Vibration Serviceability of Floors: A Probabilistic Framework

Submitted by Zandy Omer Muhammad to the University of Exeter
as a thesis for the degree of
Doctor of Philosophy in Engineering
in December 2018

This thesis is available for Library use on the understanding that it is copyright material and that no quotation from the thesis may be published without proper acknowledgement.

I certify that all material in this thesis which is not my own work has been identified and that no material has previously been submitted and approved for the award of a degree by this or any other University.

Signature: .....

Abstract

Industry feedback and research investigations have reported that problematic vibration responses in floor structures can create significant problems for both their occupants and facility owners. A critical drawback of contemporary design procedures is the lack of realistic loading scenarios and reliable vibration descriptors, since considerable complaints of unpleasant floor vibrations have been reported, even when such guidelines have been employed. A systematic investigation into realistic dynamic loading and patterns of floor occupants is of paramount importance.

This thesis investigates and describes a comprehensive procedure to carry out vibration serviceability assessment of floors on the basis of probabilistic design approach. A novel probabilistic walking load model is introduced and developed in this study using individual right and left footfalls. The load model results in more realistic force time histories than Fourier-based models, since it incorporates significant components of the spectra that are omitted in Fourier series approaches. Also, the model is applicable for probabilistic designs of multiple pedestrian input forces, regardless of the cut-off frequency.

Moreover, a simulation model of spatial distributions of pedestrians is implemented using agent based modelling. This occupant pattern model provides a realistic insight into in-service activities of multiple pedestrians on office floors, in terms of statistical distributions of their walking paths. It was found that the numerical model is capable of mimicking the actual movements to a very good extent, which makes this simulation model ideal for vibration serviceability of floors under footfall excitations.

Finally, spatial distribution of vibration responses is calculated using different statistical perspectives integrating both the probabilistic walking load model and spatial distributions of multiple pedestrians. The established approach showed a realistic way of assessing occupant exposure to vibration at specific locations of interest as well as over the entire floor area. This methodology, therefore, is expected to produce a more accurate and reliable assessment of vibration serviceability of floors.

Acknowledgements

My warmest appreciation and deepest gratitude are due for my supervisor Professor Paul Reynolds. He provided invaluable advising throughout the years of this study. His very broad knowledge, continuous encouragement and support, inspiring yet challenging ideas, keen supervision and meticulous revisions enormously helped me achieve this work. I learned a lot through my rich experience with him on the academic, professional, industry and personal levels. Special thanks are also due for Professor Alex Pavic providing valuable input through our fruitful discussions and Professor James Brownjohn for providing access to the database of measured walking forces.

I would like also to express my gratitude to Mrs Katy Manning for providing technical and administrative services. My sincere appreciation is due for Mr James Bassitt and Mr Ian Moon for facility support and professional technical service for the experimental phase of this work.

I want also to extend my thanks to wonderful members of VES for being true friends and whose help in the experimental part of this study is much appreciated, especially Emma Hudson and Karen Faulkner. Thanks to Atheer Al-Anbaki for his friendship and his assistance in the test preparation, to Ahmed Mohammed for our friendship and great technical discussions, and to Donald Nyawako and Vincent Ao for their moral support and valuable friendship. Special Thanks are due for Hiwa Fakhradin for his brotherhood and continuous prayers for me.

Special thanks are due for Qatar National Research Fund (QNRF; a member of the Qatar Foundation) via the National Priorities Research Program (NPRP), Project Number NPRP8-836-2-353. Thanks also go to colleagues at the University of Sulaimani, Kurdistan for being supportive to achieve this work.

Finally, I would like to express my sincere love and warmest gratitude to my beloved wife Sally and family to whom this thesis is dedicated; my great parents Mr Omer Muhammad and Mrs Layaqa Maruf, my mother-in-law Mrs. Parwin Ali, my sisters Mrs Rozha Omer, Mrs Kurdy Nabaz and Ms Rasyan Omer; my brothers Mr Hardy Omer, Mr Nahry Omer, Mr Nali Nabaz, Mr Khani Nabaz. Their continuous support, encouragement and prayers greatly helped me achieve this work.

List of Contents

List of Tables

List of Figures

List of Abbreviations

ABM	Agent Based Modelling
ACB	Asymmetric Cellular Beam
AISC	American Institute of Steel Construction
CCIP-016	Concrete Centre Industry Publication 016
CCTV	Closed-Circuit Television
CRSI	Concrete Reinforcing Steel Institute
CSTR43	Concrete Society Technical Report 43
DLF	Dynamic Load Factor
EMA	Experimental Modal Analysis
FE	Finite Element
FRF	Frequency Response Function
HFF	High-Frequency Floor
HiVoSS	Human Induced Vibration of Steel Structures
IP	Internet Protocol
ISO	International Organization for Standardization
LFF	Low-Frequency Floor
LTI	Linear Time Invariant
MAC	Modal Assurance Criterion
MC	Monte Carlo
MDOF	Multiple Degrees Of Freedom
MTVV	Maximum Transient Vibration Value

OS-RMS One-Step Root-Mean-Square

R factor Response factor

RFCS Research Fund for Coal and Steel

RMS Root-Mean-Square

SCI Steel Construction Institute

SDOF Single Degree Of Freedom

SFM Social Force Modelling

SRSS Square-Root-Sum-of-Squares

TP Test Point

UB Universal Beam

UC Universal Column

VDV Vibration Dose Value

Chapter 1

Introduction

1.1 Introductory statement

With the advance of modern design methods and construction technologies, floor structures featuring slender architectural designs have become more common. Coupled with reduced damping due to modern open plan layouts, these floor structures have become more susceptible than ever to excessive vibrations induced by pedestrians, even when strength criteria are satisfied. This rational design trend shifts the governing criterion from strength capacity to vibration serviceability [1, 2].

Industry feedback and previous research investigations have shown that annoyance can result from excessive vibration levels and create significant problems for building occupants and owners. These arise from the unpleasant and annoying feeling of the occupants rather than a safety or life-threatening problem, yet accompanying well-being issues [3] and psychological fear [4] are highly probable.

Over the last four decades, research efforts have tended to focus on the single pedestrian loading scenario and vibration serviceability assessment has been based on simplified design procedures. These efforts have resulted in a range of guidance documents to provide practitioners with tools to perform vibration serviceability assessments.

However, there has been much less research into potential excitation paths from multiple pedestrians, their probabilistic walking forces and statistical distributions of vibration responses. There is also very scarce published data in the public domain concerning vibration responses of multi-person floor environments and their vibration performances.

1.2 Problem statement

The majority of the available literature on vibration serviceability assessment of floors is dedicated to the single pedestrian loading scenario at a single stationary location. This individual, according to contemporary guidelines [5–8], is able to excite a floor, whose fundamental frequency decides which of two forcing functions should be used, corresponding to two well-known “classes” of floors. They are (1) a deterministic walking model for low-frequency floors (LFFs) that consists of distinct frequency components at integer multiples (harmonics) of a pacing frequency (i.e. a Fourier series model) and (2) an impulsive excitation force for high-frequency floors (HFFs) due to individual footfall impacts. However, examination of actual floor responses under realistic loading conditions has tended to demonstrate a lack of accuracy in prediction of vibration levels using these simplified

methodologies [9]. Real world floors accommodate multiple occupants, who walk over various paths at different times with a diverse range of potential excitation forces.

In addition, studies into human perception of vibrations show that subjective assessment of floor vibrations cannot necessarily be based on a binary accept/reject approach. There is a lack of research into reliable vibration descriptors that cover a range of likely responses to counter the observation that single thresholds of perception generally do not perform well to evaluate human comfort [3]. These have been observed by a significant number of practitioners, i.e. structural designers, who have received considerable complaints regarding unpleasant floor vibrations [10]. This implies that current design approaches, despite being recent (e.g. AISC DG 11 published in 2016 [5]), do not provide a reliable tool for engineers to evaluate vibration performance of modern floor design trends. A probabilistic design, therefore, is required to account for variations in human walking and hence the corresponding response predictions. There is currently no design methodology that includes multiple pedestrian spatial distribution integrated with a statistical walking model to carry out vibration serviceability assessment.

1.3 Research aim and objectives

The scope of this study is to understand and develop a probabilistic multiple pedestrian vibration design approach to predict vibration responses of floors of any type, and without recourse to an artificial low/high frequency threshold. These are crucial gaps in existing studies and design methodologies. As such, the following objectives are targeted using a combination of experimental campaign and advanced numerical modelling:

1. Conducting a comprehensive literature review of previous studies and models concerned with human walking, pedestrian excitation walking paths, design methods and vibration responses.
2. Evaluating the performance of contemporary design guidelines when implemented to actual floor structures.
3. Experimental investigation of the effect of pedestrian patterns and walking paths with respect to single and multiple pedestrian excitations, via the use of video monitoring of in-service activities.
4. Developing a numerical simulation of multiple pedestrians for vibration serviceability of floors, which includes spatial distribution of pedestrians.

5. Introducing and developing a probabilistic walking load model accommodating multi-person excitations and appropriate for probabilistic design.

6. Developing a sound analytical model to predict vibration responses, using any metric, under multiple pedestrians' walking for long durations and as such carrying out reliable vibration serviceability assessments.

1.4 Thesis organisation

This research document is organised in seven chapters. Following Chapter 1, Chapter 2 presents a critical review of the current state of knowledge on the behaviour of vibration serviceability of floors under human walking. Single pedestrian walking methods currently in use, the importance of probabilistic multiple pedestrian approaches and response predictions are also discussed in that context.

Chapter 3 thoroughly investigates, describes and criticises contemporary design guidelines to highlight the key design procedures conducted worldwide to assess vibration serviceability performance of floors. Different shortcomings based on real world floors are identified and presented.

Chapter 4 is concerned with developing an understanding of pedestrian walking patterns upon using floors. This task is performed through video monitoring techniques and quantification of multiple pedestrian walking path patterns. The test results and the effects of single and multiple pedestrians are also discussed. As a result of actual measurements, a novel multi-person simulation model is developed and integrated with actual pedestrian movements. Finally, spatial distribution of pedestrians are presented based on the proposed model.

In Chapter 5, a probabilistic multi-person walking load model is developed. The model is based on a comprehensive database of measured walking with a wide array of individuals. The model accounts for subject-variabilities and possess frequency content of those measured walking.

Chapter 6 presents spatial response analysis and probabilistic response predictions based on the details of the experimental programme carried out at two real life floors. The primary goal of the programme was to provide a thorough understanding of multiple pedestrians actual in-service response and analytical models. Further evaluation of response predictions is also discussed in the light of test results and numerical spatial distribution of pedestrians.

Chapter 7 presents a summary of the conducted research as well as concluding remarks based on the experimental and analytical work performed in this research. Suggestions for future research are also presented.

Chapter 2

Literature Review and Research Direction

This chapter is a literature review addressing current limitations of the available walking models and the corresponding vibration response assessment. In particular, the literature survey highlights the need for models of statistical multiple pedestrian walking load, identification of walking paths coupled with spatial distribution of pedestrians, and production of a statistical spatial response approach for vibration serviceability assessment of floors. The content of this chapter, in a slightly amended form, has been published in journal of Vibration under the following title:

Muhammad, Z.O., Reynolds, P., Avci ,O. and Hussein, M. “Review of pedestrian load models for vibration serviceability assessment of floor structures”, Vibration, Vol. 2, no. 1 , pp. 1-24, 2019.

2.1 Introduction

2.1.1 Background

Vibration serviceability has become increasingly important in recent years and it is now a critical design aspect of modern civil engineering structures. Nowadays, buildings and their constituents, especially floors, are becoming increasingly slender, flexible and lightweight as well as having open-plan layouts, as a result of architectural trends and much lighter forms of construction (Figure 2.1). These factors all result in significant reductions in mass and stiffness as well as low inherent damping. These tendencies and expectations on modern structures have set forth in-service functioning as increasingly important [11] due to the undesirable vibration originating from human-induced loadings. Excessive vibration in building floors [11–15], footbridges [16], staircases [17, 18], and stadia [19, 20] are examples of civil engineering structures, where normal human activities (e.g. walking, crowds bouncing and jumping) can cause significant annoyance to occupants and knock-on management and financial consequences for facility owners.

Human movements, such as walking, a common load case scenario on floor structures, can produce resonant, near-resonant or impulsive structural vibrations that are uncomfortable and intolerable for some occupants [21], may cause psychological fear or panic [4] and can adversely affect the performance of sensitive equipment or machinery [22, 23]. Some serviceability problems have required structural retrofits [24, 25], which may be difficult and expensive to implement. Hence, understanding and avoiding these problems is imperative at early stages of design, requiring development of improved methodologies for prediction of vibration response and also novel techniques for mitigation of human-induced vibrations.

Disturbing vibrations under human excitations in building floors have also been observed despite the prevalence of contemporary design guidelines[5, 6, 8]. Notwithstanding a number of attempts in recent years, one of the key deficiencies is the lack of realistic walking patterns. This is essential to provide a realistic assessment of floor structures under pedestrian loadings. In this work, office building floors are considered under walking-induced dynamic loading, since they are more likely to suffer vibration serviceability problems due to modern efficient construction and they are used mostly by professionals for long periods of time each day hence maximising exposure to problematic vibrations [26, 27].

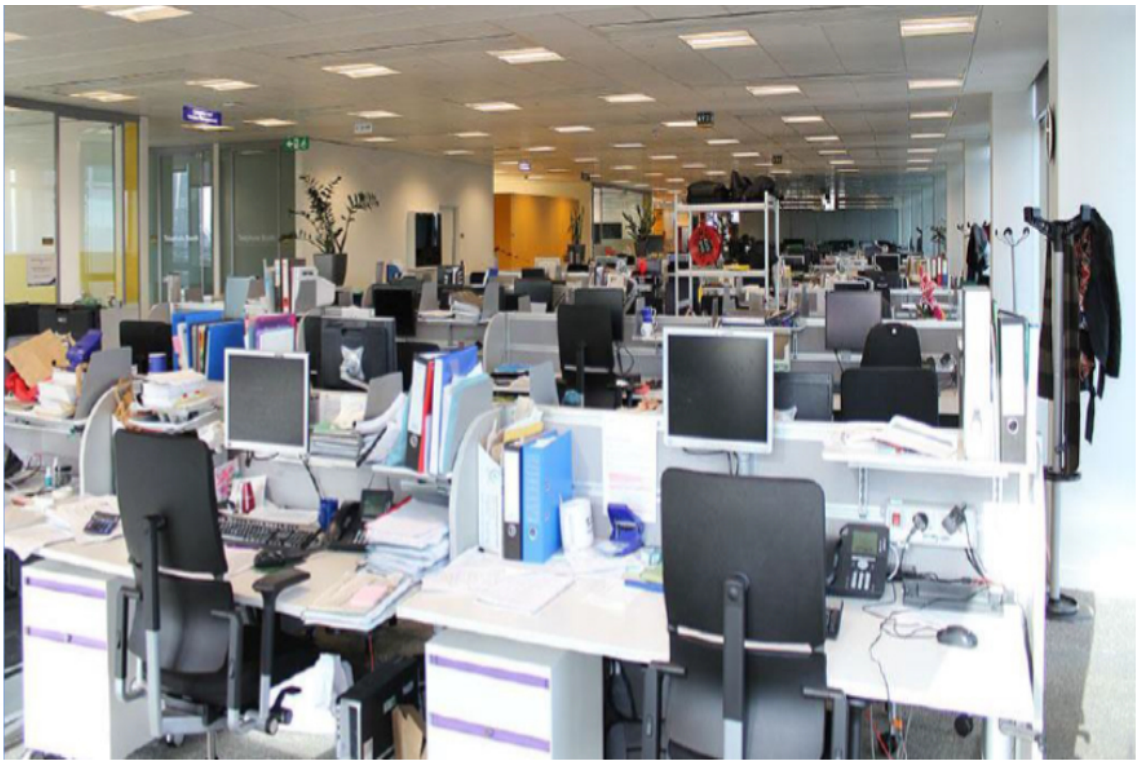

Figure 2.1: Typical modern office floor with open-plan layout.

2.1.2 Key problems

Predicting vibration magnitude in floors is an important step so that possible problems may be anticipated and prevented. Annoyance or discomfort has been reported in various types of floors such as shopping malls, office buildings, residences, restaurants and airport terminals [28–31]. Building floors for which available guidelines for floor vibrations [5–8, 32, 33] have been applied have often been found to have unacceptable performance [10], thereby demanding costly remedial measures [34, 35].

An ideal approach would be to cater for realistic walking excitations at early stages of design via appropriate probabilistic walking models. Such forcing models should be amenable for design engineers to estimate a realistic vibration exposure [36]. It is well known that human walking is a significant source of excitation for floors [6, 12] and load models derived to date can be categorized into two broad classes; deterministic load models and (more recent) probabilistic load models. The former have been used by almost all guidelines to date [5–7, 32, 33], yet the latter approach has attracted increasing interest in recent years [15, 37, 38]. Walking has been proven to be a stochastic phenomenon or narrow band random process [39], which implies that there are clear variations during walking among pedestrians and even within the same person.

In modern office floors the mass of non-structural elements has decreased due to the tendency for more open and multifunctional space environment, which increases the likelihood of unpleasant vibrations [40]. The effect of mass reduction has leaded to more problematic vibration serviceability in modern construction [2, 40]. Also, it is now widely known that in building floors the modes of vibration are often closely spaced [41]. Thus, methods to predict the vibration response should yield results that reflect actual floor behaviour in a statistical sense rather than an accept-reject method based on discrete excitation frequencies. An improved method would consider a probabilistic assessment of structural responses to walking-induced forces applied probabilistically both temporally and spatially to the structure.

In general, floors are often categorised into two types, namely low-frequency floors (LFFs) and high-frequency floors (HFFs) due to lack of a unified walking load model to cover both low and high frequency content. Floors with fundamental frequency below the threshold of approximately 10 Hz are termed as LFFs and they tend to develop a resonant build-up response. However, when the fundamental frequency exceeds approximately 10 Hz the floor does not undergo a resonant response, but rather a transient response due to individual footfall impacts [22, 42]. This work will focus on existing walking models pertinent to low-frequency floors as they are more frequent in modern office floors [43].

This chapter serves as a comprehensive review of preceding studies on approaches for modelling human loads suitable for office buildings. The intent is to identify limitations of the available walking models and the corresponding vibration response assessment and to propose where future research and direction efforts may be targeted. In particular, it is also to highlight the need for models of statistical multiple pedestrian walking loading characterised by incorporating probabilistic aspects of both temporal and spatial entities of human loading, and including randomness in walking paths on floor structures. These have not been covered comprehensively by any previous reviews [12, 13, 24, 44] into human pedestrian loadings of floors. With probabilistic forcing functions established, a statistical spatial response assessment can be produced. This probabilistic framework will be verified to be a more reliable assessment tool for vibration serviceability assessment of floors.

2.2 Characteristics of vibration in floors

Modern methods of vibration serviceability assessment should, if properly formulated, define three key parameters; the vibration source, the vibration transmission path, and the vibration receiver [45]. Rationalisation of floor vibration serviceability

into these three characteristics is simple in concept, but can be difficult to implement in practical analysis and design [11].

2.2.1 Vibration source (Input)

According to ISO 10137:2007 [45], the vibration source inside buildings can be defined as a force that generates dynamic actions that have both temporal variations (i.e. vary with time) and spatial variations (i.e. move in location) [11]. Examples are walking, which varies in both time and space, and stationary equipment operation, which varies in time only. A single pedestrian is considered to be the most appropriate source of excitation for floors typically found in quiet offices [43, 46] due to lack of synchronisation among a group of people in this environment. However, there is an increasing realisation [38, 47] that a single person loading is rather rudimentary for assessment of vibration serviceability of floors and a more realistic approach is needed. Hence, the focus of this thesis is on more sophisticated modelling of the vibration source for walking on floors.

2.2.2 Transmission path (System)

The physical medium through which the vibration is transmitted (conveyed) to the receiver can be defined as the transmission path [45]. Such a path incorporates all structural and non-structural elements attached to floor systems [11]. Dynamic properties of the transmission path are crucial to vibration serviceability. Mass can be computed fairly accurately from available physical and mechanical characteristics of floors, whereas stiffness is subjected to a high degree of uncertainty due to the influence of support conditions. Damping, a key parameter when resonance occurs, is not estimated as accurately [48]. Hence, information on floor system, mass, stiffness, damping, and support conditions has to be taken into account as precisely as possible to estimate reliably the dynamic properties and thus vibration responses [49, 50]. Typically, the lowest natural frequencies and mode shapes of floor structures can be obtained to a reasonable degree of accuracy using detailed numerical models but there is much more uncertainty with other dynamic properties such as modal masses [51] and hence magnitudes of frequency response functions, particularly for higher modes. As such, there is more research required in this area.

2.2.3 Receiver (Output)

The vibration receiver is a person or an instrument within a building that experiences the structural motion [45]. Human comfort to floor vibrations is a subjective assessment based on the magnitude and perhaps the occurrence rate of vibration, whereas the performance of sensitive equipment may be impaired if the vibration magnitude is high. There are several established criteria in various design guidance documents, using various descriptors and metrics, to evaluate the vibration for human comfort. However, the available vibration assessment procedures and associated criteria are reported to be unreliable [9, 52] and fail to deliver a satisfactory evaluation when compared to the actual human perception of vibrations in real life environments as will be discussed in Chapter 3. Therefore, improved understanding and reliable limits need to be produced to reflect more accurately the actual vibration experience of the receiver.

2.3 Human induced loading

2.3.1 Walking parameters

Human dynamic loading on floors can be categorised into two broad areas; walking and aerobic (rhythmic) loading. The former is when people walk on floors in different patterns, which may cause annoyance to occupants in quiet environments; this is a serviceability problem. The latter occurs when people exercise or perform strenuous physical activities on floors due to groups and crowds bouncing and jumping. In such cases, the force magnitude is relatively high and, if resonance occurs, it might cause the floor to suffer excessive movements thus becoming both a serviceability and strength issue at the same time [49]. It is argued that human-induced dynamic loads are complex due to individual pedestrian effects and their manner of dynamic excitation [53, 54]. Such complexity can be attributed to the dependency of human-induced dynamic loading on a large number of parameters. Information on these parameters, well recognized in biomechanics [55, 56], yet less well recognized in civil engineering, is of paramount importance in better understanding walking force functions and therefore floor vibration responses under walking excitation [57]. The reader is referred to [58] for more details.

2.3.1.1 Spatio-temporal gait parameters

Walking is considered to be a temporal-spatial phenomenon [56]. This means that it can be described in terms of temporal and spatial parameters in addition to characteristics of a pedestrian (i.e. height, weight and so on). Temporal parameters can be grouped as: step frequency (cadence), speed, stride time, stance time, swing time, single and double support and similar. Spatial parameters, whose values change with location, are: step length, step width, foot angle, attack angle, end-of-step angle and trunk orientation [55, 56, 59], as shown in Figure 2.2. The reader is referred to [58] for more information on gait cycle.

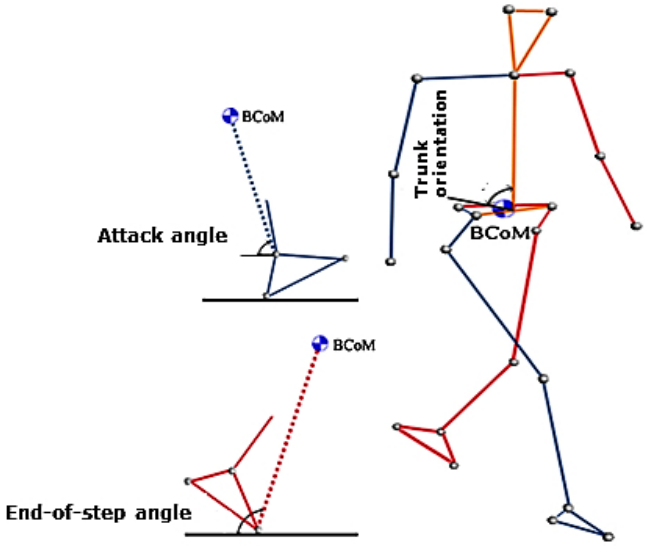

(a) Angle of different parameters with respect to Body Center of Mass (BCoM).

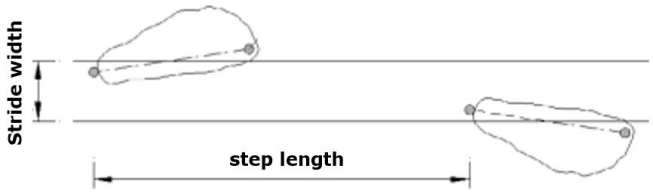

(b) Step width and step length in one step cycle.

Figure 2.2: Spatial walking parameters (after [59]).

The temporal parameters are familiar to engineers, in particular step frequency and walking speed. The spatial gait parameters, however, are not fully investigated or incorporated in the context of vibration serviceability [59]. Lack of thorough studies for gait parameters may in fact result in inadequate walking force model.

2.3.1.2 Controlled walking Vs. free walking

The findings of gait parameters in available studies, such as [15, 60–63] with respect to number of parameters measured, statistical distribution of parameters, test protocol and environment, in many instances are inconsistent. Such discrepancies could be attributed to several aspects. Firstly, the diverse environments and methods of experimentation, which often are rather artificial. For example, the majority of the studies paid attention to temporal parameters measured mostly in laboratories. It is reported that in controlled environments and/or using metronome "high level of vibration are preserved and variabilities are missed" [47]; thus, pedestrians may not walk "naturally" [62]. Also, lack of extensive experimental data due to inadequate technology in different environments has resulted in a limited number of or insufficient parameters. Secondly, it is acknowledged that people from different locations have dissimilar parameters [37], which may be due to differences in lifestyle, well-being and characteristics of walking. Lastly, the inability to describe inter- and intra-subject variability that occurs for individual pedestrians. These variations in walking have a great effect on the walking forcing function, which will be discussed in detail in Section 2.3.1.3. Therefore, it can be concluded that identification of characteristic features of the walking process is a crucial stage in developing a walking model; clearly past studies have not yet reached a consensus regarding which are the critical parameters except pacing frequency. Although correlations can be observed between walking parameters and pedestrian forcing functions, there is no single parameter that can individually provide a complete description of the walking process by itself [64]. The spatial parameters have just as much influence on walking as temporal parameters [59], in particular on floors where different walking patterns usually occur. Hence, a way forward might be to implement monitoring exercises, for example in real office environments, with advanced motion tracking technologies (presented in Section 2.6) in order to advance our knowledge of these phenomena.

2.3.1.3 Subject variability

It has been reported that there are variations between real walking and mathematical models which result in mismatch of vibration responses. The differences are mainly due to subject variabilities and human-structure interactions [65]. The aspect of human-structure interaction (HSI) is not covered in this study since in normal office floors their effect is insignificant compared to footbridges [66, 67]. Hence, this section provides insights into definition of two main subject variabilities in human walking. The occurrence of variabilities is caused by complexity of walking, which arises from inherent randomness within the bipedal locomotion.

The intra-subject variability is variations that occur within the same pedestrian during walking. The variation that exists between pedestrians, such as walking speed and step frequency, is named inter-subject variability [22, 50, 58, 59, 65, 68, 69]. The variances that exist between individuals are a result of differences in gender, age, fitness, location, etc. [62]. These are uncertainties in walking that affect vibration response level and its assessment [12].

For assessment of vibrations induced by walking, accurate prediction of vibration responses depends on a walker, in terms of force level, body weight, pacing frequency, walking velocity and so on [53, 70]. Willford et al. [71] suggests choosing a "sensible" value to account for walking variabilities, however there is no quantification for an appropriate range. This implies that there is a need to investigate walking variabilities and quantify their effect. These variabilities by their nature affect real walking, whereas previous studies that used Fourier series lost this significant information and hence inaccurate data reduction was made [35].

2.3.2 Walking models

Dynamic loading induced by pedestrians in normal walking involves loadings in the vertical, lateral and longitudinal directions. The vertical direction is exclusively considered in this study since it is the major component that causes vertical vibration and it is the most common source of annoyance and discomfort in floors [28, 72]. In the literature, available models for forcing functions are generally expressed in two forms; deterministic and probabilistic. The former have been given significant attention in past research whereas the latter is comparatively less researched. Each of these groups of load models can either be expressed in the time domain or frequency domain.

2.3.2.1 Deterministic walking models

It is assumed that the force generated in the time domain by a single walking person can be approximated by a perfectly repeating footstep at a fixed pacing frequency [57]. The assumption of perfect repetition is also used in modelling loads generated by small groups [73]. Hence, this type of forcing model is deterministic. The force produced by a person walking consists of distinct frequency components at integer multiples (harmonics) of the pacing frequency [57, 74].

Using Fourier analysis, any periodic loading can be represented as the sum of a series of simple harmonic components and the response will also occur at these same frequencies for a linear structural system. Any forcing function $F(t)$ that is periodic and has a period T can be represented by a Fourier series as

given by Equation 2.1. In 1972, Jacobs et al. [64] were the first ones who, in the biomechanics field of study, proposed and used the Fourier series to express the walking forcing function and it was supported by [75, 76]. This method was then adopted by Blanchard et al. [77] for application in civil engineering to footbridge structures. Later, many researchers adopted the same method to produce a dynamic forcing function, to name a few [21, 49, 60, 78–80]. Equation 2.1 consists of two main parts; a static part related to the weight of an individual and a time-varying part associated with the dynamic load [54]. As such, the dynamic load of the walking force is represented as follows:

$$F(t) = G\left[1 + \sum_{n=1}^{N} \alpha_n \sin(n2\pi f_p t + \Phi_n)\right] \tag{2.1}$$

where, $F(t)$ is the dynamic load (N); G is the static weight of a person (often assumed between 700 N and 800 N); n is order of harmonic of the pacing rate (integer values) (n = 1, 2, 3...); α_n is the Fourier coefficient (also known as Dynamic Load Factor - DLF) of harmonic n; f_p is pacing frequency (Hz); t is the time variable (s); Φ_n is the phase angle of harmonic n; N is the total number of harmonics considered.

It has been considered that the most significant parameters are DLFs and pacing frequency, since they are the main inputs in Fourier series. Hence, the focus of much prior research has been computing DLFs based on Fourier decomposition of measured time histories. Such quantifications of DLFs are the most common model when assuming deterministic dynamic forces [37] under walking. There are different suggestions on how many harmonic components, with corresponding DLFs, should be used. Previous studies considered different number of harmonics which generated deterministic values of DLFs, such as [57, 60, 74, 78, 79, 81]. Although methods of measurements used and the number test subjects were different, the results exhibit clear indications of variation of DLFs among people during walking. The reader is referred to [15, 16, 57] for more insights into DLFs and their values.

It is noted that LFFs can exhibit near-resonant behaviour due to pedestrians walking where the step frequency or one of its harmonics is close to a natural frequency of the floor. Conversely, HFFs tend to exhibit transient responses to individual footfalls. As such, two types of loading were deemed necessary [42] for LFFs and HFFs. This is owing to the lack of fundamental walking data and adequate mathematical models to describe the full amplitude spectrum of individual walking loading [58]. Nevertheless, there are indications [10, 34, 82] that walking has significant energy both at low harmonics and also at higher frequencies

and hence the demarcation between LFFs and HFFs lacks “scientific basis” [10], despite the fact that the cut-off frequency is commonly used.

From a frequency domain standpoint, a number of studies have remarked that footfall forces may be well represented in frequency domain [12, 21, 39, 40, 83]. Ohlsson [84] and Eriksson [46] used power spectral density to examine the energy of walking in frequency domain. Eriksson [46] concluded that walking is a narrow-band random process. As such, Brownjohn et al. [39] emphasised that walking is a stochastic phenomenon and any forcing model should reflect the natural randomness in forcing function. Frequency domain analysis for LFFs is carried out by [10]. It is shown that frequency domain approach is less expensive in terms of time and storage spaces than the time domain analysis for a single person excitation. However, the extent of analysis was not investigated for multiple pedestrians.

It can be concluded that there is a need for more actual walking datasets to be expressed statistically, even though studies to date have shown the actual nature of walking to an extent and provided some useful data. Also, deterministic force models for floors, in their current forms, are no more an effective method to be used by design engineers, since they contain many simplifications, such as stationary excitations, a single average person. These are not realistic representations of the actual loading [58]. It is noted that the majority of studies address walking of a single person in spite of existing multiple pedestrians traversing floors in daily uses of floors. There are indications showing that a single person excitation force model is not the best way of loading scenario, especially for office floors where many routes of walking are excited [38].

2.3.2.2 Probabilistic walking models for individual pedestrians

Probabilistic walking models can be regarded as statistical approaches through which the randomness of walking parameters, such as pacing frequency, weight and walking speed, can be taken into account. These approaches can model walking of an individual that, in principle, is incapable of producing a perfectly periodic load time history.

Early works of probabilistic approaches were provided by [21, 73, 85], who considered step length, step duration and footfall function for individuals walking as a function of pacing frequency. Moreover, Brownjohn et al. [39] highlighted that past researchers had given little attention to the randomness of walking forces found in the various measurements of higher harmonics. They used an instrumented treadmill to measure the continuous walking force of three test subjects walking freely to investigate actual nature of walking. Due to the stochastic nature of walking loads and energy dispersion (see Figure 2.3a), a frequency domain

model was proposed as an alternative approach to most previous work where time domain analyses were implemented to derive deterministic load models (as shown in Figure 2.3b). This study showed that there is a leakage of energy around the main harmonics of the pacing rate [22], which is due to the inherent randomness in walking. It is worth noting that the randomness has different levels at various pacing rates. Hence, a load model was proposed to include this randomness using pacing frequency as the input. This model lacks adequate statistical data to include subject variability due to insufficient number of test subjects in the experiments.

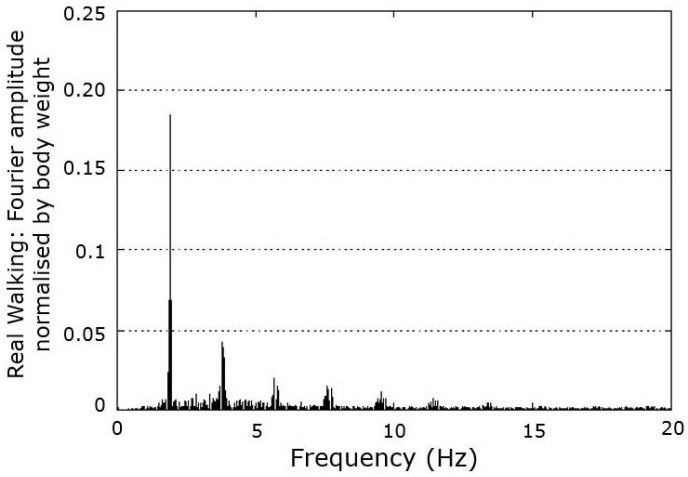

(a) Fourier amplitude of measured walking.

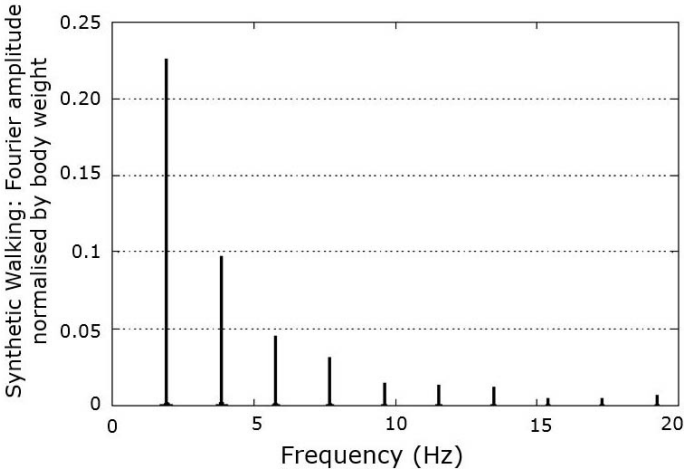

(b) Fourier amplitude of synthetic walking from deterministic models.

Figure 2.3: Frequency component of measured walking and deterministic models (after [39]).

Several studies have proposed that different parameters in the Fourier series, which is used primarily in the deterministic methods, should be modelled probabilistically [34, 68, 69, 86]. The parameters are DLFs, human weight, arrival time, walking frequency and phase angle. It was claimed [87] that a 'fully' stochastic loading model, based on walking parameters, can be established for footbridges.

The proposed model used only step frequency as the most significant parameter affecting the response rather than other parameters, which were used deterministically. This seems to be an inaccurate method since in statistical modelling, there are some interconnections which cannot be defined deterministically [88], or at least they vary from one structure to another. In addition, Racic and Brownjohn [35] proposed a synthetic loading model based on a database of forces from an instrumented treadmill. The walking load model relies on random parameters being drawn from the experimental database, resulting in a detailed representation of both temporal and spectral features of the walking force. However, access to the experimental database is a prerequisite to implement the above model, which is not available to the public domain. A possible improvement would be to provide open-access measured walking datasets so as to use the model appropriately. Middleton [51] proposed a footfall model using a quadratic spline to model walking that is suitable for floors. However, this model relied on several fixed points, i.e. using 17 points, to reconstruct the dynamic load based on the force level. This model can be improved by incorporating a wider range of frequency energy content and including subject variabilities in a statistical manner.

Recently, a study on a composite steel floor was conducted by Nguyen [15] in which a probabilistic force model based on Fourier series was proposed that defines both inter- and intra-subject variation. The weight of the human body was considered to be a mean weight of 750 N and standard deviation of 50 N. The intra-subject variability was considered by using a standard deviation (of 90 biomechanic participants) on step frequency, walking speed and step length of each participant with a probability of 5-10% chance of being exceeded; for example, the standard deviation of the step frequency is 0.083 Hz. This model is lacking in several ways. Firstly, as mentioned earlier using Fourier series approach fundamental variability in walking will be lost. Secondly, the method assumed a straight walking path in the considered office floor, which appears to be unrealistic due to obstacles usually present in office developments that can have a significant effect on the floor response. Thirdly, the walking model was only applied on one configuration of floor and the effectiveness of the model on other floor systems is not clear. Hence, further investigations are required to include these parameters statistically since, as far as modelling of walking is concerned, a stochastic approach is more appropriate as random walking paths and random parameters are considered [89, 90].

In the light of the above discussion, it follows that vibration response of floors is sensitive to forcing function, and simplified forcing models may not be reliable for assessment of floor vibration serviceability. A probabilistic approach is essential to better estimate the floor response under human walking excitation. To achieve that, actual floors, in terms of construction materials and configurations, should be

monitored and numerical simulations developed based on a universal load model under a probabilistic framework.

2.3.2.3 Response spectrum in walking models

Similar to other dynamic forces, such as seismic and wind, a number of researchers have been inspired by the response spectrum method, which is widely used in earthquake design. Despite the inherent simplifications in response spectra as it is only applicable to single degree of freedom (SDOF) structures as claimed in [91], the intent is to produce a unified load model for excitation and hence response estimation [82].

Georgakis and Ingolfsson [92] proposed a response spectrum approach based on the probability of occurrence of an event of response using numerical simulations. Mashaly et al.[91] proposed a response spectrum approach via a deterministic walking model on a footbridge to find vertical acceleration response. However, the forcing function was assumed to be stationary at the midspan. Chen et al. [63] paid attention to measured forces, using force plates and optical motion capture, to acquire statistics of test subjects for two sets of walking. One set was guided by a metronome and the other was free walking. Then, a response spectrum load model for DLFs was proposed, as shown in Figure 2.4.

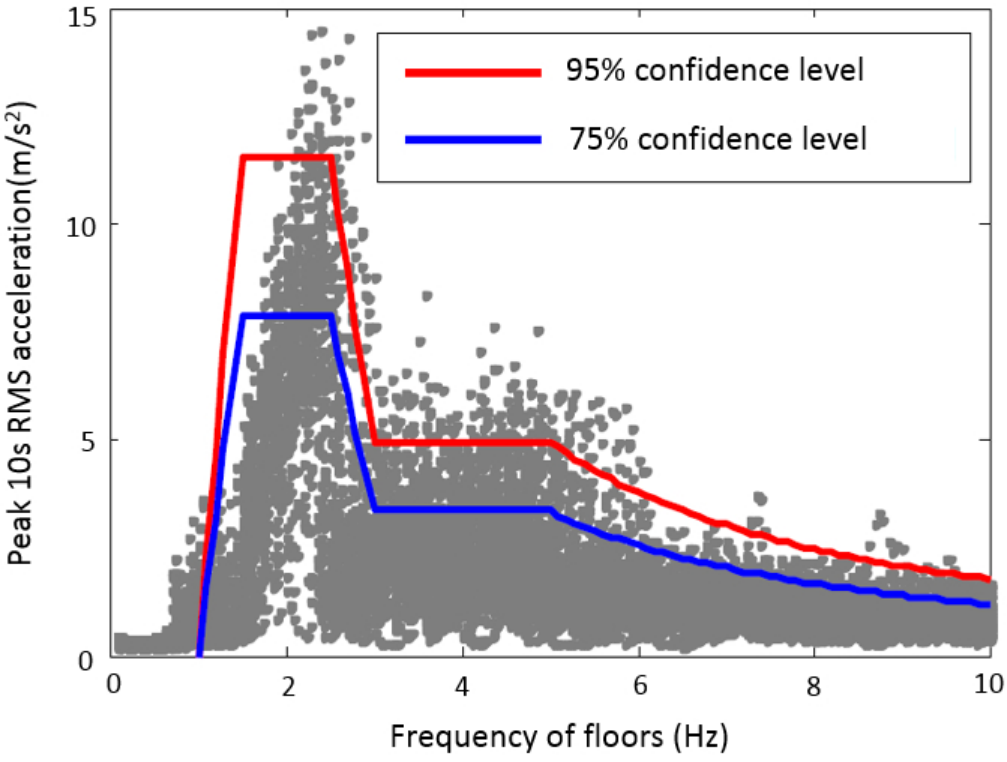

Figure 2.4: Response spectrum for floors under walking loading (after [63]).

An interesting observation made by this study is that there are sub-harmonics between the main harmonics, which are due to imperfection of the right and left steps in the gait cycle and thus a statistical method was deemed more appropriate.

Based on a large database of records from treadmills, Brownjohn et al. [82] proposed a response spectrum method for floors to evaluate vibration response measurements. This approach considers mode shape configurations and modal mass as important information to produce reliable vibration responses. It can be said that the response spectrum approach, even though it is generated under a number of simulations, is actually a deterministic method since both the input and output are actual maximum values. Hence, the application of this methodology may not provide realistic vibration serviceability assessment of floors for actual multiple pedestrians using different walking paths, despite being flexible and fast for vibration response estimation [82, 92].

2.3.3 Statistical modelling approaches for multiple pedestrians

Floors are usually used by a number of people, who they walk across the structure within certain existing walking paths [93]. Although, some multi-pedestrian loading models are available for crowd loads on footbridges [94, 95] and grandstands [96], there is a considerable lack of information about realistic multi-pedestrian loading in floors [47]. So, the resulting response could potentially lead to human discomfort and adverse comments.

Existing guidelines [5–8, 33] specify walking loading for individual pedestrians, where the load models consider a person as a stationary harmonic force. There are, however, indications [10, 97] that none of the guidelines deliver a reliable vibration assessment process that allows a designer to predict realistically the vibration performance of a structure [9, 34, 47]. The main reason is that there is not a multiple pedestrian loading model available for floors for analysis of vibration response at the design stage, uncertainties related to dynamic properties and a lack of understanding associated with tolerance levels of occupants. In other words, the actual loading situations are simplified to an average single person loading, which does not represent real use of floors. Also, the available single person force models in design guidelines are applied at a stationary position with a reduction factor to account for a walking path. However, spatial positions at different time instants would be imperative for multiple pedestrian walking excitation for which stationary harmonic forces cannot serve as a base function for such loading scenarios. Hence, the aforementioned load models do not tend to reflect the true nature of pedestrian excitation. These mechanisms to apply a probabilistic de-

sign process considering spatial patterns in walking excitation are not available, and hence the methods ignore human walking variabilities with respect to a walking path, duration of action performed and the actual frequency content of forces generated in the process [85]. Generally, pedestrians walk across floors randomly at different patterns (i.e start point and end points [38]), walking paths (discussed in Section 2.3.4), entry into or exit from room, the number of active people at a particular time, walking characteristics, walking habits of people using the floor and so on [98].

There are some experimental data regarding the stochastic treatment of people arrival time in general [99] and particularly for floors [93, 98], which follows a Poisson distribution. However, there is no experimental study to take into account spatial walking patterns of multiple pedestrians to drive a realistic relationship for existing patterns. In the case of insufficient experimental data, further developments use a probabilistic approach and numerical simulations to represent various start and end points within a typical office floor [38]. This approach is utilized to introduce parameters to quantify the main characteristics of walking and derive stochastic loads for various walking patterns.

The importance of numerical simulations, primarily Monte Carlo (MC) simulations, has been emphasised by many researchers, especially when the performance of a structure is of concern and experimental data are scarce. Although Sim et al. [96] point out that a sufficiently large dataset should be used for statistical analyses, MC simulations are in widespread use with random values generated from assumed normal distributions. Substantial simulations are chosen to get robust results by [15, 100]. It was reported around 500,000 MC simulations is found to be a reasonable value to stably estimate statistical response distribution [87]. However, performing such a large number of simulations could be time-consuming, which is a downside of the MC approach. Therefore, a better pedestrian simulation model is needed to account for multiple pedestrians' pattern upon using floors. Pedestrian models exist based on techniques such as agent-based modelling (ABM) [101] and social force modelling (SFM) [102, 103]. These models have been regarded to be effective in the context of human-induced bridge vibrations [67, 104]. These advanced models also can model individual and independent pedestrians within a virtual model, which could overcome some of the limitations in MC models considering multiple pedestrians interaction.

Actual walking paths and activities of occupants along different routes are a step forward towards establishing a reliable and stochastic load model in contemporary design. This should include the randomness in walking paths (covered in the next section) chosen by different individuals and both temporal and spatial features of the force. There is a lack of fundamental data for many relevant load

case scenarios, especially for multiple pedestrians, where different walking patterns are chosen by individuals. As a result, more experimental data are required over long periods so that realistic multiple pedestrian excitations and corresponding vibration responses can be collected. Utilising a sophisticated load model is essential to generate multiple pedestrian loads and predict the vibration response in a sufficiently accurate manner, i.e significant overestimation and considerable underestimation of the response should be avoided. More advanced numerical modelling of multiple pedestrians could pave the way for more reliable estimates of floor vibration response.

2.3.4 Walking path (route of pedestrian)

In the context of vibration response prediction, the walking path plays a major role [105], yet has not received enough attention in previous research. Most studies consider route of walking as a deterministic parameter based on the assumption that a particular walking path produces a worst case-scenario. This is an inherent simplification which raises concerns about the reliability of the response assessment.

It has been reported that the walking path is an important parameter in considering vibration of a floor; the path can traverse several mode amplitudes of a mode shape which in turn could generate resonance or near resonant response. This will vary according to which mode needs to be excited [89]. For a vibration floor assessment conducted by Reynolds and Pavic [43], pre-determined walking paths and pacing frequencies were used to create worst-case scenarios for vibration response measurements. Three walking paths, one through the middle and the other two along the diagonal of a floor, were used based on engineering judgements to excite the vibration modes of interest. Other researchers have sought a relation between walking path and entering time of individuals [21]. Through this it is assumed that the randomness of arrival time amongst multiple pedestrians is defined. However, this alone is not a realistic estimation of various paths and their realistic effect on the response prediction, since different individuals have different excitation potentials along various paths [53].

Willford et al. [71] stated that pedestrian walking paths are one of the parameters that is difficult to obtain or define at the design stage, which makes vibration response prediction difficult. Hicks and Smith [105] ascertained that different walking paths considerably affect vibration responses. However, no explanation has been given on how the route of walking can be included or estimated. The significance of walking path, particularly in low frequency floors, is that a pedestrian traversing a floor can cause resonant build-up of response if the walking path is

sufficiently long. The duration of walking and the relevant mode shape modulation need to be considered along the walking path. However, it is acknowledged that the modulation of mode shape is not easily accounted for in the current forms of vibration serviceability assessment. As a consequence, overestimation and underestimation of the response have been reported in the current guidelines [10, 22] and Section 3.4.1.2. Smith et al. in the Steel Construction Institute publication (SCI P354) [6] stated that the walking path along with the length of walking have effects on the vibration response, yet no comprehensive procedure is given on how they can be incorporated into the vibration assessment. Only very rudimentary techniques formulated in terms of "build up factors" are given in some of the design guidance documents, such as [5–7, 32].

In his doctoral thesis, Nguyen [15] assumed that the walking path "follows the configuration of a mode shape". The walking path was considered to excite the "relevant" mode shape, which was thought to produce maximum response. However, this assumption results in no definitive outcome since in floors the vibration mode shapes are quite closely spaced due to the repetitive geometry. Therefore, walking path should be considered on that part of a floor where the vibration "tolerance" is expected to be low. This could be done by simulating a number of walking paths under different walking forces so as to determine vibration responses in a statistical manner and via a spatial distribution of walking paths. This approach will take into account probabilistic distribution of various (random) routes across the whole floor, including the obstacles avoided by the pedestrians.

Considering floor monitoring, Živanović et al. [47] monitored an office floor during a normal working day. The focus was more in preselected paths with controlled walking which were thought to be most responsive. The study points out that usually a single pedestrian excitation would not give realistic estimates when compared with actual in-service vibrations of floors. It is argued that [47, 98] all responses measured during single person walking tests had considerably less than 1 percent chance of being exceeded during normal daily use of an office floor. Therefore, the single person loading scenario is not the best way to estimate vibration serviceability of floor structures (as discussed in Section 2.3.3).

In a comprehensive way Hudson and Reynolds [38] implemented various start and end points in an actual office floor where office occupants used the most; for example, near corridors are considered as walking paths. This approach gave more realistic consideration of the most used paths and gave good probabilistic assessment of the response. The probabilistic approach could entail realistic paths through a spatial distribution of multiple routes traversed by floor occupants. This in turn can generate a spatial response distribution (as discussed in Section 2.5) so that response assessment can be carried out on the basis of probabil-

ity of exceedance. Thus, a more reliable vibration assessment of floors can be obtained.

In conclusion, the walking path has a significant effect on the vibration response on floors. This parameter, along with other walking parameters, should be considered statistically in the forcing function. The way forward is to develop a walking model in which spatial walking paths and walking parameters are characterized by their stochastic nature. There is a need for including pedestrian paths into walking models so that a more accurate yet reliable approach is utilised in the context of probabilistic response assessment. As such, a statistical approach would result in a better estimate of floor performance when subjected to multi-pedestrian walking. In addition, acquisition of experimental data on floor responses via monitoring techniques (covered in Section 2.6) accompanied by occupant activities and actual walking paths utilised during normal working days are of crucial importance to establish reliable and non-conservative models.

2.4 Contemporary design guidelines and codes of practice

This section considers briefly currently available guidance documents [5–8, 32, 33, 106–108] used for vibration serviceability assessment of floors at the design stage. A more rigorous analysis of these guidance documents is presented in Chapter 3.

A range of footfall loading functions have been presented from vibration design guidelines that are deemed to be applicable to a range of structural systems. These guidelines demonstrate clear differences with respect to the frequency threshold (cut-off frequency), which are not realistic [2], nor in accordance with scientific method [10]. The key deficiencies of these guidelines can be summarised in three points. Firstly, the walking model is considered to be periodic and a single pedestrian is the only loading scenario. All of the design procedures introduced assume that walking is deterministic. Not all guidelines provide necessary information to model inherent variabilities, which results in errors in vibration response estimation. Secondly, the walking path is noted to be of great importance but existing guidelines nevertheless lack procedures to incorporate it. In other words, the excitation force is generally assumed to be stationary, i.e. a person excites a single point in space. Thus, significant overestimation or underestimation of responses predictions are often produced by the guidelines. Finally, a single peak value of the response is the sole descriptor for vibration assessment, which is not representative of the overall temporally varying vibration environment to which oc-

cupants are exposed, and hence is unrepresentative and unreliable [47, 71, 97, 105, 109].

2.5 Probabilistic response distribution

Stochastic nature of walking will yield profiles of a response that is non-deterministic and can more appropriately be defined in a statistical sense [110]. In essence, the response, in any metrics, of human-induced loading should be considered probabilistically for vibration serviceability assessment.

In order to assess the vibration serviceability of floors and its effect on occupants, there are well-known existing metrics, such as R factors, acceleration, root-mean-square acceleration (RMS) and vibration dose values (VDVs) [11]. Reynolds and Pavic [43] highlighted that there seems to be difficulty in defining which parameter provides the best response evaluation. Currently, R factors are used by some guidelines (Concrete Society 2005 [32], Concrete Centre 2006 [7], SCI P354 2009 [6]). R factor in Equation 2.2 is calculated by a running RMS with 1 s or 10 s integration time. The peak of this running RMS is termed maximum transient vibration value (MTVV). MTVV divided by the baseline acceleration, which is 0.005 m/s^2 [45], is used for assessment [43, 111]. However, it is reported that assessment of responses based on peak acceleration is "highly sensitive" to short duration peaks in the response [9, 52]. Hence, it is stated that assessing vibration responses using peak RMS is not a "reliable" descriptor and a more appropriate parameter should be defined [89, 112].

$$\mathrm{R} = \frac{max_t \left(\sqrt{\int_{t-T/2}^{t+T/2} a_w^2(t)\, dt} \right)}{0.005} \tag{2.2}$$

where:

R is the Response factor

T is the period used for the running RMS in seconds, and

$a_w(t)$ is the $\mathrm{W_b}$ frequency weighted acceleration time history in m/s^2 [113].

The vibration dose value (VDV), shown in Equation 2.3, is currently considered to be the most appropriate evaluation parameter [9, 114] in assessing vibration serviceability, as it takes into account duration of exposure and is applicable for all types of vibration (periodic, transient and random) [11, 71, 112, 114–117].

$$\text{VDV} = \left[\int_0^{T_t} a_w^4(t)dt\right]^{1/4} \tag{2.3}$$

where:

VDV is the Vibration Dose Value in m/s$^{1.75}$,

T_t is the total time period in seconds, and

$a_w(t)$ is the W_b frequency weighted acceleration time history in m/s^2 [113].

A potential problem with VDVs is that the available limits (such as limits in BS6472 [118]) are considered to be too high when compared with actual in-service monitoring of floors [9]. It is observed that a reasonable VDV limit for 16-hour daytime exposures in office buildings is around 0.15 m/s$^{1.75}$, above which adverse comment might be expected [9], which is far less than the available limits (0.4-0.8 m/s$^{1.75}$). In addition, Setareh [114] has recently proposed a new VDV limit for footbridges, which is 0.2 m/s$^{1.75}$ for low possibility of adverse comment of a standing person. Hence, vibration measurements of existing structures have revealed that the current limits, both for the VDVs and R-factors, are inaccurate and may result in clearly unsatisfactory structures to be deemed satisfactory. It should be stressed that the design guidelines ([5–7, 32, 33]) provide some of the aforementioned metrics with various limits without giving distinction of their interpretations in assessment procedures. Pedersen [119] accordingly stated that the reason that several codes and guidelines propose various parameters to assess vibrations imply that there is not a “consensus” among international committees to use a unified parameter, let alone a probabilistic assessment.

In this context, the majority of studies either use RMS or R factor in assessing vibrations. However, an important question may arise in which whether a single maximum value of these parameters or a cumulative probability distribution will yield better results. Increasing number of studies [34, 38, 67] indicate that a single value evaluation does not represent actual responses. For example, Reynolds and Pavic [9] as well as Hudson and Reynolds [38] produced a cumulative probability distribution function (PDF) of the R factors of an office floor monitored under normal operation for several days, as shown in Figure 2.5. Such probabilistic response distribution gave a realistic insight into the response over a long period of time in actual environments. Similarly, Živanović and Pavic [34] generated the cumulative distribution of the running RMS. These studies highlight that a single maximum value of R factor is unrepresentative and inaccurate compared to the actual response, for it tends to occur only at rare time intervals. However, the run-

ning R factor using cumulative distribution gives better impression of the response distribution with a probability of exceedance.

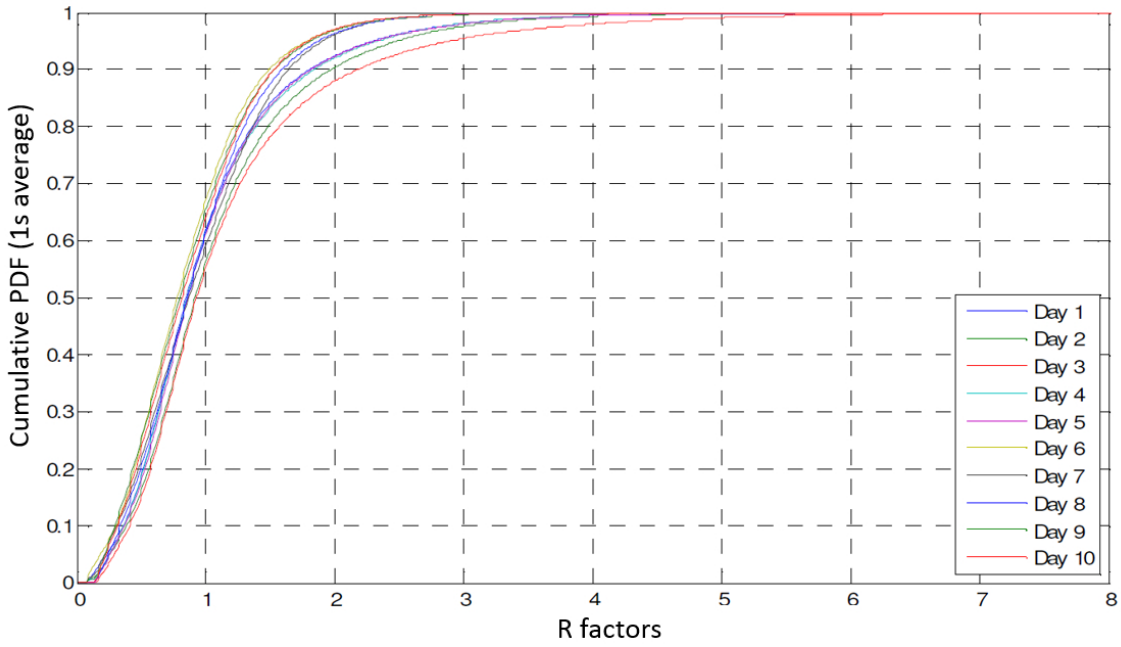

Figure 2.5: Cumulative distribution of R factors in office floor buildings (after [9]).

The majority of available literature considers evaluation of responses over time, this could be a single peak value or a statistical evaluation which is still under investigation. However, it is also imperative for accurate prediction of the response to take into account the spatial distribution of the vibration response. This is particularly essential where multiple pedestrians are crossing floors in normal operations and stay on their desks for a long period of time, which maximise their dose exposure to vibration. Combining both the spatial and the temporal response over the floor areas at the design stage may predict the possible areas with higher responses and their occurrence rates. This area of research is lacking thorough examination. Hudson and Reynolds [38] indicated that the spatial distribution of response can be very reliable as it highlights which areas experience higher vibrations (Figure 2.6). Of these areas, the vibration response may have a predetermined limit in order to be assessed and if that limit exceeded what would be the probability of occurrence. Devin et al. [120] also ascertained this method under a single person loading to produce a “contour plot of responses”. In addition, there are a number of commercial software packages, such as Oasys GSA [121], Autodesk Robot Structural Analysis [122], SAP2000 [123] and ETABS [124], that define harmonic footfall analysis for a single person excitation at stationary positions based on design guidelines, such as Concrete Centre [7], SCI P354 [6] and AISC DG11 [5]. Results of the analysis produce contour plots of vibration responses at all nodes in terms of peak R factor or acceleration. How-

ever, there is no mechanism to include moving pedestrians along different walking paths.

Identifying spatial response distributions of floors seems to provide better indications of the level of response expected for assessment in accordance with the relevant vibration criterion. Pedestrian pattern modelling, i.e. microscopic and macroscopic models [104], for multiple pedestrians movements can provide significant insights for spatial response distributions. The way forward therefore would be to include knowledge of spatial positions of pedestrians at different time instants combined with a stochastic walking load model to generate vibration responses. Introducing spatial response distributions would capture the exposure route and exposure time under actual loading scenario.

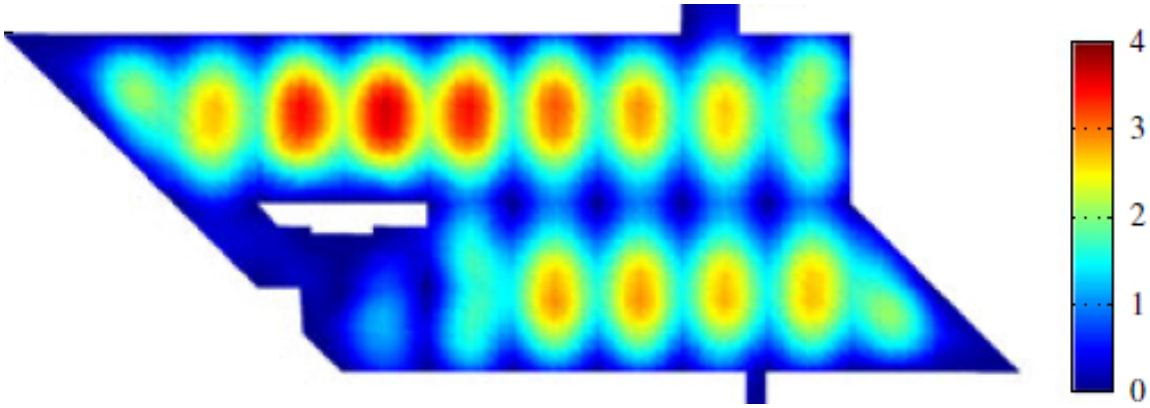

Figure 2.6: Spatial distribution of R-factor in a typical office floor (after [38]).

Therefore, it is necessary to evaluate vibration response of floors in a probabilistic framework, similar to the loading function. Better assessment of floors may be achieved by using the appropriate metric parameters and their values should be on the basis of probability of occurrence over the floor area, where multi-pedestrian walking occur. The spatial response coupled with the cumulative distribution of vibration responses might provide a more reliable and realistic approach for use at the design stage, for which there currently is no analytical procedure. As such, development of analytical techniques verified through experimental investigations might provide a mechanism for improved vibration response assessment.

2.6 Pedestrian monitoring techniques

This section gives an overview of existing in-service monitoring techniques using motion tracking [125–128]. The main purpose is to better utilize these new techniques in establishing spatio-temporal variation data of walking and thereby

developing a realistic loading model. However, the rational for using the monitoring techniques is to take into account the unconstrained floor spaces; that is experimental data should reflect the natural environments of the structures being monitored.

Monitoring tracking techniques can be categorised into the following systems for the purpose of acquiring pedestrian data. Vision-based motion tracking systems that use tracking markers, called marker-based systems, such as Codamotion and Vicon [63]. Video cameras, termed as marker-free systems, involve image processing. The third category is motion tracking inertial sensors. These can be wired (standard accelerometers) and wireless (such as inertial sensors Xsens and Opal). It is noted that using these technologies are situation-dependent [129] and their use can be limited in different environments. For example, marker-based systems tend to become less effective in areas where there is daylight interaction, whereas wireless inertial sensors are costly and the wireless range is limited [129]. Video cameras coupled with vision tracking system have been used mainly for indoor activities. Extra care should be taken to avoid occlusion of cameras field of view when this system is deployed. Thus, selection of any of these systems should be able to capture spatio-temporal data realistically and as accurately as possible.

Use of motion monitoring techniques to track human walking on building floors is rare. Several researchers [93, 125, 130] have utilised video cameras to investigate normal pedestrian traffic, walking parameters and the vibration of as-built footbridges. Kretz [131] attempted to investigate the counterflow of people walking, using three cameras, in a 1.98 m wide by 34 m long corridor. The study focused more on the walking speed, passing time and the effect of a large flux of people. In office floors, however, the situation is different due to the open-plan layout and various routes of walking. Thus, it is important to implement a number of video cameras coupled with vision tracking software to track pedestrian routes and hence produce a spatial distribution of different paths, which can be described with the probability of occurrence.

Most recently, vision based motion tracking systems have made significant advancements due to developments in computer sciences requirement for security (surveillance) purposes, where special cameras are integrated with in-built software or wireless markers. However, there seems to be no application of using a tracking system for people in civil engineering structures. Such systems would create a potential for studying human walking on floors and their movements [126]. Recently, Chen et al. [63] used a Vicon motion capture system in a laboratory to monitor the spatial trajectory of 73 test subjects during walking. Dang and Živanović [59] used a motion tracking system coupled with a treadmill

in a laboratory to monitor body movements and hence key elements of walking parameters were focused on. Also, Van Nimmen et al. [127] used motion tracking system in a laboratory to obtain step frequency of test subjects. The findings of the laboratory results were then used on a full-scale footbridge. Another contribution related to human evacuations of buildings has used Microsoft Kinect system [132] in a corridor to track the "head trajectory" of people's location, where pedestrian flow and counter flow were of interest.

There are other methods in which CCTV cameras are linked with vision tracking software. For example, Brandle et al. [133] used IP surveillance cameras with human tracking software in a railway station to capture where people stop and which areas are more concentrated. It was concluded that number and location of cameras are important. However, multiple human tracking was not included due to the complexity.

A more thorough study was carried out by [129], in which a method is proposed based on video-based algorithm to detect people on a camera then validated by Codamotion and Opal ground data (marker based). The conclusion was that the vision-based system has the potential to be used without any markers attached to people, in spite of some possible errors.

Therefore, use of new advancements and techniques in vision tracking system to capture key parameters of human walking in as-built floor structures will, possibly, pave the way for better understanding of occupants' location and their walking paths on floors. Despite challenges and errors that are inevitable in any new system, the vision tracking systems might be feasible for use on floor structures to further investigate their vibration behavior.

These technologies and techniques can provide information regarding the location of people, patterns of walking under normal working days and the statistical distribution of walking paths. These data assist in producing a probabilistic spatial variation of walking patterns where floor occupants using most. Thus, a better, yet realistic pedestrian load model can be developed based on the data collected from the vision tracking systems.

2.7 Conclusions

This chapter has presented a state-of-the-art review on pedestrian load models proposed for assessing vibration serviceability of floors. It has addressed the importance of available walking parameters and walking paths in order to develop a reliable probabilistic model. Although none of the existing models is regarded as the most reliable and accurate in predicting vibration responses, the temporal

coverage of walking parameters may be inadequate alone for a spatio-temporal loading such as walking.

A number of models have been reported to model walking of a single pedestrian, both deterministic and probabilistic. Many of these either have no pedestrian subject variabilities included and contain unrepresentative simplifications or are probabilistic in the sense that they focus on particular walking parameters and neglect other important entities. In particular, the spatial parameters and walking paths are not covered by all of these models, i.e. the routes covered by floor occupants in normal floor operations are not incorporated. Typical floors often accommodate multiple pedestrians with various walking patterns. Actual walking path and activities of occupants along different routes are a crucial step to establish a reliable loading model. This should include the randomness in walking paths chosen by different individuals and both temporal and spatial features of the force. As a result, more experimental data collected over long periods are required so that realistic multiple pedestrian excitations and thus corresponding vibration responses could be measured. Utilising a probabilistic loading model is essential to generate multiple pedestrian loads and predict the vibration response sufficiently accurately, i.e large overestimation and considerable underestimation of the response should be avoided. The loading model integrated with numerical simulations would pave way for more reliable estimates of the vibration response of floors. It is suggested that a spatio-temporal multiple pedestrian loading of walking could be a more reliable model in vibration assessment and further work should focus on developing such models.

Following the review of different walking models, a review of vibration response assessment has been presented. Most of the vibration descriptors and tolerance limits provided by the prevalent guidelines and studies are highly dependent on a single peak value, where the assessment procedure fails to deliver a reliable prediction. However, as walking is a spatio-temporal dynamic load, the vibration response tends to become a spatial distribution of response. A more reliable load model with response prediction can be developed to obtain a probabilistic unified walking loading model through which cumulative probabilistic responses are generated, not only at a sole location, but over the entire floor area for a duration of walking activity. The probabilistic approach could entail realistic paths through a spatial distribution of multiple routes traversed by floor occupants. This in turn can generate a spatial response distribution so that the response assessment can be carried out on the basis of probability of exceedance. This provides motivation for further research on the statistical relationships and development of improved spatio-temporal models for both the load and response. A probabilistic response distribution may have a predetermined limit with a probability of exceedance in order to assess floors adequately with respect to a vibration criterion.

It is essential to merge experimental and analytical activities in the research and definition of spatial distribution of walking paths traversed by floor occupants in order to produce methods for calculation of probabilistic spatial response. Experiments can inform the development of analytical models to describe the actual walking paths obtained utilising advanced vision tracking technologies. A stochastic approach, in both the walking loading and the vibration response will serve design engineers sufficiently precise in predicting the response and hence a more reliable vibration assessment.

In the light of these conclusions, the following chapters aim to propose a new framework for vibration serviceability. First, a more rigorous analysis of the design guidelines will be investigated in Chapter 3 to expand on Section 2.4. Walking patterns under multiple pedestrians will be investigated experimentally and numerically in Chapter 4. This is to address the shortcomings identified in Section 2.3.4. Also, a probabilistic walking load model is suggested in Chapter 5, which will provide a better frequency content and can be applied to multiple pedestrians in comparison to Fourier-based models as mentioned in Section 2.3.3. Finally, Chapter 6 will be built upon Chapter 4 and 5 to provide a spatial response framework for long durations of walking activity utilising probabilistic approaches to address Section 2.5.

Chapter 3

Performance Evaluation of Contemporary Design Guidelines

This chapter aims to provide a reader and/or an engineer, conversant with human-induced vibrations of floor structures, with the limitations of existing vibration design guidelines and tolerance limits which are used worldwide. Real world floors with actual pedestrian response measurements are used to evaluate the reliability of contemporary guidelines. Some content of this chapter has been published as a technical article under the following reference:

Muhammad, Z.O. and Reynolds, P.“ Vibration serviceability of building floors: Performance evaluation of contemporary design guidelines”, Journal of Performance of Constructed Facilities, Vol. 33, No. 2, 04019012, 2019.

3.1 Introduction

This chapter provides further insights into the available design guidelines presented in Section 2.4. Floors, as an integral element of any building, not only characterised by larger spans, lighter weight and relatively less damping due to the growing drive towards open-plan layouts with fewer partition walls, but also possess particular dynamic features, such as closely-spaced mode shapes [41], higher uncertainties in modal parameters [43] and subjective judgements on vibration magnitude by different occupants [134]. As discussed in Section 2.7, the potential for annoying vibrations remains high under human-induced loadings. As a consequence, vibration serviceability design is a major challenge in modern floor design whereby the prediction of vibration responses under human-induced footfall remains a difficult task.

Several design guidelines, as listed below, are available at the design stage to predict the vibration responses and provide methodologies for assessment of vibration serviceability of floors under pedestrian-induced vibrations.

- American Institute of Steel Construction Design Guide 11 (AISC DG11) [5]
- Design Guide for Vibrations of Reinforced Concrete Floor Systems, Concrete Reinforcing Steel Institute (CRSI) [33]
- Steel Construction Institute publication 354 (SCI P354) [6]
- European guideline, Human Induced Vibration of Steel Structures 2007 (HiVoSS) [8, 106]
- Concrete Centre Industry Publication 016 (CCIP-016) [7]
- Concrete Society Technical Report 43 Appendix G (CSTR43 App G) [32]

The application of current guidelines is generally for a single pedestrian at the design stage, where a simplified periodic walking load model is utilised to represent actual walking. Even though numerous studies [39, 68] have shown that such an approach is unable to reliably describe walking and its innate variabilities, nevertheless contemporary guidance documents display significant dependence on that force model. Thus, the provided design methods often result in inaccurate vibration responses [10, 82, 97]. The main shortcomings can be summarised as follows [107]:

- Lack of a pedestrian load model with sufficient reliability as the excitation source; thus a probabilistic approach is needed [15, 37].
- Incorrect characterisation of floor properties in terms of their modal parameters (modal mass, natural frequency and damping ratio), in particular modal masses [51].

- Uncorroborated simplifying assumptions, such as considering partition walls as damping elements and ignoring their mass and stiffness contribution [120].
- Imprecise assessment of floor response according to relevant vibration descriptors [134] and tolerance thresholds. In some cases, different tolerance limits are given in different guidelines for the same vibration metric (e.g. Response factor (R factor)).

The main objective of this chapter is to appraise a number of widely used vibration guidelines (AISC DG11, SCI P354, HiVoSS, CCIP-016 and CSTR43 App G) and evaluate the methodologies applied in the analysis and design of floors whose vibration responses are of concern. The CRSI guidance document is not used as it is not applicable to the case study floors chosen in this study. The procedures given in each guideline are based on certain assumptions and simplifications, but a systematic assessment of the actual efficacy is required to reflect current design practice with respect to full-scale floors under normal in-service conditions. The efficacy and assessment of the design guidance are carried out through tested full-scale floors involving their respective finite element (FE) modelling. Both simplified and FE approaches recommended by the guidance documents are used to predict the vibration response. To facilitate reliable evaluations, the predicted response metrics are compared with those from measurements.

3.2 Contemporary design guidelines

The following section gives a brief overview of vibration design methodologies included in the current guidelines. The design methods are pertinent to both low-frequency floors (LFFs) and high-frequency floors (HFFs).

3.2.1 AISC DG11

AISC DG11 [5] deals with the vibration serviceability of steel framed structures. This guidance's response methodology used in this chapter is summarised in Figure 3.1, including the relevant guidance chapter designation, and essential equations as shown in Table 3.1. The vibration response is computed based on the frequency threshold; if the fundamental frequency is below 9 Hz, the response under walking is predominantly resonant and can be described by a sinusoidal peak acceleration (equivalent R factor=sinusoidal peak acceleration x 0.707 divided by the reference value of 0.005 m/s^2 [45]). The formula for R factor is given in Equa-

tion 2.2. In the case of floors whose fundamental frequency is above this limit, a transient response to a single impulse footstep is deemed more appropriate.

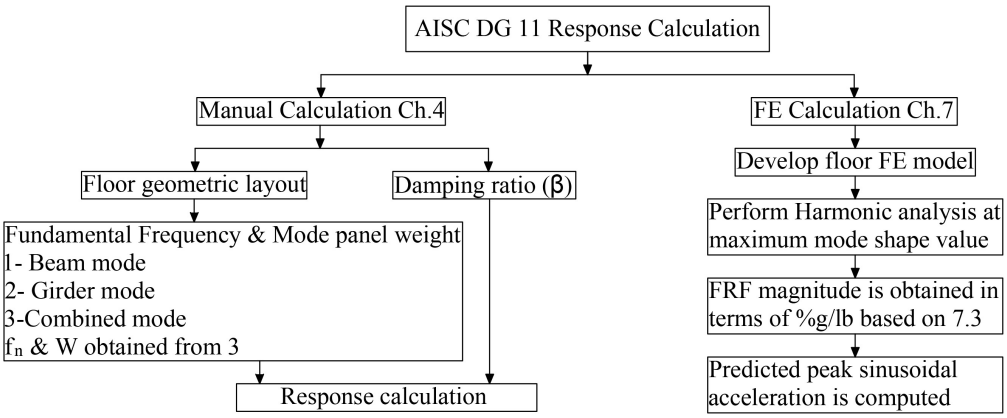

Figure 3.1: AISC DG11 vibration analysis procedure and chapter designation.

Walking is considered as a periodic force that can be reproduced by the combination of integer multiples of the basic frequency, i.e step frequency (f_p) as represented by a Fourier series. AISC DG11 implements simple equations to manually estimate modal properties of regular floor bays, shown in Table 3.1. Moreover, FE analysis is also suggested to estimate the vibration response of the floor bays by calculating Frequency response functions (FRFs), i.e frequency domain analysis. This approach has been considered in order to determine the dominant mode shapes and frequencies. The FRF magnitudes are computed via harmonic or steady-state analysis for a unit load at the walking load location (i.e a stationary location) and the response location along the walking path in close proximity to the peak mode amplitude [5]. A resonant build-up factor is considered to account for the walking path.

Table 3.1: AISC DG11 vibration analysis essential equations

Analysis type	Modal Properties	Response Prediction
Manual Calculation	$f_n = 0.18\sqrt{\frac{g}{\Delta_j+\Delta_g}}$ $W = \frac{\Delta_j}{\Delta_j+\Delta_g}W_j + \frac{\Delta_g}{\Delta_j+\Delta_g}W_g$	$a_p = \frac{P_o\, e^{-0.35\, f_n}}{\beta\, W}\, g$ for LFFs $a_p = \left(\frac{154}{W}\right)\left(\frac{f_{step}^{1.43}}{f_n^{0.3}}\right)\sqrt{\frac{1-e^{-4\pi h\beta}}{h\pi\beta}}\, g$ for HFFs
FE LFFs	Harmonic analysis up to 9 Hz	$a_p = \text{FRF}_{max} \times 0.09e^{-0.075 f_n} \times 168\rho$
FE HFFs	Harmonic analysis up to 20 Hz	$a_{p,m} = 2\pi f_{n,m}\phi_{i,m}\phi_{j,m}\left(\frac{f_{step}^{1.43}}{f_n^{1.3}}\right)\left(\frac{168}{17.8}\right)$ $a(t) = \sum_{m=1}^{N_{modes}} a_{p,m}e^{-2\pi f_{n,m}\beta t}\sin(2\pi f_{n,m}t)$ $a_p = \sqrt{2}\sqrt{\frac{1}{T}\int_0^T a^2(t)dt}$

f_n : fundamental natural frequency, Hz
g : acceleration of gravity , 386 in/s^2
Δ_j : beam midspan deflection due to the weight supported, in
Δ_g : girder midspan deflection due to the weight supported, in
W_j : effective panel weights for the beam, lb
W_g : effective panel weights for the girder panels, lb
W : effective weight supported by the beam and girder panel, lb
P_o : amplitude of the driving force, 65 lb
β : damping ratio
f_{step} : step frequency, Hz
h : step frequency harmonic matching the natural frequency
a_p : sinusoidal peak acceleration, in/s^2
ρ: resonant build-up factor
$\phi_{i,m}$, $\phi_{j,m}$: mth mode mass-normalised shape values at location i and j.
T : footstep period = $\frac{1}{f_{step}}$, s

3.2.2 SCI P354

SCI P354 [6] gives guidance to assess the vibration serviceability of composite steel-concrete floors. SCI P354 response calculation is demonstrated in Figure 3.2, including the relevant guidance chapter designation, and essential equations as shown in Table 3.2. The forcing function is assumed to be periodic and in essence the Fourier series can be used up to the fourth harmonic. Mode superposition is suggested to obtain the total vibration response under stationary walking at locations of maximum likely response (i.e. a walker excites a single point in space), with mode amplitudes of all relevant modes within the frequency range being extracted from the FE model to predict response.

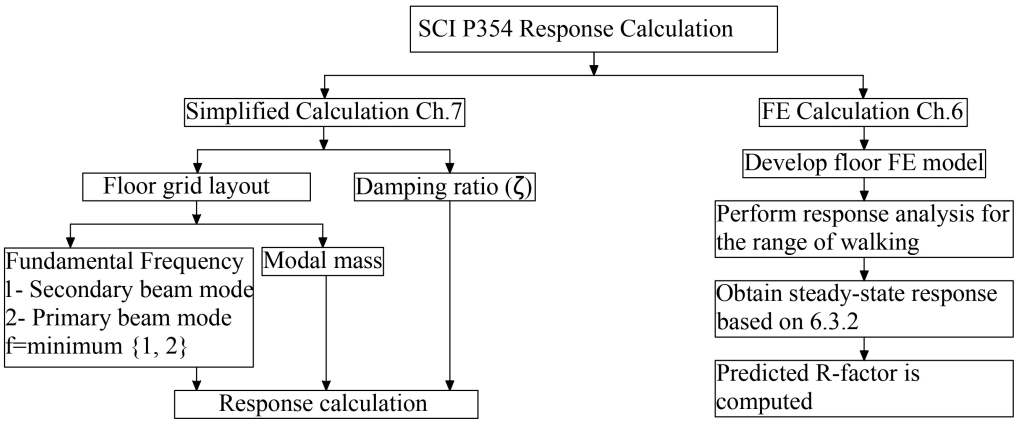

Figure 3.2: SCI P354 vibration analysis procedure and chapter designation.

The cut-off fundamental frequency between LFF and HFF is 10 Hz; above this limit the floor is assumed to undergo transient response under impulsive foot-fall loading. For LFFs, the vibration response is determined from contribution of modes up to 12 Hz (i.e. using mode superposition) and is assessed based on a single peak value, which is defined in terms of a R factor. This is shown in Table 3.2. The R factor is the peak of the running root-mean-square (RMS) acceleration for 1 second integration (termed as maximum transient vibration value, MTVV) divided by the reference value of 0.005 m/s^2 [45]. This value may then be evaluated against recommended tolerance limits for different floor functions.

From a practical point of view, a reduction factor ρ (Equation 3.1) may be applied to the peak RMS value to take into account the effect of resonant build-up for a specific walking path. This reduction factor in Equation 3.1 seems to be incorrectly written in this guideline [135]. The correct form should include the harmonic number term "H_n", as shown in Equation 3.2.

$$\rho_{\text{SCI,incorrect}} = 1 - e^{-2\pi\zeta f_p \frac{L}{v_p}} \tag{3.1}$$

$$\rho_{\text{correct}} = 1 - e^{-2\pi\zeta H_n f_p \frac{L}{v_p}} \tag{3.2}$$

where: ζ is damping ratio, f_p is step (pacing) frequency in Hz, L is length of walking path in m, and v_p is velocity of walking in m/s.

Table 3.2: SCI P354 vibration analysis essential equations

Analysis type	Modal Properties	Response Prediction
Simplified Calculation	$f_o = \frac{18}{\sqrt{\delta}}$ $M = mL_{eff}S$	$a_{w,rms} = \mu_e\mu_r\frac{74.6}{2\sqrt{2}M\zeta}\,W\rho$ for LFFs $a_{w,rms} = 2\pi\mu_e\mu_r\frac{185}{Mf_o^{0.3}}\frac{746}{700}\frac{1}{\sqrt{2}}\,W$ for HFFs
FE LFFs	include modes up to 12 Hz	$a_{w,rms} = \sum_{n=1}^{N_{modes}}\mu_{e,n}\mu_{r,n}\frac{F_{h,n}}{M_n\sqrt{2}}D_{n,h}W\rho$ $D_{n,h} = \frac{h^2\beta_n^2}{\sqrt{(1-h^2-\beta_n^2)^2+(2h\zeta\beta_n)^2}}$
FE HFFs	include modes up to two times fundamental mode	$a_{w,e,r,n} = 2\pi f_n\sqrt{(1-\zeta^2)}\mu_{e,n}\mu_{r,n}\left(60\frac{f_p^{1.43}}{f_n^{1.3}}\right)\left(\frac{746}{700M_n}\right)W_n$ $a(t) = \sum_{n=1}^{N_{modes}} a_{w,e,r,n}e^{-2\pi f_n\zeta_n t}\sin(2\pi f_n\sqrt{(1-\zeta_n^2)}t)$ $a_{rms} = \sqrt{\frac{1}{T}\int_0^T a(t)^2dt}$

f_o or f_n : natural frequency, Hz
δ : total deflection of the slab, secondary beam and primary beams, mm
M or M_n : modal mass, kg
m : floor mass including dead load and imposed load present in service, kg/m^2
L_{eff} : effective floor length, m
S : effective floor width, m
W or W_n : weighting factor for human perception based on floor frequency
ζ or ζ_n : damping ratio
μ_e, μ_r : mode unity-normalised shape values at location e and r.
f_p : step frequency, Hz
ρ : resonant build-up factor
F_h : excitation force for the hth harmonic, N
h : number of hth harmonic
β_n : frequency ratio taken as f_p/f_n
$a_{w,rms}$: root-mean-square acceleration, m/s^2
T : footstep period = $\frac{1}{f_p}$, s

3.2.3 HiVoSS

Research Fund for Coal and Steel (RFCS) has published HiVoSS [8, 106] for vibration design of steel structures. Specifically, this guideline is for composite steel-concrete floors under walking-induced vibration. It is applicable only for floors with natural frequency less than 10 Hz [107, 108], even though it is not stated explicitly within the guideline document (e.g [106]).

Walking is modelled by a polynomial fit function with eight terms, as illustrated in Section 3.2.6. HiVoSS approach for response calculation is summarised in Figure 3.3, including the relevant guidance chapter designation, and essential equations as shown in Table 3.3. This guideline treats individual modes from an

MDOF system with multiple modes of vibration as individual SDOFs and hence the response of each mode is determined separately and combined using the square-root-sum-of-squares (SRSS) approach. However, it is not clear how many modes should be included when the contributions of all modes are combined.

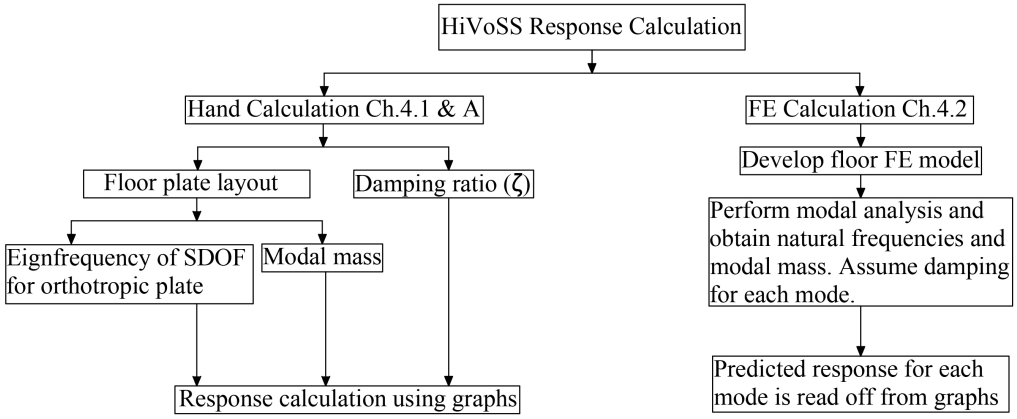

Figure 3.3: HiVoSS vibration analysis procedure and chapter designation.

Table 3.3: HiVoSS vibration analysis essential equations

Analysis type	Modal Properties	Response Prediction
Hand Calculation	$f = \frac{\pi}{2}\sqrt{\frac{EI_y}{\mu l^4}}\sqrt{1+\left[2\left(\frac{b}{l}\right)^2+\left(\frac{b}{l}\right)^4\right]\frac{EI_x}{EI_y}}$ $M_m = \mu l b\left[\frac{\delta_x^2+\delta_y^2}{2\delta^2}+\frac{8}{\pi^2}\frac{\delta_x\delta_y}{\delta^2}\right]$	use graphs to read off OS-RMS
FE LFFs	include modes up to 10 Hz [107, 108]	use graphs to read off OS-RMS
FE HFFs	include modes up to 20 Hz (from graphs)	use graphs to read off OS-RMS

f : natural frequency, Hz
μ : floor mass, kg/m^2
l : length of the floor panel (x-direction), m
b : width of the floor panel (y-direction), m
E : Youngs-Modulus, N/m^2
I_x : moment of inertia of bending about x-axis, m^4
I_y : moment of inertia of bending about y-axis, m^4
δ_y : deflection of the slab, mm
δ_x : deflection of the beam, mm
δ : total deflection of the slab and beam, mm
M_m : modal mass, kg

One-step root-mean-square (OS-RMS) is used as the vibration descriptor and it is computed as shown in Equation 3.3

$$\text{OS-RMS} = \sqrt{\frac{\sum_0^n (v_n)^2}{n}} \tag{3.3}$$

where: v_n is the weighted velocity response m/s and n is the number of samples within one step duration.

The OS-RMS multiplied by a factor of 10 gives an equivalent R factor [106]. Vibration tolerance limits are defined for different floor classes and assessment is made against these limits. The HiVoSS document states that limits specified in ISO10137 [45], which are used as a basis for limits in SCI P354, CCIP-016 and CSTR43 App G, are “unnecessarily harsh” and proposes limits that are much higher, for example OS-RMS upper limit of 3.2 for offices (equivalent to R=32).

3.2.4 CCIP-016

CCIP-016 [7] is applicable for all types of floors and footbridges. This guidance’s approach for response calculation implemented in this chapter is summarised in Figure 3.4, including the relevant guidance methodology, and essential equations as shown in Table 3.4. The walking excitation is assumed to be periodic and the first four harmonics of the Fourier series can represent the walking force. Unlike AISC DG11 and SCI P354, this guideline formulates its dynamic load factors (DLFs) based on a probability of 25 % of being exceeded. Response calculations, similar to other guidelines, are separated into resonant response, for LFFs whose natural frequency is less than 10 Hz, and impulsive response for HFFs above 10.5 Hz. However, it is stated that if the structure is “potentially susceptible to both resonance and impulsive response”, both calculation methods should be used and the highest response should be selected for assessment.

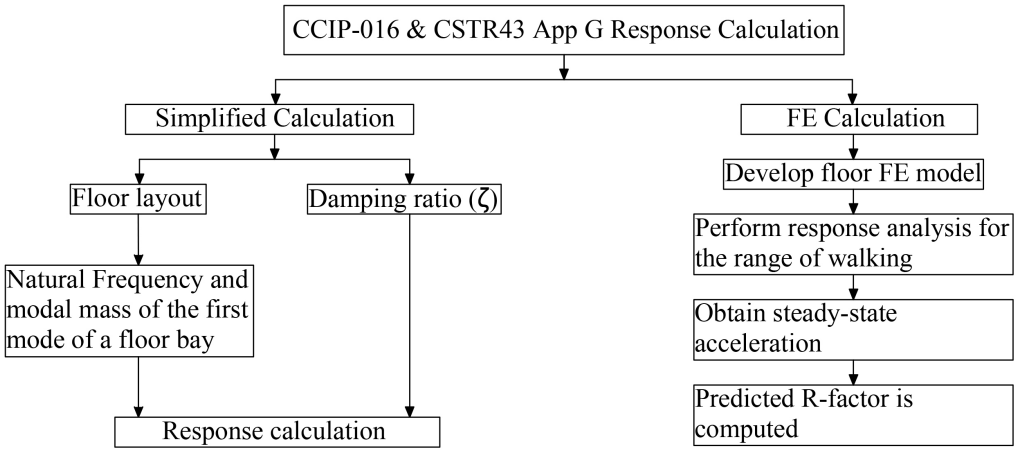

Figure 3.4: CCIP-016 and CSTR43 App G vibration analysis procedure.

Table 3.4: CCIP-016 vibration analysis essential equations

Analysis type	Modal Properties	Response Prediction
Simplified Calculation	$f = K_{f,m} K_f \frac{\pi}{2} \sqrt{\frac{D_y}{mL^4}}$ $M = \frac{mLWK_{m,m}}{4}$	$a_t = K_{r,m} \frac{\rho F_h}{2\zeta M_n}$ for LFFs $v_{rms} = 0.3 \frac{54}{M_n} \frac{f_p^{1.43}}{f_n^{1.3}}$ for HFFs
FE LFFs	include modes up to 15 Hz	$a_{real,h,n} = \left(\frac{f_h}{f_n}\right)^2 \frac{F_{h,n}\mu_{e,n}\mu_{r,n}\rho_{h,n}}{M_n} \frac{A_n}{A_n^2+B_n^2}$ $a_{imag,h,n} = \left(\frac{f_h}{f_n}\right)^2 \frac{F_{h,n}\mu_{e,n}\mu_{r,n}\rho_{h,n}}{M_n} \frac{B_n}{A_n^2+B_n^2}$ $A_n = 1 - \left(\frac{f_h}{f_n}\right)^2$ and $B_n = 2\zeta_n \frac{f_h}{f_n}$ $a_h = \sqrt{\left(\sum_{n=1}^{N_{modes}} a_{real,h,n}\right)^2 + \left(\sum_{n=1}^{N_{modes}} a_{imag,h,n}\right)^2}$
FE HFFs	include modes up to two times fundamental mode	$v_n = \mu_e \mu_r \frac{54}{M_n} \frac{f_p^{1.43}}{f_n^{1.3}}$ $v(t) = \sum_{n=1}^{N_{modes}} v_n e^{-2\pi f_n \zeta_n t} \sin(2\pi f_n t)$ $v_{rms} = \sqrt{\frac{1}{T}\int_0^T v(t)^2 dt}$

f or f_n: natural frequency, Hz
m : floor mass, kg/m^2
D_y : stiffness of the floor in major direction, Nm
K_f : multiplier on the frequency to account for two-way spanning
$K_{f,m}$: multiplier on the frequency to account for adjacent row of parallel bays
L : length of the floor bay, m
W : width of the floor bay, m
M or M_n : modal mass, kg
$K_{m,m}$: multiplier on the modal mass to account for adjacent row of parallel bays
$K_{r,m}$: multiplier on the response to account for contribution of higher modes
F_h : harmonic force amplitude, N
h : harmonic number
f_p : step frequency, Hz
ρ : resonant build-up factor
f_h : harmonic forcing frequency = hf_p, Hz
μ_e, μ_r : mode unity-normalised shape values at location e and r.
ζ or ζ_n : damping ratio
a_t : acceleration response, m/s^2
a_h : harmonic acceleration for all modes, m/s^2
v_{rms} : root-mean-square velocity, m/s
T : footstep period = $\frac{1}{f_p}$, s

The vibration response is determined from contribution of all modes up to 15 Hz and is expressed as a maximum value of RMS acceleration with integration time of $1/f_p$. The essential calculation procedure is shown in Table 3.4. Then, the R factor is computed from the peak RMS acceleration, as mentioned before. Similar to SCI P354, a reduction factor is introduced to take into account the resonant build-up

of vibration. The R factor is then compared against tolerance limits for various types of floor usage.

3.2.5 CSTR43 App G

CSTR43 App G [32], similar to CCIP-016, is versatile in its use in terms of construction materials for floors. Walking forcing function is based on Fourier analysis with DLFs based on the probability of 25 % of being exceeded. The response calculation is separated based on the fundamental natural frequency. The threshold frequency is 10 Hz between LFFs and HFFs, which corresponds with resonant and transient response, respectively.

Table 3.5: CSTR43 App G vibration analysis essential equations

Analysis type	Modal Properties	Response Prediction
Simplified Calculation	$f = \frac{\pi}{2}\left(\frac{r^2}{L^2} + \frac{s^2}{W^2}\right)\sqrt{\frac{D_y}{m}}$ [136] $M = \frac{mLW}{4}$	for LFFs same as FE LFFs for HFFs same as FE HFFs
FE LFFs	include modes up to 12 Hz	$a_{e,n}(hf_p) = \mu_{e,n}\mu_{r,n}\left(\frac{hf_p}{f_n}\right)^2 \frac{P_{e,h}}{M_n} \cdot DMF$ $DMF = \frac{1}{\left[1-\left(\frac{hf_p}{f_n}\right)^2\right]+i\left[2\zeta_n\left(\frac{hf_p}{f_n}\right)\right]\rho}$ $a_e = \sqrt{\sum_{h=1}^{4} a_e^2(hf_p)}$ $a_{rms} = 0.707 a_e$
FE HFFs	include modes up to two times fundamental mode	$v_n = \mu_e \mu_r \frac{54}{M_n}\frac{f_p^{1.43}}{f_n^{1.3}}$ $v(t) = \sum_{n=1}^{N_{modes}} v_n e^{-2\pi f_n \zeta_n t}\sin(2\pi f_n \sqrt{1-\zeta_n} t)$ $v_{rms} = \sqrt{\frac{1}{T}\int_0^T v(t)^2 dt}$

f or f_n: natural frequency, Hz
m : floor mass, kg/m^2
D_y : stiffness of the floor in major direction, Nm
L : length of the floor bay, m
W : width of the floor bay, m
M or M_n : modal mass, kg
r and s : number of sine wave curvature in x and y direction
$P_{e,h}$: harmonic excitation force amplitude at location e, N
μ_e, μ_r,f_p,h,ρ, and ζ or ζ_n : as defined in Table 3.4.
a_{rms} : root-mean-square acceleration, m/s^2
v_{rms} : root-mean-square velocity, m/s
T : averaging time taken as 1 s

CSTR43 App G approach for response calculation is summarised in Figure 3.4, including the relevant guidance methodology, and essential equations as shown in Table 3.5. The vibration response is computed, similar to SCI P354, from all

modes up to 12 Hz and the resonant reduction factor is applied similar to the aforementioned procedure. Thus, the evaluation is based on a single peak value of R factor with corresponding recommended limits.

3.2.6 Nature of forcing functions used in design guides

The aforementioned design guidelines use deterministic forcing functions based on either Fourier series or polynomial expressions (in HiVoSS as presented in Equation 3.4):

$$F(t)/G = K_1 t + K_2 t^2 + K_3 t^3 + K_4 t^4 + K_5 t^5 + K_6 t^6 + K_7 t^7 + K_8 t^8 \tag{3.4}$$

Where, $F(t)$ is the dynamic force due to a single step, G is bodyweight, K_n are polynomial coefficients described as a function of step frequency, summarised in Table 3.6, and t is the time. The standard walking force then can be done by adding the step load to this function repeatedly at intervals of $1/f_p$.

Table 3.6: Polynomial coefficients for step load walking as per HiVoSS

Coefficients	Range of step frequency (f_p)		
	f_p≤1.75 Hz	1.75 Hz < f_p < 2.0 Hz	f_p≥2.0 Hz
K_1	-8 × f_p +38	24 × f_p -18	75 × f_p -120
K_2	376 × f_p -844	-404 × f_p + 521	-1720 × f_p + 3153
K_3	-2804 × f_p +6025	4224 × f_p -6274	17055 × f_p -31936
K_4	6308 × f_p -16573	-29144 × f_p +45468	-94265 × f_p +175710
K_5	1732 × f_p +13619	109976 × f_p -175808	298940 × f_p -553736
K_6	-24648 × f_p +16045	-217424 × f_p +353403	-529390 × f_p +977335
K_7	31836 × f_p -33614	212776 × f_p -350259	481665 × f_p -888037
K_8	-12948 × f_p +15532	-81572 × f_p +135624	-174265 × f_p +321008

These are compared in Figure 3.5, which shows the forcing functions of each guideline overlaid and normalised by the human body weight at step frequency 2 Hz. It can be seen that, with the exception of HiVoSS, the various guidelines result in quite similar forcing functions. The HiVoSS forcing function is something of an outlier, with peak force amplitude much larger than those from the other guidelines. None of the guidelines has forcing functions that incorporate the random variability of walking that is observed in real human pedestrians [39] due to the “narrow band random process” of walking which has energy at all frequencies [107].

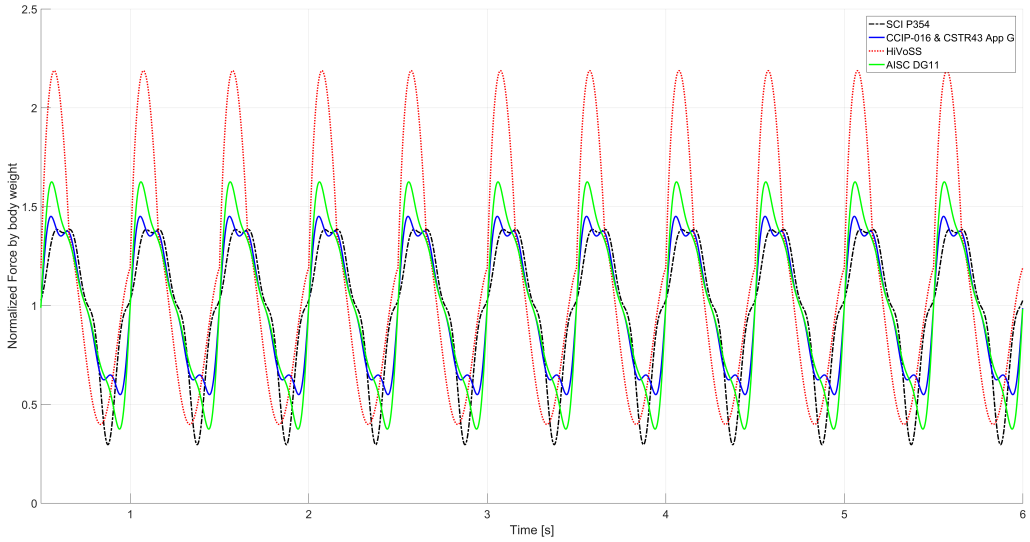

Figure 3.5: Comparison between pedestrian forcing functions.

Most of the above guidelines make a distinction between LFFs, which exhibit primarily resonant response to multiple footfalls at a pacing frequency f_p, and HFFs, which exhibit primarily a transient response to individual footfalls. However, when carrying out a detailed analysis of the performance of the CSTR43 App G guidelines, [34] highlighted that there is a 'grey region' between the LFF and HFF thresholds, where both resonant and transient responses contribute to the overall response. This implies that the cut-off frequency and separation of floors based on their fundamental natural frequency may be an unwarranted assumption [10, 34] and a universal forcing function might be a better approach. This was also examined in detail by [82], who proposed a response spectrum approach valid for both LFFs and HFFs.

To summarise the aforementioned discussion, Table 3.7 shows key similarities and differences of the guidelines:

Table 3.7: Summary of key parameters from guidelines

Guidance	Floor type	Cut-off frequency	Mode number	Pedestrian weight (N)
AISC DG11	Steel composite construction	9 Hz	LFFs up to 9 Hz HFFs up to 20 Hz	748
SCI P354	Steel composite construction	10 Hz	LFFs up to 12 Hz HFFs up to 2 × first mode	746
HiVoSS	Steel composite construction	10 Hz	modes up to 10 Hz modes up to 20 Hz	from 295 to 1225
CCIP-016	All floor construction	10.5 Hz	LFFs up to 15 Hz HFFs up to 2 × first mode	700
CSTR43 App G	All floor construction	10 Hz	LFFs up to 12 Hz HFFs up to 2 × first mode	700

3.3 Testing and FE analysis of floors

This section presents the experimental data and analytical modelling of five full-scale floors. All of these exhibited a perceptible level of vibration in service and one of these had also provoked adverse comments from occupants over the excessive vibration magnitude. The measurements were carried out by the author and members of the Vibration Engineering Section (VES). For each tested floor, a detailed FE model was developed to facilitate response prediction using methodologies from each of the aforementioned design guidelines. Experimental modal analysis (EMA) was also performed on each floor to provide experimental modal parameters, which were used to update the FE model and predict responses. The reason to tune the analytical modal properties to the measured ones was to eliminate inaccurate FE modelling as a source of error in the evaluation of vibration serviceability; therefore, the analysed floors were verified against measurement data. All modes that have been extracted from FE or EMA were unity-normalised mode shapes as per each guidelines procedure. In addition, walking response measurements were carried out during the experimental campaign to determine the actual vibration response for comparison with the numerical response predictions. Selection of a walking path (WP) for the pedestrian walking response was entirely based on the measured mode shapes so as to excite key modes along the walking path.

3.3.1 Floor Structure 1 (FS1)

3.3.1.1 Description of the floor

FS1 is a floor structure within a recently constructed multi-storey office building, which has an open-plan layout. The details of this floor were presented in detail by [38] and are summarised here for completeness. The floors are of steel-concrete composite construction, within a steel building frame of irregular geometry. Primary beams (girders) have spans of up to 10 m, secondary beams (beams) are at 3 m spacing with spans up to 13 m and steel columns lie roughly on a typical grid of 13 m $\times$ 9 m, as shown in Figure 3.6. Also, there was a full height partition wall shown in brown colour in Figure 3.6, while the rest of the floor was open-plan layout.

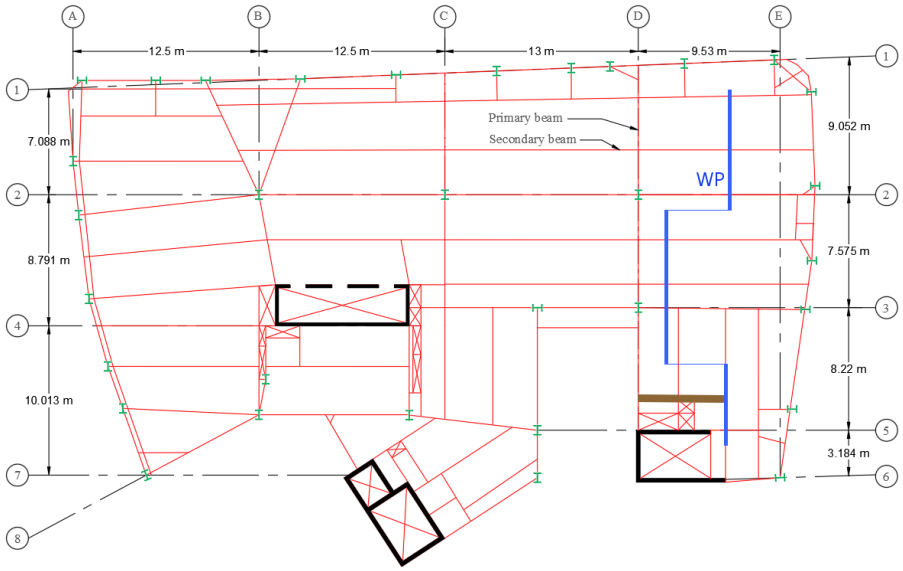

Figure 3.6: Plan layout of FS1.

Construction drawings were used to determine the size of structural members. 130 mm thick light-weight concrete is poured upon 60 mm trapezoidal steel profile decking to form the floor slab, which acts compositely with the secondary beams. Details of the structural elements vary due to the irregular geometry, but in a typical bay secondary beams are cellular with asymmetric form. The section sizes are lower tee 610×229×113 UB and upper tee 457×191×89 UB, with hole diameter of 500 mm at 750 mm centres. Primary beams are 792×191/229×101 ACB sections and column members are 254×254×73 UC. There are three reinforced concrete core walls to provide lateral resistance to the whole structure; these have been included in the FE model due to their significant effect on the structural modes.

3.3.1.2 Experimental modal analysis (EMA)

Experimental modal properties of the floor were determined from in-situ modal testing using multi-reference uncorrelated random excitation from four APS Dynamics shakers (2× APS113 and 2× APS400). A test grid of roving accelerometers (Honeywell QA750) was used with 65 test points (TPs), as shown in Figure 3.7. The modal testing was carried out (by members of VES) using continuous uncorrelated random excitation at shaker locations (i.e. multi-input multi-output modal testing). Time domain data blocks were 20 s in length giving a frequency resolution of 0.05 Hz at a sampling rate of 204.8 Hz. A total of 100 averages was used with 75% overlap and Hanning window was applied to all data blocks.

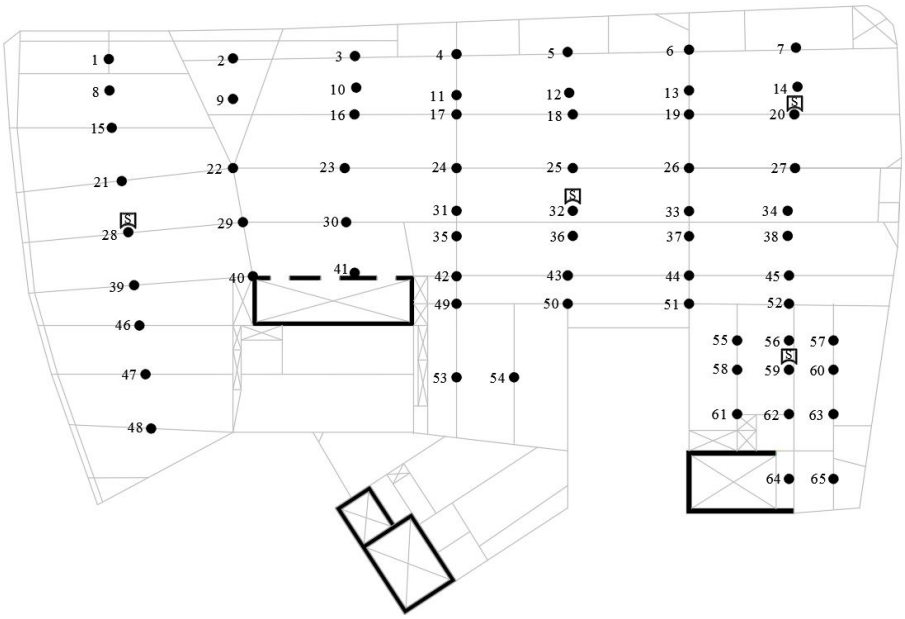

Figure 3.7: TPs locations on FS1. Excitation locations are shown by letter “S”.

Frequency response functions (FRFs) were acquired using a Data Physics Mobilyzer DP730 digital spectrum analyser, and polyreference FRF curve fitting was utilised to determine the experimental modal properties. The ME’scope [137] suite of modal parameter estimation software was used by the author to extract modal properties using a multi-polynomial method to provide reliable estimates of mode frequency, damping, shape and modal mass.

3.3.1.3 Development of FE model and analysis

The structural members were modelled in ANSYS. The composite steel-concrete floor was modelled using SHELL181 element, which is a four-node element with six degrees of freedom at each node. Orthotropic properties were assumed (flexural stiffness in the direction of the ribs is higher than the perpendicular direction).

Beams and columns were modelled using BEAM188 element, which is a two-node element with six degrees of freedom at each node. The composite action between the beams and slabs was modelled through a vertical offset of the shell element as recommended in the design guidelines [6, 7]. The concrete core walls were modelled as SHELL181 elements. The modulus of elasticity (E) of 22 GPa for light-weight concrete and density of 1800 kg/m^3 were assumed [32]. Following current practice and guidelines, one storey level of the building was modelled including top and bottom columns at a storey height of 4 m. Also, boundary conditions were assumed fixed at the end of columns. A modal analysis was carried out to obtain modal frequencies, mode shapes and modal masses.

Updating the FE model using manual tuning was conducted by introducing a full height partition wall modelled using SHELL181 elements with assumed E of 5 GPa and density of 2500 kg/m^3 as presented above. Also, sensitivity analysis was conducted to obtain the most appropriate parameters of E and density of both concrete and steel. After modal updating, the final values that gave a close match to the measured modes were 24 GPa and 210 GPa for E of concrete and steel, respectively. Material density of steel was 7830 kg/m^3 and concrete 1800 kg/m^3, as determined from the literature. The final results after tuning are shown in Figure 3.8. Numerical FRF plots were also produced to compare and reconcile with those from the measured data, as demonstrated in Figure 3.9. To generate these FRF plots, a level of damping ratio had to be assumed. The value chosen for this floor was an average of 2.4% based on measurement for all modes. It is apparent that, despite matching the mode shapes quite well (see Figure 3.8), the FE FRF does not match very well with the measured FRF. However, the modal assurance criterion (MAC), shown in Table 3.8, exhibits a good consistency. This might be associated with some of the difficulties related to modelling civil engineering floor structures, where uncertainty in modelling parameters may affect the accuracy of the FE model.

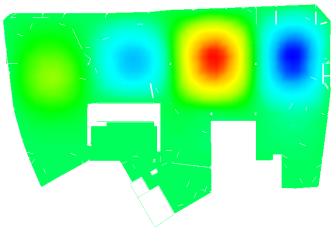

(a) FE analysis, f_1 = 5.23 Hz, m_1 = 36.02 tonnes

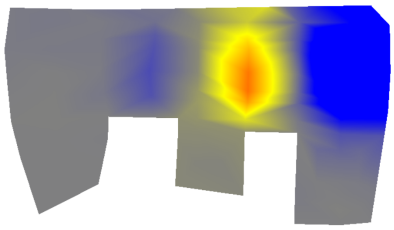

(b) EMA f_1 = 5.24 Hz, ζ_1 = 3.16 %, m_1 = 36.98 tonnes

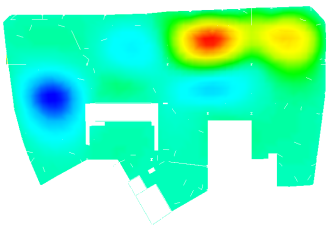

(c) FE analysis, f_2 = 6.52 Hz, m_2 = 28.54 tonnes

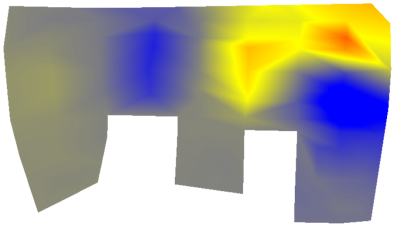

(d) EMA f_2 = 6.06 Hz, ζ_2 = 2.24 %, m_2 = 55.89 tonnes

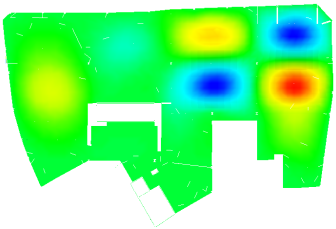

(e) FE analysis, f_3 = 6.33 Hz, m_3 = 35.95 tonnes

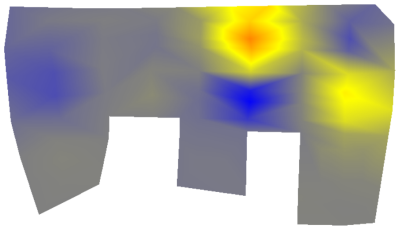

(f) EMA f_3 = 6.58 Hz, ζ_3 = 1.87 %, m_3 = 40.48 tonnes

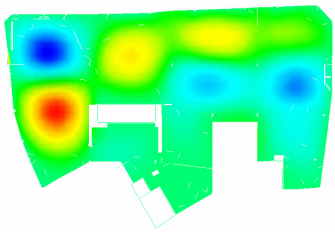

(g) FE analysis, f_4 = 6.87 Hz, m_4 = 39.95 tonnes

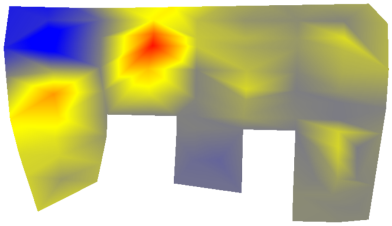

(h) EMA f_4 = 7.31 Hz, ζ_4 = 1.7 %, m_4 = 38.44 tonnes

Figure 3.8: FS1 vibration modes from FE Analysis and EMA.

Table 3.8: MAC values FS1

		Analytical			
	Mode No.	1	2	3	4
Measured	1	0.9013	0.1214	0.0245	0.1167
	2	0.2162	0.8721	0.027	0.1088
	3	0.026	0.191	0.912	0.16
	4	0.2383	0.1071	0.132	0.8899

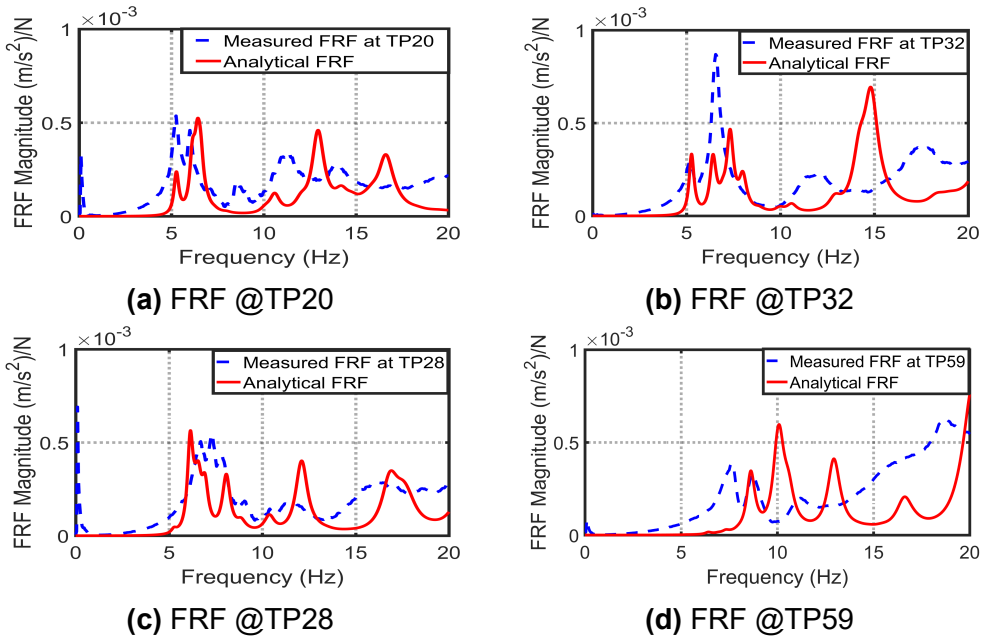

(a) FRF @TP20 **(b)** FRF @TP32

(c) FRF @TP28 **(d)** FRF @TP59

Figure 3.9: Comparison of experimental FRFs and those from the updated FE model at four locations on FS1.

3.3.2 Floor Structure 2 (FS2)

3.3.2.1 Description of the floor

This is the second case-study floor, which has the longest span of all case studies. This floor was tested at its bare stage (construction stage). It is a steel-concrete composite floor with normal weight concrete poured into a 51 mm trapezoidal steel profile decking slab, which forms a total thickness of 130 mm. Secondary beams span 15 m at a spacing of 3.125 m. The primary beams have a span of 6.25 m. The columns are situated at the intersection of beams, with typical bay sizes of 15 m × 6.25 m, as shown in Figure 3.10. Details of the structural elements in a typical bay are; secondary beams are cellular section sizes 720.5×152/229×81 UB, with hole diameter of 500 mm at 750 mm centres. Primary beams are 762×267×134 UB and column members are 305×305×158 UC. There are two reinforced concrete walls with 300 mm thickness for lateral resistance. In addition, there were lateral bracing members available on gridline F1-F3, O3-O5 and T5-U8 as well as masonry concrete blocks were placed beneath the perimeter of the floor. The discontinuous columns shown in Figure 3.10 represent three columns where the top floor supported by these columns were not completed during the testing.

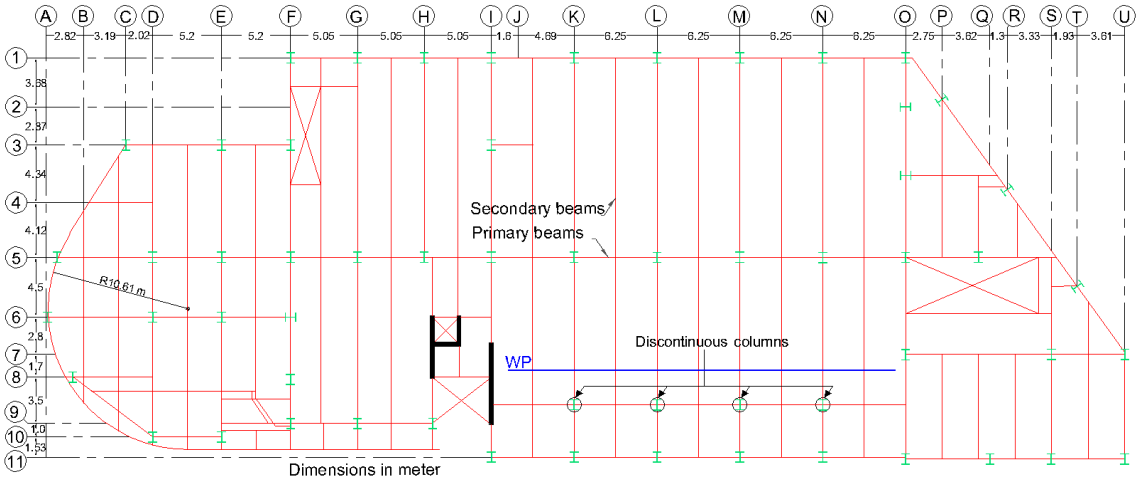

Figure 3.10: Plan layout of FS2.

3.3.2.2 Experimental modal analysis (EMA)

A modal test was performed (by members of VES) using two APS Dynamics Model 400 electrodynamic shakers as excitation sources. The structural response was measured using Honeywell accelerometers (model QA750). Digital data acquisition was performed using a portal spectrum analyzer model Data Physics DP730, similar to FS1. The shakers were driven with statistically uncorrelated random signals so that FRFs corresponding with the individual shakers could be evaluated. The force and vibration response data were sampled using a baseband setting of 40 Hz on the spectrum analyser, corresponding with a sampling rate of 102.4 Hz. Each data acquisition window was 20 s in length. For each FRF estimation, a total of 80 acquisitions were made using the Hanning window and 75% overlap, which were averaged to estimate the FRFs. The analyzer provides immediate calculation of the FRFs so that the quality of measurement data can be checked during the test. The measurements were acquired over a test grid of 93 test points, as shown in Figure 3.11. These test points were utilised to acquire the modal properties between gridelines F and O. Similar to FS1, the ME'scope [137] suite of modal parameter estimation software was used by the author to extract the modal properties.

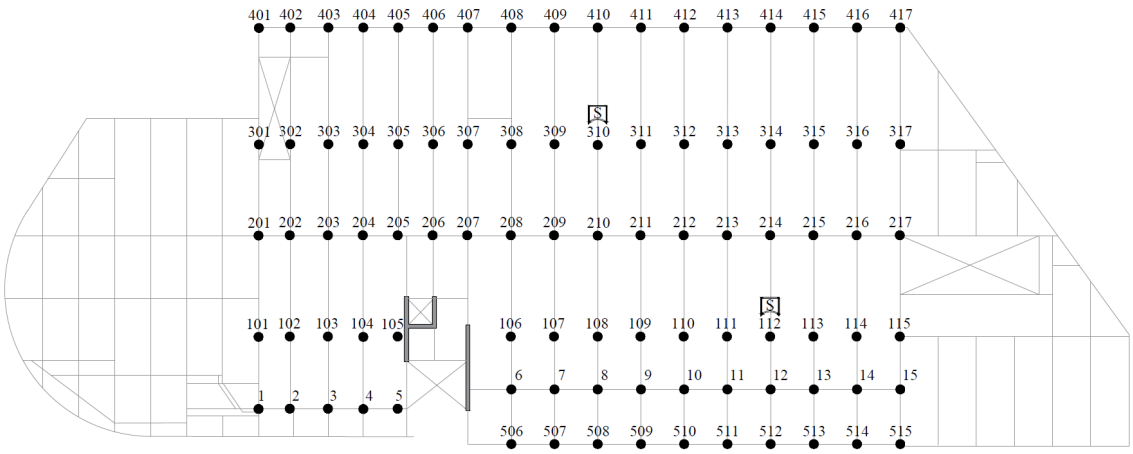

Figure 3.11: TPs locations on FS2. Excitation locations are shown by letter “S”.

3.3.2.3 FE analysis

The ANSYS FE software was utilised to model all components of the floor structure. Orthotropic properties were applied to the SHELL181 elements to model the floor slab with vertical offset to incorporate composite action. All beams and columns were modelled as BEAM188 with both their ends assumed to have rigid connections [6]. Due to the construction stage and uncompleted top floor (there was only steel deck and partial beam members with no concrete), COMBIN40 was used to model the vertical constraint of “discontinuous columns” in Figure 3.10. COMBIN40 is a single degree of freedom (SDOF) mass/spring element in ANSYS, which mass (M) and stiffness (K) were assigned. Since there was no concrete at that floor, COMBIN40 tends to behave as a connection for top columns during modal analysis. Similarly, a single storey level was modelled including top and bottom columns at a storey height of 3.5 m using fixed boundary conditions at the end of vertical members.

The initial model required a number of updating iterations to reconcile with the measured modal analysis and hence manual model updating was conducted for global parameters. The parameters updated were E and density of concrete and steel, COMBIN40 properties, lateral bracing members and partition wall installed beneath the exterior frame. After modal updating, the final values that gave a good reconciliation with measured modes were 37 GPa and 210 GPa for E of concrete and steel, respectively. The material density of steel was 7830 kg/m^3 and that of concrete was 2300 kg/m^3. Masonry concrete block beneath the perimeter of the floor of 150 mm thick with E of 22 GPa and density of 2000 kg/m^3 were assumed. COMBIN40 parameters were K=12500 N/m and M=15000 kg. It is worth noting that partition walls beneath the exterior frame had a significant effect on the mode sequences and family of modes; therefore, their modelling improved significantly the FE model. Predicted modal frequencies and mode shapes after

tuning are illustrated in Figure 3.12. Average damping ratio of 0.8% was used for FRF generation based on the measurements. Numerical and experimental FRFs are shown in Figure 3.13. It is obvious that there is a good matching between the two FRFs, albeit with some inconsistencies. Also, the modal assurance criterion (MAC), presented in Table 3.9, exhibits a good consistency; this indicates the FE model is comparably reconciled with the experimental data.

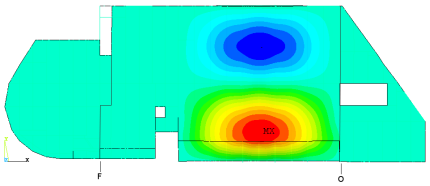

(a) FE analysis, f_1 = 4.88 Hz, m_1 = 85.15 tonnes

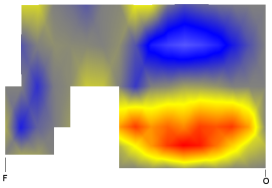

(b) EMA f_1 = 4.92 Hz, ζ_1 = 0.66 %, m_1 = 102.03 tonnes

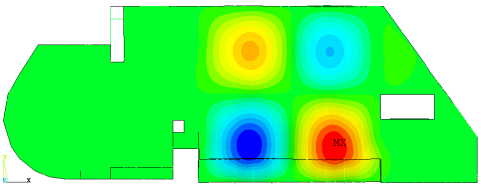

(c) FE analysis, f_2 = 5.43 Hz, m_2 = 92.89 tonnes

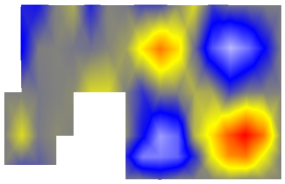

(d) EMA f_2 = 5.51 Hz, ζ_2 = 0.74 %, m_2 = 97.66 tonnes

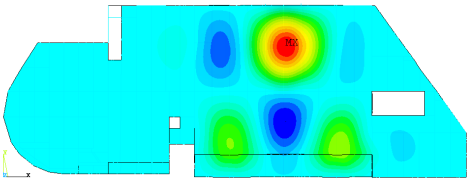

(e) FE analysis, f_3 = 6.41 Hz, m_3 = 32.02 tonnes

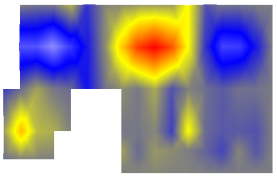

(f) EMA f_3 = 6.12 Hz, ζ_3 = 0.32 %, m_3 = 49.16 tonnes

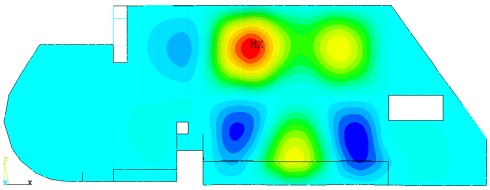

(g) FE analysis, f_4 = 6.48 Hz, m_4 = 33 tonnes

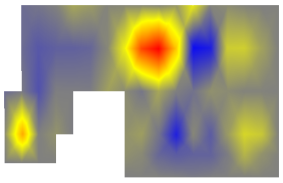

(h) EMA f_4 = 6.55 Hz, ζ_4 = 0.32 %, m_4 = 57.78 tonnes

Figure 3.12: FS2 vibration modes from FE Analysis and EMA.

Table 3.9: MAC values FS2

		Analytical			
	Mode No.	1	2	3	4
Measured	1	0.989	0.0752	0.0912	0.0599
	2	0.0313	0.942	0.0951	0.099
	3	0.0959	0.0868	0.939	0.142
	4	0.0677	0.107	0.129	0.9125

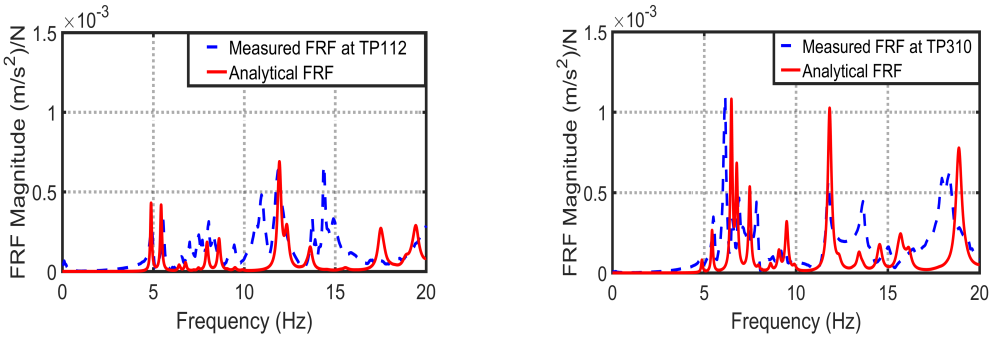

(a) FRF @TP112 **(b)** FRF @TP310

Figure 3.13: Comparison of experimental FRFs and those from the updated FE model at two locations on FS2.

3.3.3 Floor Structure 3 (FS3)

3.3.3.1 Description of the floor

This test structure is the second floor in a four-storey multi-purpose building. It is fully furnished composite steel and concrete floor spanning 9.754 m in the direction of secondary beams between gridlines H to C and 6.09 m in the direction of primary beams between gridlines 24 to 30 (Figure 3.14). Steel decking supports the in-situ cast normal weight concrete slab, which spans in the direction orthogonal to the secondary beams. At the time of testing, mechanical services and raised flooring were mounted beneath and on top the floor. The slab thickness varied from 150 mm to 200 mm due to refurbishments. The shaded area in Figure 3.14 indicates an area which was originally intended to be a swimming pool, but was never used for this purpose. In this area the slab thickness is 200 mm and there is additional mass loading from demolished partition walls that were used bring the floor surface up to the same level as the rest of the floor.

Secondary beams in a typical bay are 457×152×60 UB, whereas primary beams are 533×210×92 UB. Column members are 254×254×89 UC and bracing members are 193.7×12.5 CHS. Lateral stiffness is provided by the bracing members along the edges of the structure.

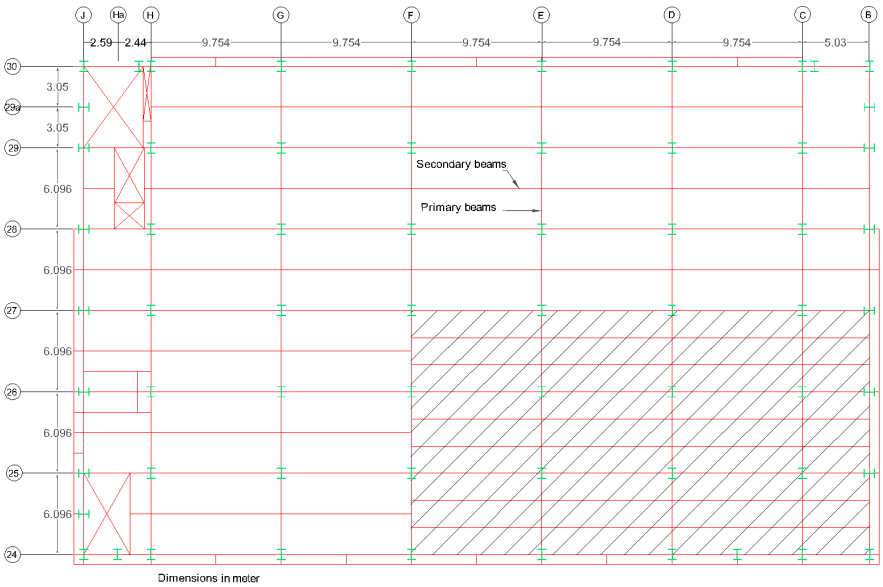

Figure 3.14: Plan layout of FS3.

3.3.3.2 Experimental modal analysis (EMA)

Natural modes were estimated for this floor (by members of VES) using EMA with four electrodynamic shakers and an array of response accelerometers in the same way as described for FS1. FRF measurements were made over a test grid of 81 points, as shown in Figure 3.15, using a portable spectrum analyzer. Similar to the previous floors, the shakers were driven with statistically uncorrelated random signals. The force and vibration response data were sampled using a baseband setting of 20 Hz on the spectrum analyser, corresponding with a sampling rate of 51.2 Hz. Each data acquisition window was 40 s in length. A total of 40 acquisitions were made using the Hanning window and 75% overlap. To estimate modal properties curve fitting of the FRF data was carried out by the author using the ME'scope [137] parameter estimation software. In-service monitoring was carried out on this floor for a duration of 12 hours under normal operation, which provided the actual vibration performance of the floor.

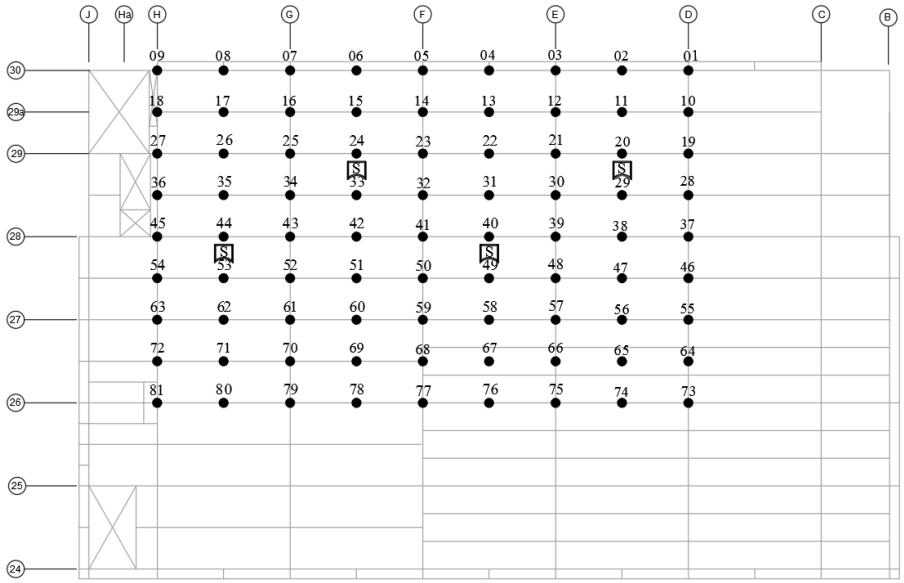

Figure 3.15: TPs locations on FS3. Excitation locations are shown by letter “S”.

3.3.3.3 FE analysis

Model of the structure was developed in the ANSYS FE software. Floors were modelled using SHELL181 elements, whereas beams and columns were modeled using BEAM188 elements. Orthotropic properties were assumed for the floors. The shaded area in Figure 3.14 was modeled using SOLID165 elements, which is an element to model volumes and it is used for the volume of the additional mass of the intended swimming pool. As mentioned for FS1 and FS2, a single storey was modelled and columns were fixed for top and bottom at a height of 4 m.

Initial modelling did not result in good matching and as such the top floor together with some substantial full height partition walls, were added to the model. This led to a better matching of mode shapes in terms of frequency and mode sequences, as shown in Figure 3.16. Similar to the two previous case-study floors, manual updating was used to update the FE model. The updating process progressed by altering floor material properties such as density and E, as well as properties related to the partition walls. The model resulted in closely-spaced modes due to repetitive geometry and orthotropic properties, which is expected in floors [41]. The final results after tuning for modal frequencies and mode shapes are shown in Figure 3.16. The FE mode shapes shown are for the considered floor and top level floor is excluded, for illustration purposes. FRF plots were generated from FE modelling to display the matching trend with experimental data at shaker points. Figure 3.17 shows the analytical and experimental FRFs at four shaker locations. Average damping ratio of 1.2% was used based on the measurements. The MAC values in Table 3.10 show to an extent a good match and

the analytical FRF plots seem to correlate with those of measurements and thus the FE model appears to be in agreement with the EMA. This is a clear indication of the need to include partition walls and top floors in the model when carrying out evaluation of vibration responses.

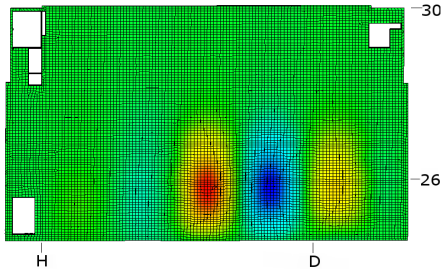

(a) FE analysis, f_1 = 6.57 Hz, m_1 = 114.6 tonnes

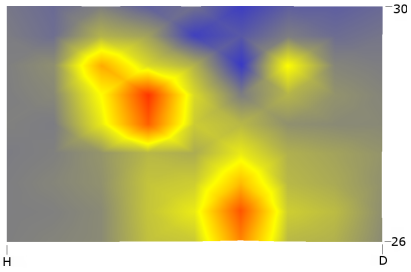

(b) EMA f_1 = 6.56 Hz, ζ_1 = 1.0 %, m_1 = 93.5 tonnes

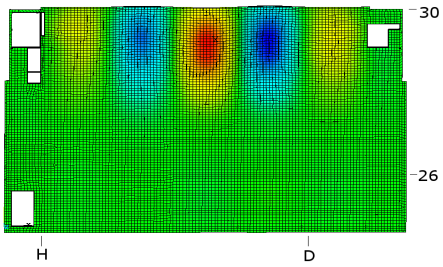

(c) FE analysis, f_2 = 6.84 Hz, m_2 = 96.15 tonnes,

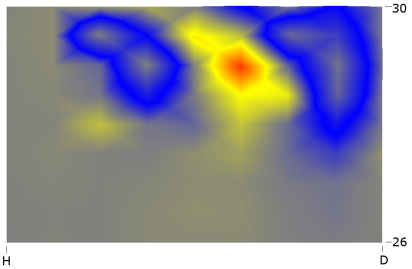

(d) EMA f_2 = 6.89 Hz, ζ_2 = 1.04 %, m_2 = 89.64 tonnes

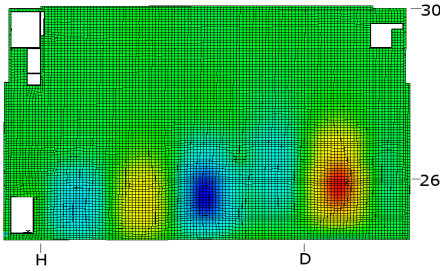

(e) FE analysis, f_3 = 7.23 Hz, m_3 = 104.13 tonnes

Mode not measured

(f) EMA f_3 = NA, ζ_3 = NA %, m_3 = NA

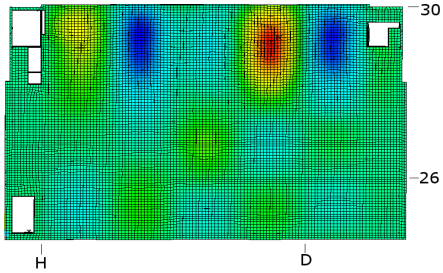

(g) FE analysis, f_4 = 7.4 Hz, m_4 = 104.53 tonnes

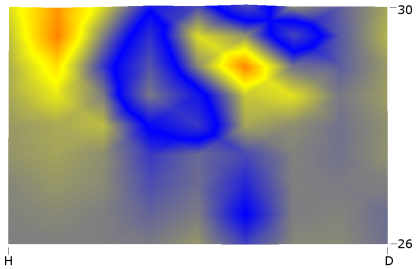

(h) EMA f_4 = 7.39 Hz, ζ_4 = 0.62 %, m_4 = 98.9 tonnes

Figure 3.16: FS3 vibration modes from FE Analysis and EMA.

Table 3.10: MAC values FS3

		Analytical			
	Mode No.	1	2	3	4
Measured	1	0.88	0.117	0	0.129
	2	0.195	0.851		0.282
	3	0	0	0	0
	4	0.142	0.228	0	0.879

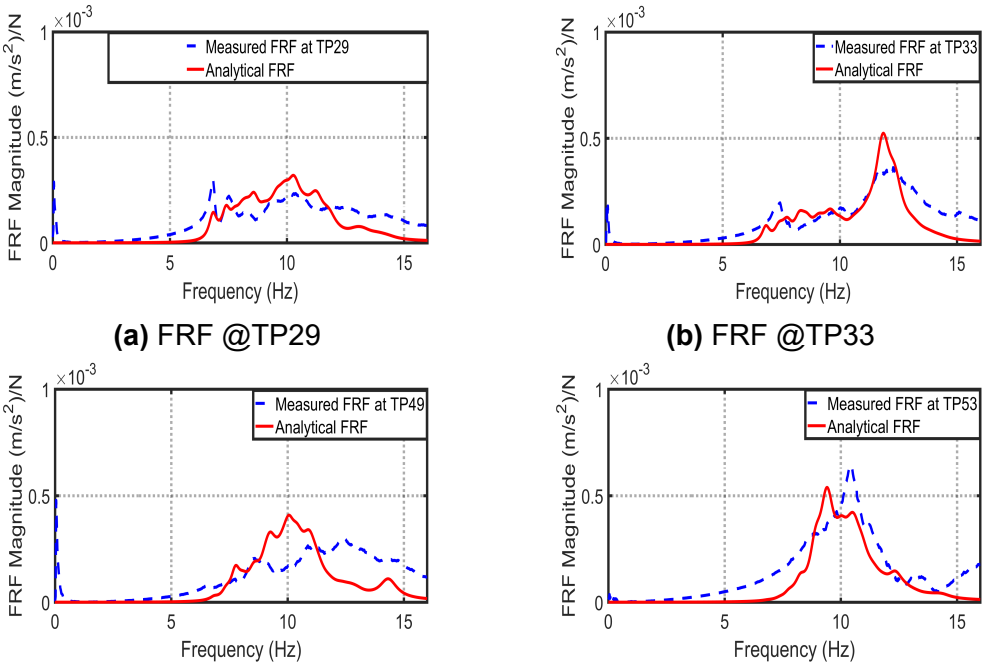

(a) FRF @TP29 **(b)** FRF @TP33

(c) FRF @TP49 **(d)** FRF @TP53

Figure 3.17: Comparison of experimental FRFs and those from the updated FE model at four locations on FS3.

3.3.4 Floor Structure 4 (FS4)

3.3.4.1 Description of the floor

This floor structure is an office floor located on the first level of a three-storey building, which comprises timber joists spanning between steel beams. Masonry brick walls and steel columns are the main vertical structural elements in the frame. The floor is an open-plan office space with a typical layout, as illustrated in Figure 3.18. There were no construction drawings, i.e. structural member details, available. This makes developing FE model quite difficult and as such the measured modal model will be used for response predictions.

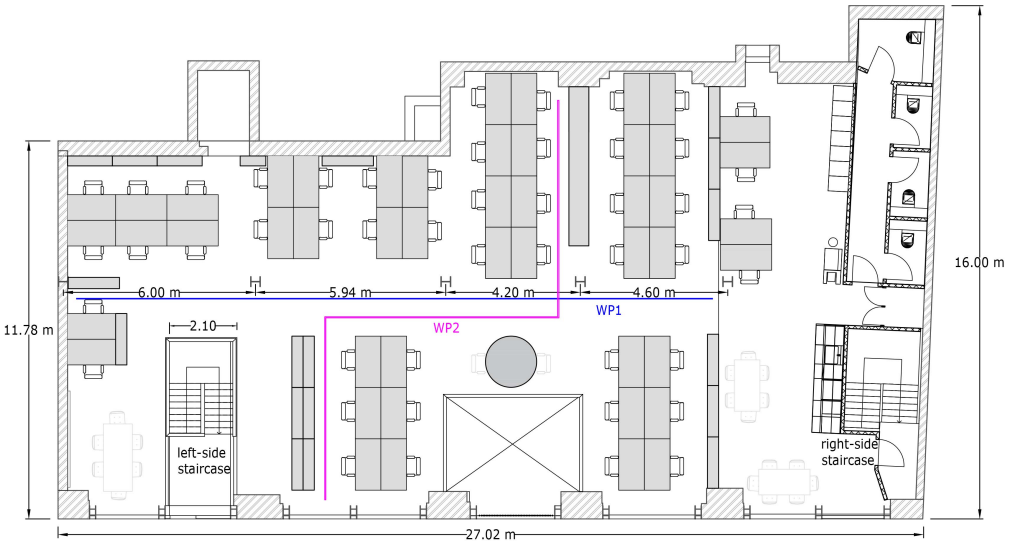

Figure 3.18: Plan layout of FS4.

3.3.4.2 Experimental modal analysis (EMA)

A modal test was performed by the author, with assistance from members of VES, using three APS Dynamics shakers (2 × APS400 and 1 × APS113) as excitation sources. The structural response was measured using array of response accelerometers (model Honeywell QA750). Digital data acquisition was performed using a portal spectrum analyser model Data Physics DP730. The floor was excited using uncorrelated random excitation between 0-80 Hz, yielding a sampling rate of 204.8 Hz. 50 averages of 40 s duration giving a frequency resolution of 0.025 Hz were used with the Hanning window and 75% overlap. The analyser provides immediate calculation of the FRFs so that the quality of measurement data can be checked during the test. The measurements were acquired over a test grid of 64 test points, as shown in Figure 3.19. These test points were utilised to acquire the modal properties over the majority of the floor area. The ME'scope parameter estimation software [137] was used by the author to estimate modal properties by carrying out curve fitting of the measured FRF data.

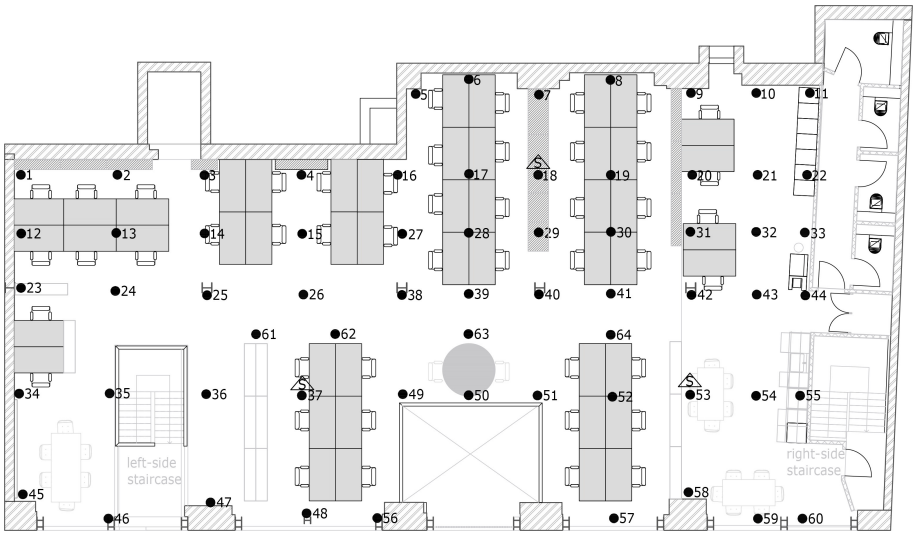

Figure 3.19: TPs locations on FS4. Excitation locations are shown by letter “S”.

The EMA modes, natural frequencies, damping ratios and modal masses extracted from the measurements are shown in Figure 3.20.

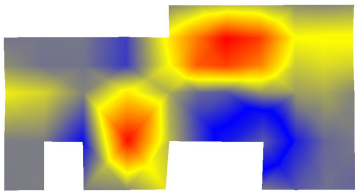

(a) EMA f_1 = 7.62 Hz, ζ_1 = 4.03 %, m_1 = 23.24 tonnes

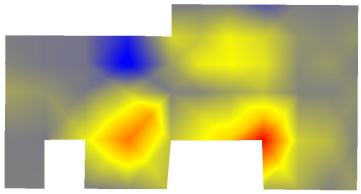

(b) EMA f_2 = 8.62 Hz, ζ_2 = 2.84 %, m_2 = 19.33 tonnes

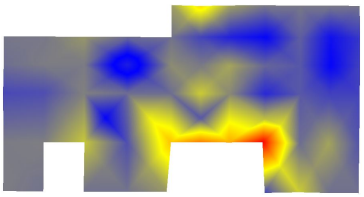

(c) EMA f_3 = 12.2 Hz, ζ_3 = 3.1 %, m_3 = 13.25 tonnes

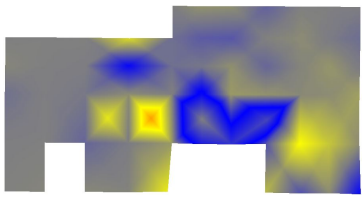

(d) EMA f_4 = 13.4 Hz, ζ_4 = 4.33 %, m_4 = 16.79 tonnes

Figure 3.20: FS4 vibration modes from EMA.

3.3.5 Floor Structure 5 (FS5)

3.3.5.1 Description of the floor

This floor is the seventh level of a recently constructed multi-storey office building. Light-weight concrete was poured into 280 mm deep slab with Comflor 210/1.2 mm profile decking to form a composite steel-concrete floor structure. Beams have spans of up to approximately 7.47 m. The columns are situated at the intersections of beams, with typical bay sizes of 7.47 m × 4.88 m, as shown in Figure 3.21. Details of the structural elements in a typical bay are; beams are

cellular section sizes 298×254/368×130.5 USFB, with hole diameter of 140 mm at 300 mm centres. Column members are 203×203×86 UC. There are three reinforced concrete walls/cores with 225 mm thickness for lateral resistance. Also, external curtain walls are EWS-101 series double-glazed cladding.

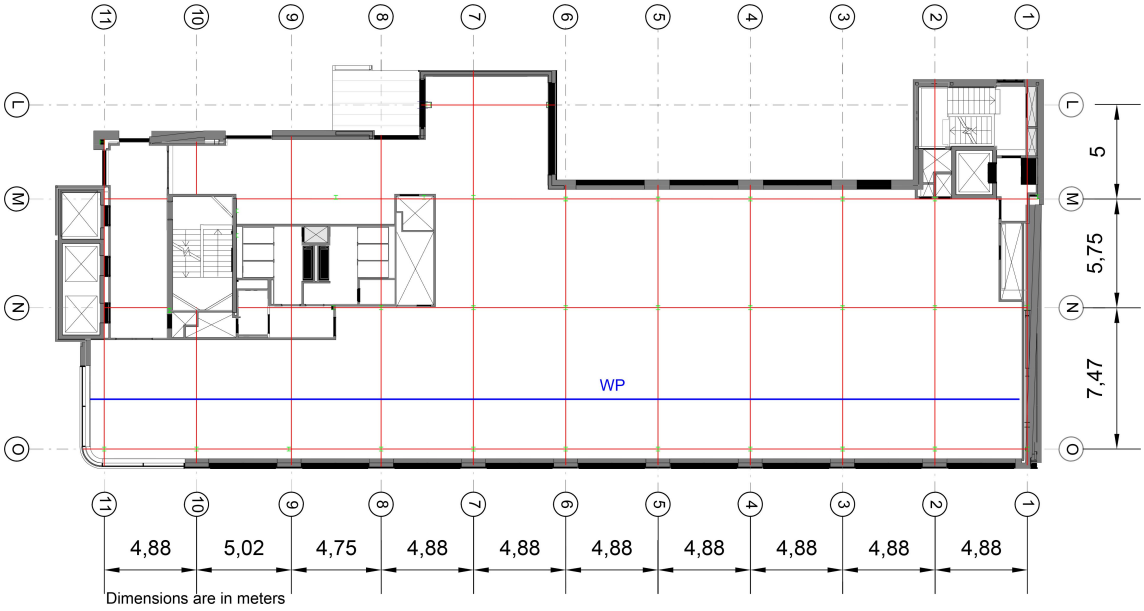

Figure 3.21: Plan layout of FS5.

3.3.5.2 Experimental modal analysis (EMA)

The floor structure was tested by the author, with assistance from members of VES, at two different stages; at construction stage prior to installing external walls and at completion stage just before fit-out. Results of the latter will be presented since it is most pertinent to this study. Experimental modal properties of the floor were obtained from modal testing utilising multi-reference uncorrelated random excitation from three APS Dynamics shakers (1× APS113 and 2× APS400) and a test grid of roving Honeywell QA750 accelerometers, as shown in Figure 3.22. The force and vibration response data were sampled at using a baseband setting of 80 Hz, corresponding with a sampling rate of 204.8 Hz. 100 averages with acquisition window of 40 s were made using the Hanning window and 75% overlap. Data Physics Mobilyzer DP730 digital spectrum analyser was used to acquire FRFs. The ME'scope software package [137] of modal parameter estimation was used by the author to extract modal properties using a multi-polynomial method to provide reliable estimates of mode frequency, damping, shape and modal mass. The final mode shape results are shown in Figure 3.23.

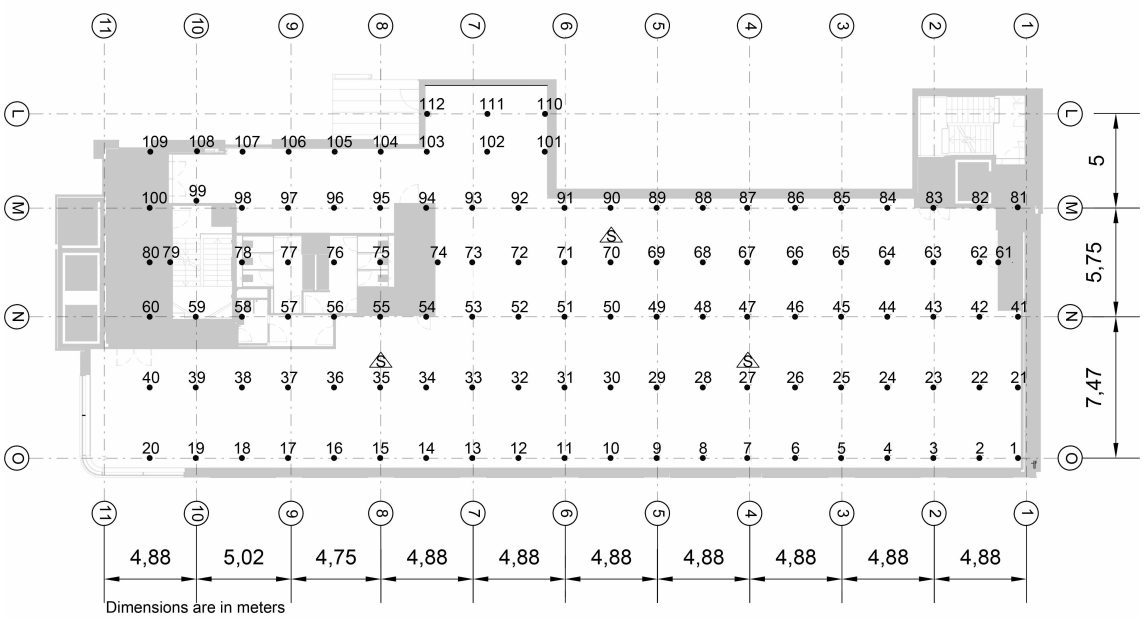

Figure 3.22: TPs locations on FS5. Excitation locations are shown by letter “S”.

3.3.5.3 FE analysis

An FE model of the structural system was developed using the ANSYS FE software. Beams and columns were modelled using BEAM188 elements. The composite steel-concrete floor was modelled using SHELL181 elements and orthotropic properties were assumed. The composite action between the beams and slabs was modelled through a vertical offset of the shell element as recommended in the design guidelines [6, 7]. The modulus of elasticity (E) of 24 GPa for light-weight concrete and density of 1500 kg/m^3 were assumed [7]. In a similar way, a single storey level with all vertical members, top and bottom, at a height of 4 m was modelled using fixed boundary conditions. Modal properties (modal frequencies, mode shapes and modal masses) were obtained via modal analysis.

The FE modal was further improved by introducing full height partition walls around grid line N7-N10 to M7-M10 and external cladding walls. This model is to show a realistic FE model that would be developed by an engineer. This was carried out as discussed in aforementioned floors, since the walls have an effect on mode shapes and their sequences. The walls were modelled as SHELL181 element. Partition walls of 110 mm thick with E of 2.1 GPa and density of 800 kg/m^3 and external cladding walls of 200 mm with E of 10 GPa and density of 2400 kg/m^3 were used as per construction details. The final results are shown in Figure 3.23.

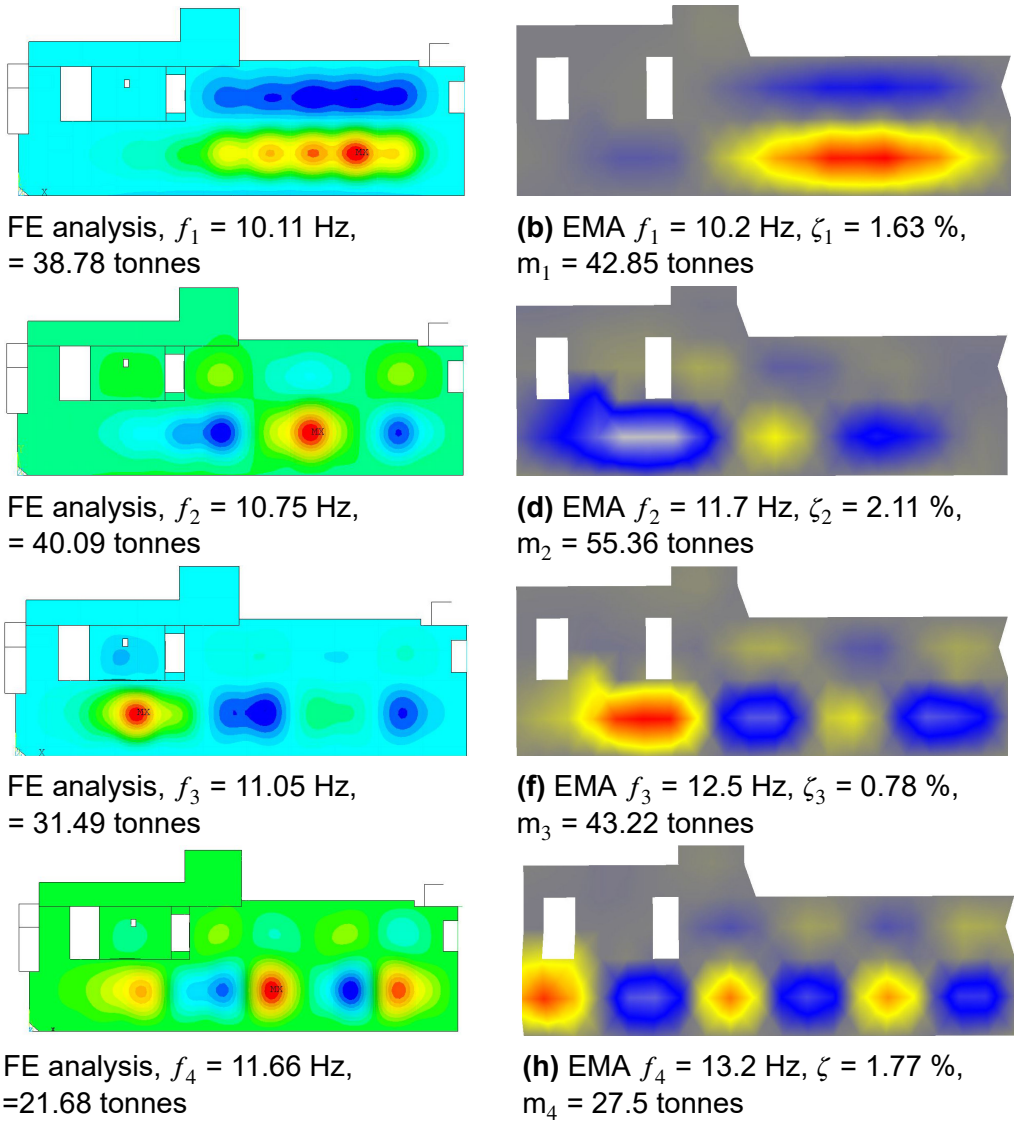

(a) FE analysis, f_1 = 10.11 Hz, m_1 = 38.78 tonnes

(b) EMA f_1 = 10.2 Hz, ζ_1 = 1.63 %, m_1 = 42.85 tonnes

(c) FE analysis, f_2 = 10.75 Hz, m_2 = 40.09 tonnes

(d) EMA f_2 = 11.7 Hz, ζ_2 = 2.11 %, m_2 = 55.36 tonnes

(e) FE analysis, f_3 = 11.05 Hz, m_3 = 31.49 tonnes

(f) EMA f_3 = 12.5 Hz, ζ_3 = 0.78 %, m_3 = 43.22 tonnes

(g) FE analysis, f_4 = 11.66 Hz, m_4 =21.68 tonnes

(h) EMA f_4 = 13.2 Hz, ζ = 1.77 %, m_4 = 27.5 tonnes

Figure 3.23: FS5 vibration modes from FE Analysis and EMA.

The MAC values in Table 3.11 show to an extent a good match and thus the FE model seems to correlate with those of measurements. As stated in earlier models that there is a need to include partition walls and claddings in the FE model when carrying out evaluation of vibration responses. It is worth noting that FRF plots were not generated for this model since MAC values provided a good correlation.

Table 3.11: MAC values FS5

		Analytical			
	Mode No.	1	2	3	4
Measured	1	0.98	0.0552	0.0622	0.09
	2	0.0223	0.932	0.101	0.0723
	3	0.0556	0.0372	0.964	0.133
	4	0.0367	0.097	0.123	0.901

3.4 Evaluation of response prediction using guidelines

3.4.1 Pre-construction: Design stage

This sections presents the evaluation of response using each of the guidelines to calculate modal properties, vibration responses and applying the recommended evaluation procedures.

3.4.1.1 Modal properties estimation

- **FS1:** FS1 has an irregular plan configuration except for a few bays, to which the simplified formulae of the guidance are applicable. Hence, modal properties are determined for floor gridline C2-D3 (see Figure 3.6). Methodologies and simplified equations or recommended values provided by each guideline are utilized to estimate the dynamic properties shown in Table 3.12. CSTR43 App G does not provide any simplified techniques and as such formulae given in structural dynamics textbooks (e.g. [136] or [138]) can been used (see Table 3.5). Similar formulae are also applicable to the other case study floors.

Table 3.12: Modal properties of first mode of FS1 from design guidance simplified formulae

Guidance	Natural frequency (Hz)	Modal mass (t)	Damping ratio (ζ)
Measured	5.24	36.98	3.16%
AISC DG11	4.99	51	3%
SCI P354	5.23	17.47	3%
HiVoSS	5.18	15.9	3%
CCIP-016	2.89	7.95	3%
CSTR43 App G	4.52	7.95	3%

- **FS2:** Modal properties are determined for a typical floor gridline L1-M5 (see Figure 3.10), since the floor is regular and the dimensions of most bays are the same. Simplified equations and recommended values provided by each guideline are utilized to estimate the dynamic properties, shown in Table 3.13.

Table 3.13: Modal properties of first mode of FS2 from design guidance simplified formulae

Guidance	Natural frequency (Hz)	Modal mass (t)	Damping ratio (ζ)
Measured	4.92	102.03	0.66%
AISC DG11	4.48	83.6	1%
SCI P354	4.99	17.26	1.1%
HiVoSS	4.78	14.77	1%
CCIP-016	4.1	7.4	1.15%
CSTR43 App G	6.5	7.4	1%

- **FS3:** Modal properties are determined for a typical floor gridline F29-E28 (see Figure 3.14), due to regular plan of the floor. Simplified equations and recommended values provided by each guideline are utilised to estimate the dynamic properties, shown in Table 3.14.

Table 3.14: Modal properties of first mode of FS3 from design guidance simplified formula

Guidance	Natural frequency (Hz)	Modal mass (t)	Damping ratio (ζ)
Measured	6.56	93.5	1%
AISC DG11	6.03	60.8	3%
SCI P354	6.61	20.98	3%
HiVoSS	6.55	12.4	3%
CCIP-016	5.47	6.2	3%
CSTR43 App G	7.24	6.2	3%

- **FS4:** As far as simplified calculation is concerned, there were no available (structural) drawings to estimate dynamic properties for this floor. Therefore, as mentioned in Section 3.3.4.1 neither FE model nor manual calculations will be considered.

- **FS5:** Modal properties are determined for this regular floor plan, floor bay O5-N6 was chosen as a typical bay (see Figure 3.21). Simplified equations and recommended values provided by each guideline are utilised to estimate the dynamic properties, shown in Table 3.15.

Table 3.15: Modal properties of first mode of FS5 from design guidance simplified formula

Guidance	Natural frequency (Hz)	Modal mass (t)	Damping ratio (ζ)
Measured	10.2	42.85	1.63%
AISC DG11	10.3	18.1	3%
SCI P354	14.66	15.73	3%
HiVoSS	14.56	6.2	3%
CCIP-016	10.76	3.1	3%
CSTR43 App G	13.03	3.1	3%

3.4.1.2 Response prediction

Prediction of vibration responses in this chapter using measured modal properties, FE analysis and hand calculations is based on the methodology of each guideline as illustrated in Figures 3.1, 3.2, 3.3 and 3.4 and Tables 3.1, 3.2, 3.3, 3.4 and 3.5. When using FE analysis, mode coordinates are extracted for excitation and response points. Contribution of more than one mode is then combined through a mode superposition approach. The guidelines that utilise such method are SCI P354, CCIP-016 and CSTR43 App G. In the same way, measured modal properties are also used to predict vibration responses. This was done to better understand where inaccuracies occur in guidance documents.

AISC DG11 suggests using harmonic analysis as mentioned in Section 3.2.1. A wide range of FRFs was generated at different locations of excitation and response on the entire floor area. The harmonic analysis produced the maximum FRF magnitude at the middle of the floor panel of gridline B1-C2, which is used for later analysis. The FRF plots from this analysis is shown in Figure 3.24 for FS1. Measured FRFs are also used using AISC DG11 procedure to predict vibration responses. HiVoSS assumes each vibration mode from FE analysis as a SDOF and as such the response is calculated from each mode and superimposed using SRSS. In addition, HiVoSS provides charts of vibration response, where the response can be read off from a known modal properties. It is worth mentioning that none of the guidelines defines walking routes, nor do they pay attention to non-stationary nature of pedestrians, i.e. moving pedestrian. However, it is speculated to take into account the line of strongest response (maximum modal ordinates) or mode amplitudes close to, where possible, a predefined “walking path”. Such method may yield an assumption of exciting the highest mode amplitudes in order to obtain conservatively the uppermost response. It is indicated [47] that significant inaccuracies occur due to the presence of variations in walking

loads and uncorroborated assumptions in response estimation. In the following analyses the maximum modal ordinates were used to predict vibration responses as per design guidelines procedure.

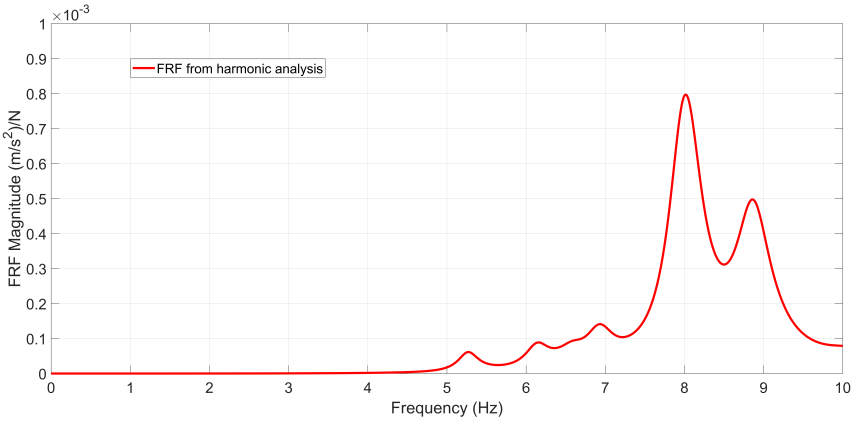

(a) FRF middle of panel gridline B1 & C2

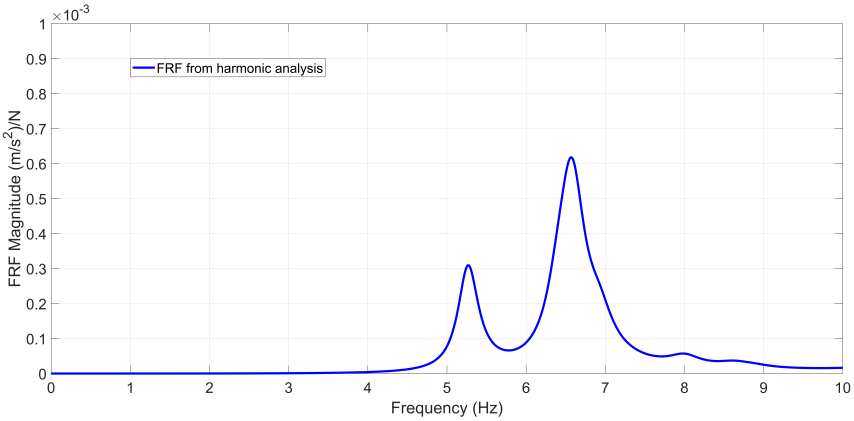

(b) FRF middle of panel gridline C1 & D2

Figure 3.24: FRF plots from FE harmonic analysis.

As far as manual calculations are concerned, the guidelines follow simple techniques to predict the vibration response. This typically includes estimating modal properties of the fundamental mode, assuming a harmonic walking load and thus predicting the response. It is worth noting that the simplified techniques can estimate accurately the modal frequency, yet an incorrect modal mass is often obtained. The vibration response can be significantly affected by such inaccuracies in modal properties and more importantly the estimation of the modal damping.

The vibration responses presented below are calculated based on the above procedure from measured modal properties, FE analysis and manual calculations for the case study floors.

- **FS1**: This is a relatively new office floor, where pedestrians use various paths during normal operations. Although floor occupants had not reported any adverse comments, perceptible vibration was obvious and thus the floor can be considered as a “borderline” case. The predicted vibration responses

following procedures in each guideline are shown in Figure 3.25. It can be seen that the predicted responses vary significantly and hence the vibration serviceability assessment can be inconclusive. In particular, use of the simplified procedures for modal parameter estimation seem to be inaccurate for estimation of floor performance. This can be seen in Table 3.16. Also, the assumption of steady state vibration response for serviceability assessment is another potential source of inaccuracy, although the measured responses can vary due to the variations in subjects' excitation and modal properties. Using measured modal properties in Table 3.16, indicate that predicted peak R factor utilising available walking load model contains large overestimations (denoted by "+" sign) as high as +67.9% in HiVoSS and underestimations (denoted by "-" sign) as low as -9.6% in SCI P354. This case study floor shows that there is a few percentage of error due to inaccurate modal properties when comparing FE calculation against measured modal properties. Reynolds and Pavic [52] remark that use of peak responses is potentially overconservative, whereas using vibration dose values or cumulative distribution of response might provide more reliable assessment.

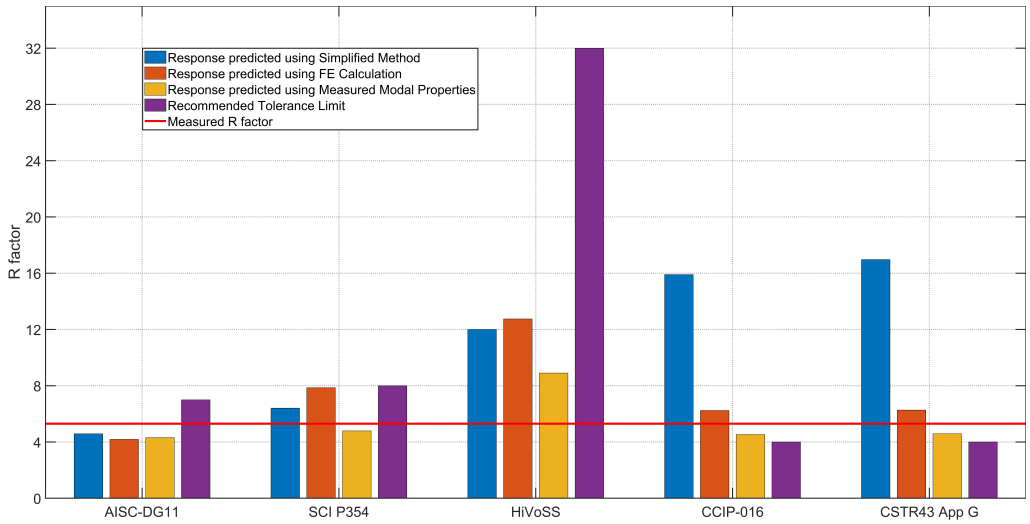

Figure 3.25: FS1 Response prediction of guidelines against actual response.

Table 3.16: FS1 percentage of error of guideline response prediction vs. actual response

Guidance	Simplified calculation	FE calculation	Measured properties calculation
AISC DG11	-13.6%	-20.9%	-18.7%
SCI P354	20.9%	48.3%	-9.6%
HiVoSS	126.4%	140.6%	67.9%
CCIP-016	200%	17.7%	-14.5%
CSTR43 App G	220%	18.3%	-13.6%

- **FS2**: This floor is a multi-purpose floor, used as a wedding venue, for meetings and as a leisure centre. During construction the floors had been reported to be highly responsive, which raised concerns of the construction contractor. The predicted vibration response compared with the measured response is shown in Figure 3.26. A good prediction is obtained via AISC DG11 methodology in terms of equivalent R factor, whereas the rest of the guidelines are dissimilar and diverse. Due to the relatively regular plan configuration, both the simplified formula and FE methodology seem to work well per AISC DG11. There are large overestimations by most guidelines, which dictate neither satisfactory or unsatisfactory condition. The percentage of error shown in Table 3.17 demonstrates that large overestimation (denoted by "+" sign) occur in the guidelines procedure even when using measured modal properties. This can provide an insight into lack of accuracy in walking models. Such discrepancies indicate the necessity for significant improvements in response prediction and tolerance limits to facilitate reliable and realistic ratings at the design stage.

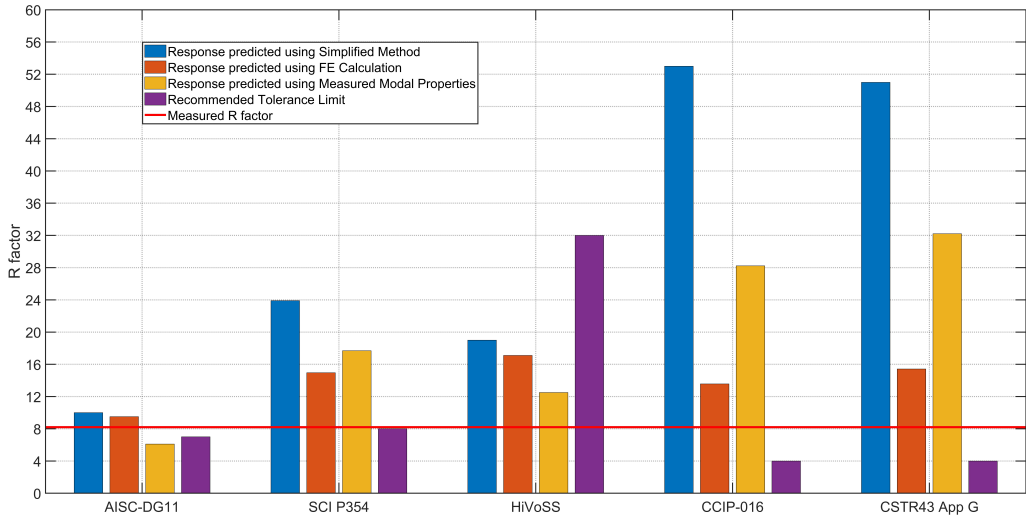

Figure 3.26: FS2 Response prediction of guidelines against actual response.

Table 3.17: FS2 percentage of error of guideline prediction vs. actual response

Guidance	Simplified calculation	FE calculation	Measured properties calculation
AISC DG11	22%	15.9%	-25.6%
SCI P354	192%	82.3%	116%
HiVoSS	132%	109%	52.4%
CCIP-016	546%	65.5%	244%
CSTR43 App G	522%	88%	293%

- **FS3**: This floor is also an office floor, which is mostly used as a library and study area. The floors had been reported to exhibit large vibration responses during in-service operation, due to the gymnasium operating on the floor above, and thus the floor occupants expressed annoyance over the magnitude of vibration. The predicted response and its measured counterpart are shown in Figure 3.27. The percentage of errors of response prediction against actual measurements are shown in Table 3.18. The significant underestimation of response observed for all guidelines is due to the difference between the loading condition assumed (i.e. single person walking) and the actual loading condition (one or more people exercising in the gymnasium above) and hence cannot be attributed to lack of performance of the guidelines. Nevertheless, this case does demonstrate an alternative loading mechanism that should be considered in buildings with multiple types of occupation.

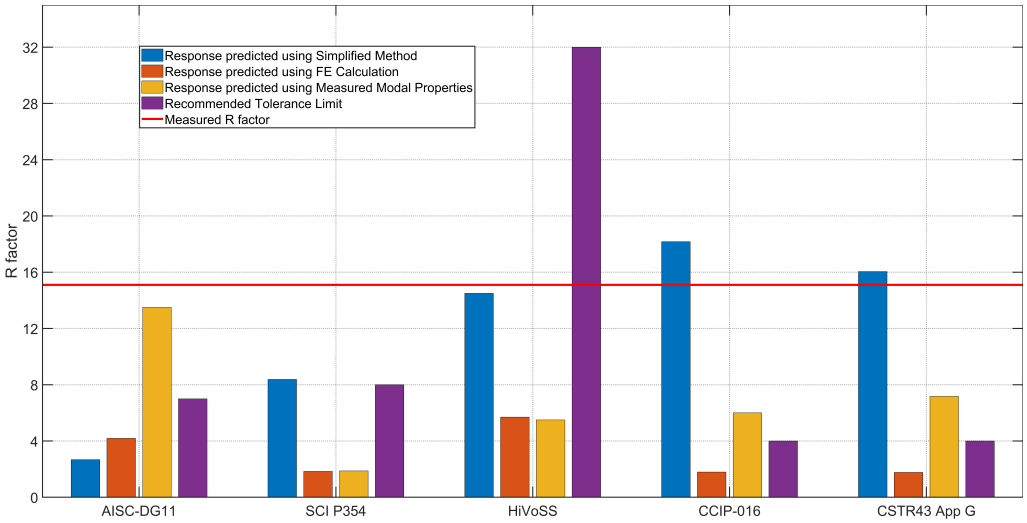

Figure 3.27: FS3 Response prediction of guidelines against actual response.

Table 3.18: FS3 percentage of error of guideline prediction vs. actual response

Guidance	Simplified calculation	FE calculation	Measured properties calculation
AISC DG11	-82.3%	-72.3%	-10.6%
SCI P354	-44.5%	-87.8%	-87.6%
HiVoSS	-4%	-62.3%	-63.6%
CCIP-016	20.3%	-88.1%	-60.3%
CSTR43 App G	6.3%	-88.3%	-52.5%

- **FS4**:This structure is an office floor that is in service. The floor is being used by a larger number of occupants and it is an open-plan floor layout. Two sets of vibration responses were measured. First set was due to a single

pedestrian walking at controlled pacing frequencies. Second set of vibration responses was due to actual in-service operation where the floor was in use by multiple occupants for a long duration. It is worth mentioning that the floor occupants had expressed annoyance over the vibration magnitude. The predicted response and its measured counterpart are shown in Figure 3.28. There is a considerable underestimation of responses by all guidelines under a single pedestrian and in-service data as it can be seen in Table 3.19, even though using measured modal properties. This can be attributed to the loading condition assumed (i.e. single person walking) and the extend to which the forcing function is limited to a few number of harmonic components. The Fourier-based models in the guidelines do not cover the wide range of spectra that is available in actual walking. Also, lack of spatial walking paths as excitation points for multiple occupants is another source of inaccuracies in design guidelines.

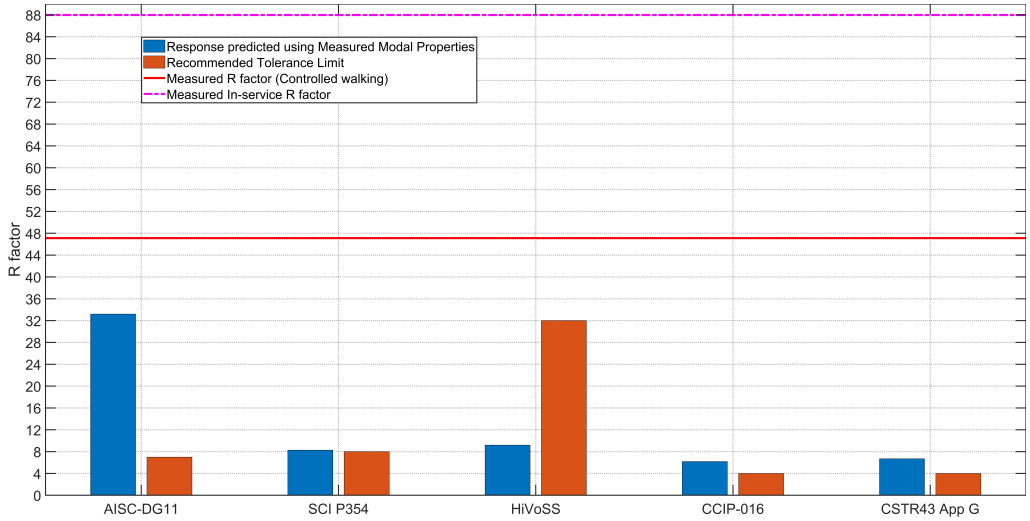

Figure 3.28: FS4 Response prediction of guidelines against actual response.

Table 3.19: FS4 percentage of error of guideline prediction vs. actual response

Guidance	Measured properties calculation: single person	Measured properties calculation: in-service
AISC DG11	-29.5%	-62.3%
SCI P354	-82.4%	-90.6%
HiVoSS	-80.5%	-89.5%
CCIP-016	-86.9%	-93%
CSTR43 App G	-85.8%	-92.4%

- **FS5**: This floor is a recently built office floor, which is not in use yet. Since this floor lies within the cut-off frequency as per guidance documents, both LFFs and HFFs methodologies were used. The maximum response from

the analysis, which was from HFFs procedure, is reported here. The predicted vibration responses following procedures in each guideline are shown in Figure 3.29. It can be seen that the predicted responses vary significantly. In particular, use of the simplified procedures for modal parameter estimation seem to be inaccurate for estimation of floor performance in some guidelines, such as HiVoSS and CCIP-016. Also, measured modal properties highlight that design procedures in some guidelines can lead to various outcomes, i.e. underestimation and overestimation results as presented in Table 3.20. However, it is worth mentioning that SCI P354 seems to have the lowest percentage of error among other guidelines. Also, the FE and measured modal properties calculations exhibit inaccuracies to a good extend due to walking models, such as AISC DG11, whereas in CCIP-016 and CSTR43 App G the inaccuracies could be due to the FE model and walking model. Hence, it can be said that there is need for a unified walking load model for a more reliable vibration serviceability assessment.

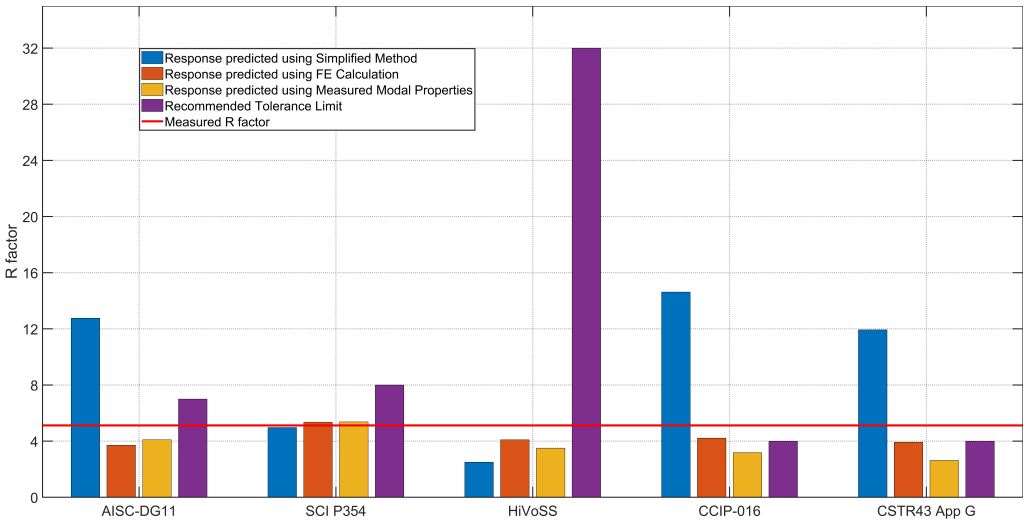

Figure 3.29: FS5 Response prediction of guidelines against actual response.

Table 3.20: FS5 percentage of error of guideline prediction vs. actual response

Guidance	Simplified calculation	FE calculation	Measured properties calculation
AISC DG11	149%	-27.5%	-20%
SCI P354	-3%	4.5%	4.9%
HiVoSS	-51.2%	-20%	-31.6%
CCIP-016	186%	-17.8%	-37.9%
CSTR43 App G	133%	-23.2%	-48.6%

3.4.1.3 Assessment criteria

- **FS1**: As indicated in Figure 3.25, this office floor has unacceptable performance according to CSTR43 App G and CCIP-016, but it is deemed satisfactory and within allowable limits (recommended floor classes in HiVoSS) with respect to AISC DG11, SCI P354 and HiVoSS. As a consequence, the assessment of the floor under walking is inconsistent.
- **FS2**: Due to the multi-functional purpose of this structure, its performance might be evaluated against a range of assessment criteria. However, in this case it is evaluated against the assessment criteria for an office floor, which is also reasonable for a meeting venue. Figure 3.26 shows the response assessed against the relevant threshold limits. It is apparent that the floor is unacceptable according to four of the guidelines, whereas it satisfies the requirements of HiVoSS for such structures.
- **FS3**: Similar to FS1, this floor is assessed under office floor requirements. It is shown in Figure 3.27 that it performs well for all guidelines. Whilst the problem with this floor was due to high levels of rhythmic excitation coming from the floor above, it can be seen that for normal office walking the floor would have been expected to perform satisfactorily. However, considering AISC DG11 procedure, the floor performance would have been unacceptable using measured modal properties. This correlated with subjective assessment made during the testing.
- **FS4**: As shown in Figure 3.28, this office floor has unacceptable performance according to all guidelines.
- **FS5**: Figure 3.29 indicated that this office floor has unacceptable performance according to CSTR43 App G and CCIP-016 FE calculations. But it is satisfactory and within allowable limits (recommended floor classes in HiVoSS) with respect to AISC DG11, SCI P354 and HiVoSS. However, the floor can be considered as satisfactory using the measured modal properties. Therefore, the assessment of the floor is not clear using binary accept-reject method.

3.4.2 Post-construction: In-service condition

- **FS1**: The actual response presented in Figure 3.25 is measured under a single person walking via the walking path (WP) in Figure 3.6. This WP was selected based on the measured mode shapes. The pedestrian weight

and height were 81 kg and 1.81 m, respectively and walked at the pacing frequency of 1.746 Hz. It is clear that this floor has a satisfactory level of vibration, despite being perceptible. The actual vibration response (red line) corresponds to an R factor of 5.3 measured at TP20 with 1 s integration period. The floor occupants had a perceptible vibration level without complaining. Hence, from standpoint of normal operation this floor can be considered as acceptable.

- **FS2**: The actual vibration response under a single person walking at 2.45 Hz, who was 90 kg in weight and 1.74 m in height, resulted in an R factor of 8.2 at TP110, as shown in Figure 3.26. Although it is predicted to be unacceptable, the actual response was measured along the walking path (WP) shown in Figure 3.10. This was done to excite the key modes in the measurements. It is clear that the predicted responses are scattered around the measured R factor. As mentioned in previous section, AISC DG 11 seems to be in close proximity to the actual response. However, it is difficult to carry out a reliable assessment due to the diverse (inconsistent) predictions of the various guidelines, even when using measured modal properties.

- **FS3**: It is shown in Figure 3.27 that this floor had very high level of in-service response, which resulted in complaints from floor occupants about the vibration. The measured R factor in service reached 15.1 at TP29 under excitation from the gymnasium above. Whilst it is not possible to draw any conclusions about the performance of the guidelines in terms of predicting the response, it is possible to assess whether the response criteria are appropriate. Examining Figure 3.27, it can be seen that the tolerance limit of the HiVoSS guideline was more than double the measured R factor, and hence it would be predicted to be acceptable. This clearly was not the case since significant complaints had been received from the building occupants. The rest of the guidelines produced an assessment that the floor is unacceptable, which correlates with the subjective assessment.

- **FS4**: As illustrated in Figure 3.18 two walking paths, WP1 and WP2, were selected based on the measured mode shapes. The actual vibration response under a single person walking along WP1 resulted in a maximum R factor of 47.11 at TP63. The pedestrian weight was 86 kg, height was 1.88 m and produced maximum R factor at the fourth harmonic of step frequency 1.905 Hz. For WP2 the same walker produced R factor of 35.2 at TP62 (not shown in Figure 3.28) at step frequency 2.2 Hz. While the in-service R factor was 87.98, as shown in Figure 3.28.

- **FS5**: The actual vibration response under a single person walking via WP (see Figure 3.21) resulted in an R factor of 5.12 at TP24, as shown in Figure 3.29. The measured R factor was due to a single pedestrian walking freely at his convenient speed, who had weight and height of 86 kg and 1.88 m, respectively. It is clear that the predicted responses are scattered around the measured R factor, whilst simplified formulae have shown the least reliable predictions. SCI P354 seems to be in close proximity to the actual response using FE and measured modal properties. However, it is difficult to carry out a reliable assessment due to the diverse predictions of the various guidelines.

3.5 Results and discussion

The analyses presented in this chapter have shown that available design guidelines do not give a consistent prediction of the vibration serviceability performance of the floor structures considered.

The results of the maximum predicted R factor for all case-studies show that the guidelines predict quite different values of R factor or equivalent. There are contradictory response predictions between CCIP-016, CSTR43 App G and SCI P354 when comparing the same vibration metric. However, for FS5 SCI P354 appears to provide relatively a good prediction when compared with its counterparts. AISC DG11 performs relatively well in terms of both response prediction and assessment for FS1 and FS2 and also gave a clear assessment of FS3 as being highly unsatisfactory, as expected. Similar performamce can be seen for FS4 and FS5. HiVoSS, however, appears to be an outlier and highly inaccurate.

None of the guidelines was able to give any insight into the frequency of event occurrence. A single peak value compared against the available tolerance limits may not be representative of the actual in-service condition, if this condition occurs only very rarely. This may lead to inconsistencies between the design stage assessment and actual performance in service. Such a wide discrepancy can cause confusion for design engineers as to whether the vibration performance is satisfactory or not, in particular when looking at measured modal properties response prediction. Another matter that could arise is the question of what is the probability of occurrence of the above predictions? In some cases, these guidelines can produce responses close to those measured on the actual structure, but it is not clear for any particular structure at the design stage whether there might be over- or under-estimation.

Simplified techniques for estimation of modal parameters giving results previously shown produce large differences in modal mass values, whereas modal frequency seems to be relatively well predicted. All guidelines tend to consider modal mass differently. As such, even larger inaccuracies appear to occur in obtaining the modal mass, which lead to potentially inaccurate estimations of vibration response. Such discrepancies in modal mass highlights that the simply-supported plate theory and empirically adjusting for a bay geometry (i.e span and width) can produce misleading values, even for regular floor configurations. This has also been observed in [51]. It is worth noting that the recommended damping ratios for the case-study floors seem to be somewhat in line with the measurements.

These case-study floors have illustrated a number of major drawbacks in contemporary guidelines in computing vibration response to pedestrian excitation. These are the simplified formulae which inaccurately estimate the modal properties and hence produce inaccurate estimates of response. The inaccurate load model used to represent actual walking in the design guidelines. The lack of a realistic vibration response descriptor with respective tolerance limits may also be a major downside in these guidelines; a single peak value of vibration response appears to be unrepresentative. Therefore, significant improvements are needed with respect to dynamic properties, expected loading scenarios and the corresponding walking-induced forces. This would result in a more reliable vibration response, which might be in the form of probability of exceedance with a realistic predefined set of values for serviceability assessment. This approach would not only give design engineers a reliable tool, but also provide a realistic response estimate for various floor usage scenarios; thus, leading to more reliable vibration serviceability assessment of floor structures.

3.6 Conclusions

This chapter has presented a back analysis of contemporary design guidelines using real-world floors that were also physically tested. The merits and demerits of the guidances have been illustrated and examined. Vibration serviceability assessment has been performed based on measured modal properties and tuned FE model for most of the floors as well as the respective simplified formula has been used. Vibration responses were calculated for a range of the floor frequencies to obtain the peak vibration response in terms of equivalent R factor (for peak acceleration and OS-RMS$_{90}$) for the guidelines due to ease of comparison.

Walking load models are represented either by Fourier series or a polynomial function. These are periodic modelling of a single person without considering the innate variabilities of actual walking and as such a probabilistic walking load model

remains absent. The frequency threshold between LFFs and HFFs is the key factor to determine vibration responses (resonant response to multiple footfalls or transient response to individual footfalls) that govern the design procedure. The methodologies presented in each guidelines predict a vibration response that may or may not match well with actual measurements. A significant over- and under-estimation can be seen in all guidelines, which can be attributed mainly to inaccurate estimation of modal properties and force models, particularly for the simplified procedures.

A peak response value appears to be misleading and unrepresentative for vibration serviceability assessment. Identifying an appropriate vibration descriptor (including tolerance limits) coupled with a probabilistic framework might be a key factor for more reliable serviceability assessment. In addition, conservative design with an accept-reject method neither results in a reliable assessment, nor describes the rare vibration events that may happen. Therefore, significant improvements and rigorous approaches are required to introduce probability of exceedance with realistic predefined set of values. The vibration ratings and tolerance limits should also reflect such a statistical manner.

Chapter 4

Experimental Testing and Spatial Pedestrian Distribution

This chapter provides both experimental and numerical investigation of pedestrian patterns in a typical office floor. The experimental campaign uses an approach of simultaneous vibration response monitoring and video monitoring coupled with a vision tracking system to locate pedestrian routes and walking patterns and to quantify occupant parameters. The dataset provides an insight into understanding actual multiple pedestrian behaviour in vibration performance of floors. The numerical simulations utilises agent-based modelling to generate occupancy patterns upon using floors via a probabilistic spatial distribution. Such method results in a realistic insight into multiple pedestrians in-service activities at the design stage. The content of this chapter, in a slightly amended form, has been submitted to Computer-Aided Civil and Infrastructure Engineering under the following title

Muhammad, Z.O. and Reynolds, P. “ Modelling and experimental verification of probabilistic walking paths for analysis of footfall-induced floor vibrations” and it is under review.

4.1 Introduction

The literature study in Section 2.3.4 has highlighted that there is a need for including pedestrian paths into walking models in the context of probabilistic response assessment. This chapter aims to address the above shortcoming in the literature.

Most studies into vibration performance of floor structures [9, 47, 105] tend to provide in-service vibration response data with insufficient information about various pedestrian patterns and their respective walking paths. Modern office floors are often characterised by open plan layouts, where diverse routes are commonly used. Also, floor occupants have different excitation potentials along various paths, which means that the assumption of a particular walking path producing a worst case-scenario is unrepresentative of the actual cumulative exposure experienced by occupants [38]. Therefore, simultaneous collection of actual vibration responses and pedestrian patterns along different routes is required to facilitate a reliable vibration serviceability assessment that can be described in a stochastic manner. This area of research requires further examination of experimental data over long periods (i.e. normal working day) to give insights about multiple pedestrian excitation paths and corresponding vibration responses.

This chapter presents the results of a unique campaign of experimental and numerical investigation of pedestrian patterns on a typical office floor. The experimental programme uses an approach of simultaneous vibration response monitoring and video monitoring coupled with a vision tracking system to locate pedestrian routes and walking patterns and to quantify occupant parameters. Acquisition of these data over a normal working day are crucial in understanding actual multiple pedestrian behaviour in vibration performance of floors. The numerical simulation utilises agent-based modelling [101] to generate occupancy patterns upon using floors via a probabilistic spatial distribution of pedestrians. Therefore, a realistic pedestrian pattern can then be used with probabilistic walking forces to carry out a more reliable vibration serviceability assessment. It is suggested that such an approach, combining both probabilistic distribution of pedestrian patterns and stochastic walking forces, will yield a more reliable assessment of vibration serviceability than the deterministic ‘worst case’ approaches of the past.

4.2 Description of the floor

The floor structure has been presented previously in Section 3.3.4.1. There was a unique opportunity to access this floor with permission given by the occupants to monitor it. The floor is an open-plan office space with a typical layout, as illustrated in Figure 4.1. There are two staircases on each side of the floor, which pedestrians

typically use to enter into or exit from the floor area. There are 48 seats in total with several filing cabinets and shelf units distributed across the floor area. There are also toilet facilities and a kitchen area as well as a storage room.

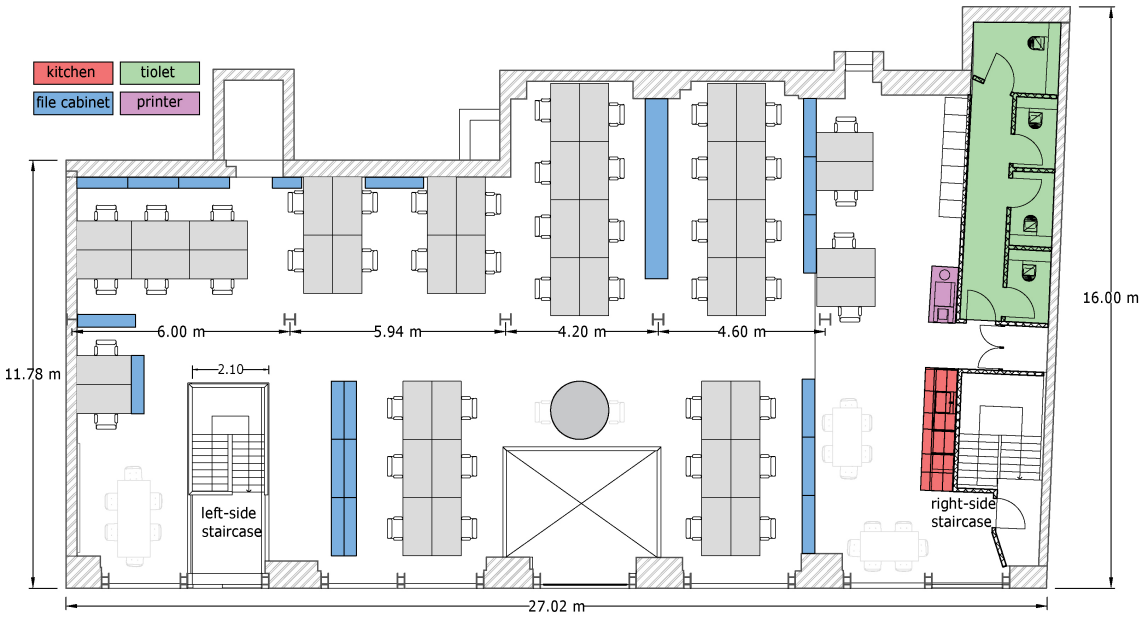

Figure 4.1: Floor plan indicating office floor layout.

4.3 Experimental monitoring program

4.3.1 Vibration monitoring data

This section presents the results of the in-service vibration monitoring in terms of response (R) factor and vibration dose values (VDVs), which are common descriptors used in vibration serviceability assessment of floors. Honeywell QA750 accelerometers were used (by the author) to measure vibration responses due to both controlled single pedestrian walking and for the in-service monitoring. Data were acquired digitally on a Data Physics Mobilyzer II spectrum analyser at a sampling rate of 204.8 Hz.

4.3.1.1 Analysis of vibration responses due to a controlled single pedestrian

A series of walking tests was performed by a single pedestrian to assess the floor response to human-induced vibrations under controlled conditions. Two walking paths (WP1 and WP2) were identified based on measured in-situ mode shapes, as shown in Figure 3.20. Walking frequencies were chosen from 1.7 to 2.2 Hz in 0.1 Hz increments, to simulate the range of pacing rates usually observed in

office environments. An additional walking frequency of 1.905 Hz was used as this was tuned to excite the observed first modal frequency of 7.62 Hz with its fourth harmonic. WP1 and WP2 were traversed once in each direction for each test. The pedestrian weight and height were 86 kg and 1.88 m, respectively. In addition, the locations of the 16 test points (TPs), shown in Figure 4.2, were intended to capture vibration responses over the floor area at key locations, which again were based on the in-situ mode shapes.

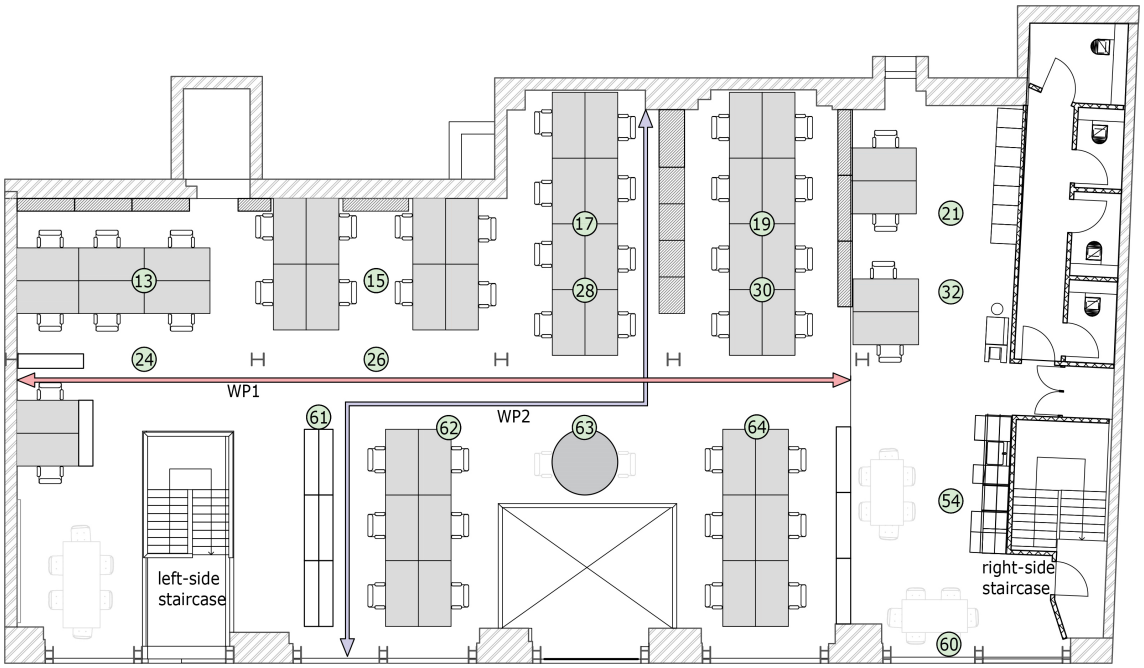

Figure 4.2: Predefined walking paths and TPs for controlled walking.

Acceleration time histories were recorded at each TP for each walking test. These were then weighted using the W_b frequency weighting curve [113, 118] for vertical accelerations. The principle of frequency weighting is based on the manner in which vibration affects the human body and that human perception of vibration is frequency dependent [113]. In other words, vibration within a certain frequency band is perceived higher than other frequency bands. There are different weighting curves in BS6841 [113], however, the most commonly used curve for vertical vibration in buildings is the W_b weighting shown in Figure 4.3. This weighting was applied to all acceleration time histories via a convolution operation using a digital filter in the time domain. This is done by convolving the input signal (accelerations) with the digital filter's impulse response (W_b weighting) [139], where the weighting coefficients are given in [113].

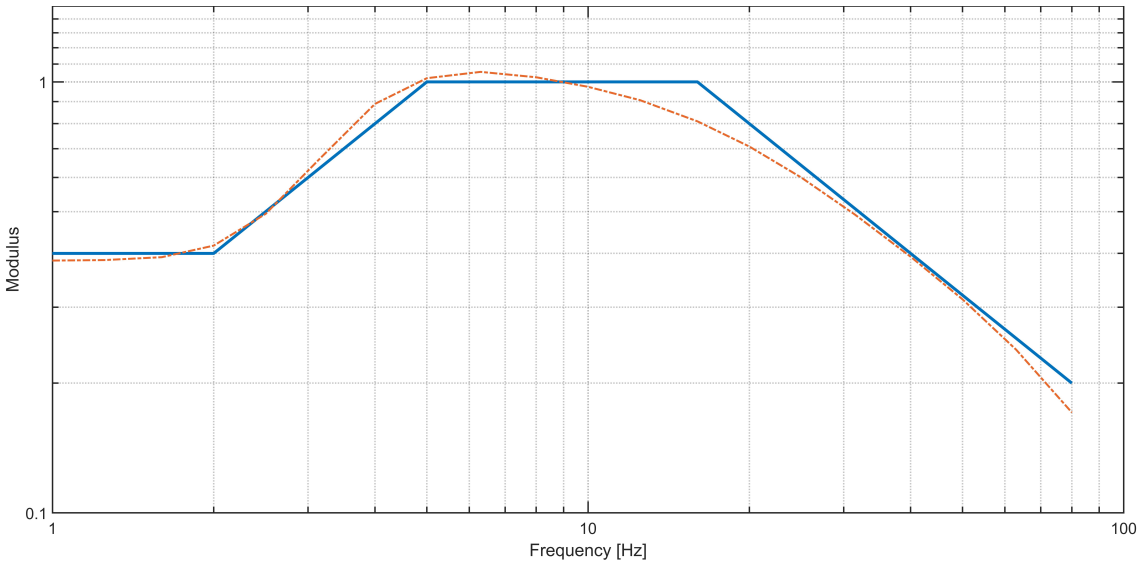

Figure 4.3: W_b weighting curve for vertical vibration (orange line) and its approximation (blue line) (after BS6841 [113]).

Maximum transient vibration value (MTVV) is calculated by running root mean square (RMS) time history with 1 s integration time. The maximum R factor was calculated for each channel by taking MTVV and normalising this by the reference value of 0.005 m/s^2 [45]. The formula for this is given in Equation 4.1.

$$\mathrm{R} = \frac{max_t \left(\sqrt{\int_{t-T/2}^{t+T/2} a_w^2(t)\, dt} \right)}{0.005} \tag{4.1}$$

where:

R is the Response factor

T is the period used for the running RMS in seconds, and

$a_w(t)$ is the W_b frequency weighted acceleration time history in m/s^2.

The time history at TP63 (Figure 4.2) at pacing rate 1.905 Hz is shown in Figure 4.4. Also, the frequency content, in terms of Fourier amplitude spectra [140], of the acceleration response is shown in Figure 4.5. The results of the controlled walking along WP1 for all walking frequencies are shown in Figure 4.6. It can be seen that the peak R factor is 47.11 at TP63 at pacing rate 1.905 Hz. The observed responses along WP2 were much lower, which the maximum R factor was 35.2 as presented in Section 3.4.2; hence they have not been shown here. According to current acceptable threshold limits for maximum R factor of 8 [6] or 4 [7] for office floors, this floor is deemed unsatisfactory.

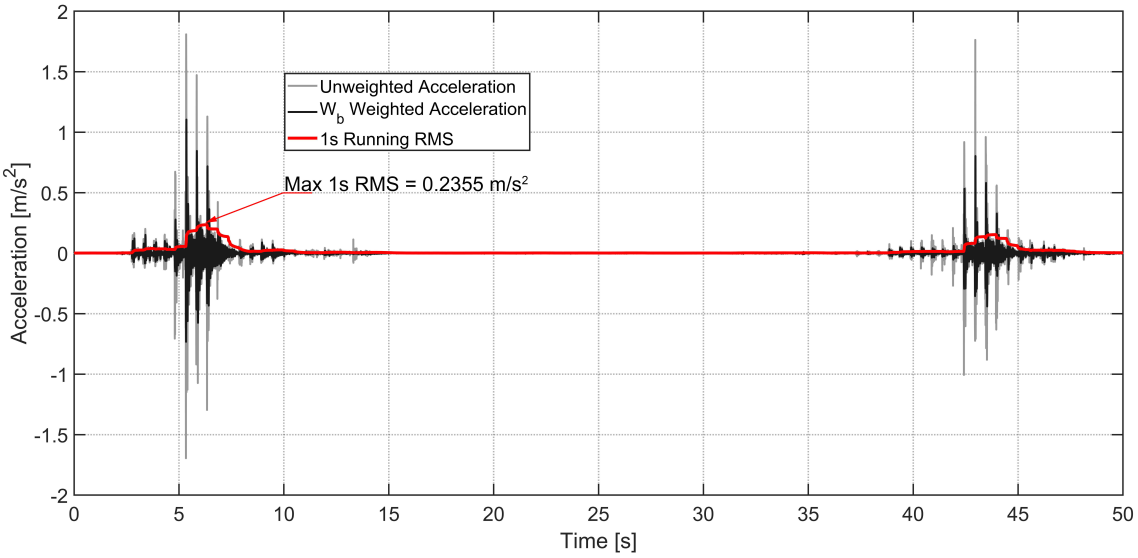

Figure 4.4: Typical time history for walking along WP1 at TP63 and pacing rate 1.905 Hz.

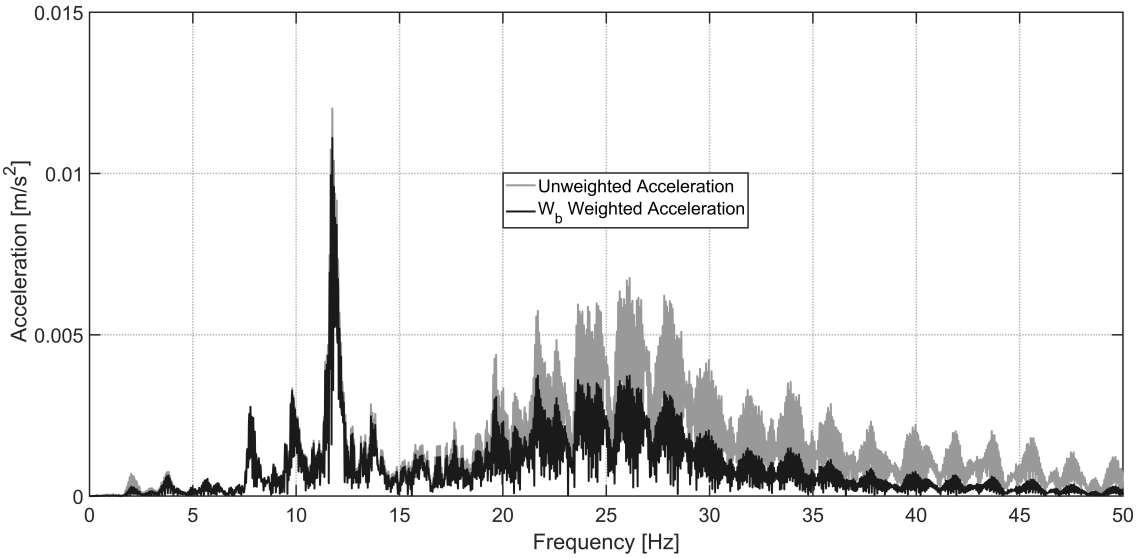

Figure 4.5: Fourier amplitude of the acceleration response of single person walking at TP63 for WP1. Acceleration in "grey" is raw data and in "black" is W_b weighted.

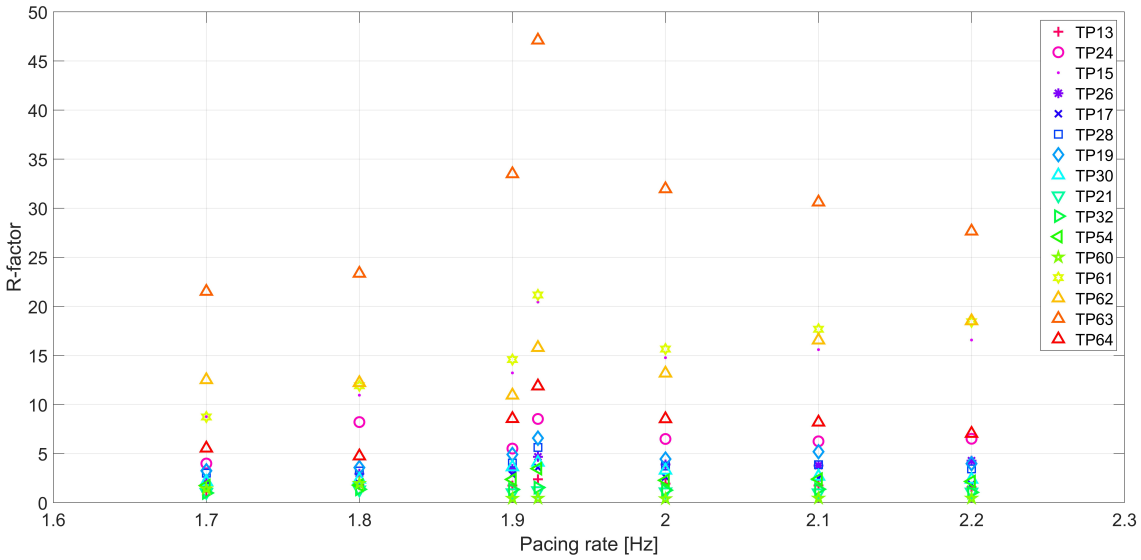

Figure 4.6: R factors observed for walking along WP1 at a range of walking frequencies.

With respect to assessment against available design guidelines, Table 3.19 presented the response predictions using measured modal properties. As mentioned in Section 3.4.2 there are large underestimations by all guidelines, which the closest value to its measured counterpart is at -42%. This indicates that current design procedures require improvements and most likely in the definition of walking forcing functions, since the structural properties used are those determined from physical testing. In addition, Figure 4.5 illustrates that there are contributions of higher modes above design guidelines limits, the highest of which is 15 Hz in CCIP-016 [7]. Therefore, these observations have highlighted some areas where design guidelines could be improved.

4.3.1.2 In-service vibration monitoring and data analysis

In-service vibration responses were monitored under normal use of the floor for 12 hours (i.e. a normal working day), with 12 accelerometer sensors (Honeywell QA750) installed over the test grid shown in Figure 4.7. The locations of sensors (i.e. TPs) were either placed under the desks or next to a furniture item to avoid being hit (accidentally mistreat the sensors) during in-service operation. Whilst it might have been ideal to put them at the exact location of single pedestrian walking in Figure 4.2, it was necessary to place them at locations that were deemed secure yet still close to walking paths based on in-situ mode shapes. There were 27 persons present during the in-service monitoring.

Figure 4.7: In-service monitoring TPs and video camera locations.

The most recent British Standard [118] recommends the use of VDV for evaluation of structural responses. The VDV descriptor incorporates both the duration of vibration exposure and the magnitude of vibration and is given by

$$\text{VDV} = \left[\int_0^{T_t} a_w^4(t) dt \right]^{1/4} \tag{4.2}$$

where:

VDV is the Vibration Dose Value in m/s$^{1.75}$,

$a_w(t)$ is the frequency weighted acceleration response time history in m/s^2, and

T_t is the total time period in seconds.

In addition, the R factor is a common measure of vibration level, even though the duration of exposure is usually not accounted for. Recent studies [3], however, suggest that motion dose, a combination of acceleration, frequency, motion type and duration of exposure is likely to provide a more reliable design criterion.

A typical acceleration time history response at TP39 from 12-hour monitoring and the corresponding Fourier amplitude spectra are shown in Figures 4.8 and 4.9, respectively. It can be seen that in the first two hours of monitoring there was no significant activity in the office. This is shown here to understand normal conditions of the floor without occupants. However, following arrival of pedestrian(s) at 08:00 and onwards, high levels of acceleration responses were observed. A

similar trend was observed for other TPs, which here only the frequency content will be shown. Fourier amplitude spectra for all other TPs are shown in Figure 4.10. Comparing the frequency content of both single pedestrian walking 4.5 and in-service 4.10, there are significant contributions of higher modes for multiple pedestrians for a wider band of frequency content than its counterpart.

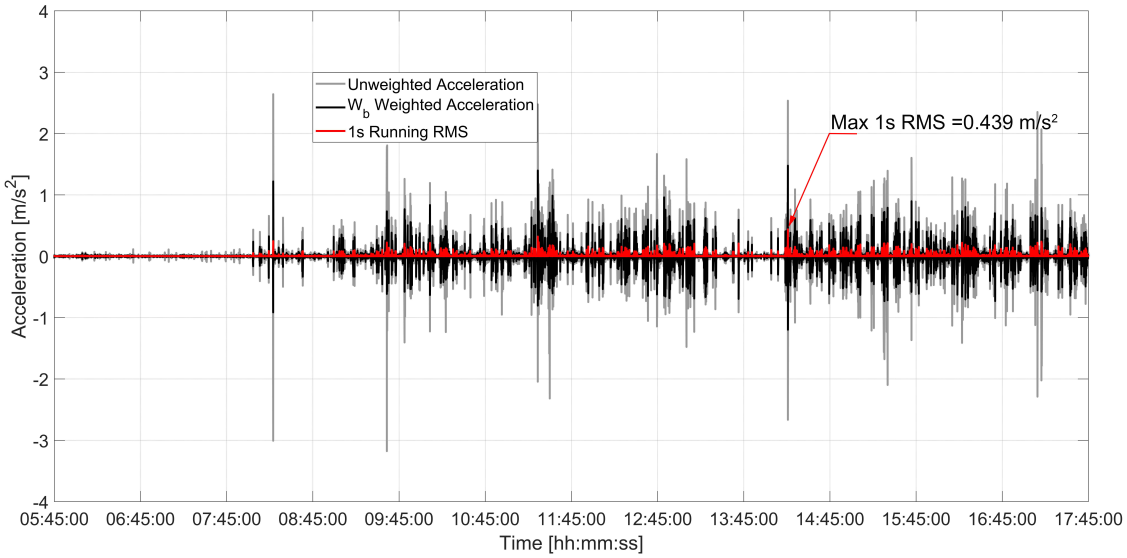

Figure 4.8: A typical in-service acceleration time history response at TP39.

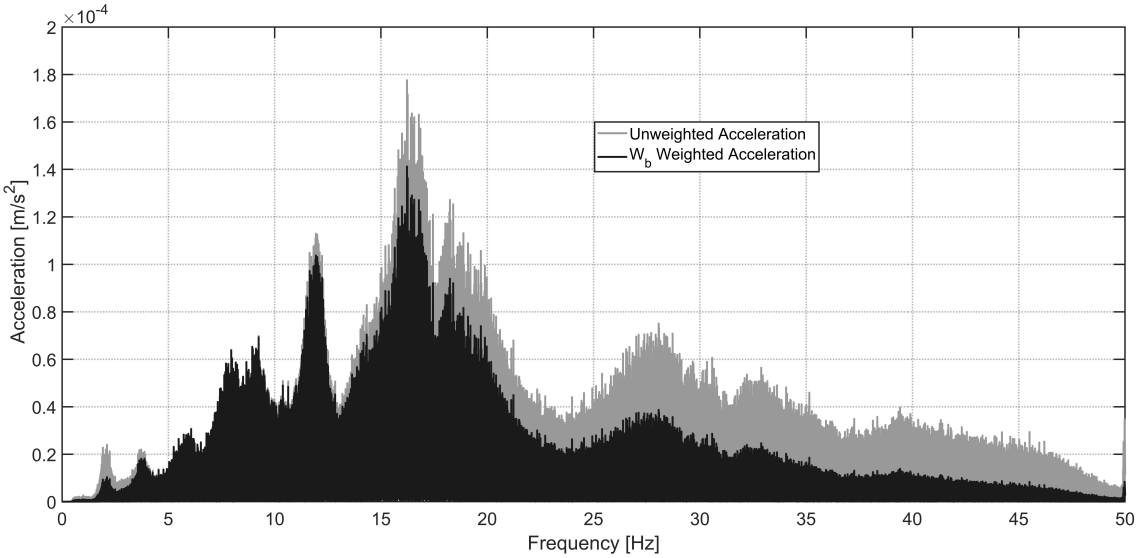

Figure 4.9: Fourier amplitude of the in-service acceleration response at TP39. Acceleration in “grey” is raw data and in “black” is W_b weighted.

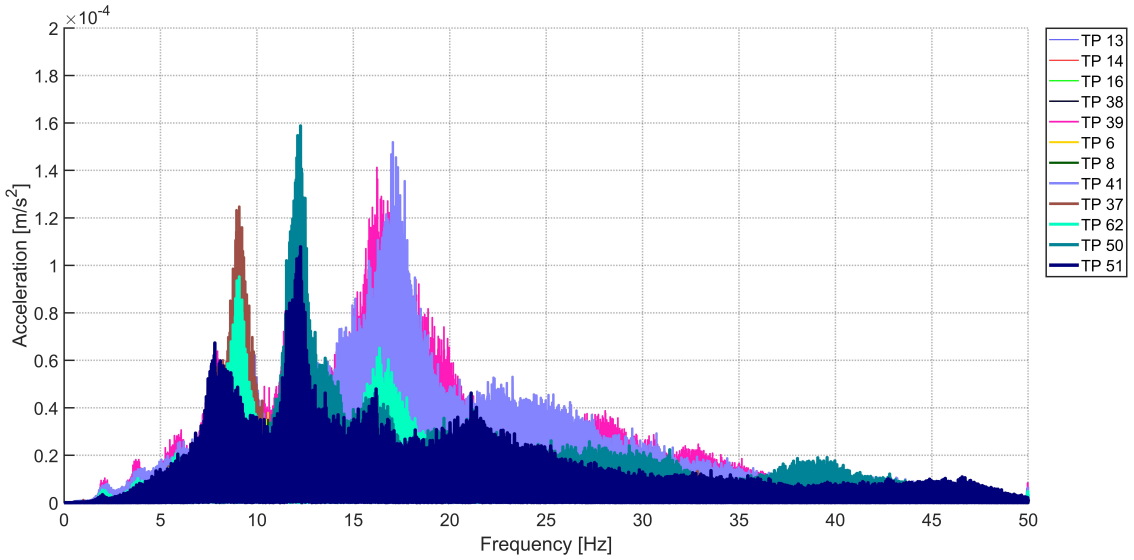

Figure 4.10: Fourier amplitude of the in-service acceleration response at all in-service monitoring TPs. Only W_b weighted acceleration is shown for clarity.

The results of the in-service vibration response in terms of VDV is shown in Figure 4.11 in the form of cumulative VDV plots (i.e. the build-up of vibration exposure throughout the monitored time period). The limit for office buildings (based on day time 16 hour exposure time) is 0.4-0.8 m/s$^{1.75}$ to ensure "low probability of adverse comment"; this limit was clearly exceeded during the in-service condition.

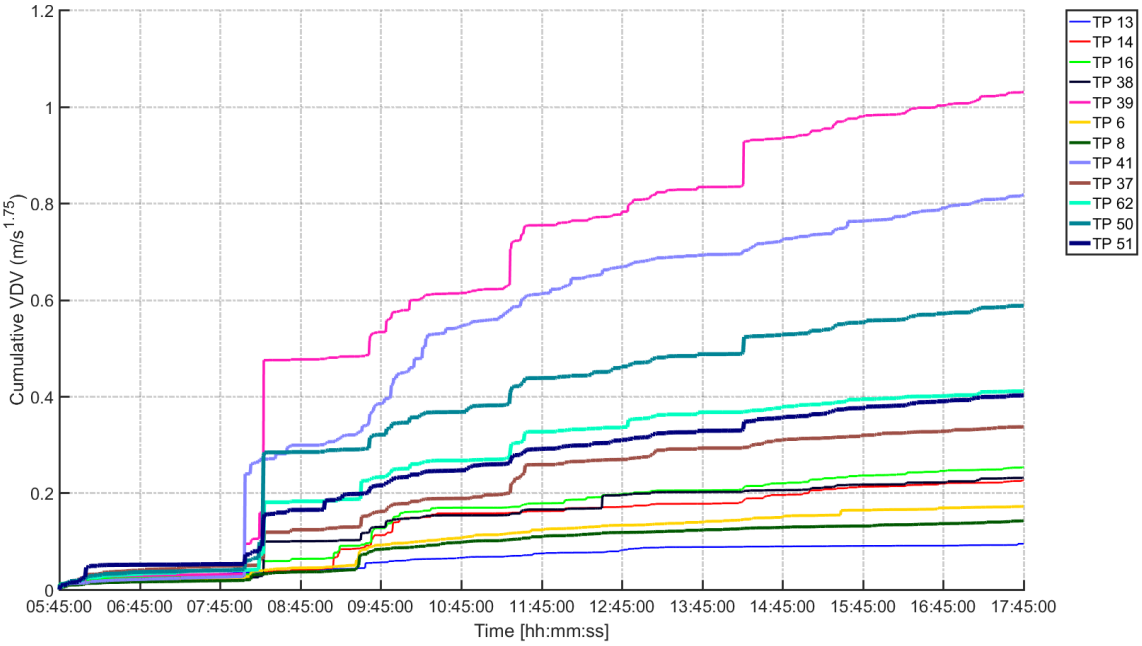

Figure 4.11: In-service cumulative VDV for 12-hour monitoring period.

Figure 4.12 shows a plot of the cumulative probability distribution functions (PDFs) calculated for 12 hours of monitoring at all TPs. These cumulative distributions are highly enlightening as they show the probability of exceedance as a function of time, and hence provide further insight into the likely 'dose' of vibra-

tions through a working day. For example, although the peak R factor was 87.98, the 95th percentile is still less than 6 (i.e. R=6 was exceeded for less than 5%) of the monitoring period.

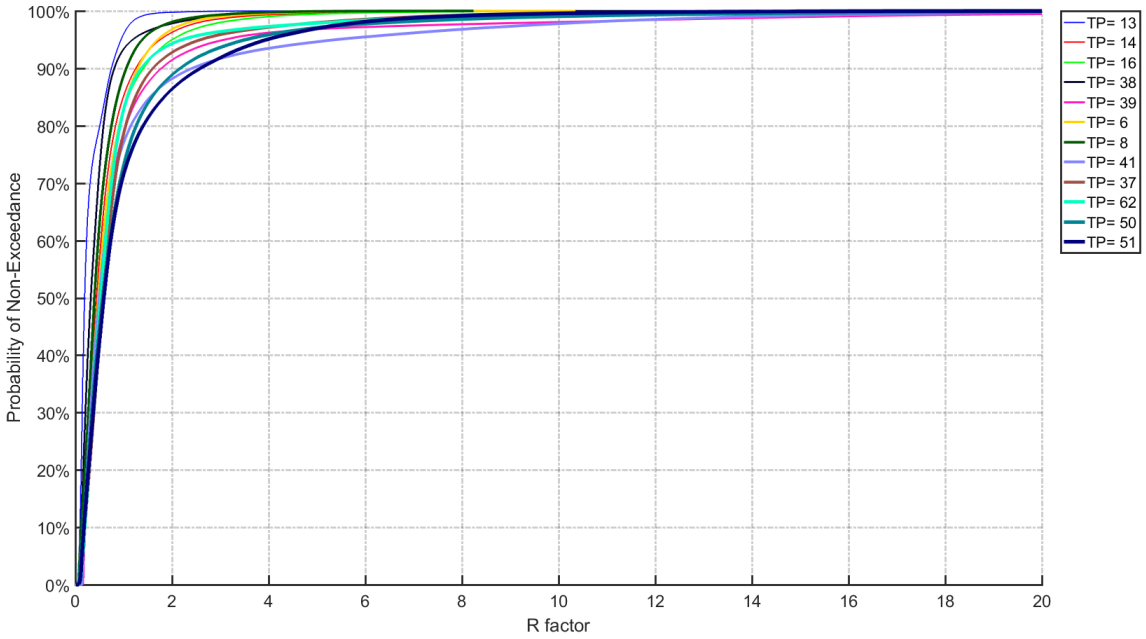

Figure 4.12: In-service cumulative PDF of R factors for 12-hour monitoring period.

As far as occupants' subjective perception is concerned, the floor was considered to be lively. It is worth mentioning that the information was anecdotal evidence. In particular, workstations in the vicinity of TP 41 and 51 were deemed annoying for most of the time. The results in Table 4.1 illustrate that the peak R factor is very high (87.98), whilst the 75th and 95th percentile values are much lower. Although R factor by itself does not account for exposure time or duration of vibration, the peak values are not representative of the majority of the exposure. In addition, the threshold limit of R factor 4 [7] is exceeded at TP 41 and 51 for 6.52% and 4.91%, respectively, of the monitoring duration, i.e. 47 and 35 minutes out of 12 hours.

Another point to note is that vibration responses under normal multi-occupant use are significantly different than those from a single pedestrian with controlled pacing rates (Figure 4.6). The VDVs in Table 4.1 have been converted to 16 hours day values using Equation 4.3, as per [118].

$$\text{VDV scaling factor} = \left(\frac{16 \times 60 \times 60}{T_t}\right)^{1/4} \tag{4.3}$$

where, T_t is the duration of exposure per day in seconds.

Table 4.1: Vibration response analysis for all TPs

TPs	75%ile R factor	95%ile R factor	% monitoring time R factor ≥ 4	Peak R factor	VDV [16 hr equivalent] $m/s^{1.75}$
13	0.38	0.94	0.01	5.86	0.102
14	0.73	1.76	0.66	13.24	0.243
16	0.79	2.0	0.99	13.61	0.272
38	0.53	1.2	0.43	12.61	0.249
39	0.88	3.1	3.8	87.98	1.107
6	0.79	1.71	0.39	10.35	0.185
8	0.65	1.39	0.23	8.24	0.153
41	0.92	5.4	6.52	44.4	0.878
37	0.91	2.6	2.86	23.45	0.362
62	0.82	2.21	2.72	23.67	0.442
50	1.06	3.53	4.15	42.19	0.632
51	1.13	3.96	4.91	28.14	0.432

In addition, the difference between single (i.e. controlled) and multiple pedestrian vibration responses, in terms of percentage of difference, has been calculated in Table 4.2 using Equation 4.4. As discussed earlier, the locations of sensors (i.e. TPs) between the two tests were not exactly the same place due to the busyness of the office during in-service conditions. Therefore, TPs in controlled walking were compared with their approximate locations of those in the in-service data. Also, both WP1 and WP2 vibration responses were compared with in-service data and the maximum value of those two was chosen for the percentage of difference. The values in positive show an increase and negative denote a decrease of the vibration responses between the controlled walking and in-service data.

$$\% \text{ Difference} = \frac{\text{in-service response} - \text{controlled response}}{\text{controlled response}} \times 100 \tag{4.4}$$

The percentage of differences in Table 4.2 illustrates an extent of higher responses in normal office operations than a single person. This shows that actual in-service responses under multiple pedestrian loading are largely different from those of a single pedestrian and as such multiple pedestrian loading scenarios should be accounted for in the design stage.

Table 4.2: Vibration response difference between controlled walking and in-service data

TPs controlled	TPs in-service	R factor WP1 controlled	R factor WP2 controlled	R factor in-service	% Difference
13	13	2.38	1.15	5.86	146.2%
15	14	20.44	15.51	13.24	-35.2%
15	16	20.44	15.51	13.61	-33.4%
26	38	4.67	5.28	12.61	138.8%
28	39	5.63	10.19	87.98	763.4%
63	39	47.11	34.69	87.98	86.7%
17	6	3.57	8.97	10.35	15.4%
19	8	6.58	14.8	8.24	-44.3%
30	41	4.1	11.77	44.4	277.2%
64	41	11.87	9.88	44.4	274%
NA	37	NA	NA	23.45	NA
62	62	18.51	35.22	23.67	-32.8%
63	50	47.11	34.69	42.19	-10.4%
NA	51	NA	NA	28.14	NA

4.3.2 Video monitoring data

This section presents in-service monitoring techniques using motion tracking. The main purpose is to utilise these new techniques to establish realistic walking patterns, taking into account the actual physical floor layouts, such as including desks, partitions and other obstacles.

There are four categories of motion tracking monitoring techniques [129]: 1) multichannel interacting model, 2) optical marker-based, 3) wireless inertial sensors and 4) video-based monitoring, as presented in Section 2.6. In this study video cameras have been selected due to their effectiveness, ease of installation and their ability to be coupled with vision tracking software to track pedestrian routes. Use of video-based monitoring techniques to track human walking on building floors is not widely implemented; thus this experimental campaign has good potential to provide insight into realistic pedestrian patterns.

In this investigation AXIS M3007-PV network cameras [141] were deployed. These cameras can be mounted on a wall or ceiling, using an ultra wide-angle lens that produces strong visual distortion. They are easy, flexible in installation and are powered via ethernet cable. The vision tracking software intuVision v8.0.11 [142] is used to analyse the acquired video data. The software tracks

walking paths of people using video image processing techniques and the outcome is pedestrian patterns, which are subsequently utilised to generate heat-map data of commonly travelled paths through the floor area. The cameras and accelerometers were synchronised manually using the time period that appears on the recording machine.

This software works on both recorded videos and live streams. In this chapter recorded videos were used for post-processing. The software configuration settings were set-up for pedestrian detection using optimised values of settings for the environment where cameras were recording. The values were obtained using a number of trials on the videos so as to achieve the best outcome. The settings are as follows. "Detection sensitivity" setting, which affects the number of detected objects (i.e. pedestrians), was set to medium level. Also, the corresponding "minimum object size" setting, in pixels, was set to 10 by 10 for width and height, respectively. This setting determines the lower size limit of detections. For smaller videos, or those with a far vantage point, this should be decreased. This will results in a bounding box around pedestrians who are walking. In addition, there is "noise filtering" setting that will decrease the number of false detections. This setting was set to the highest level. Such value is necessary for office environments so as to decrease detection around desks during sitting. Finally, in situations where an area of the video contains moving objects that are not desired detections, an "exclusion zone" was used. This was done for instance on areas outside the floor area (see Figure 4.13) or around perimeter windows (see Figure 4.16), where objects were moving outside the monitored area. The reader is referred to the software manual [142] for more information.

4.3.2.1 Laboratory validation data

To validate the image acquisition and video tracking software, a single camera was used in the Structures laboratory at the University of Exeter to provide a top-down view to cover the lab floor entirely. The camera was at height 4.0 m and positioned approximately in the middle of the floor, which has a length 7.5 m and width 5 m. Figure 4.13 shows both the original distorted image extracted from the video file and an image with reduced distortion created using the MATLAB image processing toolbox [143].

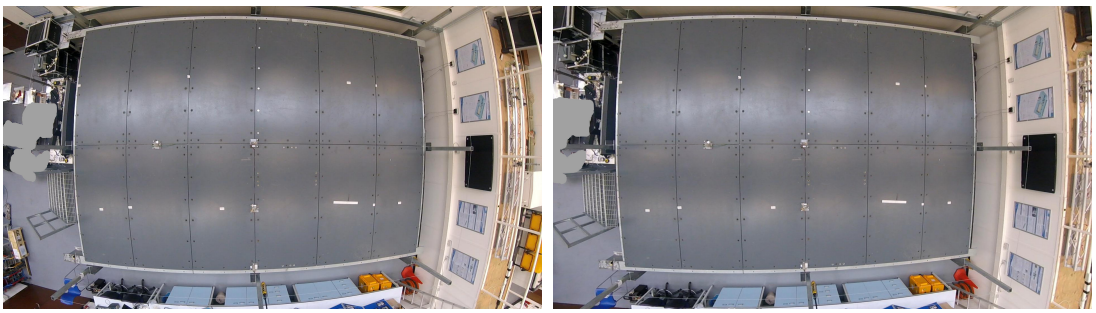

(a) Top view lab floor: distorted version

(b) Top view lab floor: image with reduced distortion

Figure 4.13: Laboratory floor at the University of Exeter.

Two pedestrians carried out simultaneous walking tests while video recording was in progress. The pedestrians walked across the diagonals of the floors at normal walking speeds for two minutes. The pedestrians were asked to walk and stop freely. This was done to mimic normal conditions. Their walking patterns were chosen to test the effectiveness of the video pedestrian tracking software to capture their walking paths. The recorded video file (raw file) was then post-processed via the IntuVsion software to obtain pedestrian walking paths and their respective usage of routes. The software captures the centroid of each pedestrian's bounding box at an instant of time. The output is a heatmap image in distorted version due to the wide-angle lens of the camera. This image then was processed to reduce distortion, so as to better understand pedestrian paths, as shown in Figure 4.14. The heatmap plot can be used as an indication of the most used areas by pedestrians collectively.

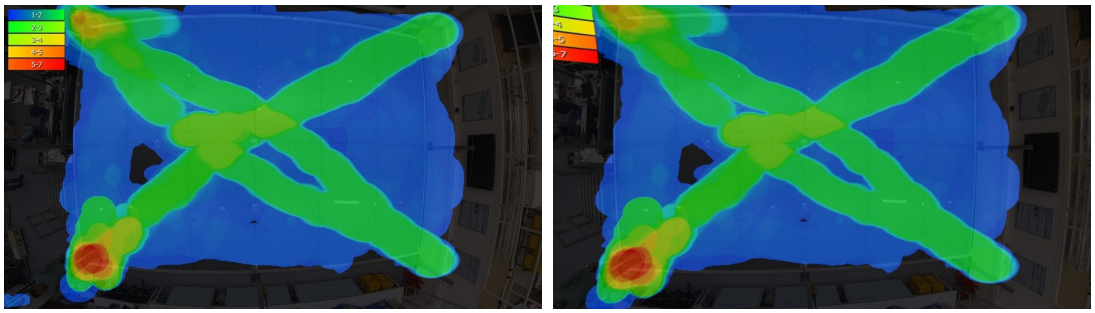

(a) Heatmap lab floor: distorted version

(b) Heatmap lab floor: less distorted version

Figure 4.14: Heatmap of two pedestrians on Laboratory floor at the University of Exeter.

The tracking software can, to a good extent, estimate pedestrian locations correctly, even when they are close to each other. In addition, the number of travelled paths was accurate when compared with manual counts from the video data. The hotspots at the corners represented nominally stationary pedestrians who were naturally unable to stand perfectly still and hence were picked up by

the analysis software. On the basis of this validation test, it was concluded that the tracking software is qualitatively accurate in locating pedestrians and their respective walking paths.

4.3.2.2 Experimental pedestrian walking path from in-service monitoring

The aforementioned office floor with a total of 27 pedestrians was monitored using three cameras to cover large areas of the floor. The cameras were fixed at a height of 2.2 m and were located at positions to give information about pedestrian patterns, as shown in Figure 4.7. The field of view of the cameras for all three cameras, approximately, are shown in Figures 4.15 and 4.16. The video recording lasted for 12 hours of a working day, in parallel with the vibration response monitoring mentioned earlier. It is worth mentioning that permission was given by the office occupants for the monitoring exercise and no identifiable features of the pedestrians will be shown in the analysis.

The video processing was carried out for 10 hours of data, because there were no pedestrians present in the first two hours. Video files were treated separately in terms of analysis to obtain pedestrian walking paths. The heatmap image for individual videos was obtained with respect to their location, as shown in Figure 4.17.

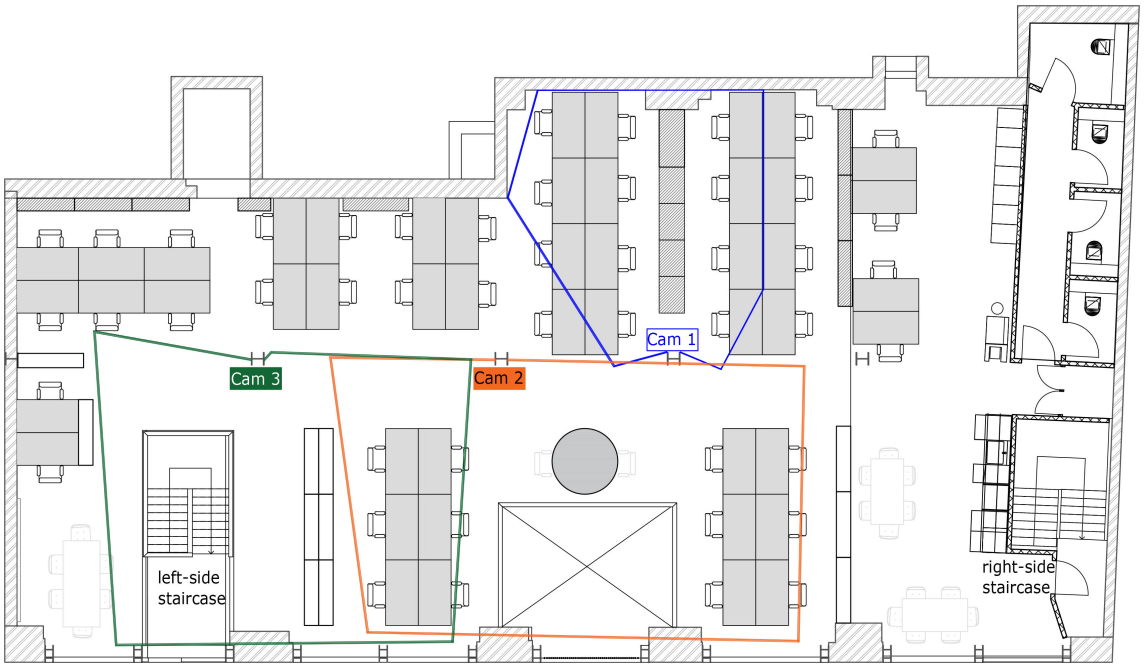

Figure 4.15: Plan of cameras top-down field of view.

(a) Camera 1 top-down view

(b) Camera 2 top-down view

(c) Camera 3 top-down view

Figure 4.16: Field of view from individual cameras.

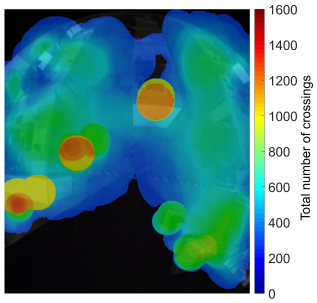

(a) Camera 1 heatmap

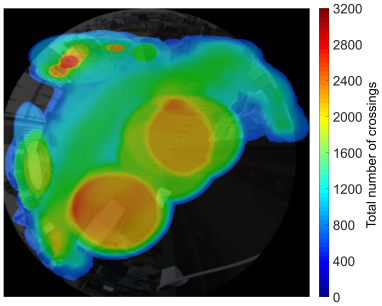

(b) Camera 2 heatmap

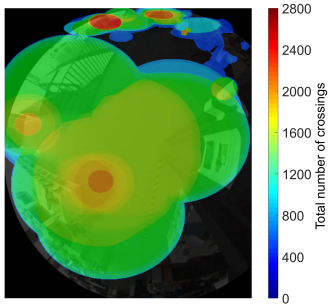

(c) Camera 3 heatmap

Figure 4.17: Heatmaps of in-service floor from individual cameras.

The software output, as mentioned, does not provide individual walking path time history, which is a shortcoming of this vision tracking software. The three heatmaps were then corrected (similar to the aforementioned section) and overlaid using MATLAB image processing onto the floor plan, as shown in Figure 4.18. This was carried out to produce the collective heatmap of the area monitored,

rather than individual locations; thus giving a more comprehensive overview of pedestrian patterns.

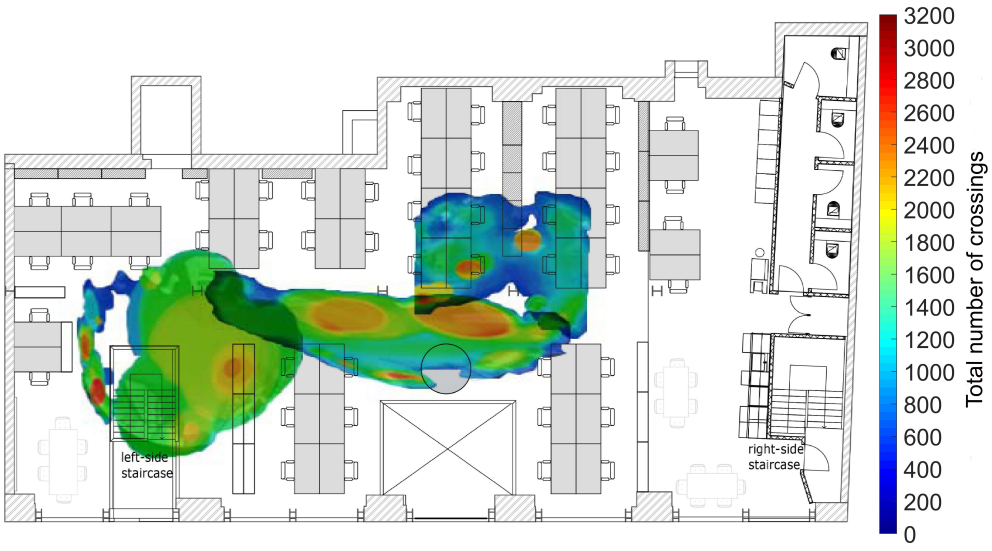

Figure 4.18: Heatmap of in-service pedestrian walking paths.

The total number of the walking paths indicated which routes were used most. It is obvious that several routes tend to be commonly in use throughout the day, in particular the walking path in the middle of the floor area. Pedestrians traversing this path produced highest vibration responses at TPs 51 and 41.

4.3.2.3 In-service pedestrian parameters

A great deal of insight into pedestrian patterns on this floor can be gained from the video data. Further analyses of movement of floor occupants were carried out to reveal a number of other parameters related to pedestrians' daily use of the floor. The analyses focused on are arrival time of occupants, walking speed, time spent at different locations and tendency to enter or exit from staircase gates.

The arrival time of pedestrians was extracted from video monitoring data. It is was calculated from (at about 08:00) when first pedestrian entered into the floor until all the remaining pedestrians arrived on the floor. It is illustrated in Figure 4.19, which has a mean of 27.5 minutes and standard deviation of 14 minutes. It is worth noting that Figure 4.19 only presents the first hour of the monitoring, a few number of occupants arrived after that time.

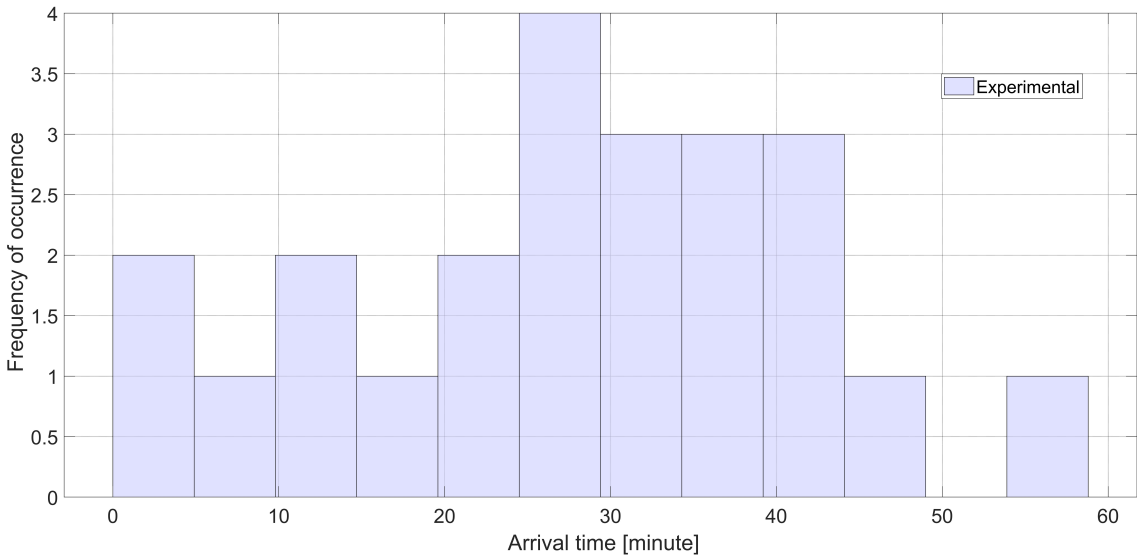

Figure 4.19: In-service pedestrian arrival time.

Walking speed during daily use varies as different pedestrians tend to have different speeds when carrying out tasks. Therefore, the collective walking speed for each pedestrian was manually estimated from the video data. Each pedestrian time along with their covered distance (from dimension of Figure 4.1) was recorded then walking speed was computed. Figure 4.20 shows a normal distribution of walking speed with a mean of 1.22 m/s and standard deviation of 0.23 m/s.

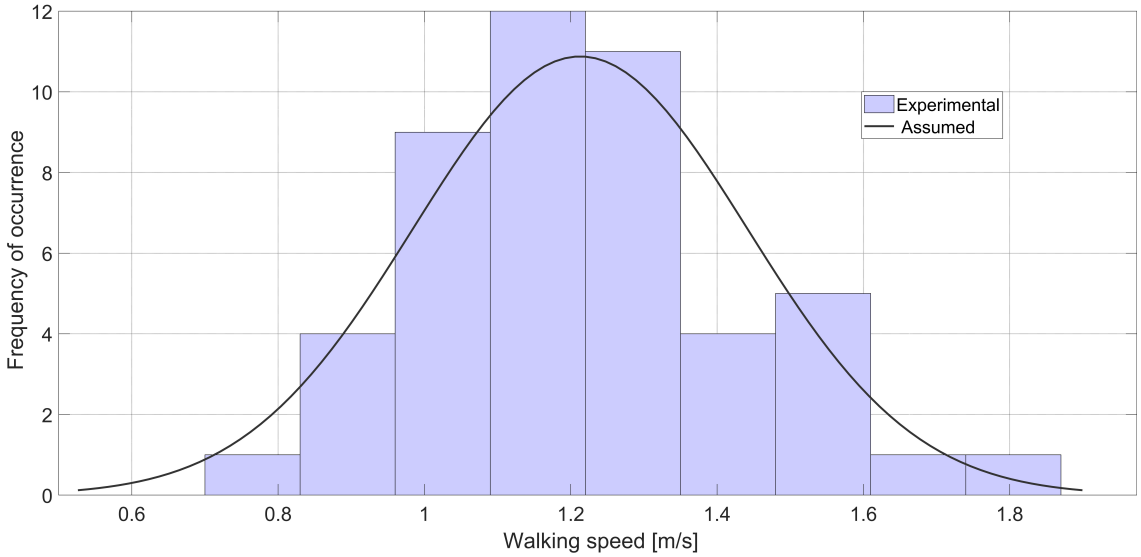

Figure 4.20: In-service pedestrian walking speed.

The results shown in Table 4.3 illustrate that pedestrian behaviour tends to be diverse and random. Each pedestrian at different times makes a trip, where s/he spends some time (active time) before returning to his/her desk. Since different occupants carry out tasks and movements randomly and infrequently, it is challenging to develop statistical relationships to represent this. However, the percentage of time to spend in any area per hour, on average, are 62%, 16%, 11%

and 11%, for the desk, kitchen, wash room and printer, respectively. As such the minimum and maximum active time during a working day were obtained to reflect their statistical distributions, which can be randomly generated within the interval. For example, 63% of pedestrians tend to use right staircase to enter into the floor (see Figure 4.7) and the pedestrians remained seated at their desks for a maximum of 4680 seconds (i.e. 78 minutes) before leaving their desk and carrying out another task. Moreover, pedestrians seem to use the kitchen area and toilet facilities quite often when they are active on the floor. The percentage of active person per an hour of the monitoring, on average, over the floor area illustrates that two or more persons are active for 16.9% of time, while for a single person it is 17.7% of time. This implies that multi-person walking activities are as important as single pedestrians. These timings help to understand how pedestrians utilise floors and which areas are used most of the time. These are specified by the results of an observation, and which can take on different values when the observation is repeated many times. As a result, further monitoring exercises will be quite beneficial in exploring pedestrian patterns in this regard.

Table 4.3: Video data analysis for different tasks and their active times

Task location	Active time
Left staircase gate	37% of pedestrians
Right staircase gate	63% of pedestrians
Seat	min= 300 seconds ; max = 4680 seconds
Kitchen	min= 5 seconds ; max = 240 seconds
Toilet facilities	min= 20 seconds ; max = 480 seconds
Printer	min= 5 seconds ; max = 63 seconds
Average percentage of active person per hour	Single person active = 17.7% of time two persons active = 11.6% of time three persons active = 3.0% of time four and more persons active = 2.3% of time No person active = 65.5% of time

4.4 Numerical simulations

There is a need to be able to model pedestrian dynamics in civil engineering structures, for analysis of their vibration serviceability. The reasons are: 1) complex behaviour of human occupants of structures, such as floors, which is quite ran-

dom and hence simplifications do not result in a suitable and accurate design; 2) anticipated patterns of loads and scenarios and plan for changes at design stage are achieved via realistic modelling; and 3) multiple pedestrian loading patterns should be developed for vibration serviceability assessment; currently available approaches neglect this aspect.

Microscopic and macroscopic models are the two common models to simulate pedestrians. Microscopic models treat each person in the virtual model as an autonomous agent (i.e. person), which occupies a certain space in time. This model accounts for factors that drive each pedestrian to their goals and also interact with the surroundings, such as social force model [102] and agent based modelling [101]. On the other hand, macroscopic models basically consider pedestrian movement as a continuous flow, which relies on the aggregate behaviour of pedestrians as a whole. Hence, microscopic models provide valuable insight into individual pedestrians performance movements in a realistic way [104].

In an actual floor environment pedestrians tend to contribute their walking-induced forces differently along walkable routes, for there are human variabilities in walking speed, pacing frequency, weight and so on. This has been demonstrated in previous sections, which implies that a multi-person model is more realistic. Modelling of crowds walking on footbridge structures have been developed by a number of studies, such as [67, 104]. However, the fundamental simulation framework has not yet been extensively extended to model in-service floors, which can be used for any other floor layouts at design stage. Therefore, this section presents a detailed numerical modelling and simulation of multiple person on the aforementioned office floor.

4.4.1 Multiple pedestrian modelling framework

Virtual models of pedestrians are widely used as a means of analysing occupant movements whilst using a particular environment for different purposes, such as panic simulation or emergences response [144]. However, for engineers, the purpose tends to be in the form of assessing the efficiency and suitability of various building layouts [104]. In particular, how multiple people whom accommodate a floor are navigating at any particular time. Hence, it is imperative to generate simulations of large numbers of autonomous and intelligent pedestrians interacting in normal-life situations, i.e. to mimic reality.

Decision making, path planning and navigation are the key components of a virtual model, where pedestrians can move as autonomous and interacting agents. In this study, the decision making aspect is implemented via an agent based model [101]. This ensures that the pedestrians make decisions by choos-

ing a task or a destination goal at any time. Path planning computes sequences of intermediate goals needed to reach a pedestrian's ultimate destination. The Dijkstra's shortest path algorithm [145] is used in this work. The navigation determines how a pedestrian moves to each intermediate goal before finally reaching its final destination. This is established via social force modelling [102, 103, 146], to prevent collisions between pedestrians and other obstacles. A schematic flow chart of the simulation modelling is shown in Figure 4.21.

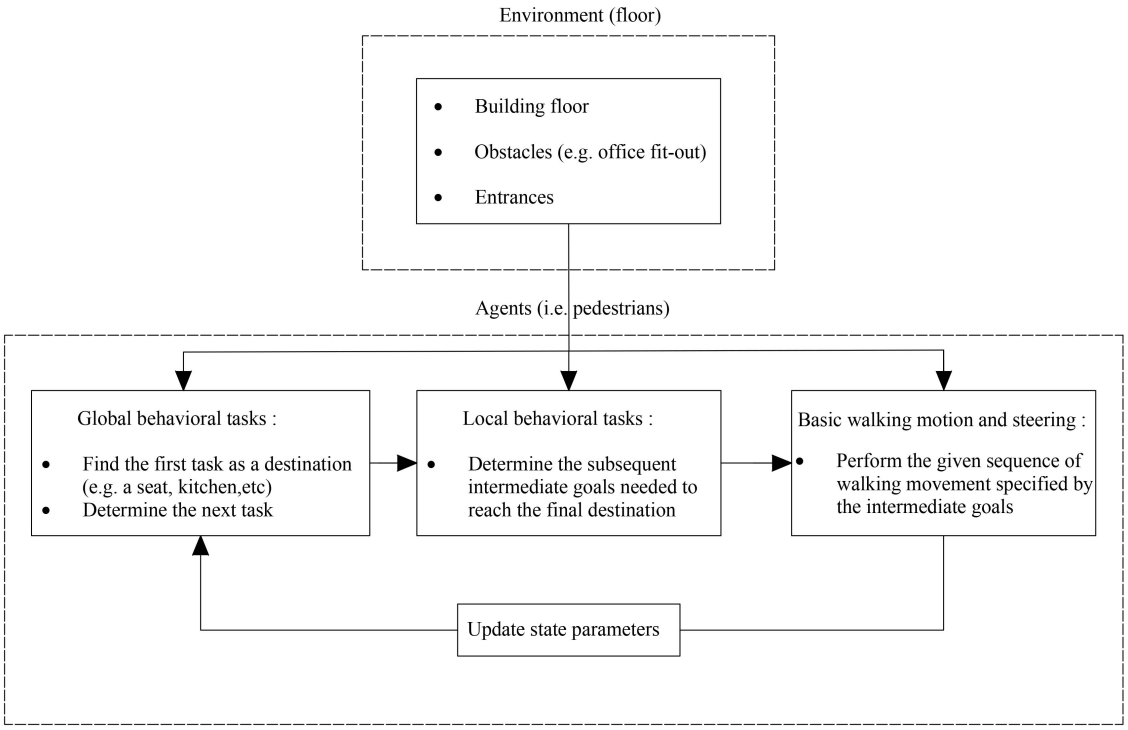

Figure 4.21: Schematic flow chart of numerical modelling of multiple pedestrians.

A pedestrian walking within a floor environment is subject to various social and physical forces as described by [102], which is assumed to follow the laws of Newtonian mechanics. The behavioural rules are modelled as forces, which each pedestrian feels and exerts on others. The social forces indicate the intention of a person to move at a given speed towards a goal in a specific direction, whilst not colliding with other people and/or with obstacles. When a person becomes close to other people or a wall that s/he is about to collide, the physical forces of pushing and friction come into account [103, 146]. In mathematical format, the change of velocity in time t is given by the acceleration in Equation 4.5 [102]. The change of position $\mathbf{r}_i(t) = \{x(t), y(t)\}_i$ is given by the velocity $\mathbf{v}_i(t) = \mathrm{d}\mathbf{r}_i/\mathrm{d}t$. Here, bold colour represents vectors.

$$m_i \frac{\mathrm{d}\mathbf{v}_i}{\mathrm{d}t} = m_i \frac{\mathbf{v}_i^0(t) - \mathbf{v}_i(t)}{\tau_i} + \sum_{i \neq j}^{N_p} \mathbf{F}_{ij}^{ped} + \sum_{w} \mathbf{F}_{iw}^{boundary} \tag{4.5}$$

where, each N_p pedestrian i of mass m_i desires to move at a certain speed $\mathbf{v}_i^0 = \{v_x^0, v_y^0\}_i$ and as such the pedestrian adapts to his/her actual velocity $\mathbf{v}_i = \{v_x, v_y\}_i$ with a certain characteristic time τ_i equal to 0.5 s. This is termed as the desired or driving force.

The term $\mathbf{F}_{ij}^{ped} = \{F_x^{Ped}, F_y^{Ped}\}_{ij}$ represents the repulsive force of pedestrians i and j, which they try to keep a distance from each other by a repulsive interaction force. This is shown in Equation 4.6 [102].

$$\mathbf{F}_{ij}^{ped} = \left[A_i\, e^{(r_{ij}-d_{ij})/B_i} + k_1 g(r_{ij}-d_{ij})\right]\mathbf{n}_{ij} + k_2 g(r_{ij}-d_{ij})\Delta\mathbf{v}_{ij}^T\mathbf{t}_{ij} \tag{4.6}$$

where, $A_i, A_w, B_i and B_w$ are constants [103] that determine the strength and range of social interaction. $d_{ij} = ||\mathbf{r}_i - \mathbf{r}_j||$ denotes the distance between centres of pedestrians, and $\mathbf{n}_{ij} = (\mathbf{r}_i - \mathbf{r}_j)/d_{ij}$ is the normalised vector from pedestrian j to i [144]. Let the radius of the i-th and j-th pedestrian be denoted by r_i and r_j, respectively and hence $r_{ij} = r_i + r_j$. When the pedestrians are within the range of $d_{ij} < r_{ij}$, the pushing force of $k_1 g(r_{ij} - d_{ij})\mathbf{n}_{ij}$ and the friction force $k_2 g(r_{ij} - d_{ij})\Delta\mathbf{v}_{ij}^T\mathbf{t}_{ij}$ should be added to the pedestrian force. $k_1 = 120000$ kg/s^2 and $k_2 = 240000$ kg/ms are constants [103]. $\Delta\mathbf{v}_{ij}^T = (\mathbf{v}_i - \mathbf{v}_j)^T$ is (transpose of) the change of velocity and $\mathbf{t}_{ij} = \{-\mathbf{n}_{ij}(2), \mathbf{n}_{ij}(1)\}$. The function $g(r_{ij} - d_{ij})$ only plays roles when the pedestrian contacts with others.

The $\mathbf{F}_{iw}^{boundary} = \{F_x^{boundary}, F_y^{boundary}\}_{iw}$ incorporates any possible obstacles or boundaries on individual i. This expression is similar to the forces between pedestrians, by substituting the quantities d_{iw}, $\mathbf{n}_{iw}$, $\mathbf{t}_{iw}$ and $\Delta\mathbf{v}_{iw}$ into the aforementioned equations and the coordinate of the closest point of the obstacles or walls is written instead of $\mathbf{r}_j$ and setting $\mathbf{v}_j$ to zero. This is shown in Equation 4.7 [102].

$$\mathbf{F}_{iw}^{boundary} = \left[A_w\, e^{(r_i-d_{iw})/B_w} + k_1 g(r_i - d_{iw})\right]\mathbf{n}_{iw} + k_2 g(r_i - d_{iw})\Delta\mathbf{v}_{iw}^T\mathbf{t}_{iw} \tag{4.7}$$

As far as values of $A_i, A_w, B_i and B_w$ are concerned, the original values suggested by [102] were set to $A_i = A_w = 2000$ N and $B_i = B_w = 0.08$ m. However, a number of studies have chosen a range of values based on the environment where occupants interact and as such they can take on a series of discrete values [147]. Therefore, the values used in the following simulations are as follows. For constants in pedestrian interactions $A_i = 1500$ N and $B_i = 0.08$ m were used, while for boundary constants $A_w = 3000$ N and $B_w = 0.02$ m were selected [147]. These values resulted in better manoeuvring for the pedestrians during simulation than the original values.

4.4.2 Pedestrian tasks and probabilistic parameters

This section presents the characteristics of pedestrians used in the simulation. The desired speed is assumed to follow a normal distribution with mean of 1.22 m/s and standard deviation of 0.23 m/s (see Figure 4.20). $\mathbf{r}_i$ is computed from a sequence of intermediate goals encoding the desired pedestrian path. The radius r_i and the mass m_i of each pedestrian have been randomly generated (assuming normal distribution) in the intervals of [0.25 m, 0.35 m] and [60 kg, 90 kg], respectively [103].

Four main tasks were defined in the numerical simulation that pedestrians will execute during the simulation; task one is take a seat, task two is use the kitchen, task three is use the toilet facilities and task four is use the printer. The sequence of tasks is randomly generated; task seat would happen more often than other tasks as pedestrian sit for a long duration. For example, a pedestrian finds a seat and dwells for a duration of time, which is randomly generated, assuming uniform distribution (see Table 4.3). When their task is fulfilled, the pedestrian would either remain or s/he would choose another task and execute it for a duration. This sequence of completing tasks remains active for the duration of the simulation.

The office floor chosen for the analysis (see Figure 4.1) was modelled in MATLAB using its actual floor dimensions and architectural layout. The model is illustrated in Figure 4.22. The two main gates were treated as an entrance when the simulation begins and also as exit when the simulation finishes; their percentage of use was with respect to Table 4.3. The arrival and exit time were selected as per normal distribution shown in Figure 4.19. The simulation was set up and run in MATLAB release 2018a [143] on Windows 10 PC with intel core i7 processor and 16GB RAM.

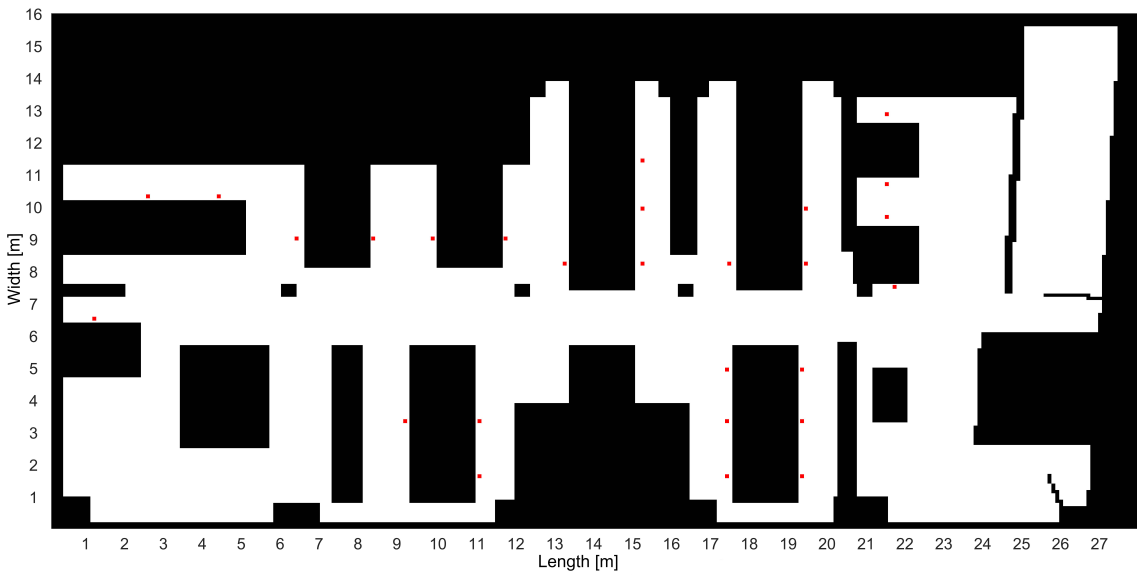

Figure 4.22: Office floor numerical model with seats.

4.4.3 Numerical walking paths

The numerical simulation was run for 27 pedestrians, similar to the actual floor, using seat locations as illustrated in red colour in Figure 4.22. The time elapsed for a 10-hour run is one hour and 35 minutes and the MATLAB file size is about 2-3 GB. This is computationally very demanding to store data in each run. All tasks performed by individuals are defined in a statistical manner (i.e. assuming normal and uniform distributions based on aforementioned discussions), thus ensuring realistic patterns. As mentioned earlier, randomised timings of tasks were defined. For example, uniform distribution was assumed to find timings of pedestrian seats using the values in Table 4.3. This was done so that the selection of any particular walking trip is randomised and as such the number of active pedestrians at any time reflects reality in an overall sense.

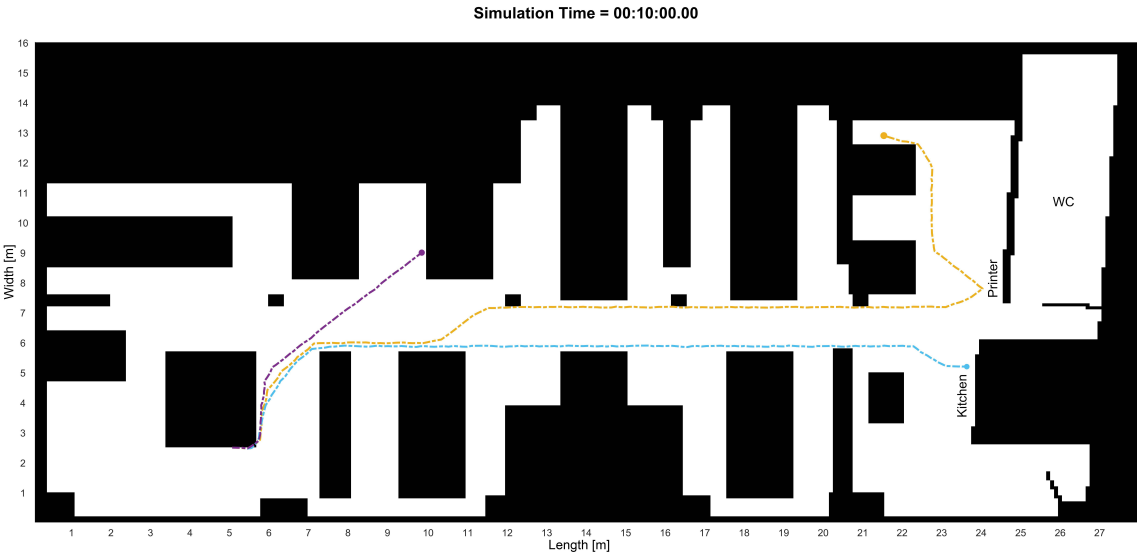

(a) Pedestrian entrance

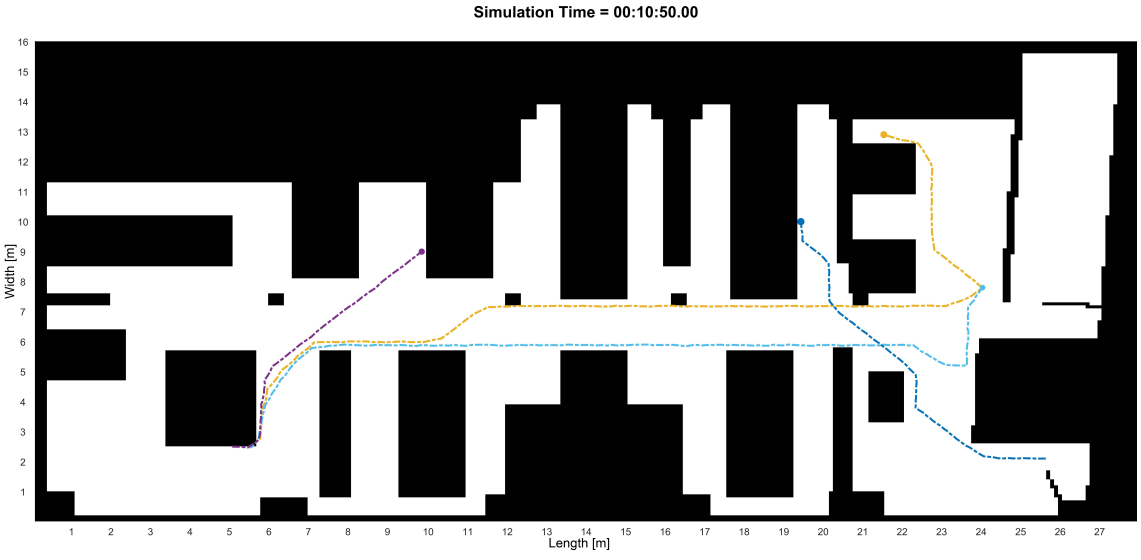

(b) Active pedestrians

Figure 4.23: Pedestrian activities in numerical simulation.

Figure 4.23a shows a screen shot from the analysis when pedestrians have entered into the floor area and taken a position at a designated seat or in the kitchen area. Figure 4.23b illustrates the case when some pedestrians are carrying out task one (sitting at desk), whereas others are either actively walking or carrying out task two (kitchen) and task four (at printer).

The location time histories for all pedestrians are stored and can be extracted for further analysis. All walking paths for 10 hours simulation for individual pedestrians are shown in Figure 4.24, which indicates pedestrian manoeuvring in a logical way, i.e. avoiding obstacles and boundaries.

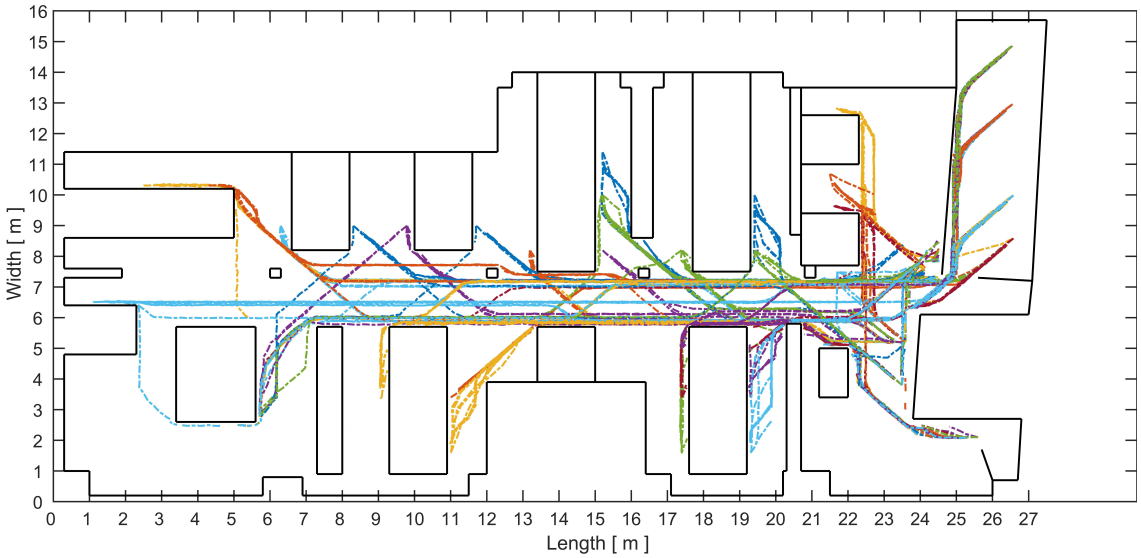

Figure 4.24: Numerical walking paths for individual occupants.

The heatmap of pedestrian walking paths also can be useful in revealing and highlighting which paths are used most. A number of runs were performed since the simulation is derived from a probabilistic approach and as such two typical results are shown in Figure 4.25. The heatmap in Figure 4.25a is obtained from all numerical walking paths as presented in Figure 4.24. It is worth noting that the heatmap shows high values around the columns or desks, this is due to the nature of a heatmap and interpolation of the data. In fact, the individual walking paths show that pedestrians are avoiding those obstacles as shown in Figure 4.24. Another reason could be Dijkstra's shortest path used in the numerical model. This is a grid-based method, which can be improved to a more advanced method such as A-star pathfinding and navigation mesh. The two heatmap results are very similar, giving confidence in the statistical approach to generate the walking paths and heatmaps. By comparing Figure 4.18 with the heatmaps derived from simulations in Figure 4.25, it can be seen there is a good similarity. In terms of total number of crossings, there is an error of less than 15%, which is deemed acceptable considering the complexity of the model. This implies that the simulation could potentially be used at design stage for analysis of floors with multiple occupants.

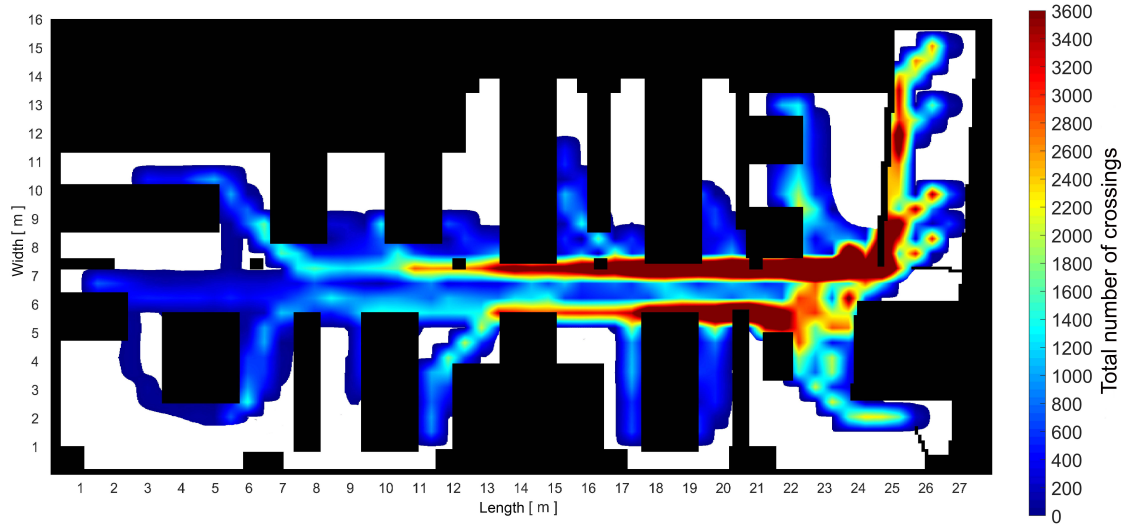

(a) Numerical walking path heatmap first run

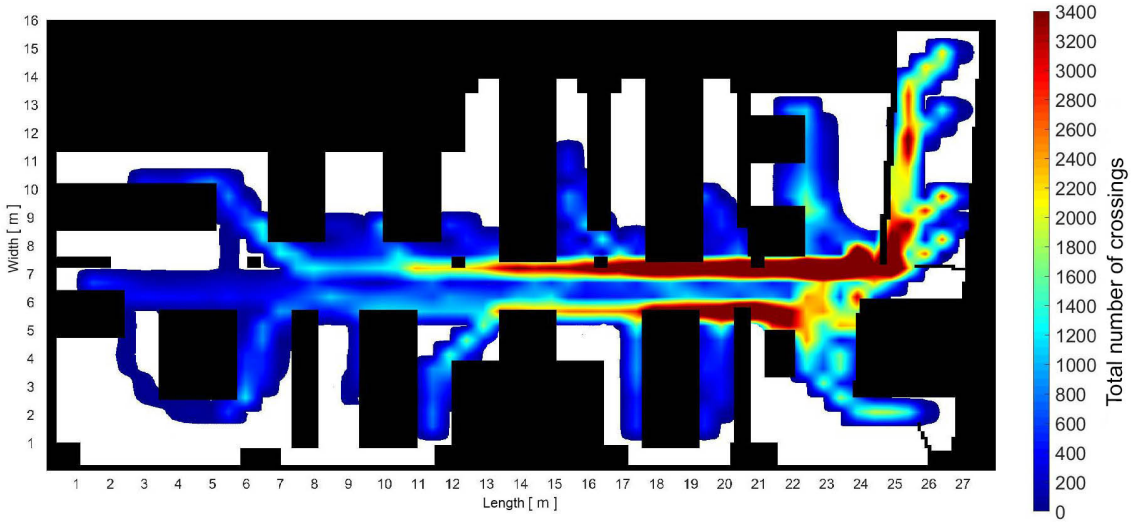

(b) Numerical walking path heatmap second run

Figure 4.25: Pedestrians activity in numerical simulation.

As far as pedestrian walking at the same time is concerned, Table 4.4 shows the outcomes from the aforementioned simulations. Only the results of the first simulation is considered here. The percentage of active person per an hour of the simulation, on average, over the floor area illustrates that a single person is 18.1% of time active on the floor. This has an error of 2.2% in comparison with actual observations in Table 4.3. Two or more persons are active for 14.3% of time in the simulation. Therefore, these values show that the pedestrian pattern model can mimic reality to a good degree, despite some differences which are acceptable taking into account the complexity of the model.

Table 4.4: Numerical simulation data analysis

Task location	Active time
Average percentage of active person per hour	Single person active = 18.1% of time two persons active = 10.3% of time three persons active = 2.2% of time four and more persons active = 1.8% of time No person active = 67.6% of time

4.5 Conclusions

This chapter has presented the outcomes of experimental in-service monitoring and novel numerical simulation of pedestrian movements in a real-world office floor. The experimental data illustrated that operational vibration responses under multiple pedestrians may be higher and have different characteristics than those from a single pedestrian. This provides an insight into relatively poor performance of current design approaches based on single pedestrian excitation.

Therefore, it was ascertained that loading patterns from multiple pedestrians should be utilised at the design stage for prediction of vibration serviceability, for which there is little consideration in the available design procedures. To achieve this, a numerical model has been developed on the basis of an agent-based model of pedestrian movements. The model generates pedestrian walking patterns in a stochastic manner, which resemble reality more closely in terms of events and locations than the arbitrary paths that are typically assumed in current design practice. It is proposed that this methodology can be further developed to provide reliable vibration serviceability predictions of floors under loading for multiple pedestrians.

The aforementioned pedestrian pattern model will be employed in spatial response predictions in Chapter 6. The aim will be to obtain vibration responses under multiple pedestrians and compare those predicted against measured data.

Chapter 5

A Unified Probabilistic Multiple Pedestrian Walking Load Model

This chapter presents a probabilistic walking load model based on a large database of continuously recorded walking forces on an instrumented treadmill for significant numbers of individuals. The model advocates using a statistical approach for generating time domain walking forces for individual and multiple pedestrians based on pedestrian walking speed. The frequency domain components of the model have features of measured walking in exhibiting the narrow band random process, which is vital for reliable vibration serviceability assessment. The content of this chapter, in a slightly amended form, has been submitted to Advances in Civil Engineering under the following title:

Muhammad, Z.O. and Reynolds, P. “Probabilistic multiple pedestrian walking force model including pedestrian inter- and intra-subject variabilities” and it is under review.

5.1 Introduction

Contemporary civil engineering structures, such as slender floors, footbridges, manufacturing facilities and operating theatres, occupied and dynamically excited by human footfall loading, require the critical design aspect of vibration serviceability to be evaluated via prediction of vibration responses and subsequent performance assessment. In the particular case of floors, present and contemporary guidance methodologies [5–8] are often followed to assess vibration serviceability. However, even if properly applied, the outcome may be unsatisfactory, leading to a knock-on effect on building or facility owners and thus litigation [82]. The key reasons for this are (1) the lack of adequate and accurate design procedures in contemporary design guidelines as presented in Chapter 3, (2) a lack of appreciation of the importance of vibration serviceability design dominance relative to other design parameters, such as strength and deflections, (3) the lack of a probabilistic modelling strategy to account for variability of excitation source and hence representative footfall loading model, and (4) the lack of appropriate assessment criteria for subjective human perception, as covered in Section 2.5. These, by nature, lead to a major challenge in modern floor design whereby the prediction of vibration responses under human-induced footfall remains demanding and uncertain[148].

Vibration analysis of floors, in design guidance documents [5–7], are commonly addressed based on a frequency threshold of first mode natural frequency. This threshold, accepted as around 10 Hz, results in two classes of floors, low frequency floors (LFF) if below the threshold and high-frequency floors (HFF) if above the threshold, irrespective of the function and usage of the floor. Forced vibrations for LFF are assumed to be deterministic, even though CSTR43 App G and CCIP-016 introduce the concept of 25% probability of exceedance on DLFs. As such the floor develops a resonant response by harmonic components of the force, whereas HFFs are assumed to undergo transient response under impulsive footfall loading. However, Chapter 3 and these studies [34, 82, 97] have shown that design guidelines do not work in many cases and require major improvements in all aspects, particularly in walking load models and design scenarios. This is owing to the fact that all the models assume walking as deterministic. The walking force is, however, not deterministic due to random variabilities inherent in real walking.

There have been a number of attempts to develop reliable synthetic walking load models by a single pedestrian for vibration serviceability assessment, such as a stochastic load model using a number of Gaussian curves by [35]. This model relies on random parameters being drawn from an experimental database, resulting in a detailed representation of a continuous walking force. However,

access to the experimental database is a prerequisite to implement the above model, which is not available to the public domain. As far as Fourier-based models are concerned, it is reported that the Fourier approach results in loss of information and introduction of inaccuracies for individual and multiple pedestrians [35]. All of these walking load models, including those from design guidelines covered in Chapter 3 tend to generate a continuous force time history rather than individual steps from both footfalls. A walking model based on individual footfalls might better describe the mechanism of walking and its parameters, as discussed in Section 2.3.1.2. Therefore, the aforementioned load models do not tend to reflect the true nature of pedestrian excitation, which has potential for the variation in pacing frequency at the same velocity or walking speed. A potential load model can be established on the basis of right and left or strong and weak legs, which could serve both single and multiple pedestrian loading scenarios. This in turn can be used as a unified load model for a wider frequency range. This could be achieved via a probabilistic framework that accounts for the inter- and intra-subject variability in the walking force modelling as well as the potential excitation at different walking speed.

The model developed in this chapter advocates using a statistical approach for generating time domain walking forces from individual steps (right and left footfalls) for individual and multiple pedestrians based on pedestrian walking speed. The established model can be reproduced from the data and equations illustrated in the following sections. In addition, the model can be used in discrete footfall analysis when individual steps are applied on different structural components. It can be implemented in any finite element (FE) package for vibration serviceability analysis. This can facilitate the application of individual walking step forces at sequential spatial positions along any walking paths. The frequency domain components of the model have features of measured walking in exhibiting the narrow band random process, which is vital for reliable vibration serviceability assessment. The model is developed based on a large database of continuously recorded walking forces on an instrumented treadmill for significant numbers of individuals. The measured database, to the authors best knowledge, is the most comprehensive collection of continuous walking forces available in the literature. The modelling strategy is followed by extracting key points on the shape of measured footfalls to develop statistical relationships for right and left steps of an individual. Therefore, the chapter presents a new unified probabilistic walking load model, which could be utilised for both LFFs and HFFs.

5.2 Continuous measurement of walking data on instrumented treadmill

Developing a realistic walking load model requires a wide range of continuously measured actual walking forces for different pedestrians, so as to retain the essence of the inherent variabilities of real walking. The measured database used in this chapter has previously been discussed and utilised by [35], but some key points are mentioned in this section.

Right and left footfalls of each person were continuously and independently recorded on an instrumented split-belt treadmill sampled at 200 Hz. The acquisition of walking records was not prompted by any stimuli such as a metronome, but instead was controlled by the treadmill speed (i.e. constant treadmill speed), which started from 0.56 m/s and increased in increments of 0.14 m/s up to the maximum comfortable walking speed. This is an inherent limitation of force measurement using instrumented treadmills. Walking forces corresponding to ten different walking speeds were collected for each person. Each person has different maximum speed due to their overall height and leg length. Each test was completed when at least 64 successive footfalls were acquired. In total 852 vertical walking forces were collected for 85 people. Their characteristic mean and standard deviation of body mass, height and age are 75.8 $\pm$ 15.2 kg, 174.4 $\pm$ 8.2 cm and 29.8 $\pm$ 9.1 years, respectively. The reader is referred to [35, 82] for more detail. In this chapter only 600 walking forces were used to develop the load model, for walking below 0.8 m/s and above 2.2 m/s have low probability [149]. A typical measured walking force time history is illustrated in Figure 5.1.

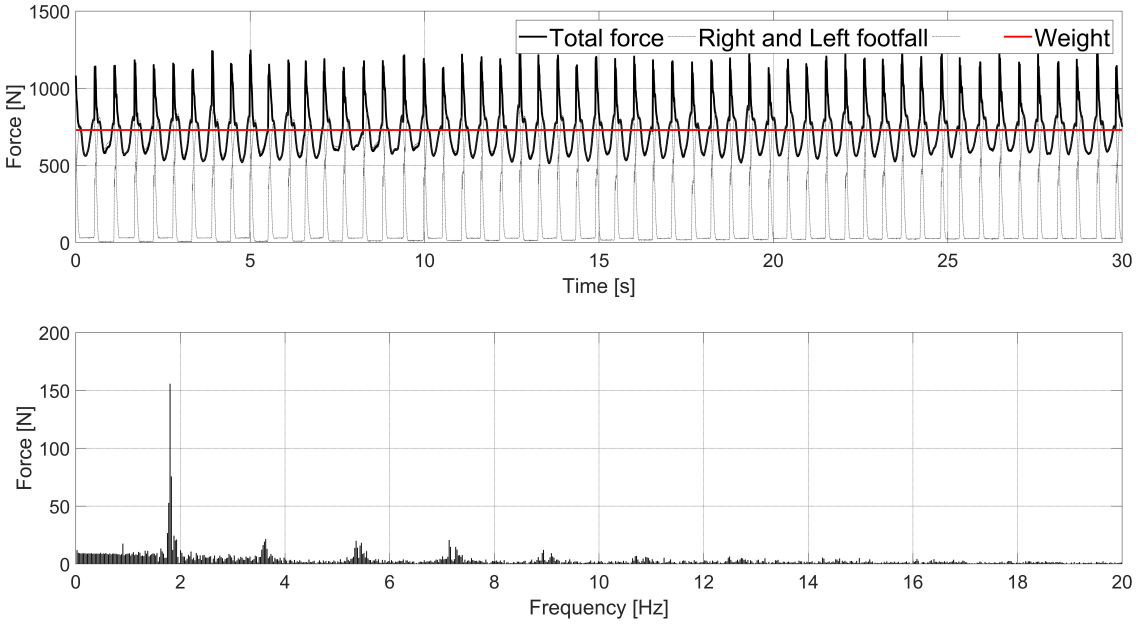

Figure 5.1: Walking force time history and Fourier spectrum at speed 1.341 m/s.

5.3 Modelling strategy of individual walking steps

This section presents the concept of the modelling approach for each footfall from analysis of the continuous measured walking. Right and left footfalls are considered separately to extract time and load components based on a single step. Establishment of these two components is based on the aforementioned measured data generated by a diverse range of pedestrians, which will provide statistical reliability in the consideration of both inter- and intra subject variabilities.

5.3.1 Key parameters for the walking step

1. **Walking speed**: walking speed has a large effect on temporal and spatial parameters of walking, and hence is considered a significant parameter in this model for a number of reasons. Firstly, numerous studies have characterised relationships between walking speed and stride-length, step-length, step-width and pacing frequency [59, 150]. Secondly, pedestrians naturally walk at different velocities that in an effortless way increase or decrease pacing frequency and spatial parameters [150]. Thirdly, individuals walking at the same speed have different excitation dynamic forces as well as different walking parameters, which could be hard to account for individually in any forcing function. Therefore, walking speed tends to be a global parameter that is inherently capable of defining distributions of several walking (temporal-spatial) parameters, which are vital in producing walking forces. The walking load model in this chapter considers walking speed as the input parameter due to the aforementioned observations, unlike any existing walking models. In this study, the range of walking speed is between 0.8 m/s for slow walking and 2.2 m/s for fast walking. These values, based on [59]'s observations, correspond to the pacing frequency of 1.4 ± 0.1 Hz and 2.3 ± 0.1 Hz, respectively.

2. **Step contact time**: step contact time or stance time is the time when a foot is in contact with the ground. The step contact time itself depends on walking speed, as presented in the next section. This will later be used in deriving relations of control points on a step. Figure 5.2 shows the shape of the force of a single walking step, where there are five main control points. The start point, which has zero load and time. The first peak load, which is the first local peak amplitude of the force. The second peak load, which is the second local peak amplitude of the force on the shape of a walking step. The valley load, which is the trough or a low point on the shape of a walking step between first peak and second peak. Also, the step contact time, which

is the last point. Any points in between these main points are called intermediate points. The intermediate points are those points that lie between first peak point and valley point or valley point and second peak point, which will be discussed later. The right and left footfall shapes are represented using a set of intermediate and control points, which have different values, probabilistically generated using mean and standard deviation, for each footfall of walking.

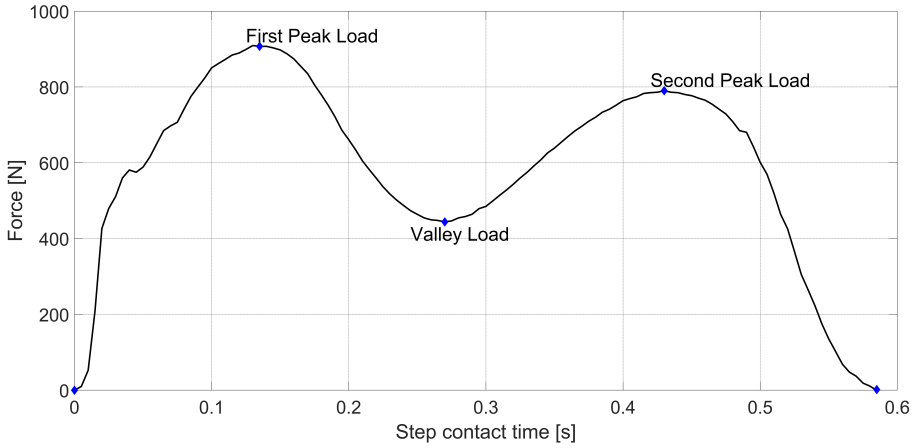

Figure 5.2: Shape of a measured walking step with time and load components.

3. **Overlap time between two consecutive steps**: overlap time or double support time is the time when both feet are in contact with the ground simultaneously. The overlap time depends on both walking speed and step contact time, based on the analysis of the measured data discussed later.

5.3.2 Timing component of a step

This section provides a statistical description of the timing components of the control points on the shape of a walking step. The relations are derived between walking speed and step contact time as well as the points described in Figure 5.2. Statistical relationships among pedestrians were also formulated to account for inter-and intra-subject variabilities in the form of probability distribution functions.

5.3.2.1 Step contact time relationship

There is a linear relationship between the walking speed and step contact time based on the aforementioned measured data, as shown in Figure 5.3. Each measured data point corresponds to an individual at that particular walking speed. It can be seen that the step contact time decreases with an increase in the walking speed. The measured data were extracted for each person's footfall for the

duration of measured walking using gradient point (i.e. slope at that point) in MATLAB. The gradient of a line is a number that describes both the direction and the steepness of the line between two points. A margin of error equal to $2dt$, where $dt = 0.005$ s, was introduced in the gradient point to achieve the lowest (ideally zero) slope due to the effect of noisiness in the data and thus obtaining a better estimate of beginning and ending of a step. Both the beginning and ending of a footfall were obtained separately and the subtraction of them gives an estimate of the step contact time. The measured data shown in Figure 5.3 are the mean values for each person for both footfalls (i.e left and right footfalls). The theoretical mean is the best fit with a high value of R^2, which indicates the goodness of fit or degree of linear correlation of the model.

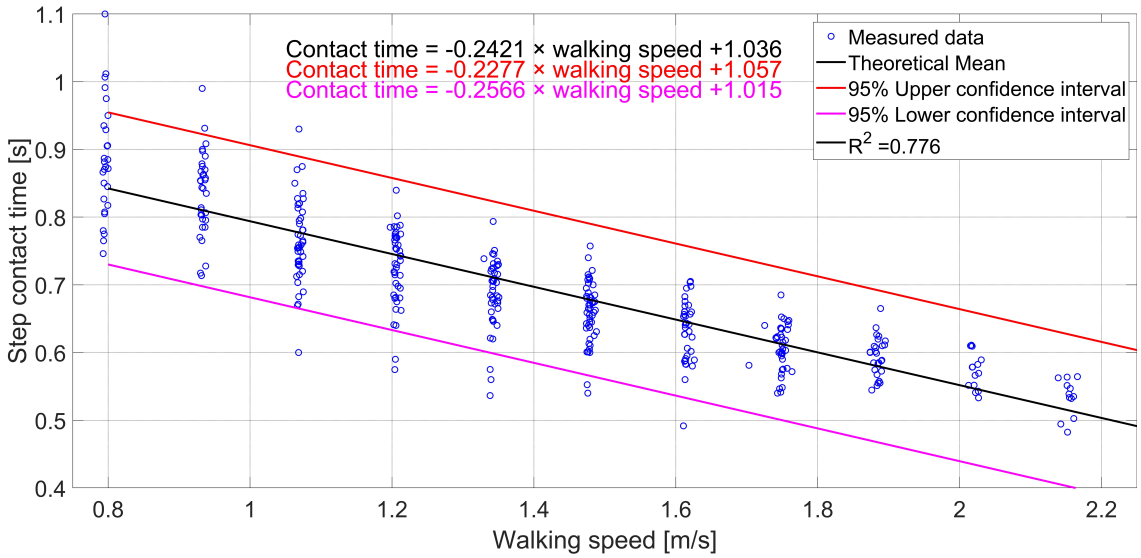

Figure 5.3: Statistical relationship between walking speed and step contact time.

Subject variabilities can be observed from the measured data and as such this chapter takes into account both inter- and intra-subject variabilities. Inter-subject variations, which exist between pedestrians, are represented by a normal distribution through mean (μ) and standard deviation (σ). The $\mu_{\text{inter-subject contact}}$ is obtained by the theoretical mean of Figure 5.3, whereas $\sigma_{\text{inter-subject contact}}$ is computed for each walking speed using both μ and σ. Since these two values are different, coefficient of variation (CoV) was calculated, which is μ divided by σ. Averaging the CoV and relating that to the mean will give the standard deviation. Thus, $\sigma_{\text{inter-subject contact}}$ is, among individuals, an average value of 6.61 % of $\mu_{\text{inter-subject contact}}$. As far as intra-subject variations are concerned, which occur within the same pedestrian, μ and σ are calculated for each person based on measured data, having $\mu_{\text{intra-subject contact}}$ of 0.0 s and $\sigma_{\text{intra-subject contact}}$ of 0.0138 s.

5.3.2.2 First peak time, Valley time and Second peak time

First peak time, valley time and second peak time of right and left footfalls are calculated as a function of step contact time as illustrated in Figures 5.4, 5.5 and 5.6. Using step contact time for all timing components is utilised due to the fact that first peak time, valley time and second peak time are all proportions of a step contact time. The reason for both footfalls is to preserve the intra-subject variabilities that are innate in actual walking and as such each footfall has its own formula. With an increase in the step contact time, the timing components increases, which is due to the slow walking. These timings are the key control points in defining the intermediate points in between them.

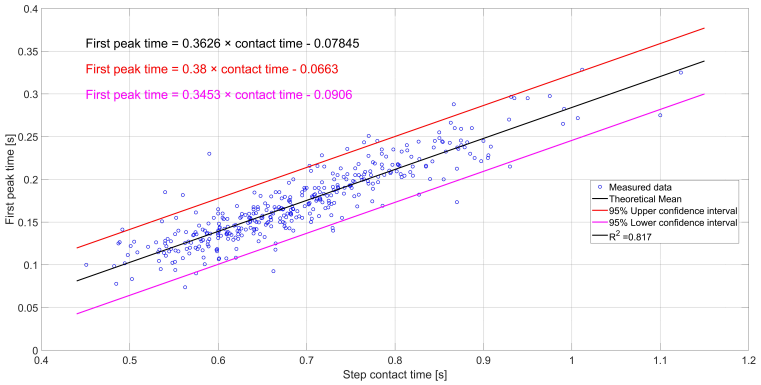

(a) Right footfall

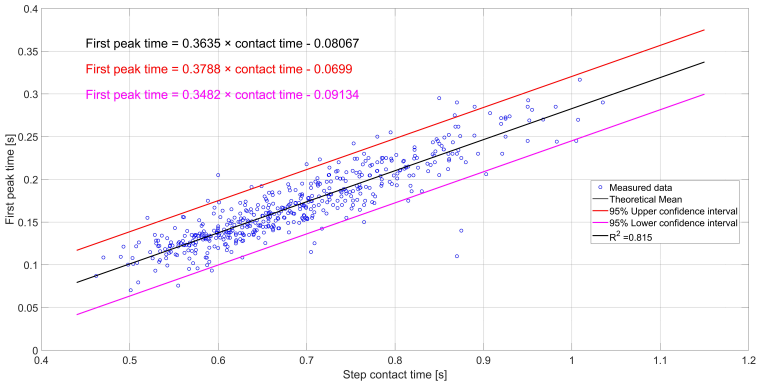

(b) Left footfall

Figure 5.4: Statistical relationship between step contact time and first peak time.

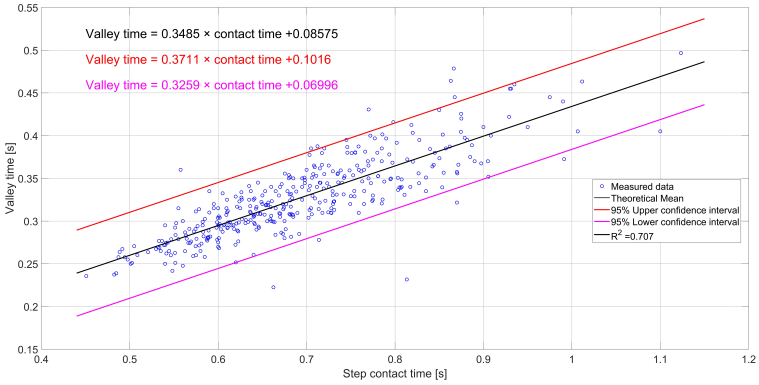

(a) Right footfall

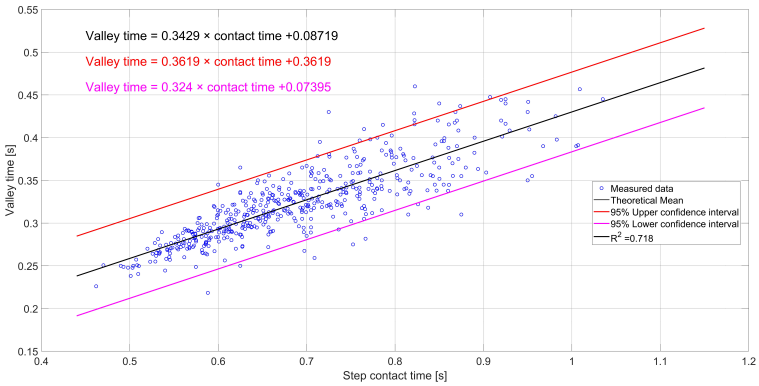

(b) Left footfall

Figure 5.5: Statistical relationship between step contact time and valley time.

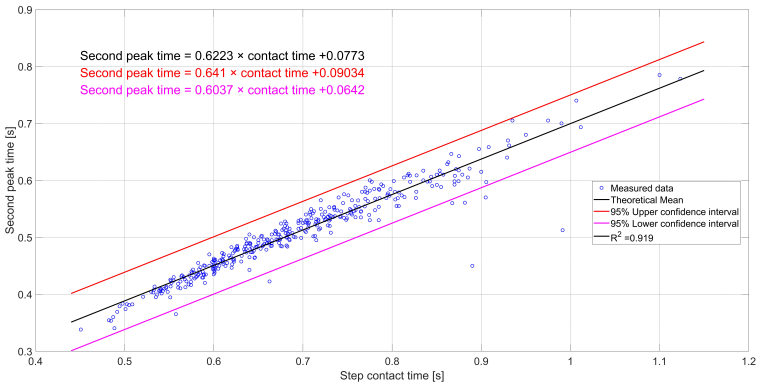

(a) Right footfall

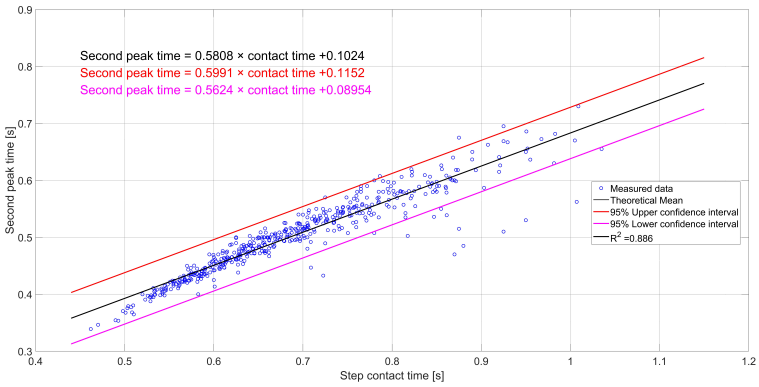

(b) Left footfall

Figure 5.6: Statistical relationship between step contact time and second peak time.

5.3.3 Loading component of a step

The relationship between walking speed and loading components of a step can be observed from the measured data. Figure 5.7 shows that first peak load (normalised by body weight) is dependent on walking speed. Statistical relationships among pedestrians were also formulated to account for subject variabilities in the form of probability distribution functions, which are assumed to follow normal distributions based on measurement observations. Therefore, $\mu_{\text{inter-subject 1st peak}}$ is given by the theoretical mean of Figure 5.7 for right and left footfalls, whereas $\sigma_{\text{inter-subject 1st peak}}$ is computed with an average value of 0.0772 and 0.06464 (units of first peak load) for right and left footfalls, respectively. As far as intra-subject variations are concerned, μ and σ are calculated, based on measurement, for right and left footfalls as $\mu_{\text{intra-subject 1st peak}}$ of 0.02929 and 0.0339 and $\sigma_{\text{intra-subjective 1st peak}}$ of 0.0218 and 0.01596 (units of first peak load), respectively.

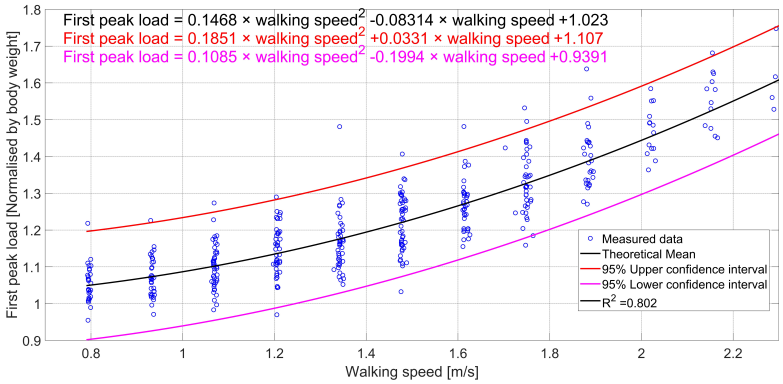

(a) Right footfall

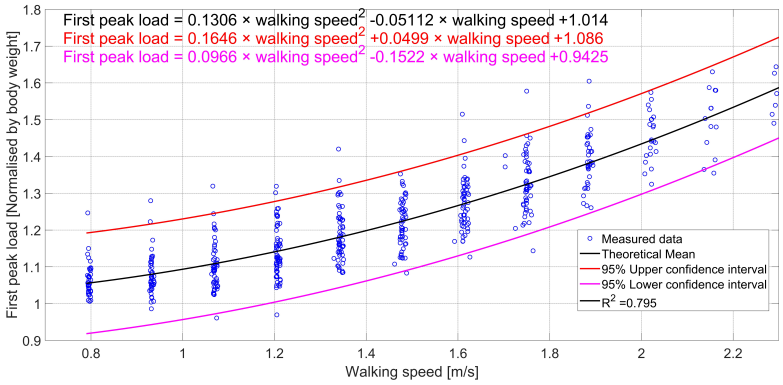

(b) Left footfall

Figure 5.7: Statistical relationship between walking speed and first peak load.

Similar relationships can be developed for the valley load, as shown in Figure 5.8. Normal distribution was assumed to govern the inter- and intra-subject variabilities, which was also in line with the measurement observation. Therefore, $\mu_{\text{inter-subject valley}}$ is given by the theoretical mean of Figure 5.8 for right and left footfalls, whereas $\sigma_{\text{inter-subject valley}}$ is computed with an average value of 0.0505 and 0.0484 (units of valley load) for right and left footfalls, respectively. As far as intra-subject variations are concerned, μ and σ are calculated for right and left footfalls as $\mu_{\text{intra-subject valley}}$ of 0.01923 and 0.0231 and $\sigma_{\text{intra-subject valley}}$ of 0.013 and 0.0104 (units of valley load), respectively.

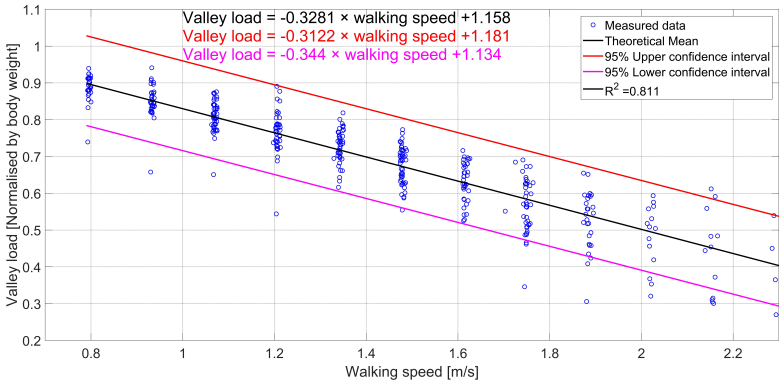

(a) Right footfall

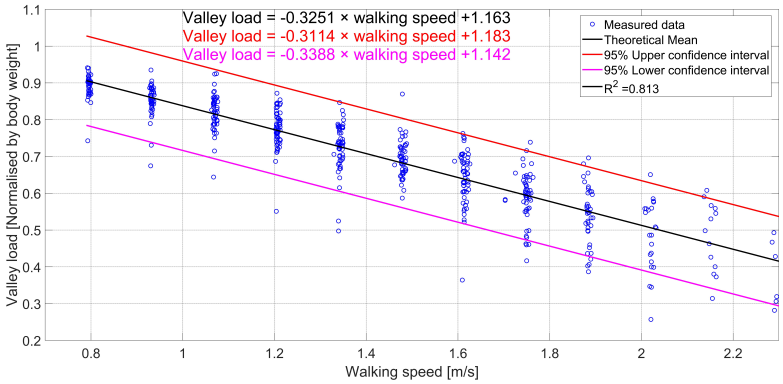

(b) Left footfall

Figure 5.8: Statistical relationship between walking speed and valley load.

As far as second peak load is concerned, the relationship is such that the second peak load depends on both walking speed and first peak load as shown in Figure 5.9. This is due to the goodness of fit, where poor relationships would result if the second peak load was derived only based on walking speed (this is not shown here for clarity). The inter-subject variabilities have already been taken into account because of dependence on the first peak load. The intra-subject variabilities, on the other hand, follow a normal distribution with μ and σ calculated for right and left footfalls as $\mu_{\text{intra-subject 2nd peak}}$ of 0.0352 and 0.0368 and $\sigma_{\text{intra-subject 2nd peak}}$ of 0.01895 and 0.01862 (units of second peak load), respectively. It is worth pointing out that this model assumes independent probability distribution of individual parameters featuring in the model and human-structure interaction (HSI) is not included.

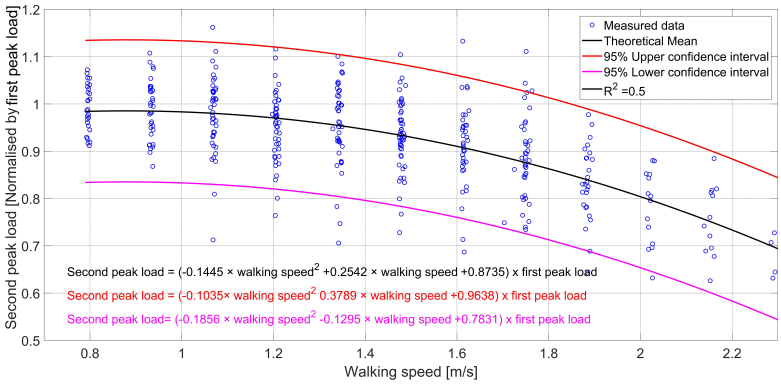

(a) Right footfall

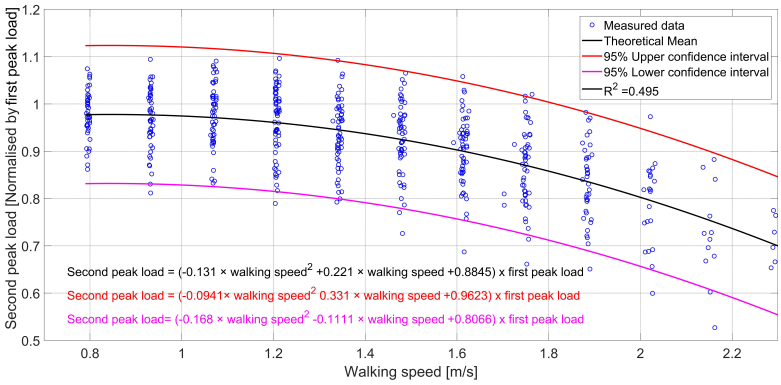

(b) Left footfall

Figure 5.9: Statistical relationship between walking speed and second peak load.

5.3.4 Model development methodology

The control points established in the aforementioned sections are critical in defining the rest of the points. The intermediate points relationships are mainly dependent on the above main control points. For example, points between beginning of a step and first peak point were estimated based on the proportion of the first peak load and/or first peak time. These criteria were set after a significant number of trials (by the author) when visually checking the walking measurements. For instance, second point (P2) is at 1% of first peak load and $\frac{1}{7.5}$ of first peak time. Third point (P3) is at 1.2% of first peak load and $\frac{1}{5.1}$ of first peak time. Satisfying both of these conditions was selected to extract the points. Similarly for all the other points different conditions were set to extract the rest of the points. This was done to capture the changes on the beginning of the step as the force value increases. For points between first peak and valley point, the conditions were: point fifteen (P15) is at a fraction ($\frac{1}{1.2}$) of time between the difference of first peak and valley point. The same methodology was followed for points between valley and second point as well as second point and end of a step. Following extraction of these points, regression analysis [151] was used to develop the statistical relationships. A number of the relationships for the points had very small R^2 (i.e.

weak relationship), thus those with $R^2 < 0.5$ were improved by relating to points with a better R^2. The relationships are shown in Table 5.1. These intermediate points, which are 34 points including the control points, tend to match the shape of an actual walking step. Spline interpolation in MATLAB is utilised to generate smooth walking steps for the above points as shown in Figure 5.10.

Table 5.1: Intermediate points between the five control points.

Pnts	Comp.	Left footfall	Right footfall	R^2
P2	Time Load	0.134 × P14 0.3496 × P3 - 0.01745	0.1374 × P14 0.4914 × P3 - 0.01233	0.98 0.51
P3	Time Load	0.1964 × P14 0.8065 × P6 - 0.02741	0.1976 × P14 0.7426 × P6 - 0.00763	0.99 0.81
P4	Time Load	0.203 × P14 0.8518 × P6 - 0.02441	0.203 × P14 0.7774 × P6 - 0.00468	0.99 0.86
P5	Time Load	0.214 × P14 0.8976 × P6 - 0.0191	0.2147 × P14 0.8443 × P6 - 0.0029	0.99 0.88
P6	Time Load	0.2413 × P14 0.6809 × P7 - 0.002679	0.2395 × P14 0.5926 × P7 + 0.02623	0.99 0.65
P7	Time Load	0.3039 × P14 0.6579 × P9 - 0.03286	0.3055 × P14 0.6622 × P9 - 0.04168	0.99 0.60
P8	Time Load	0.3567 × P14 0.8612 × P9 - 0.0705	0.3564 × P14 0.8826 × P9 - 0.0933	0.99 0.83
P9	Time Load	0.4549 × P14 1.017 × P10 - 0.176	0.4542 × P14 0.9739 × P10 - 0.1276	0.99 0.78
P10	Time Load	0.5887 × P14 - 0.00894 0.861 × P14 - 0.126	0.5892 × P14 - 0.0092585 0.8451 × P14 - 0.1059	0.99 0.63
P11	Time Load	0.6469 × P14 0.8339 × P14 - 0.03597	0.6464 × P14 0.826 × P14 - 0.0275	0.99 0.73
P12	Time Load	0.7145 × P14 0.8368 × P14 + 0.02732	0.7139 × P14 0.8392 × P14 + 0.02514	0.99 0.84

Pnts	Comp.	Left footfall	Right footfall	R^2
P13	Time	0.8331 × P14	0.8331 × P14	0.99
	Load	0.8991 × P14 + 0.0529	0.8935 × P14 + 0.05292	0.95
P14	Time	first peak time	first peak time	
	Load	first peak load	first peak load	
P15	Time	(0.8111 × (P20 - P14) + 0.0093) - P20	(0.8178 × (P20 - P14) + 0.00822) - P20	0.96
	Load	(0.9436 × (P14 - P20) - 0.00708) + P20	(0.9398 × (P14 - P20) - 0.00606) + P20	0.99
P16	Time	(0.6888 × (P20 - P14) + 0.00805) - P20	(0.6861 × (P20 - P14) + 0.00857) - P20	0.96
	Load	(0.8273 × (P14 - P20) - 0.01898) + P20	(0.8249 × (P14 - P20) - 0.0216) + P20	0.98
P17	Time	(0.5516 × (P20 - P14) + 0.00057) - P20	(0.5498 × (P20 - P14) + 0.00608) - P20	0.95
	Load	(0.6103 × (P14 - P20) - 0.02642) + P20	(0.6074 × (P14 - P20) - 0.02972) + P20	0.95
P18	Time	(0.4255 × (P20 - P14) + 0.00465) - P20	(0.4902 × (P20 - P14) + 0.00553) - P20	0.94
	Load	(0.4005 × (P14 - P20) - 0.02347) + P20	(0.4843 × (P14 - P20) - 0.0262) + P20	0.92
P19	Time	(0.3161 × (P20 - P14) + 0.00273) - P20	(0.3119 × (P20 - P14) + 0.00347) - P20	0.94
	Load	(0.4005 × (P14 - P20) - 0.02347) + P20	(0.4843 × (P14 - P20) - 0.0262) + P20	0.87
P20	Time	valley time	valley time	

Pnts	Comp.	Left footfall	Right footfall	R^2
	Load	valley load	valley load	
P21	Time	P25 - (1.026 × (P25 - P20) - 0.03)	P25 - (1.015 × (P25 - P20) - 0.0282)	0.99
	Load	(0.0631 × (P25 - P20) - 0.00098) + P20	(0.0631 × (P25 - P20) - 0.00128) + P20	0.55
P22	Time	P25 - (1.05 × (P25 - P20) - 0.0602)	P25 - (1.027 × (P25 - P20) - 0.05638)	0.96
	Load	(0.2488 × (P25 - P20) - 0.01212) + P20	(0.2485 × (P25 - P20) - 0.01766) + P20	0.67
P23	Time	P25 - (1.067 × (P25 - P20) - 0.0886)	P25 - (1.042 × (P25 - P20) - 0.0843)	0.93
	Load	(0.5145 × (P25 - P20) - 0.03621) + P20	(0.5223 × (P25 - P20) - 0.04667) + P20	0.77
P24	Time	P25 - (1.055 × (P25 - P20) - 0.119)	P25 - (1.034 × (P25 - P20) - 0.1159)	0.87
	Load	(0.8567 × (P25 - P20) - 0.06745) + P20	(0.869 × (P25 - P20) - 0.07883) + P20	0.88
P25	Time	second peak time	second peak time	
	Load	second peak load	second peak load	
P26	Time	1.071 × P25 - 0.00321	1.088 × P25 - 0.01337	0.95
	Load	0.847 × P25 + 0.1096	0.8612 × P25 + 0.09151	0.88
P27	Time	1.104 × P25 - 0.00545	1.128 × P25 - 0.01955	0.97
	Load	0.6564 × P25 + 0.2541	0.7104 × P25 + 0.1869	0.63

Pnts	Comp.	Left footfall	Right footfall	R^2
P28	Time	1.138 × P25 - 0.00654	1.171 × P25 - 0.02611	0.96
	Load	0.9204 × P27 - 0.0917	0.9204 × P27 - 0.0348	0.63
P29	Time	1.159 × P25 - 0.00755	1.195 × P25 - 0.02911	0.96
	Load	1.073 × P28 - 0.1533	1.073 × P28 - 0.1561	0.89
P30	Time	1.182 × P25 - 0.009348	1.219 × P25 - 0.03154	0.95
	Load	1.138 × P28 - 0.3101	1.092 × P28 - 0.2793	0.77
P31	Time	1.207 × P25 - 0.01035	1.248 × P25 - 0.03463	0.93
	Load	1.092 × P30 - 0.2017	1.017 × P30 - 0.1811	0.93
P32	Time	1.245 × P25 - 0.01227	1.289 × P25 - 0.03903	0.94
	Load	0.9973 × P30 - 0.321	0.841 × P30 - 0.2263	0.85
P33	Time	1.345 × P25 - 0.01648	1.399 × P25 - 0.0495	0.88
	Load	μ = 0.0634 σ = 0.029	μ = 0.0617 σ = 0.0237	
P34	Time	step contact time	step contact time	
	Load	0	0	

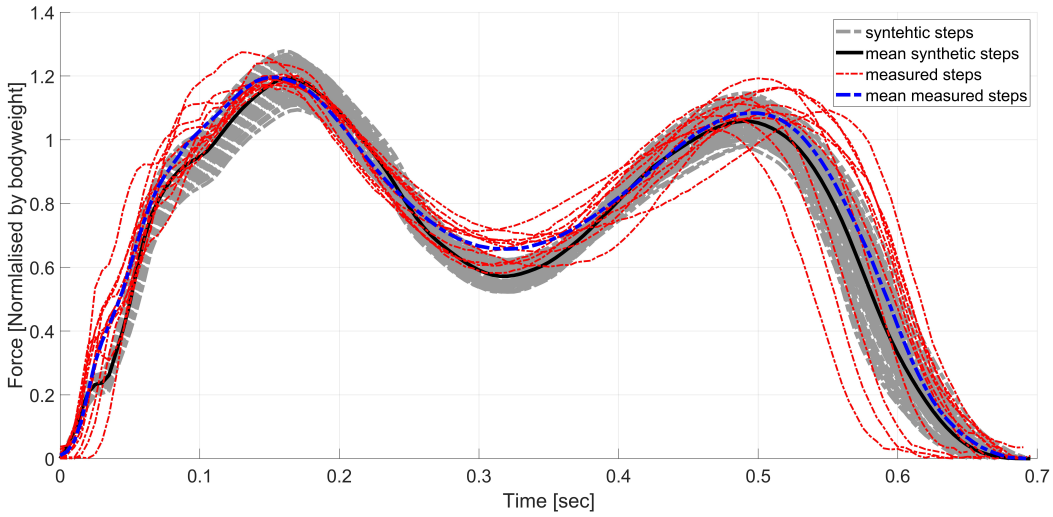

(a) pacing rate 1.8 Hz

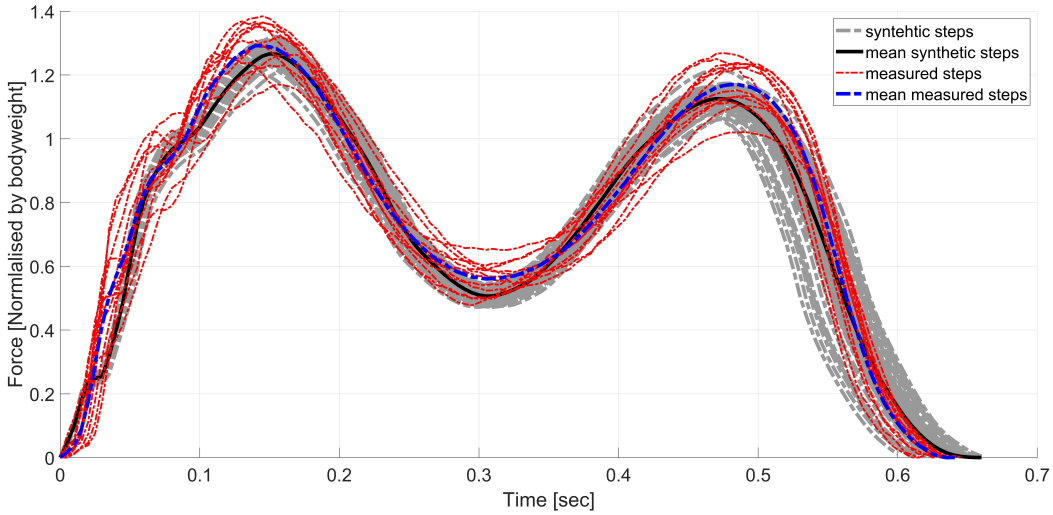

(b) pacing rate 2.0 Hz

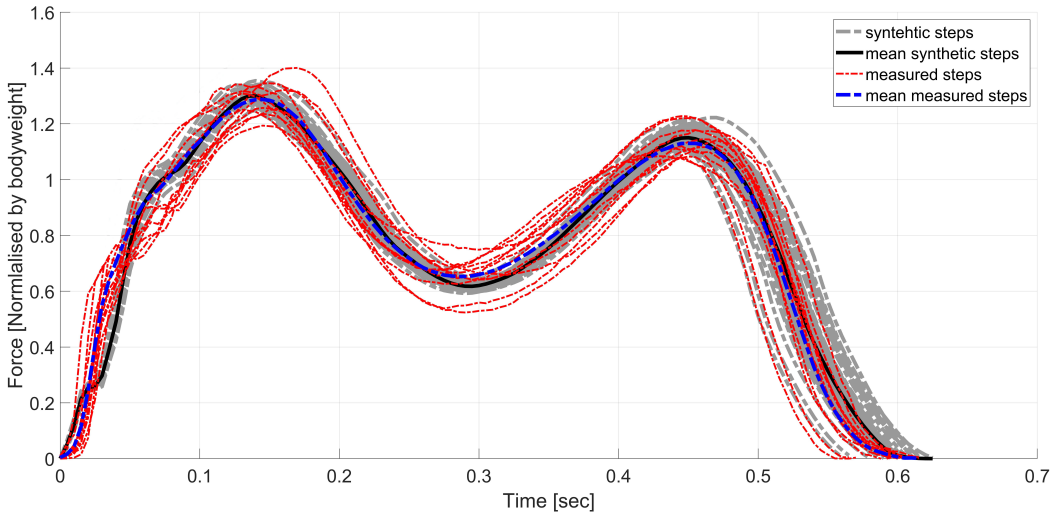

(c) pacing rate 2.2 Hz

Figure 5.10: Comparison of synthetic walking steps against measured steps.

A number of regenerated walking footfall time history for both right and left footfalls can be seen in Figure 5.10 in terms of mean and individual steps, which

matches the corresponding measured walking step closely. Since actual walking is a continuous process, continuity of walking is established via the overlap time between consecutive right and left footfalls. This was done by placing any consecutive step at a specific time slot, which is computed from previous step contact time subtracted from an overlap time. The overlap time is a function of both walking speed and step contact time as shown in Figure 5.11. The theoretical mean value only will be used to construct a continuous walking load time history, since the overlap time depends partly on step contact time, which already has taken into account the normal distribution.

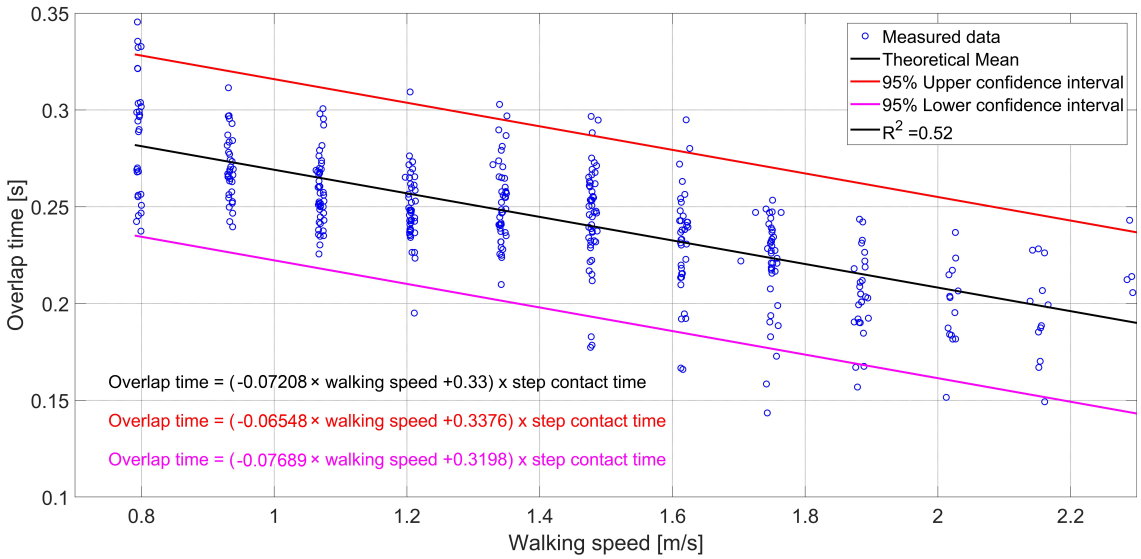

Figure 5.11: Overlap time relationship.

5.4 Development of a continuous probabilistic walking load model

A continuous walking force time history can be synthesised on the basis of individual footfall forces, with duration depending on the number of steps and its characteristics based on the statistical distributions of main control points described previously. The continuous walking algorithm illustrated in Figure 5.12 shows the complete process of creating a synthetic walking force. For a specified walking speed and number of steps (i.e. walking duration), the algorithm first estimates step contact time, first peak load, second peak load and valley load for a specific person, taking into account inter-subject variability. The load and time component intra-subject variability are selected via corresponding distribution functions, as mentioned earlier. For each component, the intermediate points are then produced. At this step the algorithm splits into two parallel actions, right footfall and left footfall.

The overlap time is selected as a function of both walking speed and step contact time to combine any consecutive footfalls. The next step integrates everything generated so far to produce the synthetic dynamic load, which is body-weight normalised. Pedestrian body mass (body weight), as a random parameter, can be generated via available databases of statistical models in the literature. Finally, a continuous synthetic walking force time history is generated after it has been scaled by the body weight.

Figure 5.13 shows examples of generated walking time histories at different pacing rates. A total of 64 successive footfalls at sampling frequency of 200 Hz was generated in the synthetic model, where the first 20 seconds are shown in Figure 5.13 for clarity. A visual comparison of the signals shows clear variations in walking steps and force amplitudes, as a result of the inherent inter- and intra-subject variability built into the algorithm.

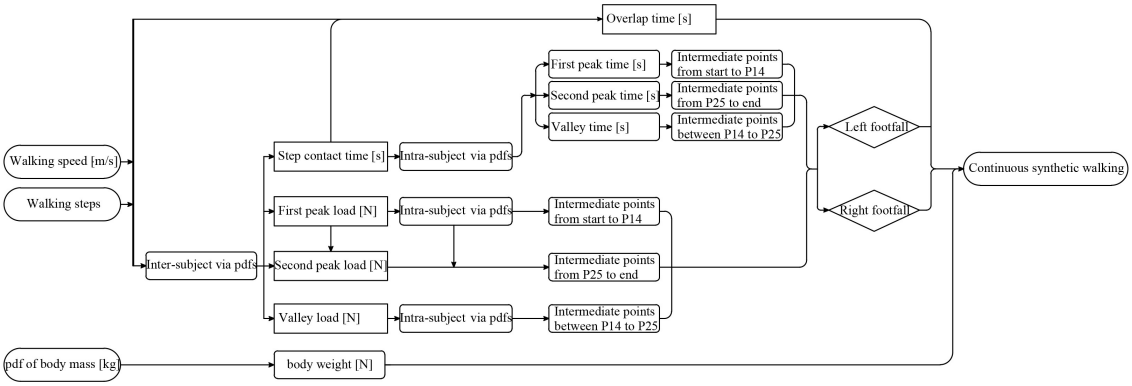

Figure 5.12: Schematic flow chart describing the procedure for generating synthetic continuous walking.

5.5 Model validation

The modelling strategy proposed in this work is validated in the frequency domain at different pacing frequencies. This was done by comparing between measured Fourier amplitude spectra of pedestrian force time histories at corresponding pacing rates and their synthetic counterparts. As mentioned, 64 successive footfalls were generated same as the measurement data for comparison. Figure 5.13 shows typical time domain signals of three pacing rates of synthetic walking, to be used for validation.

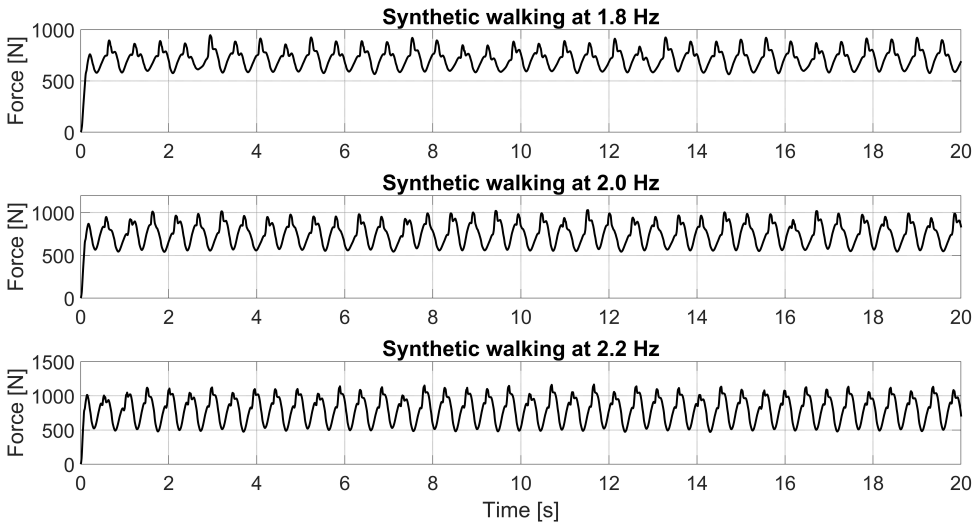

Figure 5.13: Synthetic continuous walking at three pacing frequencies.

Figures 5.14-5.16 illustrate Fourier spectra of measured and synthetic time histories corresponding with three pacing rates (f_p) of 1.8, 2.0 and 2.2 Hz, representing typical likely pacing rates for office floors. For the first four dominant harmonics, square root of sum of squares (SRSS) error in the area under the graph between the measured and synthetic spectra over 10 different walking forces for each pacing rate is less than 12%. In addition, the measure of spread of energy around the first four dominant harmonics (i.e. H harmonic number) in the aforementioned spectra was computed using area under each harmonic curve to represent the spread of energy. The values of upper frequency and lower frequency were identified as $0.95Hf_p$ and $1.05Hf_p$, respectively based on [37].

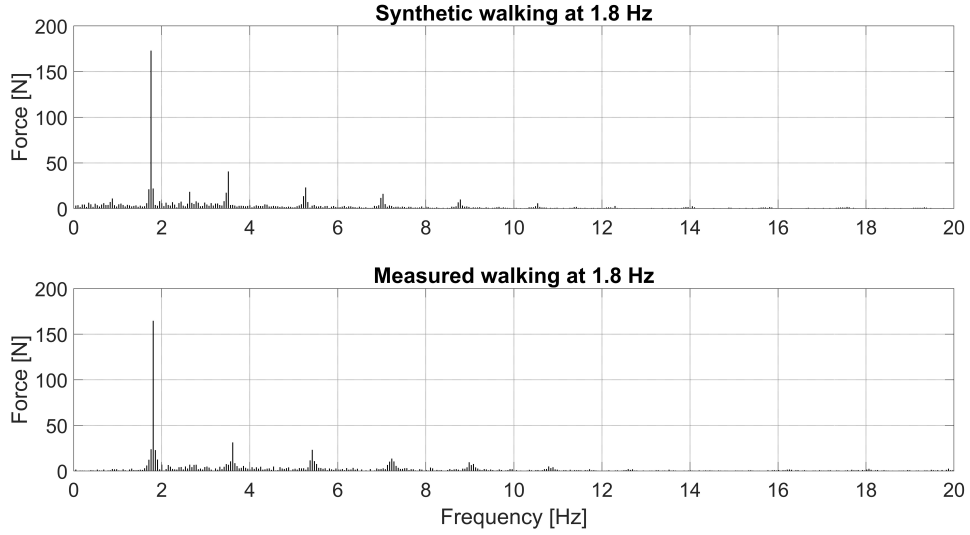

Figure 5.14: Synthetic continuous walking and measured walking at 1.8 Hz.

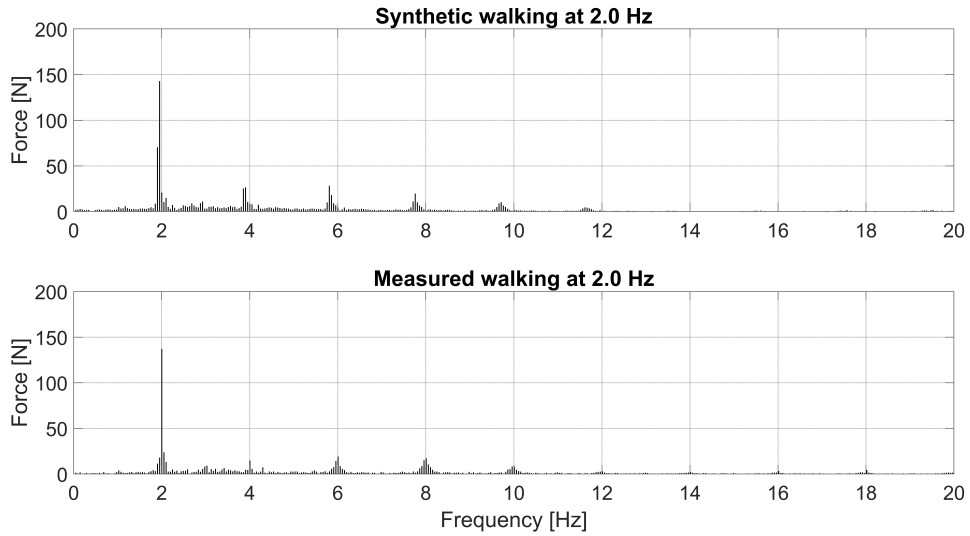

Figure 5.15: Synthetic continuous walking and measured walking at 2.0 Hz.

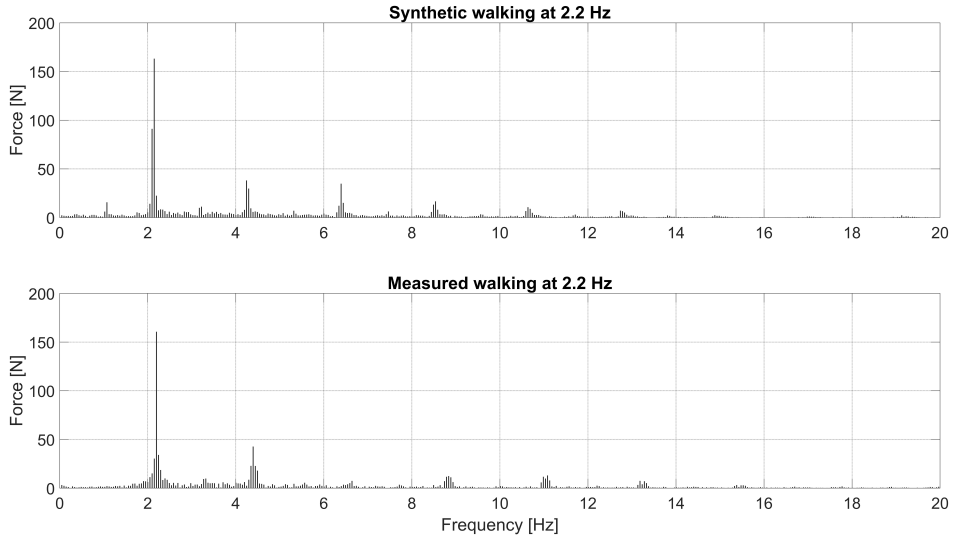

Figure 5.16: Synthetic continuous walking and measured walking at 2.2 Hz.

Table 5.2: Spread of energy in the spectra for the synthetic and measured walking

harmonic number	area synthetic walking	area measured walking	% Error
1	μ = 0.0138; σ = 0.0034	μ = 0.014; σ = 0.003	-1.43
2	μ = 0.0046; σ = 0.0012	μ = 0.0047; σ = 0.0027	-2.12
3	μ = 0.0039; σ = 0.0009	μ = 0.0032; σ = 0.001	17.9
4	μ = 0.0032; σ = 0.0006	μ = 0.0034; σ = 0.0004	-6.2

The results illustrated in Table 5.2 demonstrate the extent of spread of energy around main harmonics in terms of mean and standard deviations. Overall the

synthetic model is in agreement with measured spectra, despite some errors. All this indicates good match in the frequency content between the measured and synthesised walking force signals. Therefore, it is proposed that the synthetic forces generated by this model can be utilised as a basis for vibration serviceability assessment of civil engineering structures, such as floors and footbridges, to estimate more realistic vibration responses due to people walking than previously proposed deterministic models.

5.6 Conclusions

This chapter has presented a new probabilistic model to generate walking force time histories for specific walking speeds. The footfall forces of both left and right legs are modelled separately and then combined with an overlap time to obtain a continuous walking force. The modelling strategy can account for spatial-temporal features of real vertical walking more realistically than conventional Fourier series-based deterministic approaches. The established probabilistic model has the following advantages:

1. A set of probabilistic walking steps, taking into account intra-subject variability, is used to generate a continuous walking force signal in the time domain based on walking speed.

2. High frequency components are inherently included due to variation in walking steps in both time and load. Hence, the load model can replicate actual walking more realistically that Fourier series approaches typically based on low frequency harmonics alone.

3. Variation between walking steps for both legs in each interval of consecutive steps is possible and as such the model demonstrates the narrow band random phenomenon in frequency domain, showing the leaking of energy in the vicinity of the dominant Fourier harmonics [35]. This is a feature typical in measured pedestrian time histories.

4. Inter-subject variability is taken into account via the statistical distributions of physical characteristics of entire populations of pedestrians.

5. The walking model can be used to generate force time histories for both individual and multiple pedestrians walking via superposition.

6. The model is amenable for use in Monte-Carlo simulations of floor response, hence to provide statistical distributions of response to be used in probabilistic vibration serviceability assessment. It can also be used to predict likely

‘vibration dose’ over an extended time period of occupant exposure to vibration.

This framework of probabilistic walking forces provides an opportunity to enhance current vibration serviceability assessment, which currently typically lacks appropriate statistical perspective. The established walking model can be used to predict realistic distributions of dynamic structural responses, for assessment of civil engineering structures dynamically excited by pedestrians such as building floors and footbridges.

Chapter 6

A Multi-Person Spatial Response Prediction Framework

This chapter aims to establish pedestrian response analysis tools, where the spatial distribution of pedestrians in Chapter 4 and the probabilistic walking load model in Chapter 5 are utilised to predict vibration responses using a state space model. In this way, vibration serviceability assessment of floors can be carried out at particular occupant locations, taking into account the actual exposure time and exposure routes. It is planned to submit the content of this chapter to the Journal of Sound and Vibration under the following title:

Muhammad, Z.O. and Reynolds, P. “Vibration serviceability of floor structures: A Multi-person spatial response prediction framework”.

6.1 Introduction

Vibration serviceability is of critical importance to the design of modern pedestrian structures, due to the trends toward ever more lighter, longer and more slender structural layouts. These aspects have resulted in building floors which are increasing susceptible to vibration serviceability problems under a wide array of human activities, most commonly people walking [34]. The perception of excessive vibrations by building occupants has become more common, thus leading to human discomfort and concern in buildings that fail to provide a satisfactory vibration environment [9].

Assessment of vibration responses is often done in line with relevant design guidelines [5–8], which Chapter 3 has shown that it can be unreliable for accurate prediction of floor vibration performance. In such guidelines, a simplified design procedure is suggested to evaluate vibration responses, which neglects the actual loading situations, such as multiple pedestrians. This is most likely in normal use of floors. Moreover, vibration responses are often estimated only considering the peak value of vibration descriptors, irrespective of the exposure time, exposure route, probability of occurrences and contribution of higher modes of vibration [10]. These mechanisms to apply a probabilistic design process are not available, and hence the methods ignore human walking variabilities with respect to a walking path, duration of action performed and the actual frequency content of forces generated in the process [85].

This chapter presents a comprehensive and novel methodology to simulate pedestrian walking and predict vibration responses under multiple pedestrians using a spatially varying walking force in the time domain. The approach uses spatial pedestrian simulations on floors (Chapter 4) to establish reliable walking patterns at the design stage representing typical real floor usage. A probabilistic vertical walking force (Chapter 5) is utilised to generate walking loads for different individuals, accounting for inter- and intra-subject variabilities. The force model takes into account walking speed of individuals along different walking paths, a key advance over previously available pedestrian models, thus making the approach very useful for probabilistic design. Vibration responses then are computed using a state space model over the whole floor area, at individual seats and along pedestrian walking paths. Hence, this makes the proposed method a reliable and realistic tool for vibration serviceability of floors under human walking. The approach can be coded in any programming language to provide design engineers and researchers with a tool for carrying out more realistic vibration serviceability of floors.

6.2 Floor case studies

6.2.1 Floor A

6.2.1.1 Description of the floor

This floor structure was analysed in Chapters 3 and 4, however, a brief description is given for completeness. The floor comprises timber joists spanning on steel beams. It is an open-plan office space with typical fit-out, as illustrated in Figure 6.1. There are two staircases one on each side of the floor, which pedestrians typically use to enter into or exit from the floor area. The number of seats in total is 48, with a number of filing cabinets and shelves distributed across the floor area. It is worth mentioning that neither construction drawings nor structural member details were available. This makes developing FE model quite difficult and as such the measured modal model will be used for response predictions.

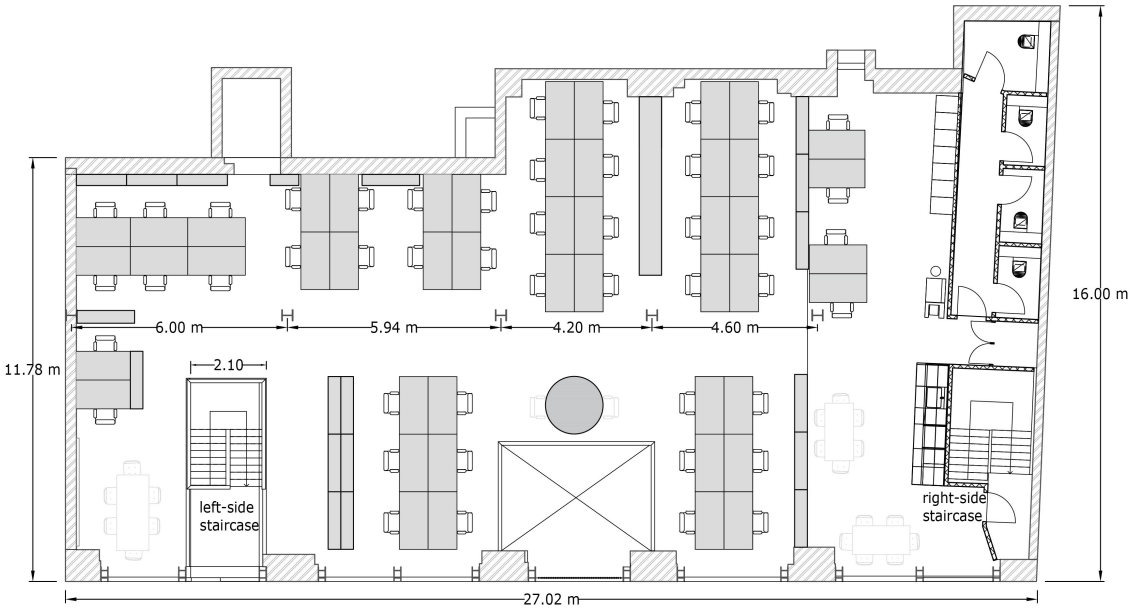

Figure 6.1: Floor A with office fit-out.

6.2.1.2 Experimental modal analysis (EMA)

A modal test was performed using three APS Dynamics shakers (2 $\times$ APS400 and 1 $\times$ APS113) as excitation sources. This was also covered in Chapter 3, however, some key points will be repeated here for clarity. The structural response was measured using array of response accelerometers (model Honeywell QA750). Digital data acquisition was performed using a portal spectrum analyser model Data Physics DP730. The analyser provides immediate calculation of the FRFs so that the quality of measurement data can be checked during the test. The mea-

surements were acquired over a test grid of 64 test points, as shown in Figure 6.2. These test points were utilised to acquire the modal properties over the majority of the floor area. The ME'scope [137] parameter estimation software was used to estimate modal properties by carrying out curve fitting of the measured FRF data.

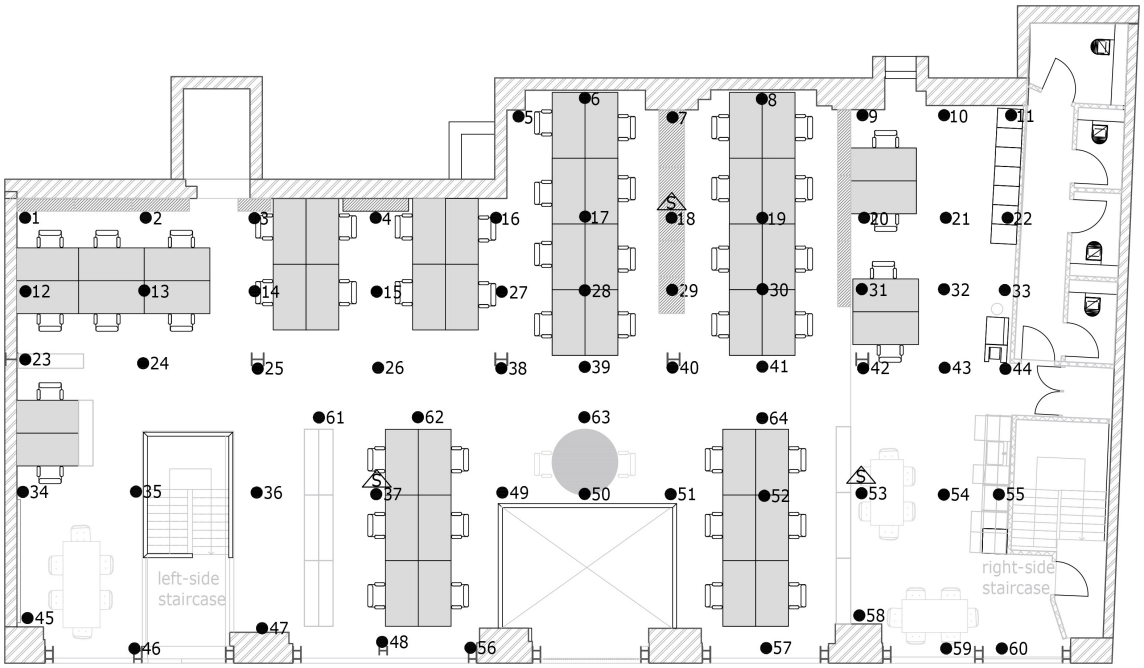

Figure 6.2: Floor A test point locations. Shaker locations are shown by letter "S".

The EMA modes, natural frequencies, damping ratios and modal masses extracted from the measurements are shown in Figure 6.3; the modes are unity normalised. The quality of curve fitting is also presented in Figure 6.4. The red colour is the curve fit obtained form ME'scope parameter estimation software and light yellow, blue and black colours are the measured FRFs. It can be seen that in the first few modes the curve fitting (i.e. red colour) overlays reasonably well over the measured FRFs both in magnitude and frequency breadth. However, for higher modes the curve fitting quality diminishes and the curve fits do not overlay so well with the measured FRFs. This could be due to some mild non-linearity and fundamental connection problems in the timber and steel members [10].

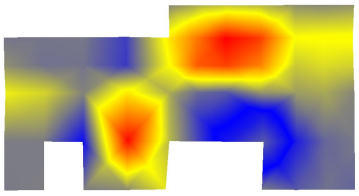

(a) EMA f_1 = 7.62 Hz, ζ_1 = 4.03 %, m_1 = 23.24 tonnes

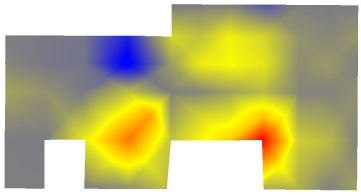

(b) EMA f_2 = 8.62 Hz, ζ_2 = 2.84 %, m_2 = 19.33 tonnes

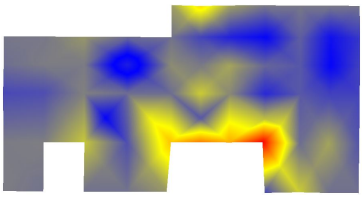

(c) EMA f_3 = 12.2 Hz, ζ_3 = 3.1 %, m_3 = 13.25 tonnes

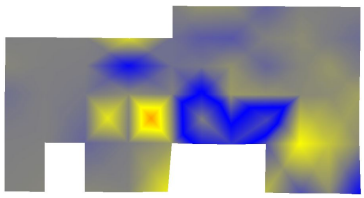

(d) EMA f_4 = 13.4 Hz, ζ_4 = 4.33 %, m_4 = 16.79 tonnes

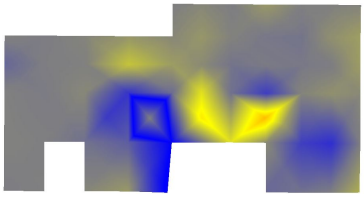

(e) EMA f_5 = 14.8 Hz, ζ_5 = 2.99 %, m_5 = 13.3 tonnes

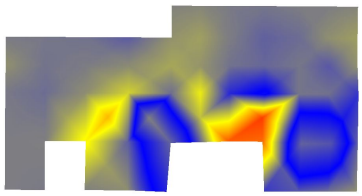

(f) EMA f_6 = 16 Hz, ζ_6 = 2.61 %, m_6 = 29.22 tonnes

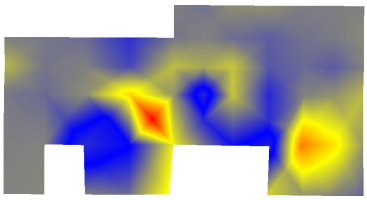

(g) EMA f_7 = 17.1 Hz, ζ_7 = 3.32 %, m_7 = 17.88 tonnes

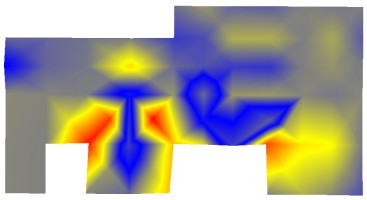

(h) EMA f_8 = 20.1 Hz, ζ_8 = 3.34 %, m_8 = 20.02 tonnes

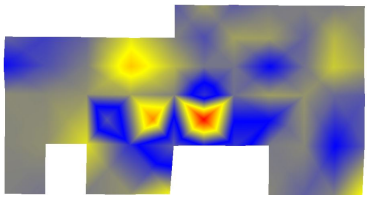

(i) EMA f_9 = 21.9 Hz, ζ_9 = 3.79 %, m_9 = 16.24 tonnes

Figure 6.3: Floor A EMA mode shapes and modal properties.

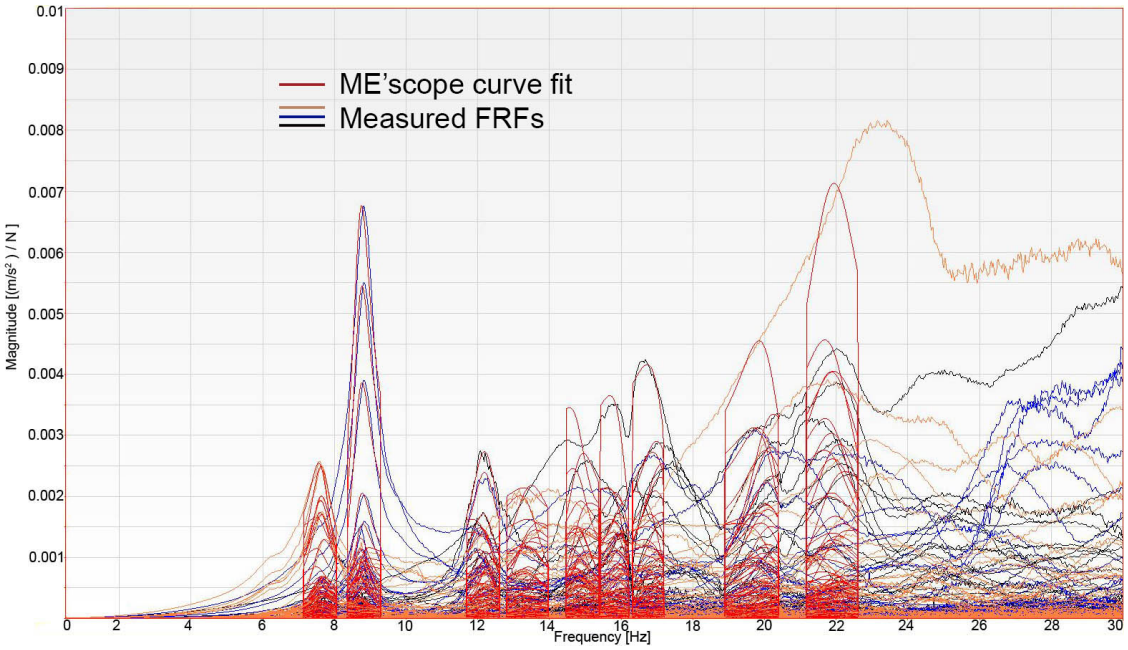

Figure 6.4: Floor A curve fitting quality.

6.2.1.3 Pedestrians spatial distribution

The spatial and temporal positions of pedestrians from agent-based modelling was discussed in Section 4.4, thus this section presents the simulation results only with brief descriptions of salient points. Figure 6.5 shows results from modelling of pedestrian motions on the floor area for a duration of ten hours. There are 27 pedestrians in total on the floor, who would carry out a range of activities. The sequences of their tasks and number of occurrences are, based on measured data and random. Also, the walking paths utilised by the occupants are different, which makes the pedestrian activity approximate actual observed activities. The walking path locations in terms of floor coordinates will be used later for excitation points. This ensures a multiple pedestrian force input along different walking paths, an approach that has not been presented previously in the literature.

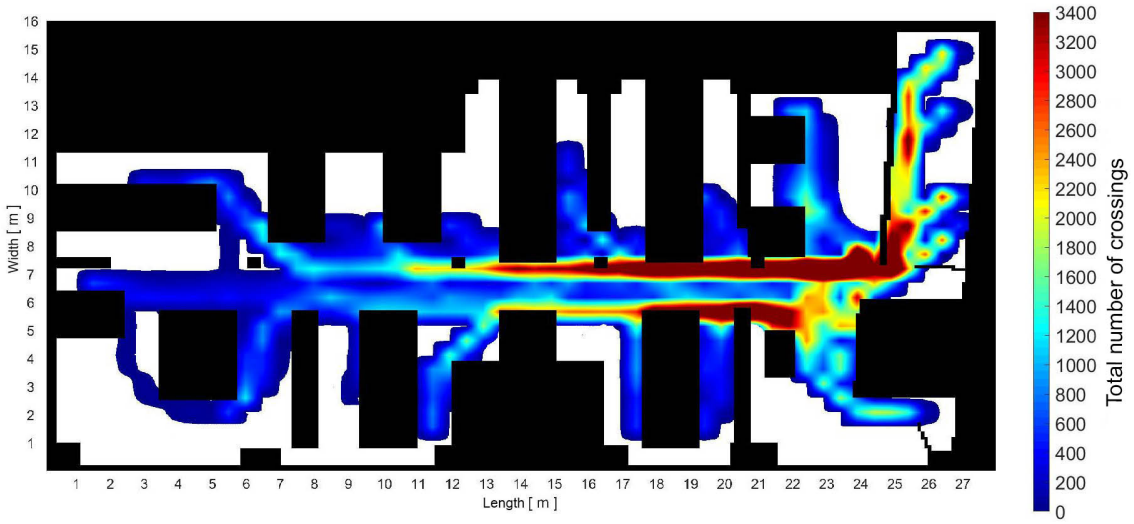

Figure 6.5: Floor A pedestrian simulation pattern.

6.2.2 Floor B

6.2.2.1 Description of the floor

This floor, covered in Chapter 3, is the seventh floor of a recently constructed multi-storey (eight storey) office building. Light weight concrete was poured into a 280 mm deep slab with Comflor 210/1.2 mm profile decking to form a composite steel-concrete floor structure spanning in the shorter direction. Beams have spans of up to approximately 7.47 m. The columns are situated at the intersections of beams, with typical bay sizes of 7.47 m $\times$ 4.88 m, as shown in Figure 6.6. Details of the structural elements in a typical bay are; beams are cellular section sizes 298×254/368×130.5 USFB, with hole diameter of 140 mm at 300 mm centres. Column members are 203×203×86 UC. There are three reinforced concrete walls/cores with 225 mm thickness for lateral resistance. Also, external curtain walls are EWS-101 series double-glazed cladding.

Figure 6.6: Floor B plan.

6.2.2.2 Experimental modal analysis (EMA)

This section was also mentioned in Chapter 3, however, some key points will be repeated for completeness. The floor structure was tested at two different stages; at construction stage prior to installing external walls and at completion stage just before fit-out. Results of the latter will be shown as it is most pertinent to this study. Experimental modal properties of the floor were obtained from modal testing utilising multi-reference uncorrelated random excitation from three APS Dynamics shakers (1× APS113 and 2× APS400) and a test grid of roving Honeywell QA750 accelerometers, shown in Figure 6.7. Data Physics Mobilyzer DP730 digital spectrum analyser was used to calculate frequency response functions (FRFs). The ME'scope software [137] package of modal parameter estimation was used to extract modal properties using a multi-polynomial method to provide reliable estimates of mode frequency, damping and shape. The final mode shape results are shown in Figure 6.8.

As far as walking response measurements are concerned, a single pedestrian walked freely at his convenient speed from TP21 to TP40 back and forth (see Figure 6.7). The pedestrian had weight and height of 86 kg and 1.88 m, respectively. The actual vibration response under a single person walking along this walking path (see Figure 3.21) resulted in an R factor of 5.12 at TP24. This was carried out to obtain vibration responses under a single pedestrian, since in-services responses could not be acquired as the the floor was not yet commissioned at the time of testing.

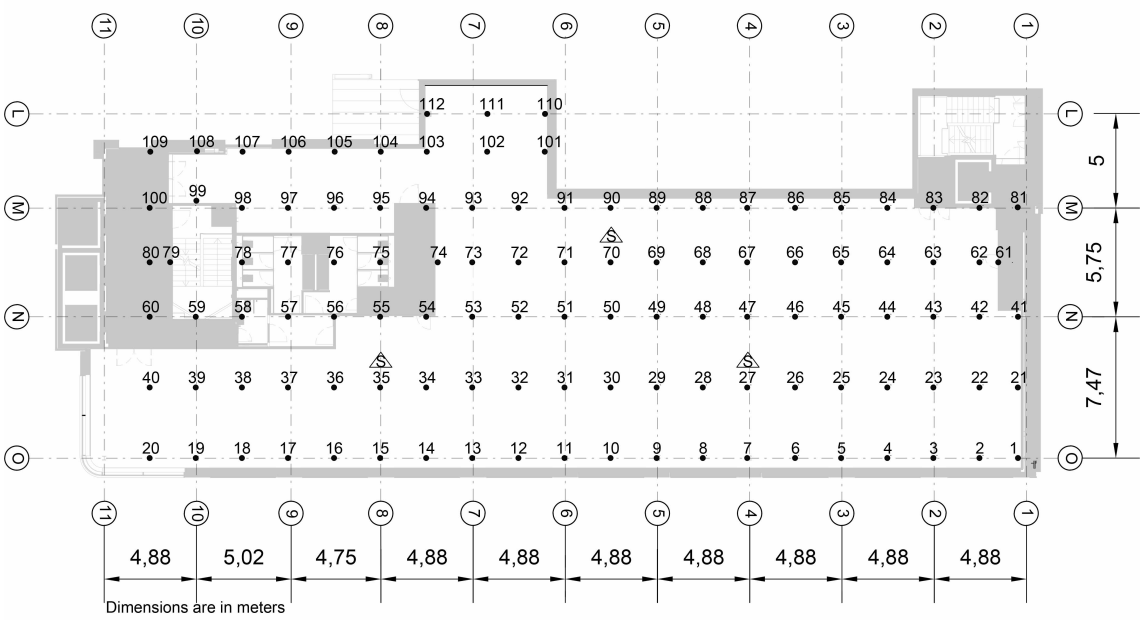

Figure 6.7: Floor B Test grid for EMA. APS shakers are shown by letter “S”.

6.2.2.3 FE model development

An FE model of the structural system was developed using the ANSYS FE software. Beams and columns were modelled using BEAM188 elements. A single storey level with all vertical members, top and bottom, at a height of 4 m was modelled using fixed boundary conditions. The composite steel-concrete floor was modelled using SHELL181 elements and orthotropic properties were assumed (flexural stiffness in the direction of the ribs is higher than the perpendicular direction). The composite action between the beams and slabs was modelled through a vertical offset of the shell element as recommended in the design guidelines [6, 7]. The modulus of elasticity (E) of 24 GPa for lightweight concrete and density of 1500 kg/m^3 were assumed [7]. Modal properties (modal frequencies, mode shapes and modal masses) were obtained via modal analysis. This was covered in Section 3.3.5.3 and as such will not be repeated here. The first few mode shapes are shown in Figure 6.8.

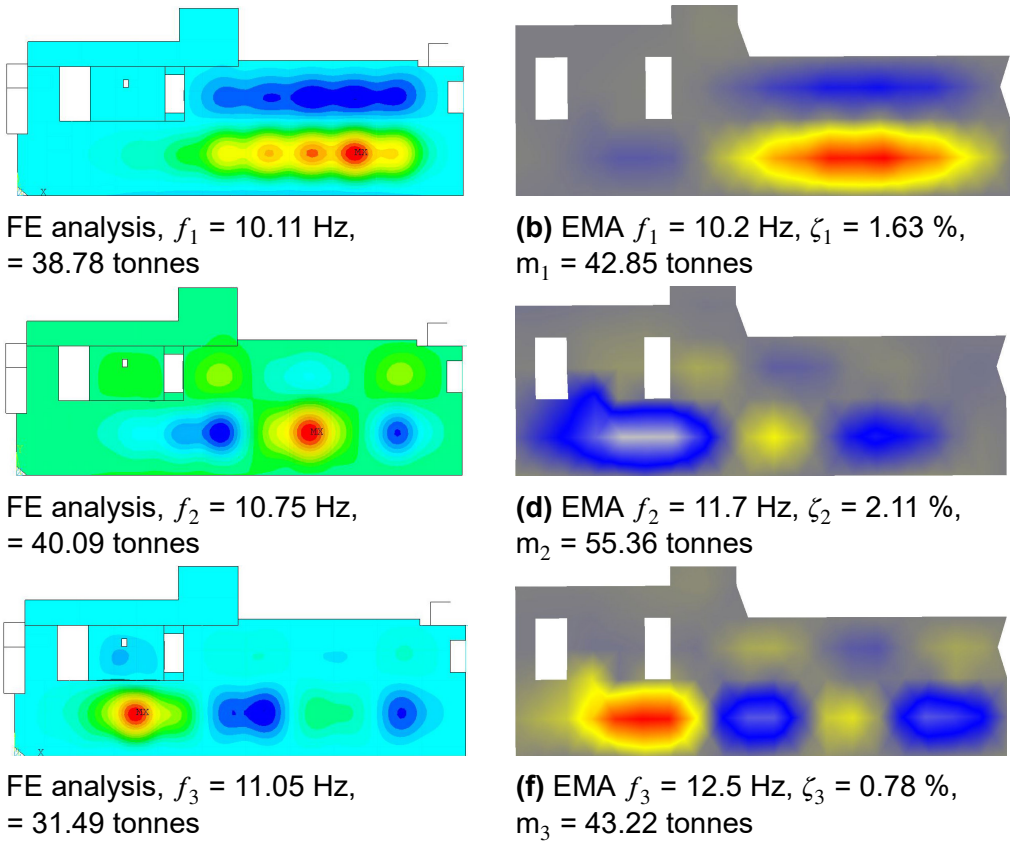

(a) FE analysis, f_1 = 10.11 Hz, m_1 = 38.78 tonnes

(b) EMA f_1 = 10.2 Hz, ζ_1 = 1.63 %, m_1 = 42.85 tonnes

(c) FE analysis, f_2 = 10.75 Hz, m_2 = 40.09 tonnes

(d) EMA f_2 = 11.7 Hz, ζ_2 = 2.11 %, m_2 = 55.36 tonnes

(e) FE analysis, f_3 = 11.05 Hz, m_3 = 31.49 tonnes

(f) EMA f_3 = 12.5 Hz, ζ_3 = 0.78 %, m_3 = 43.22 tonnes

Figure 6.8: Floor B vibration modes from EMA and FE Analysis.

6.2.2.4 Pedestrians spatial distribution

As far as the floor layout is concerned, four different plan layouts were developed to represent a range of realistic pedestrian simulation patterns. The reason for this is that the floor might be fitted out by a range of tenants for office use and thus different configurations of office layouts are possible. The four layouts designed in this work are based on experience for open-plan arrangements. This is an exercise to show the effectiveness of the pedestrian patterns upon floor usage in the context of vibration serviceability assessment. Similar approach and values are used as for Floor A.

The floor layouts with the corresponding spatial distribution of pedestrian for ten hours (corresponding to 8:00 am - 6:00 pm working hours) are shown in for layout one in Figures 6.9, 6.10; layout two in Figures 6.11, 6.12; layout three in Figures 6.13, 6.14; and layout four in Figures 6.15, 6.16, respectively. Each floor layout has different numbers of pedestrians and seats; for example, layout one has 52 seats, layout two 60, layout three 40 and layout four 50. Thus, making each arrangement produce various different excitation locations and occurrences. This is very useful to examine how different configurations and possible refurbishments impact in-service vibration responses.

Figure 6.9: Floor Layout 1 office floor open-plan: 52 pedestrians.

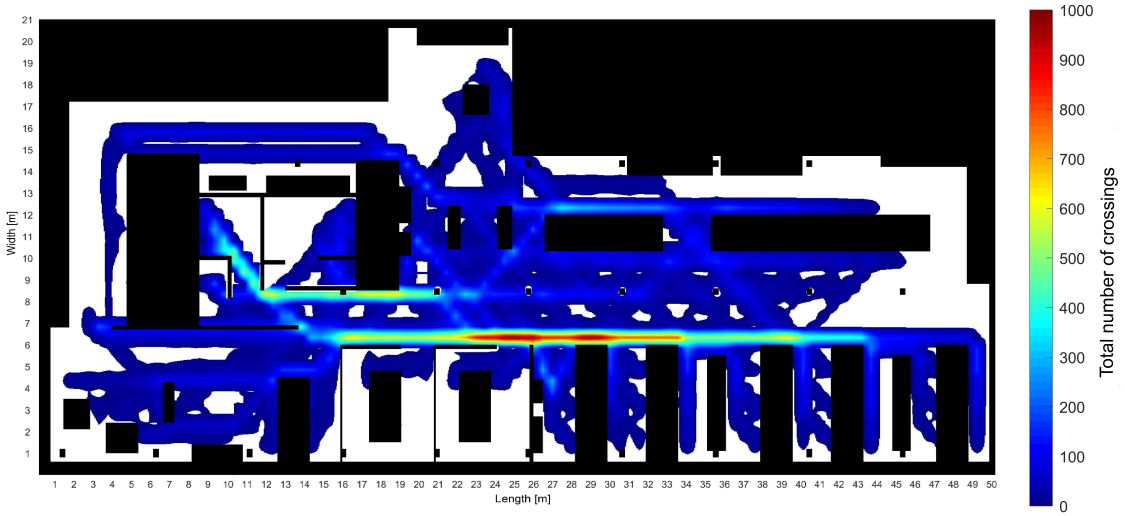

Figure 6.10: Floor Layout 1 spatial distribution of pedestrian heatmap.

Figure 6.11: Floor Layout 2 office floor open-plan: 60 pedestrians.

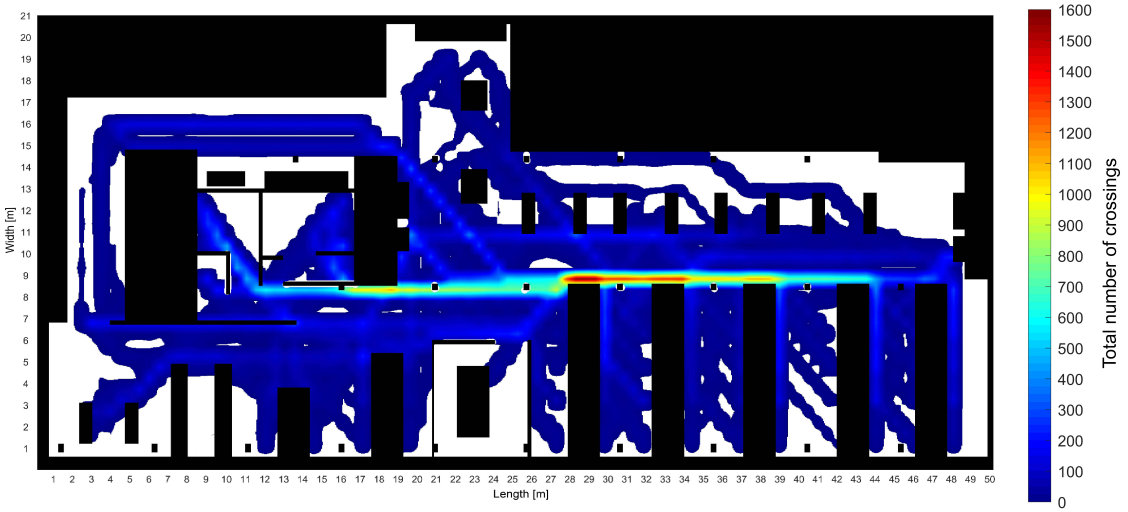

Figure 6.12: Floor Layout 2 spatial distribution of pedestrian heatmap.

Figure 6.13: Floor Layout 3 office floor open-plan: 40 pedestrians.

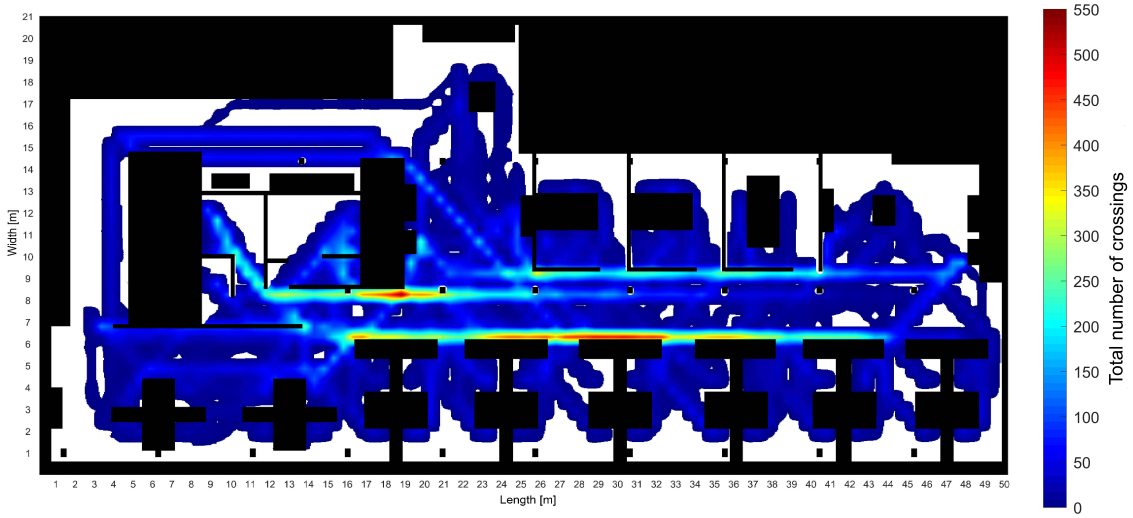

Figure 6.14: Floor Layout 3 spatial distribution of pedestrian heatmap.

Figure 6.15: Floor Layout 4 office floor open-plan: 50 pedestrians.

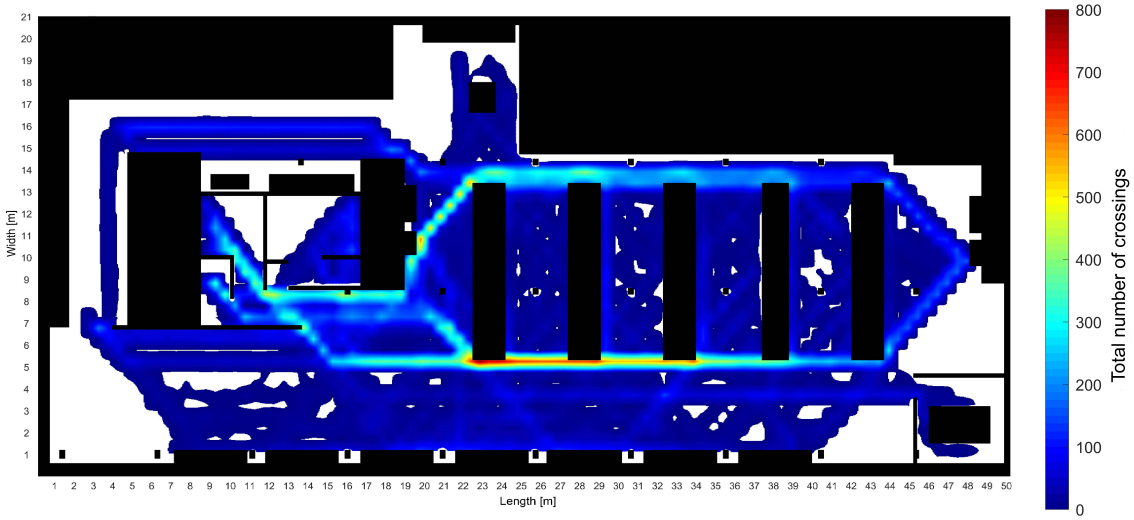

Figure 6.16: Floor Layout 4 spatial distribution of pedestrian heatmap.

6.3 Response predictions using state-space model

6.3.1 System model

This section shows the procedure for analysing a system under multiple inputs as mentioned by [1] with some modifications, such as including multiple pedestrian patterns from simulation, probabilistic walking load model, step by step application of the load and obtaining vertical acceleration as the output. The natural frequencies, mode shapes and modal masses were obtained either via measured data or predicted by the FE model. Damping ratios were obtained from measured data or assumed from vibration design guidelines. These were used to create a simulation of the floor structure. The simulation model is a transfer function (TF) relating the inputs (pedestrian forces) to the outputs (acceleration responses). In this situation, a modal system (i.e modal force to modal output) is used to facilitate modelling of multiple roving (moving) pedestrians.

Although actual building floors are continuous systems, they are approximated to a multi-degree-of-freedom (MDOF) system by the FE software. In principle, MDOF dynamic systems comprising of n nodes with one (vertical) degree of freedom per node, can be represented as a single matrix equation as follows:

$$\left[M\right]\left\{\ddot{Y}(t)\right\} + \left[C\right]\left\{\dot{Y}(t)\right\} + \left[K\right]\left\{Y(t)\right\} = \left\{F(t)\right\} \tag{6.1}$$

where

$\left[M\right]$ = mass matrix

$\left[C\right]$ = damping matrix

$\left[K\right]$ = stiffness matrix

$\left\{\ddot{Y}(t)\right\}, \left\{\dot{Y}(t)\right\}, \left\{Y(t)\right\}$ = acceleration, velocity and displacement vectors, respectively.

The displacement of any node can be represented as a linear combination of the i^{th} mode shape at location p, ϕ_{pi}, using the modal amplitude $\eta_i(t)$

$$y(p,t) = \sum_{i=1}^{N} \phi_{pi}\eta_i(t) \tag{6.2}$$

where, i is the mode number and N is the total number of modes. For displacement at n locations this results in

$$\begin{Bmatrix} y_1(t) \\ y_2(t) \\ \vdots \\ y_n(t) \end{Bmatrix} = \begin{bmatrix} \phi_{11} & \phi_{12} & \cdots & \phi_{1N} \\ \phi_{21} & \phi_{22} & \cdots & \phi_{2N} \\ \vdots & \vdots & \ddots & \vdots \\ \phi_{n1} & \phi_{n2} & \cdots & \phi_{nN} \end{bmatrix} \begin{Bmatrix} \eta_1(t) \\ \eta_2(t) \\ \vdots \\ \eta_N(t) \end{Bmatrix} \tag{6.3}$$

The mode shapes corresponding to each mode are defined as

$$\left[\Phi\right] = \begin{bmatrix} \phi_{11} & \phi_{12} & \cdots & \phi_{1N} \\ \phi_{21} & \phi_{22} & \cdots & \phi_{2N} \\ \vdots & \vdots & \ddots & \vdots \\ \phi_{n1} & \phi_{n2} & \cdots & \phi_{nN} \end{bmatrix} \tag{6.4}$$

we arrive at

$$\begin{aligned} \left\{Y(t)\right\} &= \left[\Phi\right]\left\{Q(t)\right\} \\ \left\{\dot{Y}(t)\right\} &= \left[\Phi\right]\left\{\dot{Q}(t)\right\} \\ \left\{\ddot{Y}(t)\right\} &= \left[\Phi\right]\left\{\ddot{Q}(t)\right\} \end{aligned} \tag{6.5}$$

Therefore, the above expression (Equation 6.5) represents the conversion between physical responses $\{Y(t)\}$ and modal responses $\{Q(t)\}$. Substituting Equation 6.5 into Equation 6.1 and pre-multiplying by $[\Phi]^T$ yields the following:

$$\begin{aligned} \left[\Phi\right]^T\left[M\right]\left[\Phi\right]\left\{\ddot{Q}(t)\right\} + \left[\Phi\right]^T\left[C\right]\left[\Phi\right]\left\{\dot{Q}(t)\right\} + \left[\Phi\right]^T\left[K\right]\left[\Phi\right]\left\{Q(t)\right\} \\ = \left[\Phi\right]^T\left\{F(t)\right\} \end{aligned} \tag{6.6}$$

This can be simplified by using the property of orthogonality of mode shapes with respect to mass and stiffness matrices and assuming proportional damping to

$$\left[M_N\right]\left\{\ddot{Q}(t)\right\} + \left[C_N\right]\left\{\dot{Q}(t)\right\} + \left[K_N\right]\left\{Q(t)\right\} = \left\{F_N(t)\right\} \tag{6.7}$$

where

$$\begin{aligned}\left[M_N\right] &= \left[\Phi\right]^T \left[M\right] \left[\Phi\right] \\ &= \begin{bmatrix} m_1 & 0 & \cdots & 0 \\ 0 & m_i & \cdots & 0 \\ \vdots & \vdots & \ddots & \vdots \\ 0 & 0 & \cdots & m_N \end{bmatrix}\end{aligned} \tag{6.8}$$

and

$$\begin{aligned}\left[C_N\right] &= \left[\Phi\right]^T \left[C\right] \left[\Phi\right] \\ &= \begin{bmatrix} 2m_1 w_1 \zeta_1 & 0 & \cdots & 0 \\ 0 & 2m_i w_i \zeta_i & \cdots & 0 \\ \vdots & \vdots & \ddots & \vdots \\ 0 & 0 & \cdots & 2m_N w_N \zeta_N \end{bmatrix}\end{aligned} \tag{6.9}$$

and

$$\begin{aligned}\left[K_N\right] &= \left[\Phi\right]^T \left[K\right] \left[\Phi\right] \\ &= \begin{bmatrix} m_1 w_1^2 & 0 & \cdots & 0 \\ 0 & m_i w_i^2 & \cdots & 0 \\ \vdots & \vdots & \ddots & \vdots \\ 0 & 0 & \cdots & m_N w_N^2 \end{bmatrix}\end{aligned} \tag{6.10}$$

and

$$\left\{F_N(t)\right\} = \left[\Phi\right]^T \left\{F(t)\right\} \tag{6.11}$$

where, m_i is the modal mass of mode i. ω_i and ζ_i are the circular natural frequency and damping ratio, respectively, of mode i. Hence, the MDOF system has been de-coupled into N independent single-degree-of-freedom (SDOF) systems. Equation 6.7 can be reformulated as follows:

$$\left\{\ddot{Q}(t)\right\} + \left[C^*\right] \left\{\dot{Q}(t)\right\} + \left[K^*\right] \left\{Q(t)\right\} = \left[M_N\right]^{-1} \times \left\{F_N(t)\right\} \tag{6.12}$$

where

$$\left[C^*\right] = \left[C_N\right] \left[M_N\right]^{-1} \tag{6.13}$$

and

$$\left[K^*\right] = \left[K_N\right]\left[M_N\right]^{-1} \tag{6.14}$$

At this point, it is worth noting that the MDOF system has been fully described using only the modal mass, damping, frequencies and mode shapes.

6.3.2 State space method

A state space representation is a mathematical model of a physical system as a set of input, output and state variables related by first-order differential equations. The state space representation (also known as the ”time-domain approach”) provides a convenient and compact way to model and analyse systems with multiple inputs and outputs [152, 153].

The de-coupled equation of motion in Equation 6.12, which is a second order differential equation, can be represented in state space form as a first order differential equation. For linear time-invariant (LTI) systems (i.e. those for which input and output are independent of time), the state space equations are of the general form

$$\begin{aligned} \left\{\dot{x}(t)\right\} &= \left[\mathbf{A}\right] \times \left\{x(t)\right\} + \left[\mathbf{B}\right] \times \left\{u(t)\right\} \\ \left\{y(t)\right\} &= \left[\mathbf{C}\right] \times \left\{x(t)\right\} + \left[\mathbf{D}\right] \times \left\{u(t)\right\} \end{aligned} \tag{6.15}$$

where $\left\{x(t)\right\}$, $\left\{u(t)\right\}$ and $\left\{y(t)\right\}$ are the internal state vector, input vector and output vector, respectively. $\left[\mathbf{A}\right]$, $\left[\mathbf{B}\right]$, $\left[\mathbf{C}\right]$, $\left[\mathbf{D}\right]$ are the state matrix, input matrix, output matrix and direct transmission matrix respectively [152]. $\left\{u(t)\right\}$ for multiple inputs therefore is the summation of each input element (in this case pedestrian modal force) corresponding with all modes at a particular time step.

For the dynamic system of this study, the state space equation is derived by rearranging Equation 6.7 for $\{\ddot{Q}(t)\}$ using the state vector

$$\left\{x(t)\right\} = \begin{Bmatrix} Q(t) \\ \dot{Q}(t) \end{Bmatrix} \tag{6.16}$$

When the vector of modal accelerations, $\left\{\ddot{Q}\right\}$, is chosen as the output, Equation 6.15 yields the following form of output matrix $\left[\mathbf{C}\right]$ and $\left[\mathbf{D}\right]$ [154]

$$\begin{Bmatrix} \dot{Q}(t) \\ \ddot{Q}(t) \end{Bmatrix} = \begin{bmatrix} 0 & I \\ -K^* & -C^* \end{bmatrix} \begin{Bmatrix} Q(t) \\ \dot{Q}(t) \end{Bmatrix} + \begin{bmatrix} 0 \\ M_N^{-1} \end{bmatrix} \begin{Bmatrix} F_N(t) \end{Bmatrix}$$
$$\begin{Bmatrix} y(t) \end{Bmatrix} = \begin{bmatrix} -K^* & -C^* \end{bmatrix} \begin{Bmatrix} Q(t) \\ \dot{Q}(t) \end{Bmatrix} + \begin{bmatrix} M_N \end{bmatrix}^{-1} \begin{Bmatrix} F_N(t) \end{Bmatrix} \tag{6.17}$$

The output of this modal system is then converted back to physical accelerations through Equation 6.5. A MATLAB-based time domain response analysis script was developed to perform the analysis using the aforementioned approach. It is worth mentioning that the subsequent analysis does not take into account human-structure interaction as it is beyond the scope of this study.

6.3.3 Results and discussions

The physical acceleration obtained from vibration response analyses was weighted using the W_b frequency weighting [118] for vertical accelerations, as mentioned in Section 4.3. The most recent British Standard [118] recommends the use of VDV for evaluation of structural responses, as given in Equation 4.2. The R factor, on the other hand, was calculated by taking the maximum of RMS for a one second period and normalising this by the reference value of 0.005 m/s^2 [45], as given in Equation 4.1. The R factor is most commonly used by existing guidelines [6, 7, 32] having a threshold limit of 4 or 8 for offices. The limits placed on VDV values for offices are shown in Table 6.1.

Table 6.1: Typical VDV range for office floors from BS-6472-1 [118]

Time	Low probability of adverse comment m/s$^{1.75}$	Adverse comment possible m/s$^{1.75}$	Adverse comment probable m/s$^{1.75}$
16h day	0.4-0.8	0.8-1.6	1.6-3.2
8h night	0.1-0.2	0.2-0.4	0.4-0.8

It is often recommended to convert the calculated VDVs in the simulation to 16 hrs equivalent via a scaling factor multiplication as given in Equation 6.18. In that way, the VDVs can be compared against the above limits.

$$\text{VDV scaling factor} = \left(\frac{16 \times 60 \times 60}{\text{Simulation Time [s]}} \right)^{1/4} \tag{6.18}$$

6.3.3.1 Floor A

The calculated floor responses are compared with measurements presented in Section 4.3. Pedestrian walking forces are applied at the floor coordinates as per the spatial distribution of pedestrians. To do so, the well-known relationship between walking velocity v_p, step frequency f_p and step length l_p ($v_p = f_p\, l_p$) was used. Also, the duration of footfalls was included to facilitate the step by step application of the force as discussed previously. From simulations, the walking velocity and positions of pedestrians can be obtained, however, information about f_p and l_p is missing. Thus, the following Equation 6.19 [95] is utilised to obtain f_p, which is valid in the velocity range of 0-2.5 m/s. This in turn provides the range of l_p used in the subsequent analysis, which is approximately computed in the range of 0.53-0.79 m. As a result, the individual footfall force is applied at a position obtained from the simulation and the next footfall would be at a distance l_p from the previous step taking into account both the footfall duration. It is worth mentioning that mode shape values at footfall locations were interpolated so as to replicate reality as close as possible.

$$f_p = 0.35v_p^3 - 1.59v_p^2 + 2.93v_p \tag{6.19}$$

As mentioned earlier, the physical force is converted to modal force and summed to represent multiple pedestrians. At this point, the system and input force are ready for response analysis. The vibration response values are compared with those obtained from ten hours of in-service measurements as discussed in Section 4.3.1.2.

A typical acceleration time history response at the equivalent location of measured TP39 from ten-hour simulation and the corresponding Fourier amplitude spectra are shown in Figures 6.17 and 6.18, respectively. In the same way of the measurements in Section 4.3.1.2, there are significant contributions of higher modes for the simulation of multiple pedestrians for a wider band of frequency. However, in the simulation the first mode tends to contribute higher than the measurements; for example, comparing Figure 6.18 from simulation and Figure 4.9 from measurements. This could be acceptable taking into account the probabilistic walking force and simulation of pedestrian pattern.

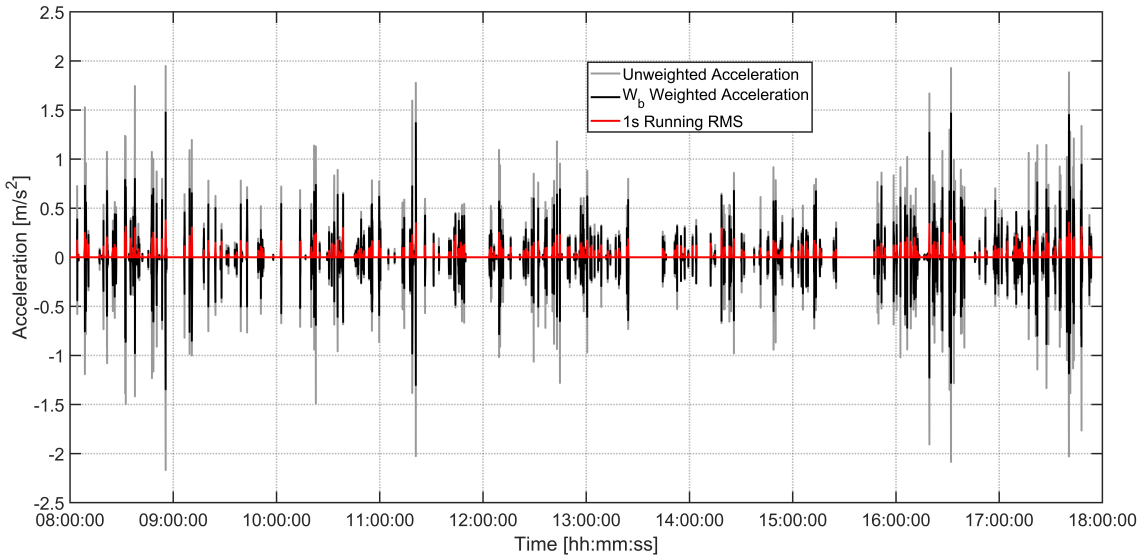

Figure 6.17: A typical simulation acceleration time history response at equivalent location of TP39.

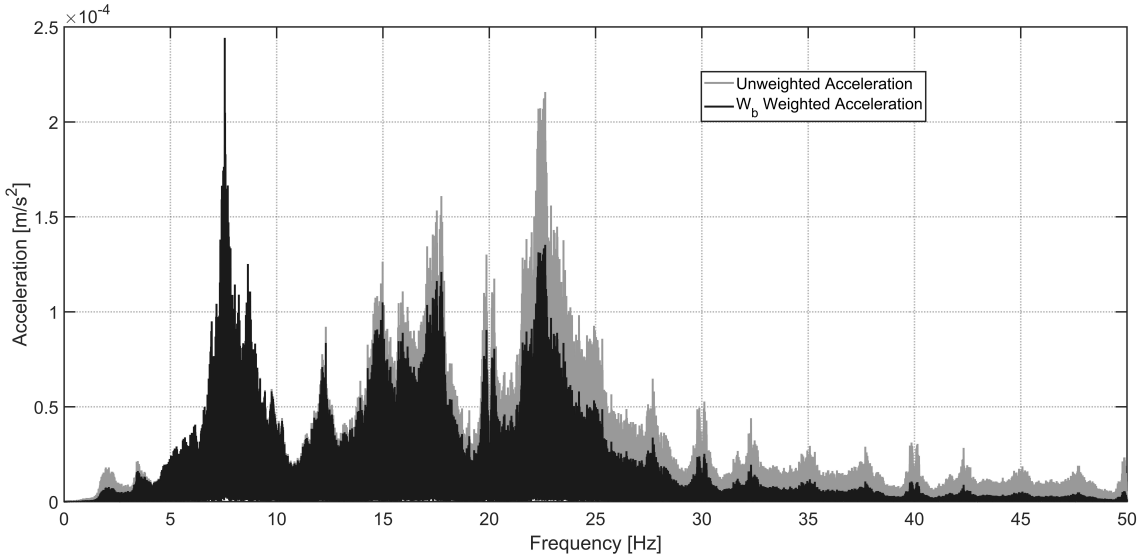

Figure 6.18: Fourier amplitude of the simulation acceleration response at equivalent location of TP39. Acceleration in "grey" is raw data and in "black" is W_b weighted.

The results of vibration response analysis for ten-hour simulation are shown in Figures 6.19 and 6.20. In addition, 5% probability of exceedance of R factor for ten-hour simulation is shown in Figure 6.21.

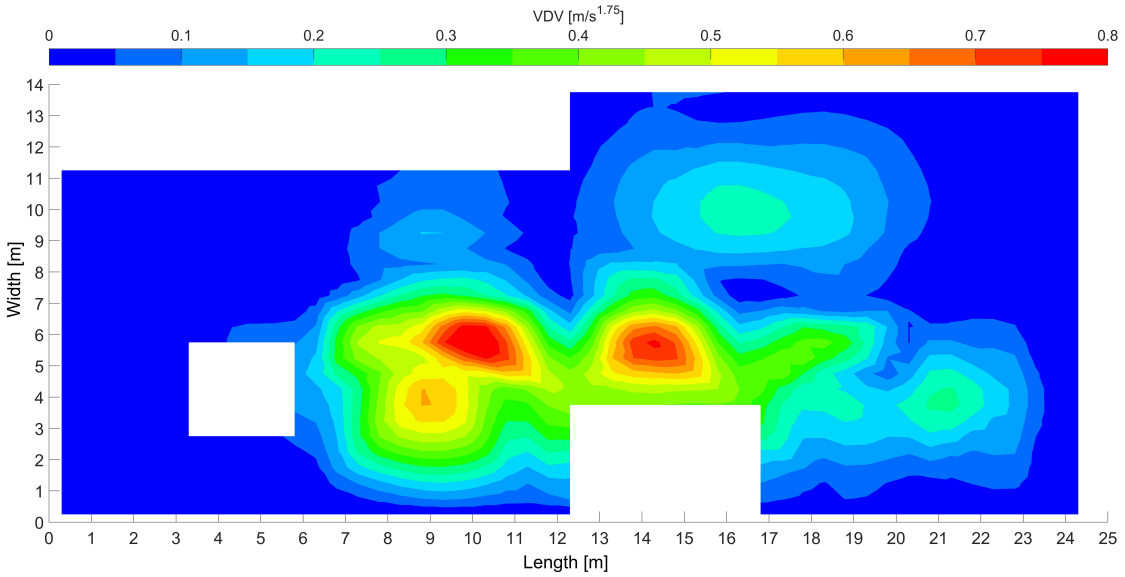

Figure 6.19: Floor A VDV spatial response.

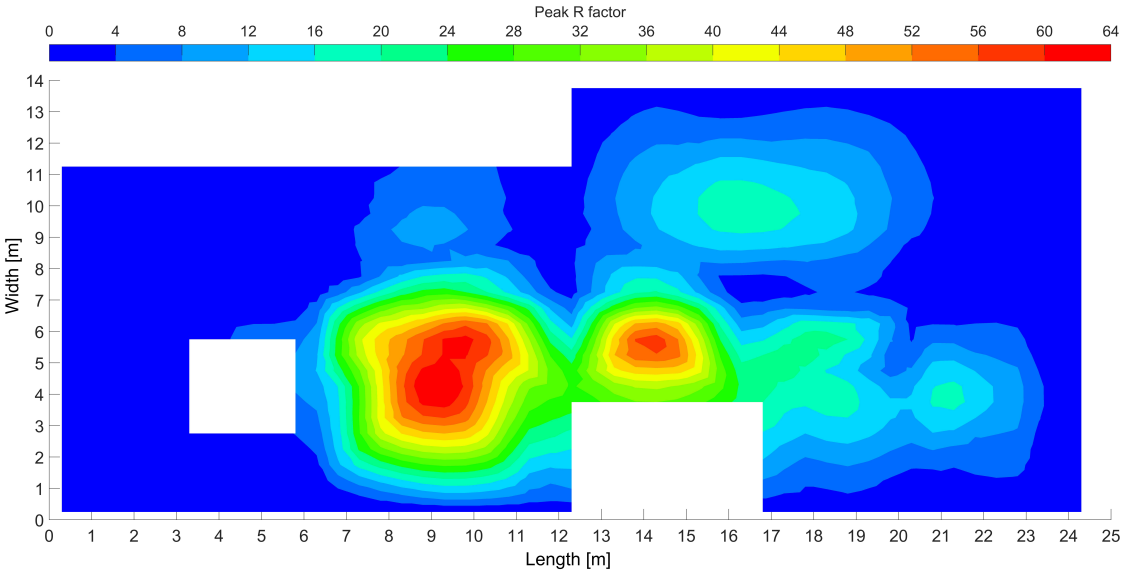

Figure 6.20: Floor A Peak R factor spatial response.

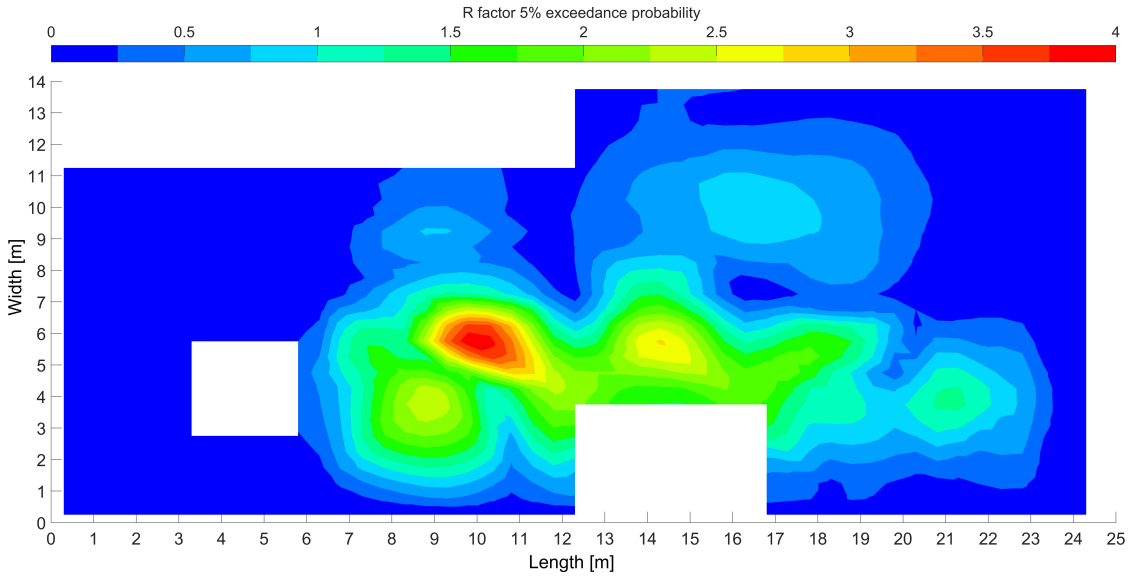

Figure 6.21: Floor A 5% probability of exceedance of R factor.

Typical comparison of both the measured TPs and simulation are shown in Figures 6.22, 6.23, 6.24, 6.24, 6.26 and 6.27. Two simulations were carried out to investigate different profiles of the response. The simulations depicted in the above figures show that the vibration level could result in different values when compared against the measurement due to the probabilistic force model and pedestrian patterns. There are some differences in these simulated responses when compared against the measured VDV and R factor, as would be expected for simulation results based on idealisations of pedestrian behaviours. The percentage of error between the simulation and the measurement, for the three locations presented in the above figures, for 5% probability of exceedance of R factor is, on average, less than 16%. Whilst, the model, in terms of VDVs, tends to replicate the trends in in-service response, some locations, such as TP39 in Figure 6.22 seems to underestimate the predictions. This could be attributed to the number of modes used in the model , which is nine modes. Another reason could be the randomness in human behaviour and further monitoring for more than a working day would be beneficial. Nevertheless, the predicted vibration response under multiple pedestrians seems to qualitatively correlate to a good extent with that measured. Hence, the methodology yields good outcomes and it is capable to provide realistic vibration serviceability assessment in this case.

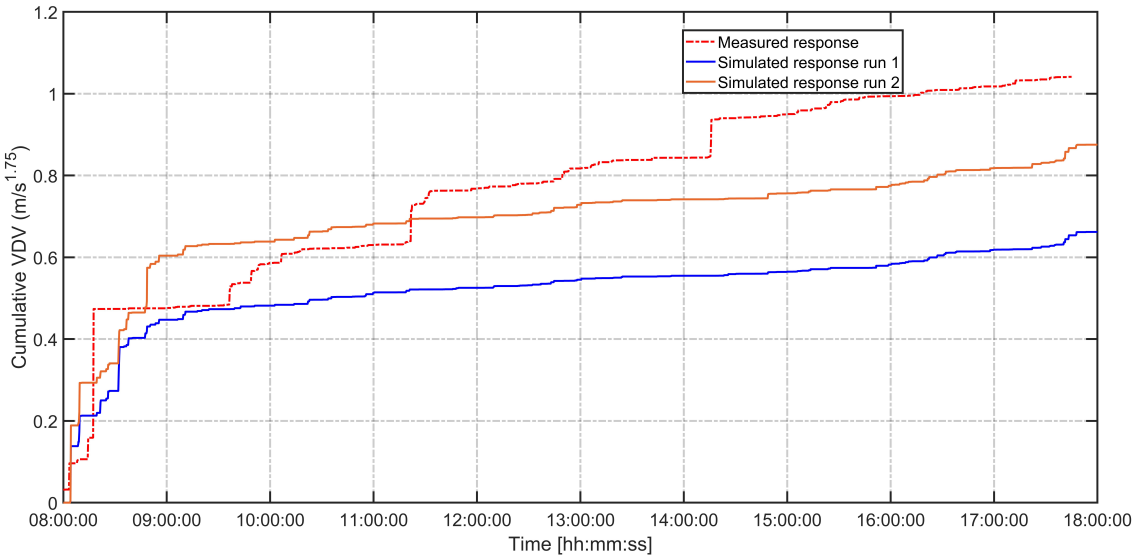

Figure 6.22: Floor A comparison of measured and simulation VDV at TP39.

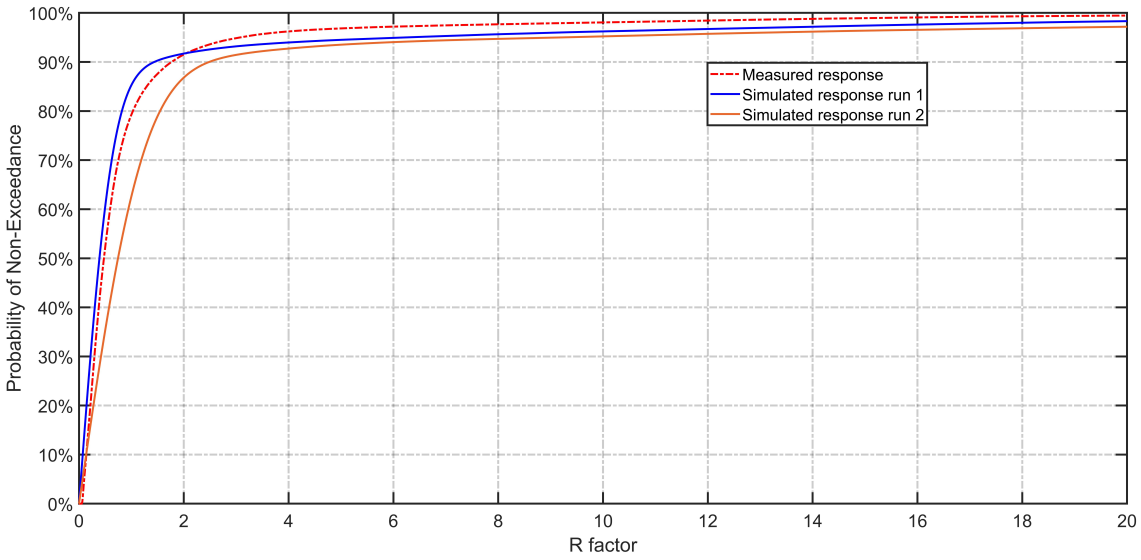

Figure 6.23: Floor A comparison of measured and simulation cumulative distribution of R factor at TP39.

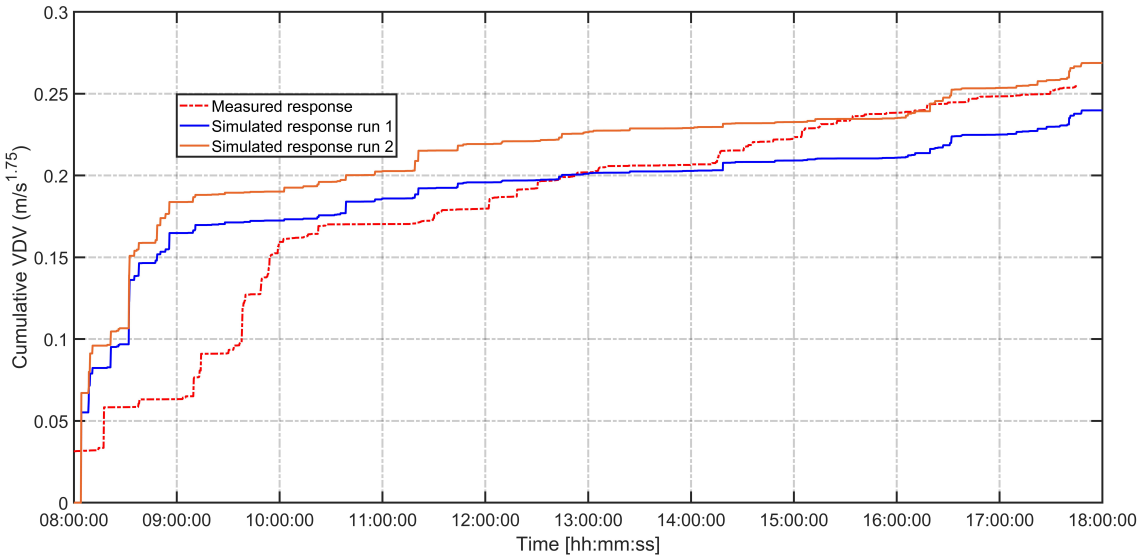

Figure 6.24: Floor A comparison of measured and simulation VDV at TP16.

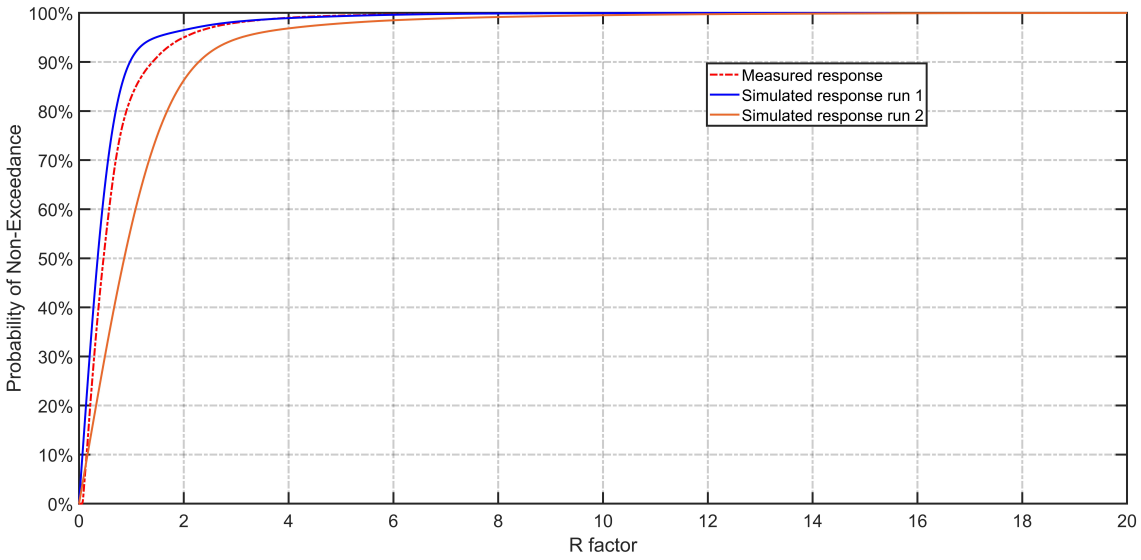

Figure 6.25: Floor A comparison of measured and simulation cumulative distribution of R factor at TP16.

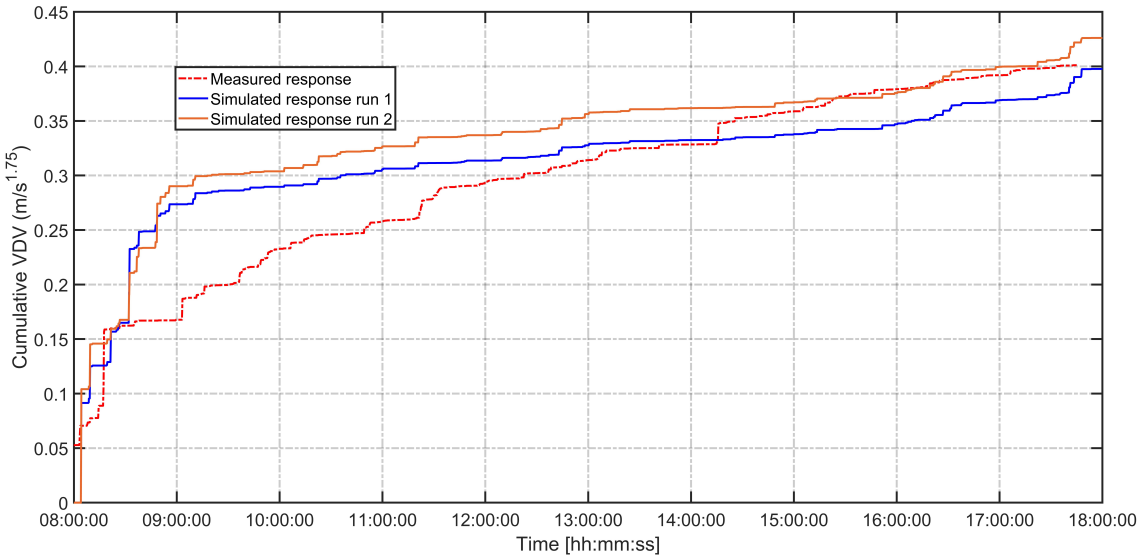

Figure 6.26: Floor A comparison of measured and simulation VDV at TP51.

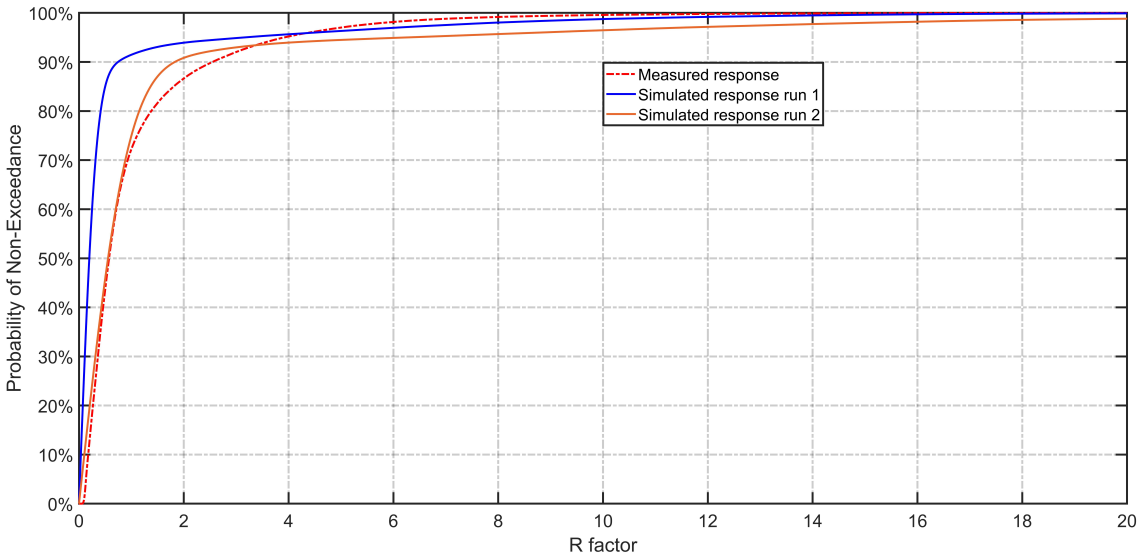

Figure 6.27: Floor A comparison of measured and simulation cumulative distribution of R factor at TP51.

6.3.3.2 Floor B

The modal properties obtained from FE analysis together with the damping ratio for each mode from measurements were used for response predictions. The methodology presented in this study accounts for a large number of modes that contribute to the response. This particular floor is in the region around LFF and HFF cut-off frequencies according to the various design guidelines, thus introducing some uncertainty as to which vibration limits are appropriate for this analysis. 50 modes from FE analysis were considered for the response calculation, which corresponds to all modes up to 30 Hz. Including more modes in the MATLAB-based time domain response analysis would have added significantly to the run

time; use of this number of modes was considered sufficient for the exercise in hand and exceeded the number of modes suggested in the CCIP-016 guidance [7], which is 15 Hz.

The results of spatial response analysis are shown as contour plots of key vibration response descriptors (VDV, R factors and 5% probability of exceedance of R factor) as determined from time histories calculated from mode superposition time integration analysis. Response distributions over the whole area for the aforementioned four layouts are illustrated in terms of 16 hrs equivalent VDVs in Figures 6.28, 6.29, 6.30 and 6.31, respectively. It can be seen that as floor occupants excite walking paths corresponding with each individual layout, some area/layouts are more prone to higher levels of response than others, and that the vibration level changes with respect to time and location. Based on these analyses, a vibration serviceability assessment can be carried out. Layout configuration 4 is, therefore, expected to have “low probability of adverse comment” according to Table 6.1. However, considering Section 2.5 where the limit for adverse comment is 0.15 m/s$^{1.75}$, that floor may have some adverse comments.

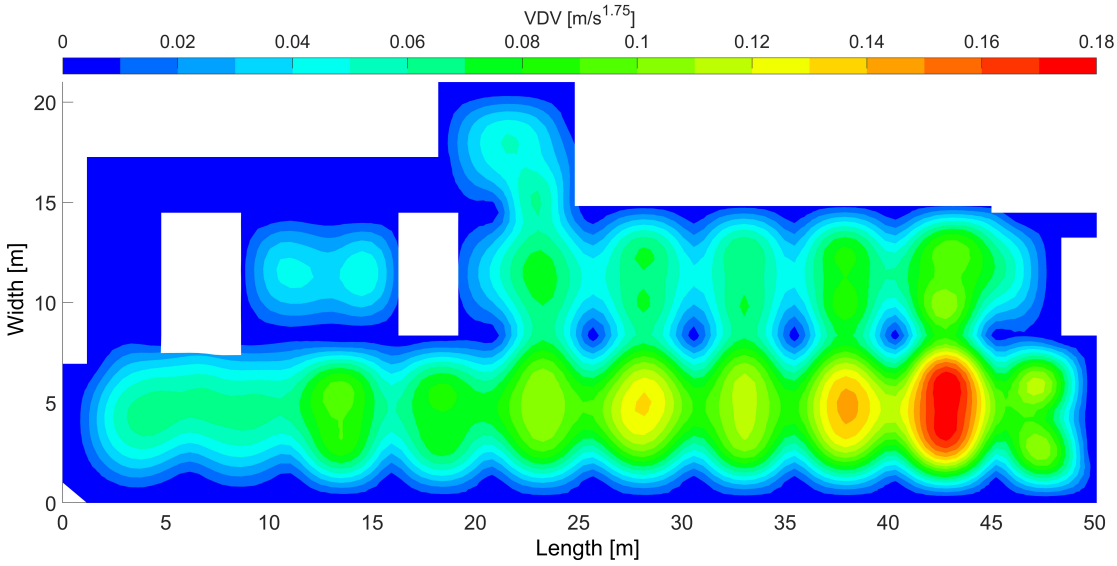

Figure 6.28: Floor Layout 1 VDV spatial response.

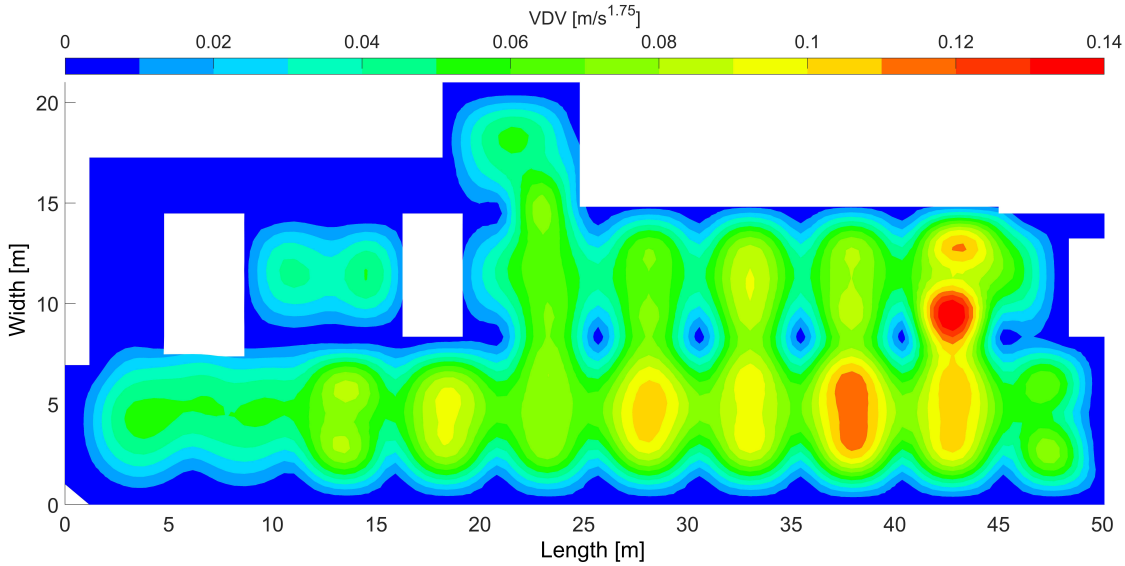

Figure 6.29: Floor Layout 2 VDV spatial response.

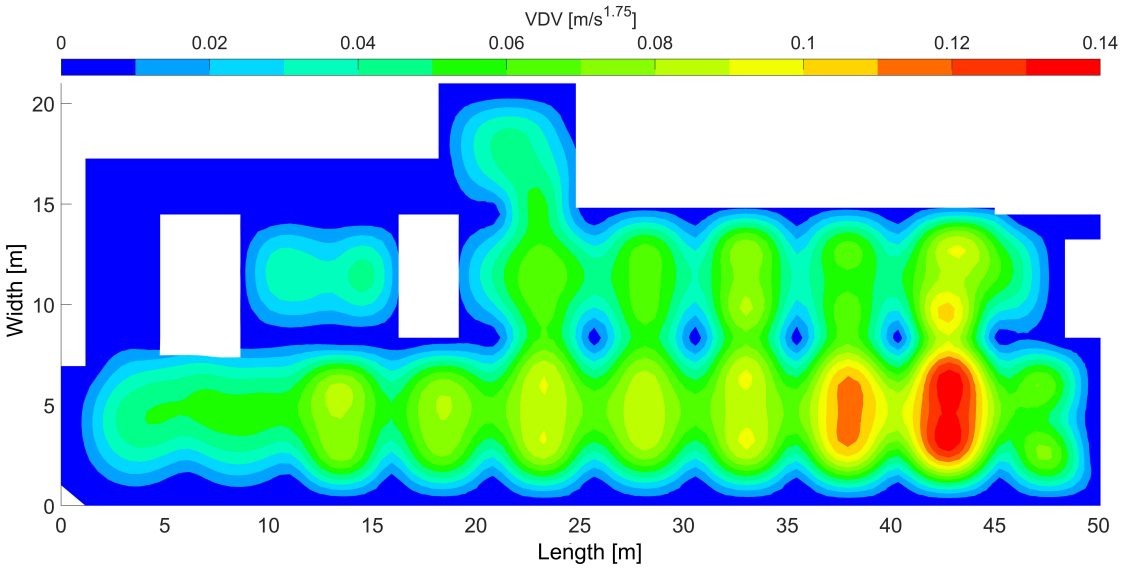

Figure 6.30: Floor Layout 3 VDV spatial response.

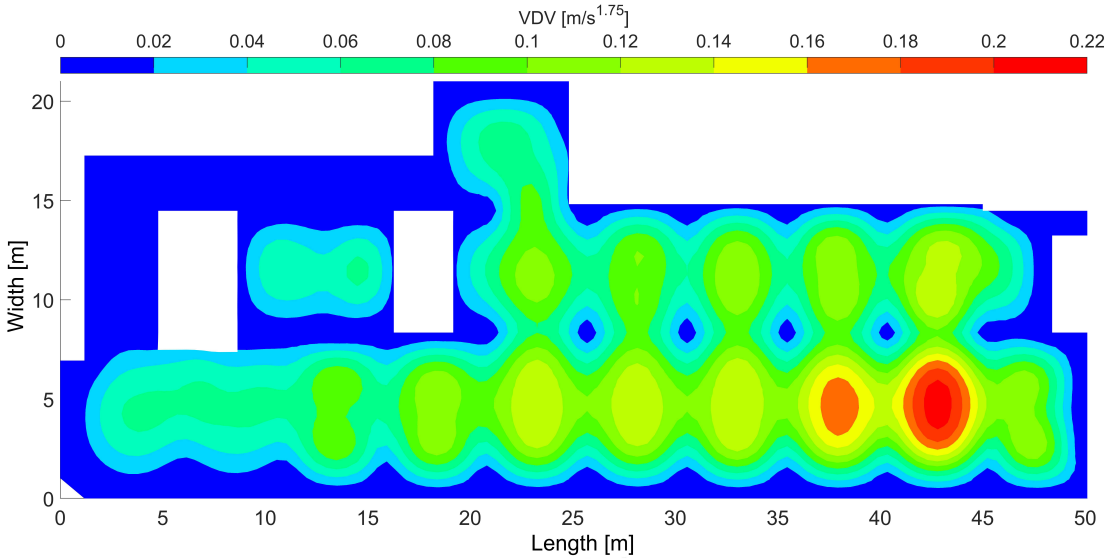

Figure 6.31: Floor Layout 4 VDV spatial response.

As far as R factor and probability of exceedance are concerned, the results are shown in Figures 6.32, 6.33 for Layout 1 and Figures 6.34 and 6.35 for Layout 4. It can be seen that the 5% probability of exceedance (i.e. 30 minutes) is far more flexible than the peak R factor in terms of describing stochastic behaviour of human-induced vibration. However, there are no specified threshold limits in the available guidance. Note that any probability of exceedance values are possible with this methodology, e.g. 10%, 25% etc.

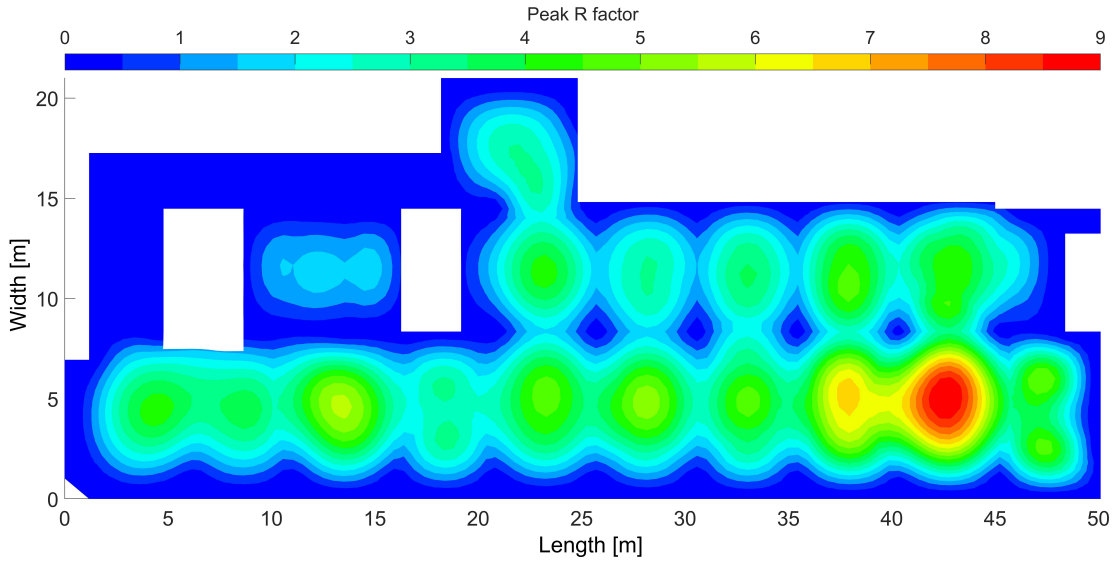

Figure 6.32: Floor Layout 1 Peak R factor spatial response.

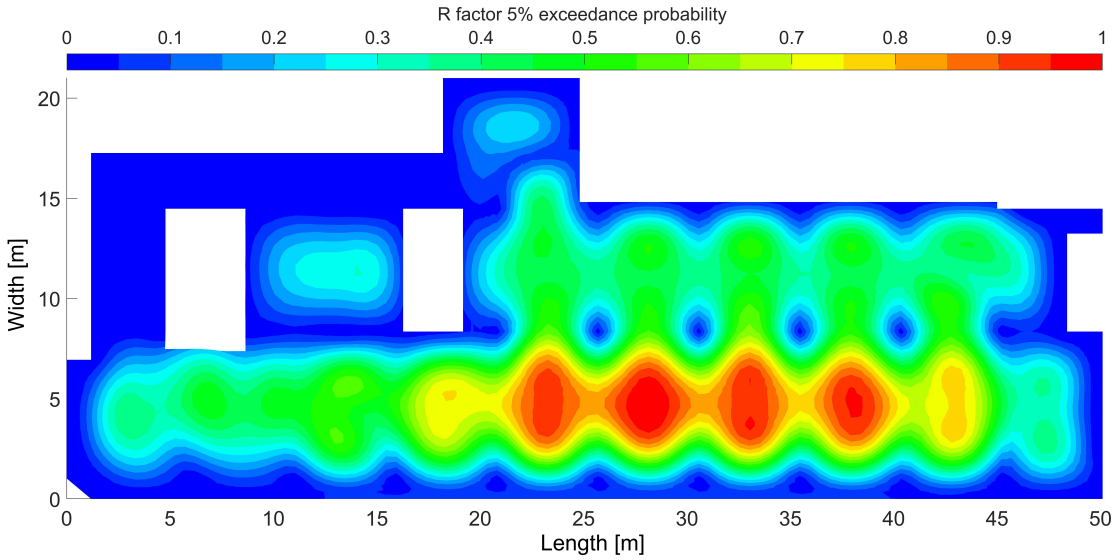

Figure 6.33: Floor Layout 1 5% probability exceedance of R factor.

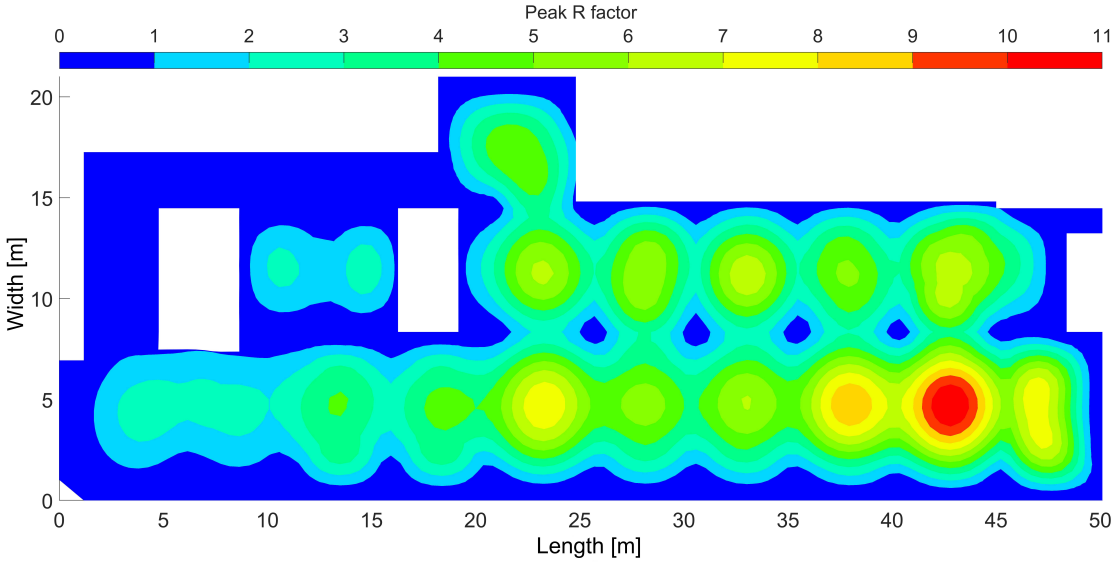

Figure 6.34: Floor Layout 4 Peak R factor spatial response.

Considering human perception of vibration, the analyses can also show results of different locations. It is worth mentioning that there may be relative differences in perception of standing, sitting and walking, which is beyond the scope of this study and future investigation should take that into account. The simulation of spatial distribution of pedestrians provides insights into timings not only at pedestrian desks, but also at a particular walking path. This in turn can yield vibration levels experienced at those locations in a probability-based approach. For example, Figures 6.36 for Layout 1, 6.37 for Layout 2,6.38 for Layout 3, and 6.39 for Layout 4, respectively, show the VDVs experienced by pedestrians in a 16 hrs equivalent time period. The 75%ile and 95%ile indicate the number of pedestrians who at their desks, i.e. while sitting, in total perceived a level of VDV at a particular time

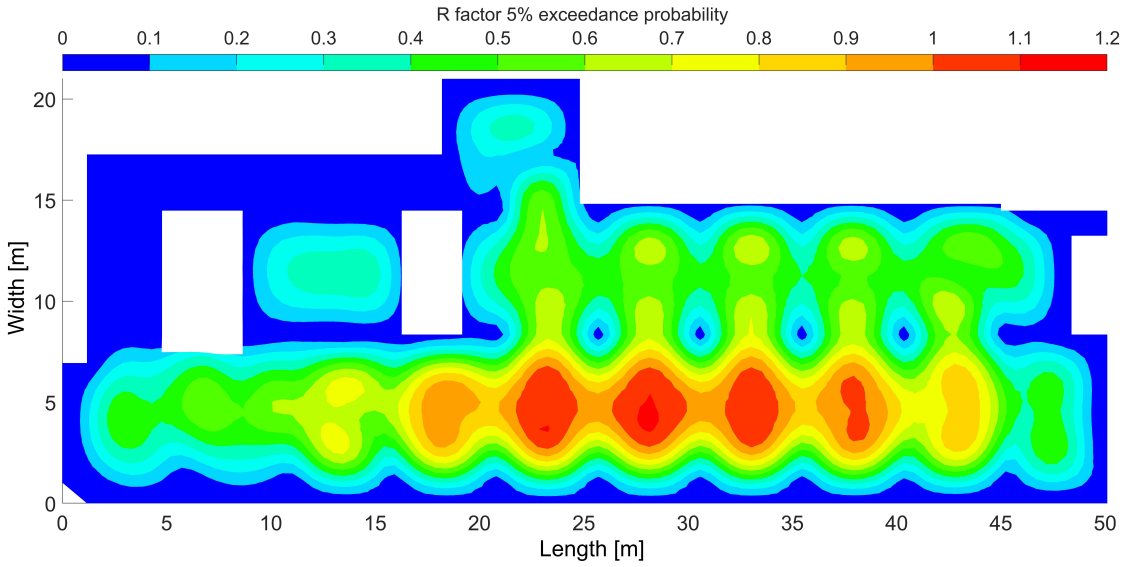

Figure 6.35: Floor Layout 4 5% probability exceedance of R factor.

of simulation time. In a similar way, while walking over a walking path, the pedestrians experienced that much level of vibration. For instance, in Figure 6.39 for the first 2.5 hours of simulation (working time) 75%ile of pedestrians while sitting felt a VDV around 0.08 m/s$^{1.75}$, whereas those walking felt around 0.143 m/s$^{1.75}$, i.e. elsewhere on the floor. This approach can provide a better understanding on how different pedestrians at various time and locations are able to perceive vibrations. It improves on current methods in the sense that a more realistic assessment of vibration serviceability can be performed.

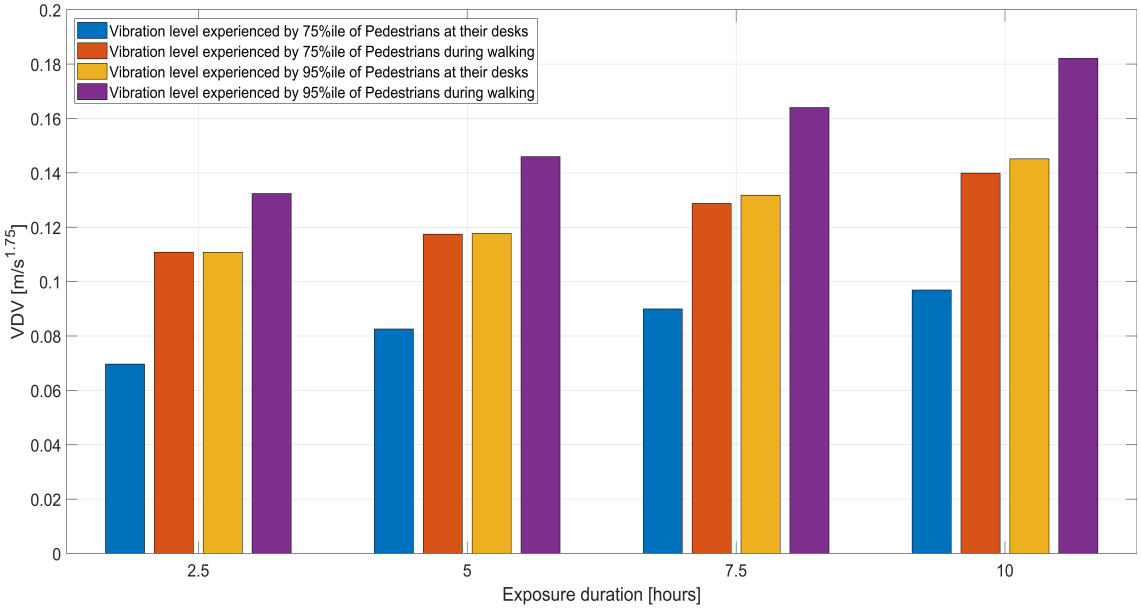

Figure 6.36: Floor Layout 1 Pedestrian vibration level experience.

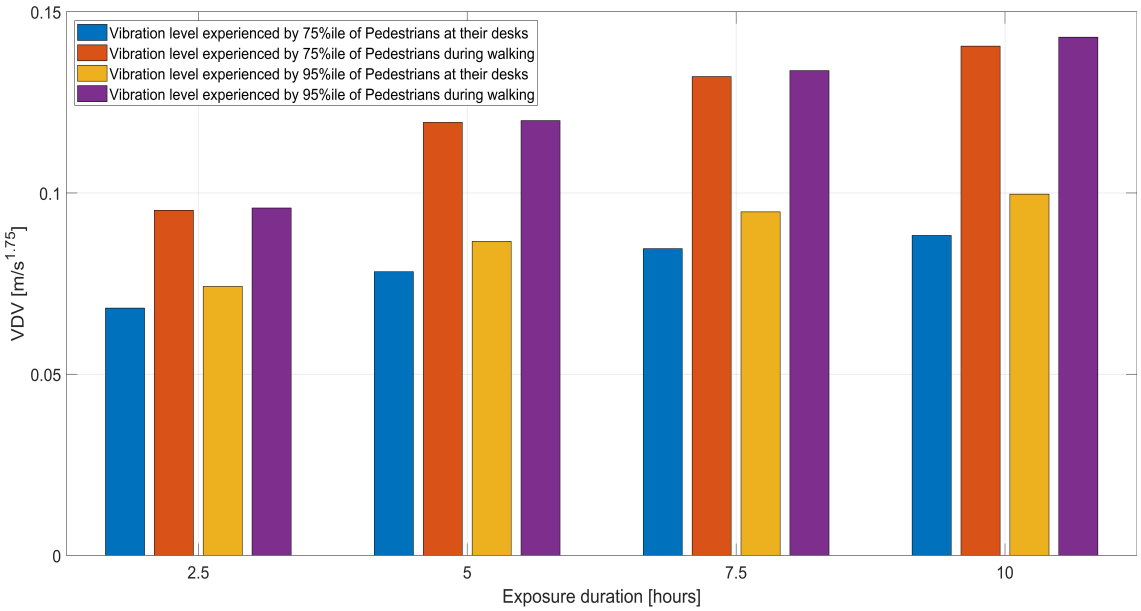

Figure 6.37: Floor Layout 2 Pedestrian vibration level experience.

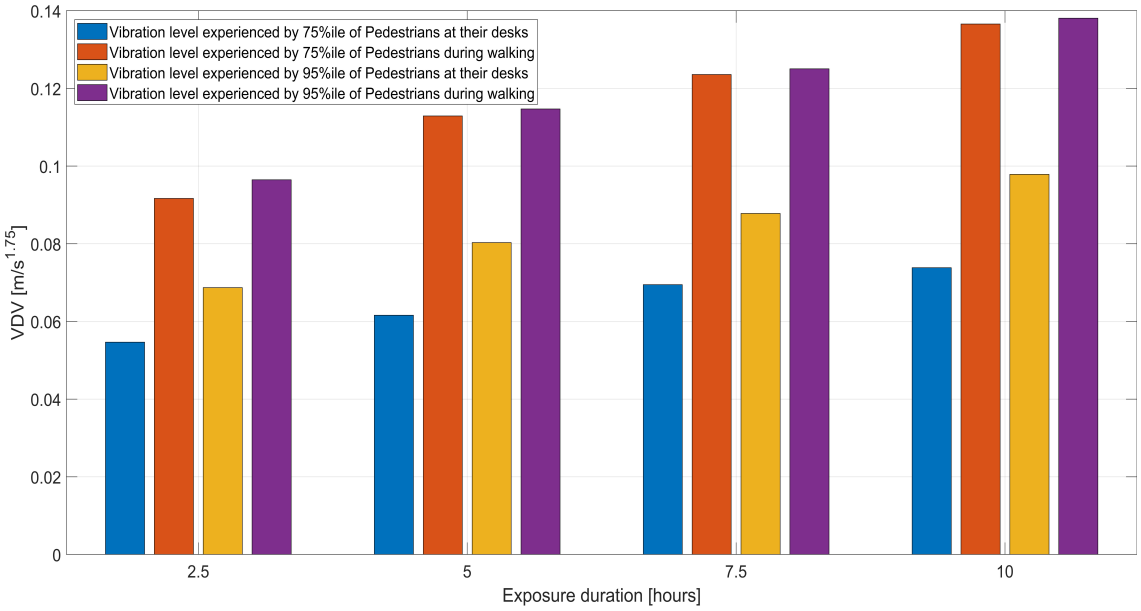

Figure 6.38: Floor Layout 3 Pedestrian vibration level experience.

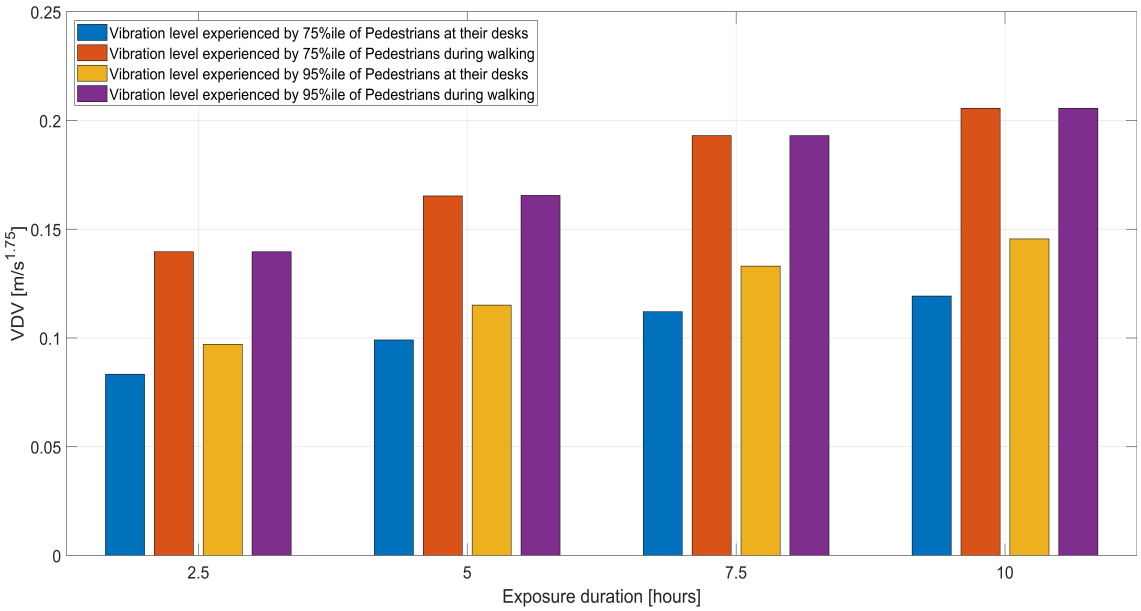

Figure 6.39: Floor Layout 4 Pedestrian vibration level experience.

Figure 6.40 shows the percentage of the floor area for Layout 4 exceeding allowable limits in Table 6.1 with respect to 16 hrs VDV. This is shown for two different vibration response runs, to assess the effect of probabilistic walking forces yielding different responses. The trend illustrates how much area of the floor has a certain value of VDVs. For example, there is approximately 5% of the floor area with a VDV higher than about 0.13 m/s$^{1.75}$. This can help in identifying percentages of areas with high vibration levels and thereby taking measures to reduce high vibration responses at the design stage.

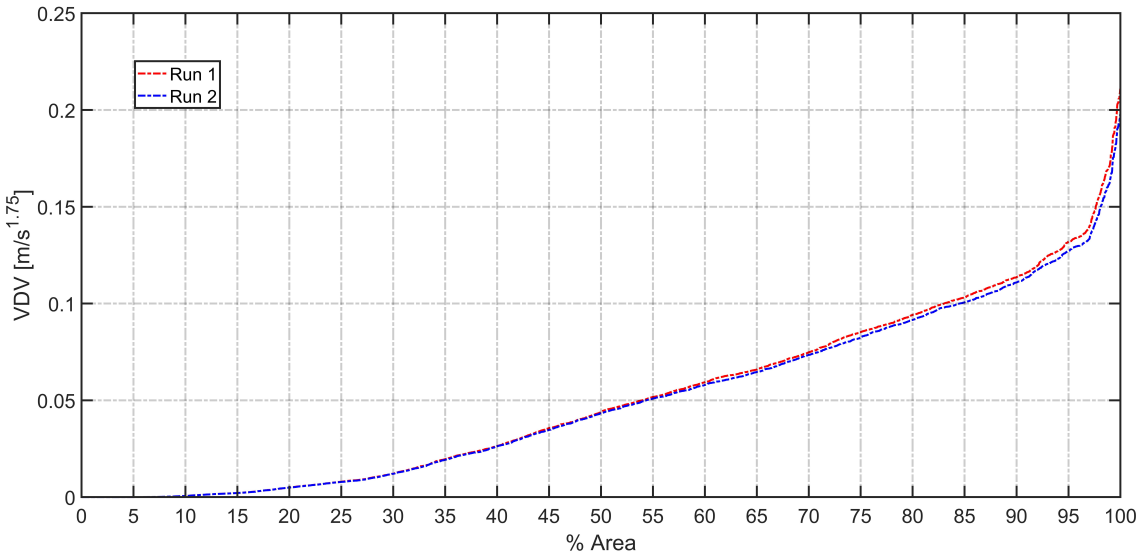

Figure 6.40: Floor Layout 4 percentage of floor area vibration experience.

6.4 Conclusions

This chapter has presented a comprehensive and compact way to predict vibration responses of floors using probabilistic time-domain response analysis. This chapter advances the field by combining a probabilistic multi-person walking model and spatial distribution of pedestrians to estimate vibration responses for long durations of time. The results are presented in terms of VDVs and R factors, and probabilistic analysis of exceedance of vibration responses at various locations, rather than a single peak value at each location. The model qualitatively represents in-service response measurements for Floor A. It was noted that overall the model tends to replicate trends in in-service response and to a good extent provides approximate vibration levels consistent with those from measurements.

It is shown that a range of walking paths can be excited by multiple pedestrians, resulting in some areas of a structure being more prone to higher levels of response than others. In particular, four different layouts for Floor B produced various levels of vibration and among those configurations, layout four was the critical case. It is important also to consider the temporal distribution of pedestrians, since individual responses can be additive, leading to a more realistic assessment of overall response than for a single person walking. Also, the methodology can provide a realistic vibration serviceability assessment in a statistical manner, where vibration levels corresponding to any probability of exceedance can be computed.

More realistic assessment of occupant perception of vibration both at their desks and during walking is another advantage of this approach. Both the exposure time and location can be used to determine how much vibration (vibration dose) is experienced by individuals. This can provide a more reliable prediction for vibration serviceability assessment of floors.

Chapter 7

Conclusions and Recommendations

The study presented in this thesis aimed to provide insights and improve understanding of vibration serviceability of floors under multiple pedestrians walking via a probabilistic approach. A comprehensive literature survey was conducted, leading to development of a probabilistic walking model and numerical models to represent spatial distributions of multi-person features. Study of the experimental tests enabled identification of the in-service vibration responses under floor occupants and the effect of different walking paths on vibration level. The key findings and outcomes of the research work conducted and presented in this thesis are summarised hereafter.

7.1 Conclusions

1. Typical floors often accommodate multiple pedestrians with a range of walking patterns. Actual walking path and activities of occupants along different routes are a crucial step to consider.

2. Contemporary vibration design guidelines are shown to produce significant over- and under-estimation of vibration responses to a pedestrian excitation. It is suggested that improvements are required with respect to dynamic properties, expected loading scenarios and the corresponding walking-induced forces.

3. A single peak value of vibration response appears to be misleading and unrepresentative for vibration serviceability assessment. Therefore, significant improvements and rigorous approaches are required to introduce measures of vibration dose or probability of exceedence with realistic perception

thresholds, to represent vibration ratings and tolerance limits in a statistical manner.

4. The research showed that assessment based on a single pedestrian vibration response is not consistent with true multiple pedestrian in-service responses. Therefore, it was ascertained that multiple pedestrians' loading patterns should be utilised at the design stage.

5. A novel numerical technique was developed using agent-based modelling incorporating a social force model to generate spatial distributions of pedestrians upon floor usage. The model includes pedestrians' patterns in a comprehensive way that resembles reality in terms of events and locations. Such techniques are rare in vibration serviceability assessment of floors. This makes simulation of pedestrian patterns at design stage a very interactive and decisive tool.

6. Utilising a probabilistic approach is essential to generate multiple pedestrian loads and predict the vibration response sufficiently accurately, i.e. both large overestimation and considerable underestimation of the response should be avoided. It is suggested that a probabilistic walking force model, irrespective to any frequency threshold, should be used.

7. The established probabilistic walking force model in this study showed an opportunity to enhance current vibration serviceability assessment guidelines, which lack appropriate statistical perspective. The walking model is applicable for walking force signals from both individual and multiple pedestrians.

8. The established model can be easily reproduced from the data and equations presented in this study. In addition, the model can be used in discrete footfall analysis when individual steps are applied on different structural components. It can be implemented in any finite element (FE) package for vibration serviceability analysis. This can facilitate the application of individual walking step forces at sequential spatial positions along any walking paths.

9. Conservative design with an accept-reject method neither results in a reliable assessment, nor describes the rare vibration events that may happen. Hence, this study has presented a comprehensive method to predict vibration responses using different statistical perspectives integrating both the probabilistic walking load model and spatial distributions of multiple pedestrians. The established approach showed a realistic way of determining pedestrians' vibration exposure at different locations as well as over the whole floor area.

7.2 Future research recommendations

1. This study examined a limited number of floors due to time and access constraints. As such, it is recommended to conduct more investigations wherein a wide array of floors in terms of functions and plan layouts are monitored for long durations to better understand pedestrians' movements and activities. This could include floor structures (FS) 1, 2 and 3.

2. Contemporary design guides do not have a methodology to consider multiple pedestrian loading scenarios. Therefore, it is recommended to initiate a collaborative committee of experts in this area, industry partners and guidance organisation body to come up with a new set of guidelines and codes of practice based on the findings of this study.

3. Non-structural elements, including partitions and cladding walls, appeared to have significant effects on dynamic properties and families of modes. This study provided some recommendation to include them in numerical modelling. However, there are no procedures in guidance documents for practitioners to follow. It is therefore suggested to carry out more thorough investigations on that aspect.

4. Time domain analysis has been the main analysis utilised in this thesis, despite some challenging aspects such as computational effort and data storage. It is suggested to develop enhanced techniques to model pedestrians' movements to reflect effectively and efficiently assessment of vibration serviceability at the design stage.

5. Investigation of pedestrians-structure interaction is also essential, particularly for ultra-light weight structures and multiple pedestrians effect. It is recommended to include that aspect to the established methodology so that a comprehensive vibration serviceability assessment can be guaranteed.

References

1. Hudson, E. J.: Incorporating active control of human-induced vibrations in floors into buildings. PhD thesis. Sheffield, UK: The University of Sheffield, 2013.
2. Mohammed, A., Pavic, A., and Racic, V.: Improved model for human induced vibrations of high-frequency floors. Eng. Struct. Vol. 168, pp. 950 – 966, 2018.
3. Lamb, S., Macefield, V. G., Walton, D., and Kwok, K. C. S.: Occupant response to wind-excited buildings: a multidisciplinary perspective. Structures and Buildings, Vol. 169, No. 8, pp. 625–634, 2016.
4. Zhou, X., Li, J., and Liu, J.: Vibration of prestressed cable RC truss floor system due to human activity. J. of Struct. Eng. Vol. 142, No. 5, pp. 1–10, 2015.
5. Murray, T. M., Allen, D. E., Ungar, E. E., and Davis, D. B.: Vibrations of steel-framed structural systems due to human activity. American Institute of Steel Construction (AISC). AISC-DG11, USA, 2016.
6. Smith, A., Hicks, S., and Devine, P.: Design of floors for vibration: A new approach. 2nd. Steel Construction Institute (SCI). SCI P354, Berkshire, UK, 2009.
7. Willford, M. and Young, P.: A Design guide for footfall induced vibration of structures. Concrete Centre(CC). CCIP-016, Surrey, UK, 2006.
8. RFCS: Human induced vibrations of steel structures (HiVoSS) -vibration design of floors: background document. European Commission-RFCS. European Commission: RFS2-CT-2007-00033, Brussels, Belgium, 2007.
9. Reynolds, P. and Pavic, A.: Reliability of assessment criteria for office floor vibrations. Proc. of EVACES. Exp. Vib. Anal. for Civ. Eng. Struct., 2011, pp. 317–324.
10. Al-Anbaki, A. F.: Footfall excitation of higher modes of vibration in low-frequency building floors. PhD thesis. Exeter, UK: The University of Exeter, 2018.
11. Pavic, A., Reynolds, P., Waldron, P., and Bennett, K. J.: Critical review of guidelines for checking vibration serviceability of post-tensioned concrete floors. Cem. and Concr. Compos. Vol. 23, No. 1, pp. 21–31, 2001.
12. Pavic, A. and Reynolds, P.: Vibration serviceability of long-span concrete building floors: part 1- Review of background information. Shock and Vib. Dig. Vol. 34, No. 3, pp. 191–211, 2002.
13. Pavic, A. and Reynolds, P.: Vibration serviceability of long-span concrete building floors: part 2- Review of mathematical modelling approaches. Shock and Vib. Dig. Vol. 34, No. 4, pp. 279–297, 2002.
14. Hicks, S. and Devine, P.: Vibration characteristics of modern composite floor systems. Proc. of ASCE Compos. Constr. in Steel and Concr. 2006, pp. 247–259.

15. Nguyen, H. A. U.: Walking induced floor vibration design and control. PhD thesis. Australia: Swinburne University of Technology, 2013.

16. Živanović, S., Pavic, A., and Reynolds, P.: Vibration serviceability of footbridges under human-induced excitation: A literature review. J. Sound and Vib. Vol. 279, No. 1–2, pp. 1–74, 2005.

17. Kerr, S. C.: Human induced loading on staircases. PhD thesis. London, UK: University College London, 1998.

18. Davis, B. and Avci, O.: Simplified vibration serviceability evaluation of slender monumental stairs. J. of Struct. Eng. Vol. 141, No. 11, pp. 1–9, 2015.

19. Jones, C., Reynolds, P., and Pavic, A.: Vibration serviceability of stadia structures subjected to dynamic crowd loads: A literature review. J. of Sound and Vib. Vol. 330, No. 8, pp. 1531–1566, 2011.

20. Catbas, F., Celik, O., Avci, O., Abdeljaber, O., Gul, M., and Do, T.: Sensing and monitoring in stadium structures: A review recent advances and a forward look. Frontiers in Built Environ. Vol. 3, No. 38, pp. 1–18, 2017.

21. Mouring, S. E. and Ellingwood, B. R.: Guidelines to minimise floor vibrations from building occupants. J. of Struct. Eng. Vol. 120, No. 2, pp. 507–526, 1994.

22. Brownjohn, J. and Middleton, C.: Procedures for vibration serviceability assessment of high-frequency floors. Eng. Struct. Vol. 30, No. 6, pp. 1548–1559, 2008.

23. Bhargava, A., Al-Smadi, Y., and Avci, O.: Vibrations assessment of a hospital floor for a magnetic resonance imaging unit (MRI) replacement. Struct. Congress 2013. ASCE Struct. Congress, 2013, pp. 2433–2444.

24. Ebrahimpour, A. and Sack, R. L.: A review of vibration serviceability criteria for floor structures. Comput. and Struct. Vol. 83, No. 28, pp. 2488–2494, 2005.

25. Avci, O.: Retrofitting steel joist supported footbridges for improved vibration response. Struct. Congress 2012. ASCE Struct. Congress, 2012, pp. 460–470.

26. Osborne, K. P. and Ellis, B.: Vibration design and testing of a long-span lightweight floor. The Struct. Eng. Vol. 68, No. 10, pp. 181–186, 1990.

27. Chen, Y. and Aswad, A.: Vibration characteristics of double tee building floors. PCI J. Vol. 39, No. 1, pp. 84–95, 1994.

28. Chen, Y.: Finite element analysis for walking vibration problems for composite precast building floors using ADINA: modeling, simulation, and comparison. Comput.and Struct. Vol. 72, No. 1, pp. 109–126, 1999.

29. Hanagan, L. M., Raebel, C. H., and Trethewey, M. W.: Dynamic measurements of in-place steel floors to assess vibration performance. J. of Perform. of Constr. Facil. Vol. 17, No. 3, pp. 126–135, 2003.

30. Barrett, A., Avci, O., Setareh, M., and Murray, T.: Observations from vibration testing of in-situ structures. Struct. Congress 2006. ASCE Struct. Congress, 2006, pp. 1–10.

31. Toratti, T. and Talja, A.: Classification of human induced floor vibrations. Build. Acoust. Vol. 13, No. 3, pp. 211–221, 2006.

32. Pavic, A. and Willford, M.: Vibration serviceability of post- tensioned concrete floors. 2nd. Concrete Society. Concrete Society Appendix G, Technical Report 43.: CSTR43 App G, Slough, UK, 2005.

33. Fanella, D. A. and Mota, M.: Design guide for vibrations of reinforced concrete floor systems. Concrete Reinforcing Steel Institute (CRSI). CRSI No. 10: CRSI-10-DG-Vibration, Schaumburg, IL, 2014.
34. Živanović, S. and Pavic, A.: Probabilistic modeling of walking excitation for building floors. J. of Perform. of Constr. Facil. Vol. 23, No. 3, pp. 132–143, 2009.
35. Racic, V. and Brownjohn, J. M. W.: Stochastic model of near-periodic vertical loads due to humans walking. Adv. Eng. Inform. Vol. 25, No. 2, pp. 259–275, 2011.
36. Živanović, S.: Modelling human actions on lightweight structures: experimental and numerical developments. MATEC Web of Conf. 2015, p. 01005.
37. Živanović, S.: Probability-based estimation of vibration for pedestrian structures due to walking. PhD thesis. Sheffield, UK: The University of Sheffield, 2006.
38. Hudson, E. J. and Reynolds, P.: Implications of structural design on the effectiveness of active vibration control of floor structures. Struct. Control & Health Monit. Vol. 21, No. 5, pp. 685–704, 2014.
39. Brownjohn, J., Pavic, A., and Omenzetter, P.: A spectral density approach for modelling continuous vertical forces on pedestrian structures due to walking. Can. J. Civ. Eng. Vol. 31, No. 1, pp. 65–77, 2004.
40. Middleton, C. J. and Brownjohn, J. M. W.: Response of high frequency floors: A literature review. Eng. Struct. Vol. 32, No. 2, pp. 337–352, 2010.
41. Pavic, A, Miskovic, Z., and Živanović, S.: Modal properties of beam-and-block pre-cast floors. The IES J. Part A: Civ.and Struct. Eng. Vol. 1, No. 3, pp. 171–185, 2008.
42. Willford, M., Young, P., and Field, C.: Improved methodologies for the prediction of footfall-induced vibration. Proc. SPIE. Buildings for Nanoscale Research and Beyond, 2005, pp. 1–12.
43. Reynolds, P. and Pavic, A.: Effects of false floors on vibration serviceability of building floors. II: Response to pedestrian excitation. J. of Perform. of Constr. Facil. Vol. 17, No. 2, pp. 87–96, 2003.
44. Younis, A., Avci, O., Hussein, M., Davis, B., and Reynolds, P.: Dynamic forces induced by a single pedestrian: A literature review. Appl. Mech. Rev. Vol. 69, No. 2, pp. 020802–1–020802–17, 2017.
45. ISO10137: Bases for testing of structures- serviceability of buildings and walkways against vibrations. International Organization for Standardization (ISO), Geneva, Switzerland, 2007.
46. Eriksson, P.-E.: Vibration of low-frequency floors –dynamic forces and response prediction. PhD thesis. Goteborg, Sweden: Chalmers University of Technology, 1994.
47. Živanović, S., Pavic, A., and Racic, V.: Towards modelling in-service pedestrian loading of floor structures. Dyn. of Civ. Struct., Vol. 1 : Proc. of the 30th IMAC, A Conf. and Expos. on Struct. Dyn. 2012. Springer Int. Publ., New York, NY, 2012, pp. 85–94.
48. Avci, O.: Amplitude-dependent damping in vibration serviceability: Case of a laboratory footbridge. J. of Archit. Eng. Vol. 22, No. 3, pp. 1–15, 2016.
49. Ji, T. and Ellis, B.: Floor vibration induced by dance type loads: theory. The Struct. Eng. Vol. 72, No. 31, pp. 37–44, 1994.

50. Hamdan, S., Hoque, M. N., and Sutan, M.: Dynamic property analysis and development of composite concrete floor (CCF) and vibration serviceability: A review. Int. J. of the Phys. Sci. Vol. 6, No. 34, pp. 7669–7693, 2011.
51. Middleton, C. J.: Dynamic performance of high frequency floors. PhD thesis. Sheffield, UK: The University of Sheffield, 2009.
52. Reynolds, P. and Pavic, A.: Reliability of assessment criteria for building floor vibrations under human excitation. 50th U.K. Conf. on Hum. Responses to Vib. Exp. Vib. Anal. for Civ. Eng. Struct., Southampton, U.K., 2015.
53. Živanović, S. and Pavic, A.: Quantification of dynamic excitation potential of pedestrian population crossing footbridges. Shock and Vib. Vol. 18, No. 4, pp. 563–577, 2011.
54. Costa-Neves, L., Silva, J. da, Lima, L. de, and Jordão, S.: Multi-storey, multi-bay buildings with composite steel-deck floors under human-induced loads: The human comfort issue. Comput. and Struct. Vol. 136, No. 5, pp. 34–46, 2014.
55. Lythgo, N., Wilson, C., and Galea, M.: Basic gait and symmetry measures for primary school-aged children and young adults whilst walking barefoot and with shoes. Gait and Posture, Vol. 30, No. 4, pp. 502–506, 2009.
56. Lythgo, N., Wilson, C., and Galea, M.: Basic gait and symmetry measures for primary school-aged children and young adults. II: Walking at slow, free and fast speed. Gait and Posture, Vol. 33, No. 1, pp. 29–35, 2011.
57. Rainer, J. H. and Pernica, G.: Vertical dynamic forces from footsteps. Can. Acoust. Vol. 14, No. 2, pp. 12–21, 1986.
58. Racic, V., Pavic, A., and Brownjohn, J. M. W.: Experimental identification and analytical modelling of human walking forces: Literature review. J. of Sound and Vib. Vol. 326, No. 1, pp. 1–49, 2009.
59. Dang, H. V. and Živanović, S.: Experimental characterisation of walking locomotion on rigid level surfaces using motion capture system. Eng. Struc. Vol. 91, No. 3, pp. 141–154, 2015.
60. Ellis, B.: On the response of long-span floors to walking loads generated by individuals and crowds. The Struct. Eng. Vol. 10, No. 78, pp. 17–25, 2000.
61. Kerr, S. C. and Bishop, N. W. M.: Human induced loading on flexible staircases. Eng. Struct. Vol. 23, No. 1, pp. 37–45, 2001.
62. Pachi, A. and Ji, T.: Frequency and velocity of people walking. The Struct. Eng. Vol. 83, No. 3, pp. 36–40, 2005.
63. Chen, J., Xu, R., and Zhang, M.: Acceleration response spectrum for predicting floor vibration due to occupant walking. J. of Sound and Vib. Vol. 333, No. 15, pp. 3564–3579, 2014.
64. Jacobs, N., Skorecki, J., and Charnley, J.: Analysis of the vertical component of force in normal and pathological gait. J. of Biomech. Vol. 5, No. 1, pp. 11–34, 1972.
65. Caprani, C. C.: Application of the pseudo-excitation method to assessment of walking variability on footbridge vibration. Comput. and Struct. Vol. 132, No. 2, pp. 43–54, 2014.
66. Mohammed, A. S. and Pavic, A.: Evaluation of mass-spring-damper models for dynamic interaction between walking humans and civil structures. Dyn. of Civ. Struct., Vol. 2 : Proc. of the 35th IMAC, A Conf. and Expos. on Struct. Dyn. 2017. Springer Int. Publ., 2017, pp. 169–177.

67. Shahabpoor, E., Pavic, A., and Racic, V.: Structural vibration serviceability: New design framework featuring human-structure interaction. Eng. Struct. Vol. 136, No. 4, pp. 295–311, 2017.
68. Živanović, S., Pavic, A., and Reynolds, P.: Probability-based prediction of multi-mode vibration response to walking excitation. Eng. Struct. Vol. 29, No. 6, pp. 942–954, 2007.
69. Piccardo, G. and Tubino, F.: Simplified procedures for vibration serviceability analysis of footbridges subjected to realistic walking loads. Comput. and Struct. Vol. 87, No. 13-14, pp. 890–903, 2009.
70. Waarts, P. H. and Duin, F. V.: Assessment procedure for floor vibrations due to walking. Heron J. Vol. 51, No. 4, pp. 251–264, 2006.
71. Willford, M. R., Young, P., and Field, C.: Predicting footfall-induced vibration: Part 1. Proc. of the Inst. of Civ. Eng. (ICE) - Structures and Buildings, Vol. 160, No. 2, pp. 65–72, 2007.
72. Setareh, M.: Office floor vibrations: evaluation and assessment. Proc. of the Inst. of Civ. Eng. (ICE) - Structures and Buildings, Vol. 167, No. 3, pp. 187–199, 2014.
73. Ebrahimpour, A., Hamam, A., Sack, R. L., and Patten, W. N.: Measuring and modeling dynamic loads imposed by moving crowds. J. of Struct. Eng. Vol. 122, No. 12, pp. 1468–1474, 1996.
74. Rainer, J. H., Pernica, G., and Allen, D. E.: Dynamic loading and response of footbridges. Can. J.of Civ. Eng. Vol. 15, No. 1, pp. 66–71, 1988.
75. Hamming, R. W.: Numerical methods for scientists and engineers. Second. McGraw Hill, New York, NY, U.S., 1973.
76. Alexander, R. M. and Jayes, A.: Fourier analysis of forces exerted in walking and running. J. of Biomech. Vol. 13, No. 4, pp. 383–390, 1980.
77. Blanchard, J., Davies, B. L., and Smith, J.: Design criteria and analysis for dynamic loading of footbridges. Symp on Dyn. Behav. of Bridges. Crowthrone, UK, 1977, pp. 1–11.
78. Murray, T. M. and Allen, G.: Floor vibrations: a new design approach. Proc. of IABSE. Zürich, Switzerland, 1993, pp. 119–124.
79. Bachmann, H., Ammann, W. J., Deischl, F., Eisenmann, J., Floegl, I., Hirsch, G. H., Klein, G. K., Lande, G. J., Mahrenholtz, O., Natke, H. G., Nussbaumer, H., Pretlove, A. J., Rainer, J. H., Saemann, E.-U., and Steinbeisser, L.: Vibration problems in structures: Practical guideline. Report. Zürich: Birkhäuser Verlag, 1995.
80. Obata, T. and Miyamori, Y.: Identification of a human walking force model based on dynamic monitoring data from pedestrian bridges. Comput. and Struct. Vol. 84, No. 8-9, pp. 541–548, 2006.
81. Bachmann, H. and Ammann, W.: Vibrations in structures induced by man and machines. Second. International Association for Bridge and Structural Engineering, Zürich, Switzerland, 1987.
82. Brownjohn, J., Racic, V., and Chen, J.: Universal response spectrum procedure for predicting walking-induced floor vibration. Mech. Syst. & Signal Process. Vol. 71, No. 3, pp. 741–755, 2016.
83. Krenk, S.: Dynamic response to pedestrian loads with statistical frequency distribution. J. of Eng. Mech. Vol. 138, No. 10, pp. 1275–1281, 2012.
84. Ohlsson, S. V.: Floor vibrations and human discomfort. PhD thesis. Goteborg, Sweden: Chalmers University of Technology, 1982.

85. Ebrahimpour, A. and Sack, R. L.: Modeling dynamic occupant loads. J. of Struct. Eng. Vol. 115, No. 6, pp. 1476–1496, 1989.

86. Piccardo, G. and Tubino, F.: Equivalent spectral model and maximum dynamic response for the serviceability analysis of footbridges. Eng. Struct. Vol. 40, No. 7, pp. 445–456, 2012.

87. Pedersen, L. and Frier, C.: Sensitivity of footbridge vibrations to stochastic walking parameters. J. of Sound and Vib. Vol. 329, No. 13, pp. 2683–2701, 2010.

88. Bocian, M., Macdonald, J., and Burn, J.: Biomechanically inspired modeling of pedestrian-induced vertical self-excited forces. J. of Bridge Eng. Vol. 18, No. 12, pp. 1336–1346, 2013.

89. Hicks, S.: Vibration characteristics of steel concrete composite floor systems. Progress in Struct. Eng. and Mater. Vol. 6, No. 1, pp. 21–38, 2004.

90. Maraveas, C., Fasoulakis, Z. C., and Tsavdaridis, K. D.: A review of human induced vibrations on footbridges. Am. J. of Eng. and Appl. Sci. Vol. 8, No. 4, pp. 422–433, 2015.

91. Mashaly, E.-S., Ebrahim, T. M., Abou-Elfath, H., and Ebrahim, O. A.: Evaluating the vertical vibration response of footbridges using a response spectrum approach. Alex. Eng. J. Vol. 52, No. 3, pp. 419–424, 2013.

92. Georgakis, C. and Ingolfsson, E. T.: Vertical footbridge vibrations: The response spectrum methodology. Proc. of Footbridge Conf. Porto, Portugal, 2008, pp. 267–275.

93. Živanović, S., Pavic, A., and Ingólfsson, E. T.: Modelling spatially unrestricted pedestrian traffic on footbridges. J. of Struct. Eng. Vol. 136, No. 10, pp. 1296–1308, 2010.

94. Carroll, S., Owen, J., and Hussein, M.: A coupled biomechanical/discrete element crowd model of crowd–bridge dynamic interaction and application to the Clifton Suspension Bridge. Eng. Struct. Vol. 49, No. 4, pp. 58–75, 2013.

95. Venuti, F., Racic, V., and Corbetta, A.: Modelling framework for dynamic interaction between multiple pedestrians and vertical vibrations of footbridges. J. Sound and Vib. Vol. 379, pp. 245–263, 2016.

96. Sim, J., Blakeborough, A., Williams, M. S., and Parkhouse, G.: Statistical model of crowd jumping loads. J. of Struct. Eng. Vol. 134, No. 12, pp. 1852–1861, 2008.

97. Hassan, O. A. B. and Girhammar, U. A.: Assessment of footfall-induced vibrations in timber and lightweight composite floors. Int. J. of Struct. Stab. and Dyn. Vol. 13, No. 2, pp. 1–26, 2013.

98. Živanović, S.: Benchmark footbridge for vibration serviceability assessment under the vertical component of pedestrian load. J. of Struct. Eng. Vol. 138, No. 10, pp. 1193–1202, 2012.

99. Matsumoto, Y., Nishioka, T., Shiojiri, H., and Matsuzaki, K.: Dynamic design of footbridges. Proc. of IABSE. 1978, pp. 1–15.

100. Nguyen, T. H., Gad, E., Wilson, J., Lythgo, N., and Haritos, N.: Evaluation of footfall induced vibration in building floor. Aust. Earthq. Eng. Soc. Conf. Barossa Valley, South Australia, 2011.

101. Macal, C. and North, M.: Tutorial on agent-based modelling and simulation. Journal of Simulation, Vol. 4, No. 3, pp. 151–162, 2010.

102. Helbing, D. and Molnar, P.: Social force model for pedestrian dynamics. Pysical Review, Vol. 51, No. 5, pp. 4282–4287, 1995.

103. Farina, F., Fontanelli, D., Garulli, A., Giannitrapani, A., and Prattichizzo, D.: Walking ahead: the headed social force model. Plos One, Vol. 12, No. 1, pp. 1–23, 2017.

104. Carroll, S., Owen, J., and Hussein, M.: Modelling crowd bridge dynamic interaction with a discretely defined crowd. J. Sound and Vib, Vol. 331, No. 11, pp. 2685–2709, 2012.

105. Hicks, S. and Smith, A.: Design of floor structures against human-induced vibrations. Steel Constr. Vol. 4, No. 2, pp. 114–120, 2011.

106. RFCS: Human induced vibrations of steel structures (HiVoSS) -vibration design of floors: guideline. European Commission-RFCS. European Commission: RFS2-CT-2007-00033, Brussels, Belgium, 2007.

107. Feldmann, M., Heinemeyer, C., Butz, C., Caetano, E., Cunha, A., Galanti, F., Goldack, A., Helcher, O., Keil, A., Obiala, R., Schlaich, M., Sedlacek, G., Smith, A., and Waarts, P.: Design of floor structures for human induced vibrations. Joint Rep No. EUR 24084 EN. Luxembourg: European Commission-JRC, 2009.

108. Sedlacek, G., Heinemeyer, C., Butz, C., Volling, B., Waarts, P., Van Duin, F., Hicks, S., Devine, P., and Demarco, T.: Generalisation of criteria for floor vibrations for industrial, office, residential and public building and gymnastic halls. Tech.Rep No. Eur 21972 EN. Luxembourg: European Commission-JRC, 2006.

109. Fahmy, Y. G. M. and Sidky, A. N. M.: An experimental investigation of composite floor vibration due to human activities. A case study. Hous. and Build. Natl. Res. Center (HBRC) J. Vol. 8, No. 3, pp. 228–238, 2012.

110. Clough, R. W. and Penzien, J.: Dynamic of structures. 3rd. Computers and Structures, Inc., Berkeley, CA., USA, 2003.

111. Pavic, A., Reynolds, P., Prichard, S., and Lovell, P. A.: Evaluation of mathematical models for predicting walking-induced vibrations of high-frequency floors. Int. J. of Struct. Stab. and Dyn. Vol. 3, No. 1, pp. 107–130, 2003.

112. Setareh, M.: Vibration serviceability of a building floor structure. II: Vibration evaluation and assessment. J. of Perform. of Constr. Facil. Vol. 24, No. 6, pp. 508–518, 2010.

113. (BSI), B. S. I.: Guide to measurement and evaluation of human exposure to whole-body mechanical vibration and repeated shock. BSI, London, UK, 1987.

114. Setareh, M.: Vibration serviceability issues of slender footbridges. J. of Bridge Eng. Vol. 21, No. 11, pp. 1–12, 2016.

115. Ellis, B. R.: Serviceability evaluation of floor vibration induced by walking loads. The Struct. Eng. Vol. 79, No. 21, pp. 30–36, 2001.

116. Ellis, B.: The influence of crowd size on floor vibrations induced by walking. The Struct. Eng. Vol. 81, No. 6, pp. 20–27, 2003.

117. Willford, M. R., Young, P., and Field, C.: Predicting footfall-induced vibration: Part 2. Proc. of the Inst. of Civ. Eng. (ICE) - Structures and Buildings, Vol. 160, No. 2, pp. 73–79, 2007.

118. (BSI), B. S. I.: Guide to evaluation of human exposure to vibration in buildings. Part 1: Vibration sources other than blasting (BS6472-1). BSI, London, UK, 2008.

119. Pedersen, L.: Dynamic model of a structure carrying stationary humans and assessment of its response to walking excitation. Dyn. of Civ. Struct.: Proce. of the IMAC-XXIV, A Conf. and Expos. on Struct. Dyn. 2007. Springer Int. Publ., 2007.

120. Devin, A., Fanning, P. J., and Pavic, A.: Nonstructural partitions and floor vibration serviceability. J. of Archit. Eng. Vol. 22, No. 1, pp. 1–9, 2016.

121. Oasys: GSA v9.0 Structural Design & Analysis Software. Oasys Software, London, UK, 2018.

122. Autodesk: Autodesk Robot Structural Analysis Professional. Autodesk, USA, 2018.

123. CSI: SAP2000 v20 Integrated Finite Element Analysis and Design of Structures. Computers and Structures Inc., Berkely, USA, 2018.

124. CSI: ETABS v17 Integrated Analysis, Design and Drafting of Building Systems. Computers and Structures Inc., Berkely, USA, 2018.

125. Živanović, S., Racic, V., El Bahnasy, I., and Pavic, A.: Statistical characterisation of parameters defining human walking as observed on an indoor passerelle. Proc. of EVACES. Exp. Vib. Anal. for Civ. Eng. Struct., Porto, Portugal, 2007, pp. 219–225.

126. Racic, V., Pavic, A., and Brownjohn, J. M. W.: Modern facilities for experimental measurement of dynamic loads induced by humans: A literature review. Shock and Vib. Vol. 20, No. 1, pp. 53–67, 2013.

127. Van Nimmen, K., Lombaert, G., Jonkers, I., De Roeck, G., and Van Den Broeck, P.: Characterisation of walking loads by 3D inertial motion tracking. J. of Sound and Vib. Vol. 333, No. 20, pp. 5212–5226, 2014.

128. Keogh, J., Duignan, R., and Caprani, C.: Characteristics of pedestrian crowd flow demand for vibration serviceability of footbridges. Bridge Maintenance, Safety, Management and Life Extension. CRC Press, 2014, pp. 370–377.

129. Zheng, F., Shao, L., Racic, V., and Brownjohn, J.: Measuring human-induced vibrations of civil engineering structures via vision-based motion tracking. Measurement, Vol. 83, No. 4, pp. 44–56, 2016.

130. Fujino, Y., Pacheco, B. M., Nakamura, S., and Warnitchai, P.: Synchronization of human walking observed during lateral vibration of a congested pedestrian bridge. Earthq. Eng. and Struct. Dyn. Vol. 22, No. 9, pp. 741–758, 1993.

131. Kretz, T., Grünebohm, A., Kaufman, M., Mazur, F., and Schreckenberg, M.: Experimental study of pedestrian counterflow in a corridor. J. of Stat. Mech.: Theory and Exp. Vol. 2006, No. 10, P10001, 2006.

132. Corbetta, A., Bruno, L., Muntean, A., and Toschi, F.: High statistics measurements of pedestrian dynamics. The Conf. on Pedestrian and Evacuation Dyn. 2014 (PED2014). Transportation Research Procedia, 2014, pp. 96–104.

133. Brandle, N., Bauer, D., and Seer, S.: Track-based finding of stopping pedestrians - A practical approach for analyzing a public infrastructure. Proc. of the IEEE Intelligent Transportation Syst. Conf. (ITSC). Transportation Research Procedia, Toronto, Canada, 2006, pp. 115–120.

134. Setareh, M.: Vibration Serviceability of a Building Floor Structure. II: Vibration Evaluation and Assessment. J. of Perform. of Constr. Facil. Vol. 24, No. 6, pp. 508–518, 2009.

135. Davis, D. B.: Finite element modeling for prediction of low frequency floor vibrations due to walking. PhD thesis. Blacksburg, Virginia, USA: The Virginia Polytechnic Institute and State University, 2008.

136. Smith, J.: Vibration of structures. Application in civil engineering desing. Chapman & Hall, London, England, 1988.

137. Vibrant Technology Inc.: ME'Scope VES-VT560 Visual SDM Pro. VES, USA, 2018.

138. Blevins, R.: Formulas for natural frequency and mode shape. Litton Educational Publ., Inc, New York, 1979.

139. Al-Hunaidi, M. O. and Guan, W.: Digital frequency-weighting filters for evaluation of human exposure to building vibration. Noise Control Eng. J. Vol. 44, No. 2, pp. 79–91, 1996.

140. Newland, D. E.: An introduction to random vibrations, Spectral & Wavelet analysis. Dover Publications Inc., 3rd ed., 2005.

141. AXIS Communications: AXIS M3007-PV Network Camera Datasheet, 2017.

142. IntuVision v8.0.11: www.intuvisiontech.com. USA, 2018.

143. The MathWorks, Inc.: MATLAB Release 2018a. MathWorks, Natick, Massachusetts, USA, 2018.

144. Helbing, D., Farkas, I., and Vicsek, T.: Simulating dynamical features of escape panic. Nature, Vol. 407, No. 9, pp. 487–490, 2000.

145. Dijkstra, E.: A note on two probelms in connexion with graphs. Numerische Mathematik, Vol. 1, No. 1, pp. 269–271, 1959.

146. Lakoba, T. I., Kaup, D., and Finkelstein, M. N.: Modifications of the Helbing-Molnar-Farkas-Vicsek social force model for pedestrian evolution. Simulation, Vol. 81, No. 5, pp. 339–352, 2005.

147. Chen, X., Treiber, M., Kanagaraj, V., and Li, H.: Social force models for pedestrian traffic – state of the art. Transport Reviews, Vol. 38, No. 5, pp. 625–653, 2017.

148. Bocian, M., Macdonald, J., Burn, J., and Redmill, D.: Experimental identification of the behaviour of and lateral forces from freely-walking pedestrians on laterally oscillating structures in a virtual reality environment. Eng. Struc. Vol. 105, No. 12, pp. 62–76, 2015.

149. Bohannon, R. W.: Comfortable and maximum walking speed of adults aged 20-79 years:reference values and determinants. Age and Ageing, Vol. 26, No. 1, pp. 15–19, 1997.

150. Smith, A. J. and Lemaire, E. D.: Temporal-spatial gait parameter models of very slow walking. Gait & Posture, Vol. 61, No. 3, pp. 125–129, 2018.

151. Draper N. R. and Smith, H.: Applied regression analysis. 3rd. John Wiley & Sons Inc., 1998.

152. Cho, W.: Introduction to dynamics and control in mechanical engineering systems. 1st. John Wiley and Sons, Sussex, UK, 2016.

153. Hatch, M.: Vibration simulation using MATLAB and ANSYS. Chapman and Hall, USA, 2001.

154. Cara, F., Juan, J., Alarcon, E., Reynders, E., and De Roeck, G.: Modal contribution and state space order selection in operational modal analysis. Mech. Syst. & Signal Process. Vol. 38, No. 20, pp. 276–298, 2013.